



Hydro-mechanical behaviour of cement kiln  
dust under saturated and unsaturated conditions

Yahya Hamza Karagoly

Geoenvironmental Research Centre

School of Engineering

Cardiff University

*Thesis submitted in candidature for the degree of Doctor of  
Philosophy at Cardiff University*

April 2020

# Dedication

*This work is dedicated to the memory of my  
father*

# Acknowledgements

In the name of Allah, the Most Gracious, the Most Merciful

I would like to express my deep and sincere gratitude to my supervisors Professor Snehasis Tripathy and Professor Peter Cleall for their support, encouragement, advices, time, and patience that they have given me throughout this study.

My deepest appreciation goes to my sponsor “ Iraqi Ministry of Higher Education and Scientific Research” for their financial support and my deep gratitude is also extended to Iraqi Cultural Attache in London for the support I received during the study period.

I would like to thank Dr Michael Harbottle for his annual reviews of my work and for his valuable comments. I am also very grateful to the technical staff at ENGIN and my appreciation is also extended to the staff of research office and financial office for their assistance and support.

I would also like to take this opportunity to thank my viva examiners, Prof Yu-Jun Cui from Ecole des Ponts Paris, France and Dr Diane Gardner from Cardiff University, for their very invaluable comments and suggestions.

Thanks to my all friends and lab mates who I have met at Cardiff University for their encouragements, accompany, support, and knowledge sharing.

My sincere gratitude goes to my father (may Allah give his mercy upon him) and my mother for their love, prayers, and support. I would like to extend my appreciation to my brothers, sisters, and relatives and their families. Especial thanks and love to my wife and lovely daughter for being in my life.

# Abstract

The importance of reusing industrial wastes has been recognised to benefit the society in various ways. Waste minimisation, natural resources conservation, reducing energy cost, effective landfill utilization, and mitigating the environmental impacts are some of key issues that are directly linked with the reuse of industrial wastes. Cement kiln dust (CKD), an industrial by-product from cement manufacturing process, has been considered as an alternative material (alone or as admixture) in various geotechnical and geoenvironmental engineering applications. Most construction materials used in various applications are compacted and hence unsaturated which in turn, may undergo wetting and drying processes due to the environmental changes. This thesis presents a comprehensive experimental investigation focusing on the hydro-mechanical behaviour of CKD. Numerous experimental techniques were used to study the volume change, compressibility, hydraulic conductivity, water retention and shear strength of a CKD. Complementary investigations were also carried out on a sand and a sand (85%)-CKD (15%) mixture. One-dimensional volume change and compressibility tests were carried out using a conventional oedometer. Pressure plate, chilled-mirror dew-point potentiometer, fixed matrix porous ceramic disc sensors, suction control oedometer, and unsaturated triaxial test set up were used to establish the water retention curves (WRCs). The shear strength parameters were determined from conventional UU, CU, CD tests and the unsaturated shear strength parameters from unsaturated CD triaxial tests.

The CKD used exhibited swelling at low applied stresses and a tendency to collapse at high stresses when wetted from unsaturated condition. The swelling strain decreased with an increase in the applied stress, whereas swelling pressure developed when hydrated under constant volume condition. Some commonly used correlations between compressibility parameters and plasticity properties of clayey soils were found to be valid for the CKD. Significant scatter was noted in the experimental WRC data that were established from various devices/techniques. The popular parametric models used for best-fitting water retention data of soils were found to be suitable for CKD. The wetting WRC remained below that of the drying WRC. Consolidation of CKD influenced the shear strength parameters. The cohesion ( $c$ ) was higher and the angle of internal friction ( $\phi$ ) was lower in the UU tests than in the CU tests. The maximum value of  $\phi$  for the CKD was obtained in CD tests. The strain rate adopted during the shearing process affected the rate of development of deviator stress and the peak deviator stress, but its effect was insignificant at large axial strain. The value of apparent cohesion ( $c$ ) decreased with a decrease in the matric suction. The suction – cohesion relationship was found to be non-linear, particularly at high suctions, whereas ignoring the non-linear relationship, the values of  $\phi$  and  $\phi^b$  (the angle of friction due to matric suction effect) were found to be similar. An addition of 15% CKD to sand did not significantly influence the hydraulic conductivity and ( $\phi$ ) of the sand, whereas  $c$  was found to increase.

# Table of Contents

<b>Abstract</b> .....	<b>iii</b>
<b>Table of Contents</b> .....	<b>iv</b>
<b>List of Figures</b> .....	<b>ix</b>
<b>List of Tables</b> .....	<b>xv</b>
<b>List of Abbreviations and Symbols</b> .....	<b>xvii</b>
<b>CHAPTER 1</b> .....	<b>1</b>
<b>Introduction</b> .....	<b>1</b>
1.1 Background.....	1
1.2 Aim .....	4
1.3 Objectives .....	4
1.4 Thesis overview .....	6
<b>CHAPTER 2</b> .....	<b>8</b>
<b>Literature review</b> .....	<b>8</b>
2.1 Introduction.....	8
2.2 Cement kiln dust and uses/applications .....	8
2.2.1 Cement kiln dust (CKD) .....	8
2.2.2 Reactivity of CKD .....	9
2.2.3 Applications of CKD .....	10
2.2.3.1 CKD-treated soils.....	11
2.2.3.2 A review of research works on CKD .....	13
2.3 Suction and water potential .....	15
2.4 Measurement and control of soil suction .....	17
2.4.1 Suction measuring techniques.....	20
2.4.1.1 Fixed-matrix porous ceramic disc water potential sensors (MPS-6) .....	20
2.4.1.2 Chilled-mirror Dew-Point Potentiometer (WP4-C) .....	22
2.4.2 Measurement of osmotic suction .....	24
2.4.3 Suction control techniques .....	26
2.4.3.1 Pressure plate extractor .....	26
2.4.3.2 Constant relative humidity desiccators .....	27
2.5 Water retention curve (WRC).....	29

2.5.1 Features of WRC.....	30
2.5.2 Factors influencing the WRC.....	32
2.5.2.1 Influence of type of soil on WRC .....	33
2.5.2.2 Influence of compaction state on WRC .....	34
2.5.2.3 Influence of stress state on WRC.....	35
2.5.2.4 Influence of stress history on WRC .....	36
2.6 Modelling of WRC .....	37
2.7 Stress state variables .....	39
2.8 Volume change behaviour of unsaturated soils .....	40
2.9 Shear strength of soil .....	43
2.9.1 Saturated shear strength .....	43
2.9.2 Unsaturated shear strength.....	44
2.9.2.1 The nonlinearity of Failure Envelope .....	48
2.9.2.2 Determination of unsaturated shear strength.....	49
2.10 Concluding remarks .....	50
<b>CHAPTER 3.....</b>	<b>52</b>
<b>Materials and methods .....</b>	<b>52</b>
3.1 Introduction.....	52
3.2 Materials used .....	52
3.3 Properties of the materials used .....	53
3.3.1 Specific gravity .....	53
3.3.2 Atterberg Limits.....	53
3.3.3 Particle size distribution.....	54
3.3.4 Compaction tests.....	56
3.3.5 Cation exchange capacity (CEC) of CKD .....	58
3.3.6 Chemical composition .....	60
3.3.7 Mineral compositions.....	62
3.3.8 Microstructural analysis (SEM study) .....	64
3.4 Experimental techniques and test procedures .....	66
3.4.1 Preparation of the material-water mixtures.....	67
3.4.2 Swelling and compressibility tests on CKD .....	67

3.4.2.1 Specimen preparation (swelling and compressibility tests on CKD).....	67
3.4.2.2 Testing procedure (one-dimensional swelling and consolidation tests on CKD) .....	69
3.4.3 Water retention tests on CKD .....	71
3.4.3.1 Pressure plate tests .....	71
3.4.3.1.1 Apparatus description .....	71
3.4.3.1.2 Testing procedure (pressure plate tests).....	72
3.4.3.2 Salt solution tests .....	73
3.4.3.2.1 Specimen preparation and testing procedure (vapour equilibrium technique).....	74
3.4.3.3 Chilled-mirror dew-point potentiometer tests .....	75
3.4.3.4 Fixed-matrix porous ceramic disc water potential sensor tests.....	78
3.4.3.4.1 Specimen preparation and testing procedure (water potential sensor).....	79
3.4.3.5 Water content-void ratio relationship (shrinkage path) .....	81
3.4.3.5.1 Clod test.....	81
3.4.3.5.1.1 Calibration of glue mass .....	83
3.4.4 Saturated and unsaturated triaxial tests.....	84
3.4.4.1 Conventional Triaxial shear Tests.....	85
3.4.4.1.1 Specimen preparation for conventional triaxial tests .....	85
3.4.4.1.2 Testing procedure (CD, UU and CU tests) .....	88
3.4.4.1.2.1 Specimen and system preparation.....	89
3.4.4.1.2.2 Saturation stage.....	89
3.4.4.1.2.3 Consolidation stage.....	91
3.4.4.1.2.4 Shearing stage .....	91
3.4.4.2 Permeability tests in a triaxial test set up.....	92
3.4.4.3 Unsaturated triaxial shear tests on CKD .....	94
3.4.4.3.1 Control of matric suction .....	98
3.4.4.3.2 Saturating a high air-entry value ceramic disk.....	98
3.4.4.3.3 Measurement of total volume change .....	99
3.4.4.3.4 Testing procedure (Unsaturated triaxial tests) .....	100
3.4.4.3.4.1 Matric Suction equalisation stage .....	102
3.4.4.3.4.2 Shearing stage .....	102
3.4.4.4 Suction-controlled oedometer tests.....	103
3.4.4.4.1 Testing procedure (suction control oedometer tests) .....	105
3.5 Concluding remarks.....	107
<b>CHAPTER 4.....</b>	<b>108</b>
<b>One-dimensional swelling and compressibility behaviour of cement kiln dust.....</b>	<b>108</b>
4.1 Introduction.....	108
4.2 Experimental programme.....	109

4.3 Results and discussion .....	110
4.3.1 Swelling strain .....	110
4.3.2 Swelling pressure .....	111
4.4 Compressibility characteristics .....	113
4.4.1 Time-deformation behaviour .....	113
4.4.2 Compression index ( $C_c$ ) and swell index ( $C_s$ ).....	115
4.4.3 Coefficient of consolidation ( $C_v$ ) .....	117
4.4.4 Coefficient of volume compressibility ( $m_v$ ).....	119
4.4.5 Coefficient of permeability ( $k$ ) .....	120
4.5 Concluding Remarks.....	122
<b>CHAPTER 5.....</b>	<b>124</b>
<b>Water retention characteristics of CKD, sand, and sand-CKD.....</b>	<b>124</b>
5.1 Introduction.....	124
5.2 Experimental programme.....	125
5.3 Results and discussion .....	127
5.3.1 Suction equilibrium time.....	127
5.3.1.1 Suction equilibration time in pressure plate tests.....	127
5.3.1.2 Suction equilibration time in vapour equilibrium tests .....	128
5.3.1.3 Suction equilibration in chilled-mirror dew-point potentiometer (WP4-C) tests .....	129
5.3.1.4 Suction equilibration in MPS-6 tests .....	130
5.3.2 Osmotic suction of CKD.....	133
5.3.3 Water retention curves (WRCs).....	134
5.3.3.1 Suction-water content WRCs of CKD .....	134
5.3.3.2 Suction-degree of saturation WRCs of CKD .....	135
5.3.3.3 Shrinkage curve of CKD.....	136
5.3.4 WRCs of compacted sand and sand-CKD mixture.....	139
5.3.5 WRC parametric model results .....	143
5.4 Concluding remarks.....	149
<b>CHAPTER 6.....</b>	<b>150</b>
<b>Effects of suction and net stress on the one dimensional volume change behaviour of cement kiln dust .....</b>	<b>150</b>

6.1 Introduction.....	150
6.2 Experimental programme.....	151
6.3 Results and discussion .....	151
6.3.1 Water volume and vertical deformation.....	152
6.3.2 Void ratio change during wetting and drying .....	154
6.3.3 Water retention behaviour of CKD during the wetting process.....	155
6.4 Concluding Remarks.....	158
<b>CHAPTER 7.....</b>	<b>159</b>
<b>Shear strength, volume change, and permeability behaviour under saturated and unsaturated conditions .....</b>	<b>159</b>
7.1 Introduction.....	159
7.2 Experimental program .....	162
7.3 Results and discussion .....	164
7.3.1 UU and CU triaxial test results .....	164
7.3.1.1 UU and CU-test results of compacted-saturated cement kiln dust (CKD) .....	164
7.3.1.2 UU and CU-Test results of sand .....	169
7.3.1.3 UU and CU-Test results of the compacted sand-CKD mixture .....	171
7.3.1.4 Peak deviator stress and axial strain under various conditions .....	175
7.3.1.5 CD triaxial test results of CKD .....	178
7.3.2 Saturated permeability from triaxial tests .....	181
7.3.3 Unsaturated Consolidated Drained triaxial test results of CKD .....	184
7.3.3.1 Matric suction equalisation .....	184
7.3.3.2 Water content, void ratio, and degree of saturation at various imposed matric suctions .....	186
7.3.3.3 Shear strength at various matric suctions.....	188
7.3.3.4 Unsaturated shear strength parameters.....	192
7.4 Concluding Remarks.....	195
<b>CHAPTER 8.....</b>	<b>198</b>
<b>Conclusions and Recommendations .....</b>	<b>198</b>
8.1 Conclusions.....	198
8.2 Recommended further studies.....	204
References.....	206

# List of Figures

Figure 2.1 Stabilisation process using the cement kiln dust: (a) Constructing a pavement base (reproduced from Adaska and Taubert 2008), and (b) Constructing stabilised subgrade soil (reproduced from Bandara and Grazioli 2009). .....	12
Figure 2.2 Details of the fixed-matrix porous ceramic disc sensor (reproduced from Tripathy et al. 2016). .....	21
Figure 2.3 Water retention curve of the fixed-matrix porous ceramic disc (MPS-6) sensors (reproduced from Tripathy et al. 2016). .....	21
Figure 2.4 a schematic of chilled-mirror dew point device (reproduced from Bulut et al. 2008) .....	23
Figure 2.5 Osmotic pressure plotted against electrical conductivity for pore water containing dissolved salts (reproduced from United States Salinity Laboratory (1954), cited in (Leong et al. 2003)). .....	25
Figure 2.6 Schematic cross section of the interface between the soil specimen and high-entry-value ceramic disc (reproduced from Murray and Sivakumar 2010). .....	27
Figure 2.7 Schematic of vacuum desiccator for equilibrating small soil specimens in a constant-relative-humidity environment created by controlled salt solution (reproduced from Alabdullah 2010). .....	29
Figure 2.8 Typical WRCs for a silt under desorption and adsorption conditions (reproduced from Fredlund et al. 2012). .....	31
Figure 2.9 A typical WRC (reproduced from Vanapalli et al. 1999). .....	32
Figure 2.10 Desorption WRCs for sand, silt, and clay soils (reproduced from Fredlund and Xing 1994). .....	34
Figure 2.11 Effect of stress history and method of specimen preparation on measured SWCC (reproduced from Fredlund et al. 2012). .....	37
Figure 2.12 A new total volume measuring system for triaxial testing of unsaturated soils (reproduced from Ng et al., 2002). .....	42

Figure 2.13 Mohr-Coulomb failure envelope for saturated soil (reproduced from Fredlund and Rahardjo 1993).....	44
Figure 2.14 Extended Mohr-Coulomb failure envelope for unsaturated soils (reproduced from Fredlund et al. 2012). .....	46
Figure 2.15 Line of intercepts along failure plane on $\tau$ versus $u_a - u_w$ plane (reproduced from Fredlund et al. 2012). .....	47
Figure 2.16 Horizontal projection of failure envelope onto $\tau$ versus $\sigma - u_a$ plane viewed parallel to matric suction ( $u_a - u_w$ ) axis as contour lines of failure envelope on $\sigma - u_a$ plane (reproduced from Fredlund et al. 2012). .....	48
Figure 3.1 Atterberg limits – curing time relationship of cement kiln dust .....	54
Figure 3.2 Particle size distribution curves of materials used.....	55
Figure 3.3 Standard Proctor compaction curve of the cement kiln dust .....	57
Figure 3.4 Standard Proctor compaction curve of the sand. ....	57
Figure 3.5 Standard Proctor compaction curve of the sand-cement kiln dust.....	58
Figure 3.6 X-ray diffraction patterns of (a) Cement kiln dust (CKD); (b) Sand and (c) Sand-CKD mixture.....	63
Figure 3.7 SEM photomicrograph of cement kiln dust (CKD) - 2 $\mu\text{m}$ scale .....	64
Figure 3.8 SEM photomicrographs of sand (a) 1mm scale; (b) 200 $\mu\text{m}$ scale.....	65
Figure 3.9 SEM photomicrographs of sand-CKD - 200 $\mu\text{m}$ scale. ....	66
Figure 3.10 (a) A photograph of the components of compaction mould and (b) the static compaction setup used. ....	68
Figure 3.11 The automatic oedometer used in this study to measure swelling pressure of CKD. ....	70
Figure 3.12 Test setup for 5-bar pressure plate extractor.....	72
Figure 3.13 Salt solution (VET) test setup: a photograph of the desiccator used and Rotronic Hydrolog relative humidity probe arrangement.....	74
Figure 3.14 WP4-C model of chilled-mirror dew point device .....	77

Figure 3.15 The water potential sensor and data logger used in this study.....	79
Figure 3.16 Experimental setup for measuring suction using MPS6 water potential sensors ....	80
Figure 3.17 Coated cement kiln dust specimens in clod test .....	82
Figure 3.18 Glue mass fraction calibration curve .....	84
Figure 3.19 Triaxial shear test set up (a) a schematic layout of the device (reproduced from Rees 2013); (b) a photograph of the experimental setup. ....	86
Figure 3.20 Triaxial compaction mould (a) a photograph of the components; (b) a compaction setup .....	87
Figure 3.21 Steps for preparing sand and sand-CKD specimens.....	88
Figure 3.22 Relationship between pore pressure parameter B and degree of saturation (reproduced from Black and Lee 1973) .....	90
Figure 3.23 Unsaturated triaxial test set up (a) A schematic of the test system (Adapted from GDS Instruments Ltd 2012) and (b) a photograph of the experimental setup .....	96
Figure 3.24 A photograph showing a CKD specimen in unsaturated triaxial test and the inner cell.....	101
Figure 3.25 Suction-controlled oedometer test: (a) components of the unsaturated consolidation cell; (b) experimental setup of test. ....	104
Figure 4.1 One-dimensional swelling strain of compacted CKD specimens at various applied vertical pressures.....	111
Figure 4.2 Constant volume-swelling pressure test results for compacted CKD specimen.....	112
Figure 4.3 Typical time-compression plots of CKD specimens at applied vertical pressures of (a) 100 kPa and (b) 800 kPa.....	114
Figure 4.4 e-log p plots of compacted and slurried cement kiln dust specimens.....	116
Figure 4.5 Effect of vertical pressure on the coefficient of consolidation. ....	118
Figure 4.6 Effect of vertical pressure on the coefficient of volume compressibility of CKD. .	119
Figure 4.7 Effect of vertical pressure on the coefficient of permeability of CKD.....	121
Figure 5.1 Elapsed time versus water content in pressure plate tests for CKD specimens.....	128

Figure 5.2 Elapsed time versus water content plot of CKD in desiccator tests .....	129
Figure 5.3 Suction measurement time in chilled-mirror dewpoint potentiometer. ....	130
Figure 5.4 Suction measurement time for CKD specimens in MPS-6 sensors.....	131
Figure 5.5 Suction measurement time for sand specimens in MPS-6 sensors.....	132
Figure 5.6 Suction measurement time for sand-CKD specimens in MPS-6 sensors.....	132
Figure 5.7 Suction–water content WRC test results of CKD using various techniques. ....	135
Figure 5.8 Suction – degree of saturation WRC test results of CKD using various techniques. .....	136
Figure 5.9 Measured volume change with elapsed time for the cement kiln dust during drying process in clod test. ....	138
Figure 5.10 Shrinkage curve for the cement kiln dust. ....	139
Figure 5.11 Comparisons of fixed-matrix porous ceramic disc (MPS-6) sensor and chilled- mirror dew-point potentiometer (WP4-C) test results for the sand used.....	140
Figure 5.12 Comparisons of fixed-matrix porous ceramic disc (MPS-6) sensor and chilled- mirror dew-point potentiometer (WP4-C) test results for the sand used.....	141
Figure 5.13 Comparisons of fixed-matrix porous ceramic disc (MPS-6) sensor and chilled- mirror dew-point potentiometer (WP4-C) test results for compacted sand-CKD mixture. ....	142
Figure 5.14 Comparisons of fixed-matrix porous ceramic disc (MPS-6) sensor and chilled- mirror dew-point potentiometer (WP4-C) test results for compacted sand-CKD mixture. ....	143
Figure 6.1 Elapsed time versus (a) water volume change and (b) vertical deformation at various applied suctions and a constant net stress of 25 kPa.....	153
Figure 6.2 Effect of the applied suction on the void ratio of cement kiln dust. ....	155
Figure 6.3 Effect of the applied suction on the water content of cement kiln dust specimens at a constant net normal stress of 25 kPa. ....	156
Figure 6.4 Effect of the applied suction on the degree of saturation of cement kiln dust specimens at constant net normal stress of 25 kPa. ....	157

Figure 7.1 Results of the triaxial compression tests for the cement kiln dust specimens: (a) deviator stress from UU-tests; (b) deviator stress from CU-tests and (c) excess pore water pressure from CU-tests.....	167
Figure 7.2 Mohr-Coulomb failure envelopes for the cement kiln dust specimens: (a) UU-tests with strain rate of 1 mm/min; (b) CU-tests with strain rate of 1 mm/min and (c) CU-tests with strain rate of 0.083 mm/min.....	168
Figure 7.3 Results of the triaxial compression tests for the sand specimens: (a) axial strain versus deviator stress from UU-tests; (b) axial strain versus deviator stress from CU-tests and (c) axial strain versus excess pore water pressure from CU-tests. ....	170
Figure 7.4 Mohr-Coulomb failure envelopes for the sand specimens: (a) UU-tests and (b) CU-tests. ....	171
Figure 7.5 Results of the triaxial compression tests for the sand-CKD specimens: (a) axial strain versus deviator stress from UU-tests; (b) axial strain versus deviator stress from CU-tests and (c) axial strain versus excess pore water pressure from CU-tests. ....	173
Figure 7.6 Mohr-Coulomb failure envelopes for the sand-CKD specimens: (a) UU-tests and (b) CU-tests.....	174
Figure 7.7 Results of saturated triaxial compression tests (UU and CU-Tests) for the selected materials: (a) confining pressure versus peak deviator stress, and (b) confining pressure versus axial strain. ....	176
Figure 7.8 Results of saturated CD-triaxial tests of cement kiln dust specimens under different confining pressures: (a) axial strain versus deviator stress, (b) axial strain versus volumetric strain, and (c) normal stress versus shear stress.....	180
Figure 7.9 Hydraulic conductivity of the selected material (CKD, Sand, and Sand-CKD) under various confining pressures.....	182
Figure 7.10 Test results of unsaturated triaxial tests for the cement kiln dust specimens during the equalisation process under different suctions at constant net confining pressure: (a) water volume change, (b) total volume change .....	185
Figure 7.11 Test results of equalisation process under various suction at constant net confining pressure: (a) water content; (b) void ratio; (c) degree of saturation.....	187

Figure 7.12 Results of the unsaturated CD-triaxial compression tests of the cement kiln dust specimens under different suctions at constant net confining pressure of 25 kPa: (a) deviator stress and (b) volumetric strain. .... 190

Figure 7.13 Mohr circles and cohesion intercepts of the saturated and unsaturated cement kiln dust specimens under different suctions at constant net confining pressure of 25 kPa. .... 193

Figure 7.14 Suction versus cohesion intercept of the saturated and unsaturated cement kiln dust specimens under different suctions at constant net confining pressure of 25 kPa. . 194

# List of Tables

Table 2.1 Summary of some devices for measuring soil suction and its components (Lu and Likos 2004; Fredlund et al. 2012; Tripathy et al. 2016). .....	19
Table 2.2 The electrical conductivity of some natural waters (Adapted from Dismuke et al. 1981). .....	24
Table 3.1 Properties of the materials used .....	59
Table 3.2 Chemical composition of materials used .....	61
Table 3.3 Relative humidity imposed by saturated salt solutions and corresponding suctions at 21°C .....	75
Table 3.4 Summary of the triaxial tests .....	84
Table 3.5 B values for different soils at complete or nearly complete saturation (reproduced from Black and Lee 1973) .....	91
Table 3.6 The confining pressures and hydraulic gradients used for determining the coefficient of permeability of CKD, sand, and sand-CKD. ....	93
Table 3.7 Descriptions of the main components of GDS triaxial testing apparatus. ....	97
Table 4.1 Compression and swell indices of the cement kiln dust specimens tested. ....	117
Table 4.2 Typical values for Coefficient of consolidation, $C_v$ (reproduced from Lambe and Whitman 1969). ....	118
Table 4.3 Typical values of the coefficient of volume compressibility and descriptive terms used (reproduced from Carter 1983). ....	120
Table 5.1 Electrical conductivity and osmotic suction of cement kiln dust.....	134
Table 5.2 Model parameters in relation to water content and degree of saturation from both equations based on the pressure plate and desiccator for the CKD. (s = suction, w = water content, $S_r$ = degree of saturation). ....	146
Table 5.3 model parameters in relation to water content and degree of saturation from both equations based on the MPS-6 and WP4-C tests for CKD, sand, and sand-CKD. (s = suction, w = water content, $S_r$ = degree of saturation). ....	147

Table 5.4 Air entry values for the materials used. ( $s$ = suction, $w$ = water content, $S_r$ = degree of saturation) .....	148
Table 7.1 Summary of saturated shear strength test results of the materials. ....	177
Table 7.2 Effective and total shear strength parameters of CKD, sand and sand-CKD based on Mohr-Coulomb failure criterion. (UU, CU, and CD - Triaxial Tests).....	180
Table 7.3 Summary of the saturated permeability tests results.....	183
Table 7.4 Summary of water content ( $w$ ), void ratio ( $e$ ), and degree of saturation ( $S_r$ ) of saturated and unsaturated cement kiln dust specimens from triaxial tests.....	192

# List of Abbreviations and Symbols

## Abbreviations

AEV	Air entry value
ASTM	American Society for Testing and Materials
C-A-H	Calcium-aluminate-hydrates
C-A-S-H	Calcium – aluminate -silicate-hydrates
CD	Consolidated drained
CEC	Cation exchange capacity
CKD	Cement kiln dust
C-S-H	Calcium-silicate-hydrates
CU	Consolidated undrained
DPT	Differential pressure transducer
DPVC	Digital pressure/volume controllers
DPT	Differential pressure transducer
DTI	Digital transducer interface
CEC	Cation exchange capacity
EC	Electrical conductivity
EPA	Environmental Protection Agency
HAE	High air entry
LL	Liquid limit
LOI	loss on ignition
LVDT	linear variable displacement transducer
OWC	Optimum water content
PL	Plastic limit
PI	Plasticity index
PVAc	Polyvinyl acetate glue
SL	Shrinkage limit
SEM	Scanning electron microscope
SWCCs	Soil-water characteristic curves
UU	Unconsolidated undrained

USCS	Unified Soil Classification System
USEPA	United States Environment Protection Agency
VET	Vapour equilibrium technique
WRCs	Water retention curves
XRD	X-ray diffraction
XRF	X-ray fluorescence spectroscopy

## Symbols

$\alpha$	van Genuchten fitting parameter related to the inverse of air-entry value
$\Delta h/ L$	Hydraulic gradient
$\Delta\sigma_3$	Increment of confining pressure.
$\Delta u$	Pore-water pressure change
$\rho_{\text{d material (t)}}$	Dry density of the material
$\rho_{\text{glue}}$	Density of the glue
$\sigma$	Total stress
$\sigma'$	Effective stress
$(\sigma - u_w)$	Effective normal stress
$(\sigma - u_a)$	Net normal stress
$(\sigma_3 - u_a)$	Net confining stress
$(\sigma_v - u_a)$	Net vertical stress
$\sigma' = \sigma - u_w$	Effective stress
$(\sigma_f - u_w)_f$	Effective normal stress on the failure plane at failure
$\sigma_{ff}$	Total normal stress on the failure plane at failure
$(\sigma_f - u_a)_f$	Net normal stress state on the failure plane at failure,
$\tau$	Shear stress
$\tau_f$	Shear stress at failure
$\tau_{ff}$	Shear stress on the failure plane at failure
$\phi'$	Angle of internal friction associated with the net normal stress
$\phi^b$	Angle of friction due to matric suction effect
$\phi'$	Effective internal friction angle.
$\psi$	Free energy per unit mass of soil pore-water comparing to that of free pure water (J/kg)

$\psi_T$	Total soil water potential
$\psi_m$	Matric potential
$\psi_o$	Solute (osmotic) potential
$\psi_p$	Pressure potential
$\psi_g$	Gravitational potentials
$\psi_o$	Osmotic suction
$\Psi_{res}$	Estimated residual suction for the soil,
$\omega_v$	Molecular mass of water vapour (18.016 kg/k mol)
$a$	Fredlund & Xing fitting parameter related to the inflection point on the SWCC
$a_{sh}$	Minimum void ratio
$B$	Pore-water pressure parameter
$b_{sh}$	Slope of the line of tangency,
$c'$	Effective cohesion
$c$	Cohesion intercept
$C_c$	Coefficient of curvature
$C_c$	Compression index
$C_s$	Swelling index
$C_u$	Coefficient of uniformity
$C_v$	Coefficient of consolidation
$c_{sh}$	Curvature of the shrinkage curve,
$e$	Irrational constant equal to 2.71828
$e_{material(t)}$	Void ratio of material specimen
$g_{f(t)}$	Mass fraction of the glue at any given time
$G_s$	Specific gravity
$G_s$	Specific gravity
$k$	Saturated hydraulic conductivity
MPS-6	Fixed-matrix porous ceramic disc sensors
ML	Inorganic silt with low plasticity ().
$M_{clod(i)}$	Initial total mass of the Clod
$M_{material(i)}$	Initial total mass of the specimen
$M_{glue(i)}$	Initial mass of glue
$M_{air(t)}$	Mass of the Clod in air
$M_{water(t)}$	Mass of Clod in water

$M_d$	Dry mass of the specimen
$m_v$	Coefficient of volume compressibility
$m$	Fitting parameter related to the curvature near residual conditions.
$n$	Fitting parameter directly related to the slope of the WRC
$R$	Universal gas constant (8.31432 J/(mol K))
$R^2$	Correlation coefficient
$S_r$	Degree of saturation
$S_{res}$	Residual degree of saturation
SP	Poorly graded sand
SM	Silty sand
$S_{res}$	Residual degree of saturation
$T$	Absolute temperature (°K)
$u_a$	Pore air pressure
$u_w$	Pore water pressure
$(u_a - u_w)$	matric suction
$u_v$	Partial pressure of pore- water vapour
$u_{v0}$	Saturated vapour pressure of free water at the same temperature
$u_v/u_{v0}$	Ratio is equal to the relative humidity (RH).
$u_{wf}$	Pore-water pressure at failure
$u_{af}$	Pore-air pressure on the failure plane at failure,
$(u_a - u_w)_f$	Matric suction on the failure plane at failure
$v_{w0}$	Specific volume of water (m <sup>3</sup> /kg) - which is the inverse of the density of water
$V_{clod(t)}$	Total volume of the Clod
$V_{material (t)}$	Volume of specimen
$V_{glue(t)}$	Volume of glue
WP4-C	Chilled-mirror dew-point potentiometer test
$w$	Gravimetric water content at any specified suction, $\psi$
$w_s$	Saturated gravimetric water content
$W_{material (t)}$	Water content of the material specimen
$W_{material (i)}$	Initial water content of the material specimen

# **CHAPTER 1**

## **Introduction**

### **1.1 Background**

Due to the growth of population, increasing urbanisation, and rising standards of living, huge quantities and variety of solid wastes are being generated by industrial, mining, domestic and agricultural activities. Globally, the estimated quantity of wastes generation was 12 billion tonnes in the year 2002 of which 11 billion tonnes was industrial wastes (Mukherjee and Ghosh 2013). Some of the industrial wastes are steel slags, plastics, glass, fly ash, cement kiln dust, silica fume, and mine tailings (Mohamed 2002; Huang et al. 2007; Gunning et al. 2010; Nidzam and Kinuthia 2010; Sabat and Pati 2014; Osinubi et al. 2015).

In many cases, native soils are unsuitable for use in barriers construction, particularly so when the water holding capacity plays an important role. For example, sands possess high permeability and low water retention capacity as compared to the fine soils. One of the most effective ways in order to address this issue is either improving the sand by adding other materials that contribute to decreasing the permeability and improving water-holding capacity or replacement with local available suitable alternative materials.

The cement kiln dust (CKD) is one of the solid industrial by-products that has received attention to be used alone or as a mixture with soil in various civil engineering applications. The worldwide cement kiln dust generation is estimated to be about 420 - 560 tonnes during year 2009 (Kunal et al. 2012). Cement kiln dust is a by-product of the Portland cement manufacturing process. This material is a fine powder with a wide range of particle sizes and poses health hazards, storage problems, and a potential pollution source (Baghdadi and Rahman 1990; Baghdadi et al. 1995). For addressing these issues and scarcity of suitable natural resources, research is being performed in different parts of the world to explore economical and effective ways of using CKD in various

applications including cement production, soil stabilization, construction of hydraulic barrier systems, pavements, low-strength backfill, mine reclamation, and agriculture (USEPA 1998; Adaska and Taubert 2008; Keerthi et al. 2013; ASTM D5050 – 08 2015).

The beneficial use of CKD in geotechnical and geoenvironmental applications, for example, stabilisation/modification of soils, pavements, barrier systems in landfills, and retaining or wing walls of hydraulic structures, have been investigated by many researchers in the past (Baghdadi and Rahman 1990; USEPA 1998; Mohamed 2002; Moses and Afolayan 2011; Hashad and El-Mashad 2014). In most of the applications, the construction soils/materials are used in compacted form above the groundwater table. Therefore, the materials often are in unsaturated state.

The unsaturated compacted soils/fills located above the water table have negative pore water pressure (Fredlund and Rahardjo 1987). The engineered structures generally experience variations in environmental and climate conditions throughout the year and therefore, the compacted soils/fills may undergo significant changes in water content and suction due to the wetting or drying process, particularly in arid and semi-arid climates. When the soil/fill is wetted, the pore-water pressures increase, tending towards positive values and consequently, considerable changes may occur in volume, shear strength and hydraulic conductivity (Fredlund and Rahardjo 1987; Fredlund and Rahardjo 1993; Ng and Menzies 2007)

Unsaturated soils/fills have commonly been referred to as a three-phase system (solids, water, and air). The importance of soil suction in explaining the mechanical behaviour of unsaturated soils has been emphasized (Fredlund and Rahardjo 1993). The soil suction has two components, namely matric and osmotic suctions. Several devices and techniques are available currently for controlling and measuring the suction of unsaturated soils/materials either in a direct or indirect manner (Lu and Likos 2004; Nam et al. 2009; Fredlund et al. 2012; Toll et al. 2015; Tripathy et al. 2016 ).

The main information that are needed for the estimation and analysis of unsaturated soil/material are water retention ability, volume change, shear strength, permeability, and seepage. Many of the information are linked to the water retention curve (WRC) (Fredlund 1997; Fredlund 1999; Fredlund et al. 2012; Goh 2012) which represents the relationship between soil suction and water content (or degree of saturation

or volumetric water content). The characteristics of WRC are influenced by many factors including type of soil/material, compaction state, applied stress, structure and fabric, and stress history (Vanapalli et al. 1999; Lu and Likos 2004; Thu et al. 2007; Fredlund et al. 2012; Tripathy et al. 2014).

Volume change in soils/fills is usually referred to either as shrinkage, swelling or collapse. The amount and type of volume change is dependent upon several factors, such as the material type and structure, the imposed stress state, the compaction state, and degree of wetting (Sridharan et al. 1986; Lawton et al. 1989; Mitchell and Soga 2005; Ng and Menzies 2007; Wijaya and Leong 2016). The volume change of unsaturated soils/fills is controlled by two stress state variables, namely the net normal stress and matric suction. Recently, the importance of considering the volume change of soils during suction change has been recognized by a number of researchers (Peron et al. 2007; Perez-Garcia et al. 2008; Lins 2009; Nuth and Laloui 2011; Fredlund and Houston 2013). Several laboratory tests are available to determine the deformation characteristics of unsaturated soils, such as the one-dimensional compression test, isotropic compression test, and wetting and drying tests under various stress conditions in triaxial and direct shear tests.

The shear strength of unsaturated soil/materials is governed by two independent stress state variables (net normal stress and matric suction) (Fredlund et al. 1977). The matric suction provides an additional shear strength component referred to as apparent or total cohesion (Taylor 1948). The rate of change in shear strength with respect to changes in matric suction is defined by the unsaturated shear strength angle,  $\phi^b$ . The effect of suction on the shear strength of soils has been investigated by many researchers (Fredlund et al. 1978; Vanapalli et al. 1996; Taha et al. 2000; Farouk et al. 2004; Estabragh and Javadi 2012; Goh 2012; Elsharief and Abdelaziz 2015; Rashedul H Chowdhury and Azam 2016; Pujiastuti et al. 2018). Various devices and techniques can be used for measuring the unsaturated shear strength in the laboratory. The axis translation technique and a suction controlled triaxial apparatus are commonly used.

Most of the previous studies on CKD have reported that the fresh CKDs with free lime content can be successfully utilised in modification/stabilisation of both fine-and coarse-grained soils (McCoy and Kriner 1971; Baghdadi and Rahman 1990; Zaman 1992; Miller and Azad 2000; Parsons et al. 2004; Sreekrishnavilasam et al. 2007; Peethamparan et al. 2008; Moses and Afolayan 2013). The studies also referred to the effectiveness of

CKD in the treatment of problematic soils (Sayah 1993; Miller et al. 1997; Parsons et al. 2004; Keerthi et al. 2013; Nasr 2015). Sand-CKD mixtures have been investigated by several researchers. For example, Oriola et al. (2012) have studied the water retention behaviour of foundry sand-CKD, Moses and Afolayan (2011) assessed the foundry sand-CKD as a compacted hydraulic barrier material, and dune sand-CKD mixture has been evaluated as a base material for highway construction (Baghdadi and Rahman 1990), and suitability of desert sand-CKD mixture with chemical additives for use in the road pavement structures has been also investigated by (Freer-Hewish et al. 1999). Additionally, CKD has been approved to be used as an alternative to soil for daily or intermediate cover at CKD landfills and proposed as a CKD liner or cap at several locations in the United States (USEPA 1998).

A review of literature showed that most of the studies in the past have evaluated the behaviour of CKD under saturated conditions. Research related to the water retention characteristics curve of CKD is very limited. Studies on the behaviour of volume change and shear strength of CKD under various matric suctions are still scarce. Further, studies related to the saturated shear strength and permeability of CKD under different conditions as well as compressibility and expansion characteristics under various initial conditions have not been explored in detail yet.

Based on the review of the literature, three materials were chosen for the investigation: a cement kiln dust, a sand and a mixture of sand and CKD.

## **1.2 Aim**

The main aim of this study is to investigate the hydro-mechanical behaviour of cement kiln dust.

## **1.3 Objectives**

The objectives of the study are:

- 1- To experimentally investigate the one-dimensional volume change behaviour (swelling and compressibility) of CKD (either initially saturated slurried or

compacted) at various applied pressures. The investigations will provide important information concerning the swelling strain, compressibility characteristics, swelling pressure and hydraulic conductivity of CKD.

- 2- To experimentally establish the water retention curves (WRCs) of CKD, sand and sand-CKD mixture and to study the influence of addition of CKD to sand on the WRC. The results from the study will provide information on the drying water retention behaviour of CKD at various initial placement conditions (initially saturated slurried and compacted), volume change during the drying process, applications of various parametric models to establish WRC of CKD and sand-CKD mixture, and the benefits of adding CKD to sand in enhancing the water retention capacity of sand.
- 3- To investigate experimentally the one-dimensional volume change behaviour of compacted unsaturated CKD during the wetting process under various matric suctions and at constant net normal stress. The results from the investigation will provide information on the wetting water retention behaviour of CKD and will allow comparing the results with the findings from the drying WRCs in objective 2 and wetting WRC in triaxial set up in objective 6.
- 4- To study the shear strength characteristics of compacted-saturated CKD, sand, and sand-CKD. The results from the investigation will enable exploring the impact of testing conditions (UU, CU and CD) on the shear strength parameters.
- 5- To study effect of confining pressure on the saturated hydraulic conductivity of the CKD, sand, and sand-CKD in a triaxial test set up. The findings from this investigation will allow comparing the impact of  $K_0$  and isotropic stress conditions on the hydraulic conductivity of CKD.
- 6- To investigate the volume change and shear strength behaviour of the unsaturated compacted CKD during the wetting process at a constant net confining pressure. The findings will allow bringing out the impact of initial saturation conditions on the volume change, WRC and shear strength parameters.

## **1.4 Thesis overview**

The thesis consists of eight chapters. The overview of the chapters is presented as follows:

CHAPTER 1 presents the background of the study, the main aim and objectives of this study and outline of the thesis.

CHAPTER 2 presents a review of literature concerning the studies undertaken. The chapter presents general information about the cement kiln dust (CKD) and its potential use. The concept of suction and water potential, suction measurement and control techniques related to the research and the methods used for determining the WRCs are briefly presented. The relevant aspects related to the volume change and shear strength of unsaturated soils are highlighted.

CHAPTER 3 introduces the physical properties and chemical composition of the study materials (CKD, sand, and sand-CKD). The mineral composition using X-ray diffraction (XRD) and scanning electron microscope (SEM) of the materials are explored. The specimens preparation procedures, experimental setup and the testing procedures are described in detail in this chapter. The devices and techniques used for various tests are also presented.

CHAPTER 4 introduces the experimental results from the one-dimensional swelling and compressibility tests on CKD under different initial conditions. The swelling strain of compacted specimens under initial pressures of 2 kPa and 25 kPa are presented. The compressibility characteristics (compression index, coefficient of consolidation and volume compressibility) of initially saturated slurried and compacted-saturated CKD are presented as well as the permeability

of CKD under different vertical stresses. The swelling pressure of compacted specimen under constant volume condition is also considered.

CHAPTER 5 presents the water retention curves (WRCs) obtained from pressure plate extractor, desiccator, chilled-mirror dew-point potentiometer, and fixed-matrix porous ceramic disk water potential sensor tests for CKD, sand and sand-CKD. Applications of the parametric models of van Genuchten (1980) and Fredlund & Xing (1994) are also presented. Further, the shrinkage behaviour of CKD based on clod tests and the osmotic suction from electrical conductivity tests are explored.

CHAPTER 6 presents the results of suction-controlled oedometer tests on compacted CKD during the wetting process under various matric suctions and at a constant net vertical stress. Comparisons of drying WRCs from chapter 5 and wetting WRC of CKD are considered.

CHAPTER 7 presents the triaxial UU, CU and CD test results of compacted-saturated CKD and unsaturated triaxial CD test results of compacted unsaturated CKD at various matric suctions and at constant confining pressure. The UU and CU test results of compacted-saturated sand and sand-CKD are also discussed. The hydraulic conductivities of compacted-saturated CKD, sand and sand CKD at different confining pressure are presented along with the wetting water retention behaviour of compacted CKD, which is compared with the results from Chapters 5 and 6.

CHAPTER 8 summarises the main conclusions drawn from this study and further presents an outlook for possible future work in this field.

## **CHAPTER 2**

### **Literature review**

#### **2.1 Introduction**

The importance of recycling and reuse of the industrial wastes has been recognised while dealing with natural resource conservation, reducing energy cost and environmental impact and effective landfill utilization. Cement kiln dust (CKD) is one of such industrial by-products. Several studies have been carried out to investigate CKD and/or soil-CKD mixtures as alternative engineering materials to be used in various civil engineering applications. This chapter presents a review of the studies that focused on the use of the CKD and soil-CKD mixtures in the geotechnical and geoenvironmental applications and the important findings derived from the research works. A review of the concept of suction, suction measurement and control techniques related to this research are presented along with the laboratory methods used for determining the drying and wetting water retention curves. The relevant aspects related to the volume change and shear strength of unsaturated soils which form the main background of the investigation on CKD in this study are reviewed.

#### **2.2 Cement kiln dust and uses/applications**

##### **2.2.1 Cement kiln dust (CKD)**

Cement kiln dust (CKD) is a waste material produced in considerable quantities during the manufacture of Portland cement. It is a fine powdery material similar in appearance to portland cement and collected from electrostatic precipitators during the production of cement clinker (Kunal et al. 2012). The principal constituents of CKD are compounds of lime, silica, alumina, and iron (Naik et al. 2003b). Over 2.8 billion tons of cement was generated throughout the world in the year 2009 (Oss 2010). The generation of CKD has been estimated to be 15–20% of clinker or cement production (EPA 1993),

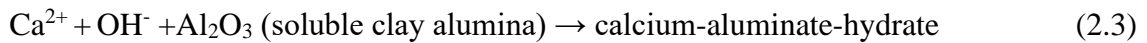
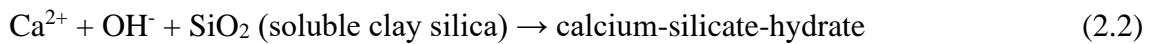
which put worldwide CKD generation at an estimated 420–560 million tonnes for the year 2009 (Kunal et al. 2012). The chemical compositions of CKD widely vary with the source of raw materials used in cement production, type of operation, dust collection facility, and type of fuel (Kunal et al. 2012). The chemical compositions of CKD influence the pozzolanic reactions while mixed with soil and consequently affect the mechanical properties of mixtures (Bhatty et al. 1996; Miller and Zaman 2000; Kim and Siddiki 2004; Pranshoo Solanki et al. 2007). CKDs usually contain insignificant amount of trace metals and hence, the concentrations of metals are not of any concern for most applications (Adaska and Taubert 2008). Studies in the past have shown that the heavy metals, such as lead, cadmium, mercury, selenium, and radionuclides are generally found in low concentrations in CKD; however, assessments of these constituents levels and their mobility in or leachability out of the CKD are important (Naik et al. 2003).

### **2.2.2 Reactivity of CKD**

CKD represents one of the chemical additives which have been recently used in various applications (e.g. geotechnical engineering, geoenvironmental engineering). The effectiveness of the additive in stabilisation or modification process depends on the amount and type (e.g. availability of free lime) of the additive, the soil treated and curing conditions (Solanki and Zaman 2002; Parsons et al. 2004; Al-Hassani et al. 2015). Although, CKD is known as a pozzolan material because it contains silica or silica and alumina, however, it has little or no cementation value itself, but under certain conditions can react with soil to produce a cementitious material (Mohamed 2002). Addition of the chemical additives to clay soils with water causes a number of reactions including cation exchange, flocculation, carbonation and pozzolanic reaction that lead to the improvement of soil properties (Al-Rawas et al. 2005). For the silt and granular materials, due to a lack of aluminacious and silicious material, the pozzolanic (cementitious) reactions do not occur (Solanki and Zaman 2002; Parsons et al. 2004; Muhunthan and Sariosseiri 2008).

(Solanki and Zaman 2012) showed that the calcium-based additives can be effectively used to improve the properties of clayey soils. In the presence of water, the calcium ions released from these stabilizers reduce the thickness of a diffuse double layer through cation-exchange and flocculation-agglomeration reactions. This is primarily responsible for the improvement in workability through reduction of adsorbed water and

decrease in plasticity index. In long-term, pozzolanic reactions occur between the calcium ions of the stabilizer and the silica and alumina of the clay minerals resulting in the formation of cementitious products such as calcium-silicate-hydrates (C-S-H), calcium-aluminate-hydrates (C-A-H), and calcium – aluminate -silicate-hydrates (C-A-S-H). The reaction may be written as:



In the presence of calcium sulfate, an additional product of hydration, known as ettringite ( $\text{Ca}_6[\text{Al}(\text{OH})_6]_2 \cdot (\text{SO}_4)_3 \cdot 26\text{H}_2\text{O}$ ) is formed (Eq. 2.4).



The formation of the aforementioned cementitious products in the soil-stabilizer matrix are responsible for an increase in the internal friction and shear strength of the stabilized soil.

### 2.2.3 Applications of CKD

Recently, a majority of CKD is recycled back into the kiln system as raw feed. In addition, there has been general trend to use the remainder of the CKD in various applications. The reuse of the CKD reduces the demand for raw materials, which saves natural resources and helps conserve energy, addresses disposal problems and mitigate the environmental impacts. There are many beneficial uses of CKD covering a wide variety of applications, such as stabilization of soils, construction of hydraulic barrier systems (liner and cover components) in landfills, low-strength backfill, inclusion in Portland cement as a materials additive, solidification of waste materials, mine

reclamation, and agricultural soil enhancement (USEPA 1998; Adaska and Taubert 2008; ASTM D5050 – 08 2015).

Many research works have been carried out to investigate the potential use of CKD in various applications particularly in the geotechnical and geoenvironmental fields. This material has been utilised in combination with other additives or alone (Adaska and Taubert 2008).

### **2.2.3.1 CKD-treated soils**

In case of using CKD as an additive in stabilisation or modification of soils, the chemical and physical properties of the modified soils get altered. The stabilisation and modification processes can be utilised to treat a wide range of soils ranging from expansive clays to granular materials.

Bhatty et al. (1996) presented a summary for a number of studies and indicated that CKD with high free lime and low alkalies exhibited improvement in the unconfined compressive strengths of clayey soils, whereas CKD with low free lime and high alkalies adversely influenced the unconfined compressive strength. A high loss on ignition (LOI) value shows that CKD is high in slow-reacting calcium carbonate and low in reactive free lime. CKDs with LOI of 28% or higher was described to possess high LOI, whereas for CKDs with moderate free lime content and low alkalies, the plasticity index, strength, and durability were improved alongside a reduction in the swelling.

Miller and Zaman (2000) found that all the CKDs used in the study showed an increase in the unconfined compressive strength and the CKD with lowest LOI exhibited the greatest increase in strength. The durability of the soils in wet-dry and freeze-thaw tests was also improved over the untreated soil. Williams (2005) showed that the soil mixtures containing CKD with high LOI (> 20%) never hardened.

For a kaolinite clay treated with 16% of CKD, the unconfined compressive strength was increased from 210 to 1100 kPa after 28 days of curing, whereas for the bentonite mixed with 8% of CKD, the plasticity index decreased from 513 to 326% (Baghdadi 1990).

One-dimensional oedometer tests indicated that the CKD can be used effectively in reducing the collapse settlement and overall compressibility (Miller et al. 1997). Studies (e.g. Adaska and Taubert 2008; Bandara and Grazioli 2009) have reported that CKDs containing free lime content can be used as stabiliser in pavement applications (Figure 2.1).



Figure 2.1 Stabilisation process using the cement kiln dust: (a) Constructing a pavement base (reproduced from Adaska and Taubert 2008), and (b) Constructing stabilised subgrade soil (reproduced from Bandara and Grazioli 2009).

Previous studies also investigated the effect of CKD on the behaviour of sandy soils. Stabilisation of a sandy soil using a CKD for pavement subgrade applications was explored by Napeierala (1983). The results indicated that an addition of 15% of CKD having 5.9% free CaO and MgO and 0.97% total alkalis ( $K_2O + Na_2O$ ) ensured a compressive strength of 0.25 MPa, which is standard practice in Poland for the subgrades within 14 days of the treatment. Baghdadi and Rahman (1990) showed that an increase in the fraction of CKD resulted in an increase in the compressive strength of a dune sand. The study suggested that CKDs may be used as an alternative for cement or lime in stabilising soils for reducing the construction cost. Another study has also been performed on the dune sand showed that there was a continuous increase in compressive strength with the amount of CKD and curing duration. It was suggested that 12-30% CKD should be sufficient to upgrade the dune sand for the light applications, whereas raising the CKD content to about 50% may be required for the heavily loaded applications (Baghdad et al. 1995). Both studies (Baghdadi and Rahman 1990 and Baghdad et al. 1995) showed that the maximum dry density increased with an increase in the CKD content (due to void-

filling) up to a point around 40 to 50% CKD content, after which the dry density decreased, whereas the optimum moisture content exhibited an opposite trend. Stabilisation of desert sand with CKD (UK commercially available CKD) and chemical additives for construction of desert road was investigated by Freer-Hewish et al. (1999). Results showed that large amounts of CKD were required for stabilising sand to meet pavement layer standards. The CKD requirement was decreased by using chemical additives (sodium metasilicate and calcium chloride).

The performance of sandy soils treated with the CKD as barrier material has been evaluated. Mohamed (2002) reported that the optimum mix design was achieved by mixing a silty sand soil with 6% of CKD. The test results showed that the shear strength increased and a hydraulic conductivity of less than  $10^{-9}$  m/s was achieved. As a result, using the treated soil as a soil-based barrier layer for containment of hazardous waste is possible. Moses and Afolayan (2011) investigated the suitability of CKD for the treatment of foundry sand as a compacted hydraulic barrier material. The results indicated that the compressive strength of foundry sand was improved with an increasing CKD content and the compressive strength values met the minimum value of 200 kPa. The hydraulic conductivity was also found to meet the regulatory requirement ( $10^{-9}$  m/s) as well as the maximum dry density generally increased and the optimum moisture content decreased with an increasing of CKD content.

The water retention behaviour was explored for a foundry sand treated with various percentages of CKD (Oriola et al. 2012). Pressure plate extractor tests were carried out and the experimental data was best-fitted by the Brooks-Corey and van Genuchten models. It was concluded that the water retention curves (WRCs) of the specimens with higher CKD content were above those of the specimens with lower CKD content showing an increase of retention capacity with CKD addition. The results of the best-fit showed that the parametric models are applicable for tracing the WRCs of foundry sand treated with CKD (Oriola et al. 2012).

### **2.2.3.2 A review of research works on CKD**

Extensive analytical studies have been carried out by Environmental Protection Agency (EPA) (USEPA 1998) for evaluating the effectiveness and efficiency of CKD for

use as liners or caps in CKD landfills. The evaluation was based on the laboratory and field test results. The findings from the studies have shown that very low hydraulic conductivity of CKD ( $< 10^{-9}$  m/sec) can be attained in the laboratory and field using heavy equipment. Further, the compression tests showed that the CKD compressibility was found to be moderate with compression index ranging between 0.25 and 0.4 in the virgin compression portion of the tests. USEPA (1998) reported that CKD can be used as a part of an alternative unit design as long as the facility can demonstrate that the design satisfies the performance standard for the ground water.

The characteristics of fresh and landfilled CKDs were evaluated and compared to an extensive database gathered from the literature by Sreekrishnavilasam et al. (2006). The results of evaluation indicated that both the fresh and landfilled CKDs can be primarily used in modification and stabilisation processes of soil. Although CKDs have limited reactivity based on the free lime content, but due to the fineness, the material may be considered as an attractive alternative for the use in low strength flowable fill mixtures. Moreover, the high water absorption capacity and low reactivity of the CKD (particularly, the landfilled CKD) potentially make this an ideal daily cover material for sanitary landfills.

Peethamparan et al. (2008) investigated the hydration behaviour of four different CKDs and their potential use as soil stabiliser. The results showed that the hydrated high free-lime content CKDs produced a significant amounts of calcium hydroxide, ettringite and syngenite and exhibited a higher unconfined compressive strength and higher temperature of hydration compared to CKDs with lower amounts of free-lime, whereas these products were nearly absent in the low free lime hydrated CKDs and the primary constituent of hydration process was calcite. Further, it was reported that both the compressive strength and the temperature of hydration of the CKD paste can be considered as indications of the suitability of particular CKD for soil stabilization. Baghdadi et al. (1995) reported that CKD specimens exhibited relatively high strengths but failed because of durability requirements.

Ebrahimi et al. (2012) explored the potential swelling of CKD. The results indicated that the CKD specimens exhibited 16% expansion after 28 days curing because of the presence of free lime and a high content of sulfur trioxide (SO<sub>3</sub>). This value decreased to 8% due to addition of 50% sand (by weight).

## 2.3 Suction and water potential

Water status in soils is characterized by both the amount of water present and its energy state (Or et al. 2005). The energy state of the pore water will be very different depending on whether its pressure is above or below the reference atmospheric pressure. In fully saturated soils that exist below the water table, this pressure will be positive and the water will be in a state of compression. On the other hand, a partly saturated soil, or an element of soil existing above the water table, will present a negative pressure and the water will be in a state of tension.

The primary forces acting on soil water held within a rigid soil matrix under isothermal conditions can be conveniently grouped (Day et al. 1967) as matric forces, osmotic forces, and body forces. The combined effects of these forces result in a deviation in potential energy (called the total soil water potential,  $\psi_T$ , relative to a reference state, The reference state is defined as the potential energy of pure water, with no external forces acting on it, at a reference pressure (atmospheric), reference temperature, and reference elevation. Soil-water potential is then determined as potential energy per unit quantity of water, relative to the reference potential of zero.

Total soil water potential ( $\psi_T$ ) can be expressed as sum of the component potentials corresponding to the different fields acting on soil water as:

$$\psi_T = \psi_m + \psi_o + \psi_p + \psi_g \quad (2.5)$$

where  $\psi_m$ ,  $\psi_o$ ,  $\psi_p$ , and  $\psi_g$  are matric, solute (osmotic), pressure, and gravitational potentials, respectively.

The theoretical concept of soil suction was developed in the early 1900's (Buckingham 1907; Edlefsen and Anderson 1943). The ability of a soil to absorb additional water, whether it is fully saturated or unsaturated, is termed soil suction and can be defined as the free energy state of soil water in soil physics (Edlefsen and Anderson 1943; Jury et al. 1991). The free energy of the soil water can be termed as the partial vapor

pressure of the soil water (Richards, 1965). Soil suction is a general term that may be used when referring to matric suction, osmotic suction or total suction. According to Aitchison (1965) and Fredlund et al. (2012), total, matric and osmotic suctions can be defined as follows:

Matric suction is the equivalent suction derived from the measurement of the partial pressure of water vapour in equilibrium with soil-water relative to the partial pressure of water vapour in equilibrium with a solution identical in composition with the soil water. In unsaturated soils, matric suction is controlled by the capillary effect and adsorption of water (Richards 1974; Murray and Sivakumar 2010). The contribution of each mechanism to matric suction as a whole depends upon soil composition and geometrical configuration of the soil structure. In engineering practice, matric suction is considered to be the pressure difference between the pore air pressure ( $u_a$ ) and the pore-water pressure ( $u_w$ ), i.e.,  $(u_a - u_w)$ .

Osmotic suction is the equivalent suction derived from the measurement of the partial pressure of water vapour in equilibrium with a solution identical in composition with the soil water relative to the partial pressure of water vapour in equilibrium with free pure water. The osmotic suction arises from retention energy due to the presence of salts in the pore water, or more precisely a difference in salt concentrations in the pore water in the system being analysed, and the surrounding water (Murray and Sivakumar 2010). Osmotic suction can attract or remove water from a system. The osmotic suction represents the ionic potential of the pore fluid in a soil (Fredlund et al. 2012). Osmotic suction can be altered by either changing the mass of water or the amount of ions in solution. However, in most practical problems encountered in geotechnical engineering, the strength of an unsaturated soil is principally governed by the matric suction, even though the presence of salts within the soil water can give rise to some fundamental changes in mechanical behaviour (Alonso et al. 1987; Fredlund et al. 2012; Murray and Sivakumar 2010).

Total suction is the equivalent suction derived from the measurement of the partial pressure of water vapour in equilibrium with the soil water relative to the partial pressure of water vapour in equilibrium with free pure water. The thermodynamic relationship between total suction and its partial vapour pressure of the soil pore water is described by Kelvin's equation (Eq. 2.6):

$$\psi = -\frac{RT}{v_{w0}\omega_v} \ln \left[ \frac{u_v}{u_{v0}} \right] = -\frac{RT}{v_{w0}\omega_v} \ln \left( \frac{RH}{100} \right) \quad (2.6)$$

where  $\psi$  is the free energy per unit mass of soil pore-water comparing to that of free pure water (J/kg),  $R$  is the universal gas constant (8.31432 J/(mol K)),  $T$  is the absolute temperature ( $^{\circ}\text{K}$ ),  $v_{w0}$  is the specific volume of water ( $\text{m}^3/\text{kg}$ ), which is the inverse of the density of water,  $\omega_v$  is the molecular mass of water vapour (18.016 kg/k mol),  $u_v$  is the partial pressure of pore- water vapour (kPa), and  $u_{v0}$  is the saturated vapour pressure of free water at the same temperature (kPa). The ratio  $u_v/u_{v0}$  is equal to the relative humidity (RH).

Fredlund et al. (2012) stated that total suction corresponds to the free energy of the soil water and comprised of matric suction and osmotic suction that are the components of free energy (Eq. 2.7).

$$\psi = (u_a - u_w) + \pi = \psi_m + \psi_o \quad (2.7)$$

where  $\psi$  = total suction, kPa,  $\psi_m = (u_a - u_w)$  = matric suction, kPa,  $u_a$  = pore-air pressure, kPa,  $u_w$  = pore-water pressure, kPa, and  $\psi_o = \pi$  = osmotic suction, kPa.

## 2.4 Measurement and control of soil suction

Experimental techniques for measuring soil suction and establishing water retention curves (WRCs) can be categorized based on the principle involved. Measurements of soil suction are considered as a great challenge in geotechnical engineering practice particularly when soil water retention characteristics curve with a wide range of suction is required.

Several devices and techniques are available for measuring matric, osmotic and total suctions in unsaturated soils (Lu and Likos 2004; Fredlund et al. 2012). Table 2.1 summarises some commonly used devices and techniques and measurement ranges. The

soil suction can be measured either in a direct or indirect manner. Direct methods measure matric suction. The pore-air pressure component of matric suction is atmospheric in the field, whereas it can be raised to the desired value in the laboratory. Indirect methods measure a variable other than the negative pore-water pressure (e.g., thermal conductivity, water content) through use of a specially designed ceramic material. A calibration of the measuring device is required to determine the matric suction in the soil when using an indirect method.

The techniques used for measuring matric suction include tensiometers, axis translation techniques, electrical/thermal conductivity sensors, and contact filter paper techniques. The axis translation technique relies on controlling the difference between the pore air pressure and pore water pressure and measuring the corresponding water content of the soil in equilibrium with the applied matric suction. The electrical or thermal conductivity sensors are used to indirectly relate matric suction to the electrical or thermal conductivity of a porous medium embedded in a mass of unsaturated soil. The contact filter paper technique relies on measuring the equilibrium water content of a filter papers in direct contact with unsaturated soil specimens. In each of these cases, water content corresponding to the measured (or controlled) suction is measured to generate data points along the soil-water characteristic curve. The resulting characteristic curve corresponds to either a wetting or drying process.

For measuring the total suction, humidity measurement techniques, humidity control techniques, and the non - contact filter paper method are used. The humidity measurement devices include thermo-couple psychrometers, chilled-mirror hygrometers, and polymer resistance/capacitance sensors. The humidity control techniques include isopiestic, or “same pressure,” techniques (e.g., humidity control using salt solutions) and “two-pressure” techniques, also known as divided-flow humidity control. The noncontact filter paper method is an indirect humidity measurement technique that relies on determining the equilibrium water content of small filter papers sealed in the headspace (i.e., in communication with the vapor phase) of unsaturated specimens. For each of these techniques, Kelvin’s equation (Equation 2.6) is used to convert the measured or controlled humidity to total suction. WRCs are generated by measuring equilibrium water contents corresponding to the applied suctions.

Table 2.1 Summary of some devices for measuring soil suction and its components (Lu and Likos 2004; Fredlund et al. 2012; Tripathy et al. 2016).

Suction measurement method	Suction component	Suction range (kPa)	Comments
Null-type axis translation	Matric	0 - 1500	Direct, limit to the air-entry value of ceramic disk
Tensiometers	Matric	0 – 100	Direct, difficulties with cavitation required daily maintenance
High suction tensiometers	Matric	0 – 1500	Direct, cavitation at high suction air diffusion through ceramic cup
Time domain reflectometry	Matric	0 - 500	Indirect, required soil water characteristic curve, expensive, sophisticated electronic device
Thermal conductivity sensors	Matric	10 - 1500	Indirect, measurement using variable-pore size ceramic sensor, temperature changes influence the accuracy
Electrical conductivity sensors	Matric	10 - 1500	Indirect, affected by salinity and temperature of soil water
Filter paper method	Matric	0 - 1000	Indirect, depends on calibration curve and equilibrium time, low cost
	Total	> 1000	
Relative humidity probes	Total	> 1000	Indirect, constant temperature required, accuracy vary by manufacturer
Chilled-mirror hygrometer	Total	100 - 300000	Indirect, error at low suction levels
Psychrometers	Total	100 - 8000	Indirect, affected by temperature fluctuation sensitivity, deteriorate with time
Pore fluid squeezer	Osmotic	Entire range	Used in conjunction with psychrometer or electrical conductivity measurement
Water potential sensors (MPS-6)	Matric	9 - 100000	Direct, laboratory and field, easy to operate, low temperature effect, insensitivity to salts

Various factors influence the selection of suction measurement devices that measure either matric or total suction (Tripathy et al. 2016), such as the suction equilibrium time, suction measurement range and accuracy, operating temperature, and resolution of the device. In situ and laboratory measurements of matric suction are usually carried out by tensiometers that can measure suction up to about 1500 kPa (Ridley and Burland 1993; Guan and Fredlund 1997; Toll et al. 2013; Lynch et al. 2019). Therefore, devices that facilitate measuring a large range of suction with reasonable accuracy and time are beneficial (Tripathy et al. 2016).

The MPS-6 sensors (fixed-matrix porous ceramic disc sensors), humidity measurement technique (WP4-C chilled-mirror dew-point potentiometer), axis-translation technique (pressure plate, suction-controlled oedometer and suction-controlled triaxial device), vapour equilibrium technique (desiccator) and indirect method for measuring osmotic suction by electrical conductivity measurements are described in the following sections that were used in this study for measuring and controlling the suction of the selected materials during the tests.

## **2.4.1 Suction measuring techniques**

### **2.4.1.1 Fixed-matrix porous ceramic disc water potential sensors (MPS-6)**

The MPS-2 and MPS-6 sensors produced by Decagon devices Inc, Pullman, WA (Meter Group, [www.metergroup.com](http://www.metergroup.com)) measure the dielectric permittivity of a solid matrix porous ceramic discs to determine its water potential. The dielectric permittivity of the porous ceramic discs depends on the amount of water present in the ceramic discs (METER Group 2017). The measured permittivity is then converted into water content that finally is transformed into a potential based on the sensor-specific moisture characteristic curve (Figure 2.2 and 2.3). As a result, the sensors enable measuring a wide range of water content and suction. The sensors are not affected by soil type since the sensors only measure the water potential of the ceramic discs in equilibrium with the soil as long as adequate hydraulic contact is attained. The MPS-6 dielectric water potential sensor is currently known as TEROS 21.

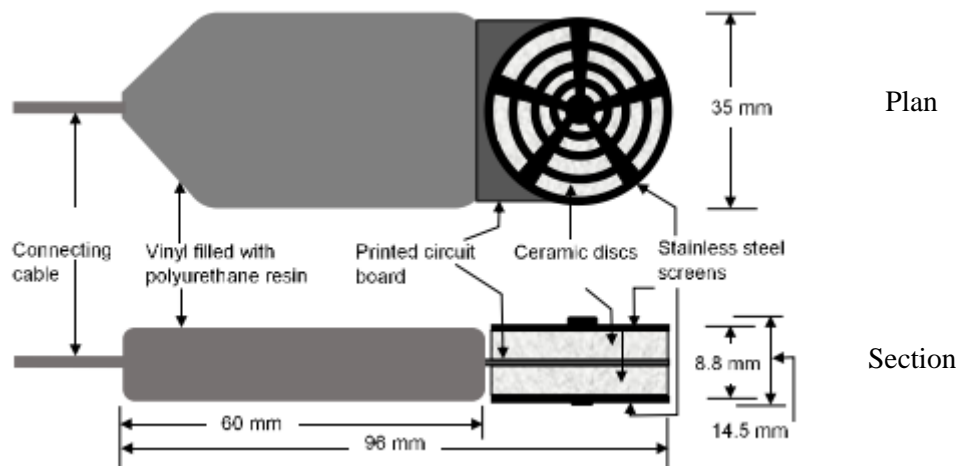


Figure 2.2 Details of the fixed-matrix porous ceramic disc sensor (reproduced from Tripathy et al. 2016).

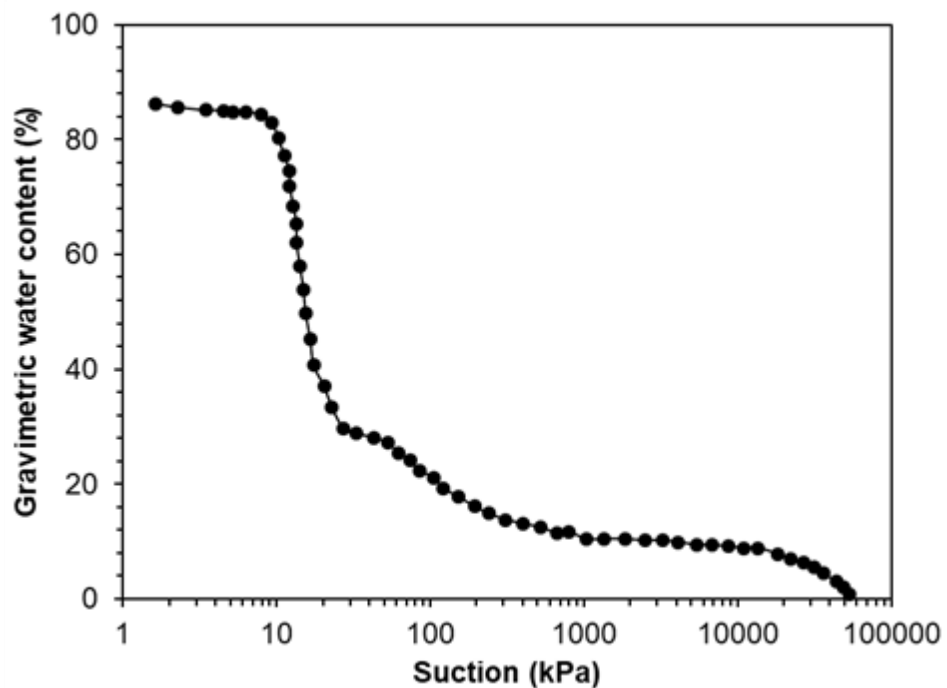


Figure 2.3 Water retention curve of the fixed-matrix porous ceramic disc (MPS-6) sensors (reproduced from Tripathy et al. 2016).

The MPS-6 sensor comprises two fixed-matrix porous ceramic discs (dielectrics) separated by a printed electric circuit board to form a capacitor. When the sensor is brought in contact with soil, the water content of the ceramic disc assembly changes and

consequently, the charge time of the capacitor is influenced. Depending on the predetermined relationship between water content and matric suction of the fixed-matrix ceramic discs (Figure 2.3), the water content of the ceramic discs is translated into matric suction. The suction of the soil and the ceramic discs tend to become equal with elapsed time. A data acquisition system is used to monitor and record the measured suction and the corresponding temperature.

As per the manufacturer's specifications, the suction measurement range of the device is from 9 to 100,000 kPa with a resolution of 0.1 kPa. The air entry potential of the largest pores in the ceramic is about 9 kPa and this value represents the lower suction limit of the sensor. The operating temperature of the sensor is between 0 and 60 °C. The accuracy of the sensor is  $\pm$  (10 % of reading +2 kPa) over a suction range of 9 – 100 kPa. At high suctions, the accuracy of the sensor depends upon the water retention characteristic of the ceramic disc (Figure 2.3).

The first release of the soil water potential sensor (MPS) was calibrated and evaluated by Malazian et al. (2011), who inferred that there was good consistency among the probes after local calibration and a low-temperature impact. Degré et al. (2017), used the MPS-2 sensor for measuring the WRC in the field and showed that the MPS-2 had good reliability in its respective range. MPS-6 soil water potential sensors were employed for suction measurements of various materials (Speswhite kaolin, MX80 bentonite, Cement Kiln Dust, and sand) and the results showed that the MPS-6 sensors were able to provide a wide range of suction measurements (Tripathy et al. 2016; Karagoly et al. 2018). In another study, in-situ suction measurements were effectively performed using the MPS-6 sensor (Tian et al. 2018).

#### **2.4.1.2 Chilled-mirror Dew-Point Potentiometer (WP4-C)**

The chilled-mirror dew-point WP4-C device uses the dew-point technique to measure the water potential of a soil or rock sample. The instrument was developed by Decagon devices Inc, Pullman, WA (Meter Group, [www.metergroup.com](http://www.metergroup.com)). The device consists of a sealed chamber with a fan, a mirror, a photoelectric cell, and an infrared thermometer (Figure 2.4). Measurements of total suction with the WP4-C is based on equilibrating the liquid phase of the water in a soil sample with the vapor phase of the

water in the air space above the sample in a sealed chamber. The thermoelectric (Peltier) cooler cools the mirror until dew forms and then to heat the mirror to eliminate the dew. The device also equipped with a temperature controller to set the temperature of the sample at which relative humidity measurement is to be made. The sample temperature is measured with the infrared thermometer. The optical sensor detects the dew formed on the mirror and the dew point temperature is measured by the thermocouple attached to the chilled mirror. The small fan circulates the air within the sample chamber and speed up vapour equilibrium. The relative humidity above the soil sample within the closed chamber is calculated based on the dew point and soil sample temperature. Kelvin's equation (Eq. 2.6) is then used to determine the total suction of the soil specimen. The calculations are carried out by software within the device and displayed on an LCD panel in MPa unit along with the specimen temperature.

The WP4-C device has a suction measurement range of 0.1 to 300 MPa. The accuracy of the potentiometer is  $\pm 0.05$  MPa for a suction range of 0 to 5 MPa and 1% for a range of suction of 5 to 300 MPa. Suction measurements using the device can be made within a selectable temperature range of 5 to 40 °C.

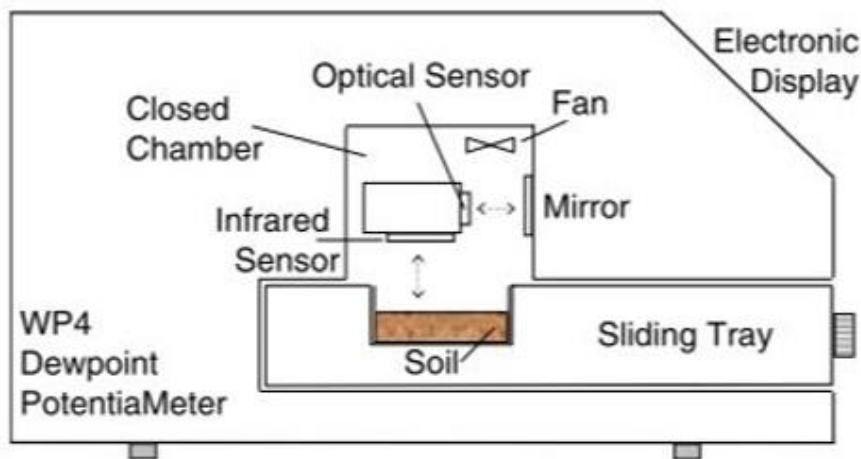


Figure 2.4 a schematic of chilled-mirror dew point device (reproduced from Bulut et al. 2008)

Prior to total suction measurement, the functionality of the device should be verified by measuring the total suction of a salt solution with a known osmotic potential. The WP4-C is the fastest, most accurate, and most reliable instrument available for

measuring water potential using the chilled-mirror dew point technique (Bulut and Leong 2008). However, Scanlon et al. (2002) reported that error can occur in case of disturbed field samples due to the drying of sample during the collection and measurement process. This problem is greatest for coarse-textured soils and dry soils. The device has been employed by several researchers to measure total suction of various materials and polyethylene glycol solutions (Leong et al. 2003; Agus and Schanz 2005; Thakur et al. 2006; Campbell et al. 2007; Tripathy and Rees 2013; Tripathy et al. 2016; Karagoly et al. 2018; Jones et al. 2019). The accuracy of chilled-mirror dew-point potentiometer has been verified using compacted soil samples and the results indicated that the measured total suctions were always greater than the sum of the matric and osmotic suctions measured independently (Leong et al. 2003).

#### 2.4.2 Measurement of osmotic suction

The osmotic suction of soil can be determined indirectly by measuring the electrical conductivity of the extracted pore-water. With an increasing dissolved salts in the pore-water the electrical conductivity is increasing and consequently, the osmotic suction. Pure water has low electrical conductivity in comparison with pore water, which contains dissolved salts (Leong et al. 2003). Typical values of electrical conductivity of some common fluids are listed in Table 2.2 (Leong et al. 2003).

Table 2.2 The electrical conductivity of some natural waters (Adapted from Dismuke et al. 1981).

Type of water	Electrical conductivity
Pure water at 25°C	0.05 $\mu\text{S}/\text{cm}$
Distilled water	2.0 $\mu\text{S}/\text{cm}$
Rainwater	50 $\mu\text{S}/\text{cm}$
Tap water	200-1000 $\mu\text{S}/\text{cm}$
Open seawater	40000-50000 $\mu\text{S}/\text{cm}$
Tropical seawater	62500 $\mu\text{S}/\text{cm}$

Several techniques are available for extracting the pore water from soil samples, namely dilution or saturation extraction, leaching, centrifuging, immiscible liquid displacement, gas extraction method and pressurised squeezing (Iyer 1990; Fredlund et al. 2012). The pore fluid squeezer method has shown to be the most reasonable measurement technique of osmotic suction (Krahn and Fredlund 1972; Wan 1996; Peroni and Tarantino 2005). This technique consists of squeezing a soil specimen to extract the pore fluid, that is used for measuring the electrical conductivity. The studies have shown that the magnitude of applied extraction pressure affects the osmotic suction.

Saturated soil paste or dilution of soil with water can also be used to measure the electrical conductivity (Leong et al. 2003; Nam et al. 2009). Using this method, air dried soil is mixed with a certain amount of de-ionized water, and the soil water is extracted by filtering with a low vacuum.

The osmotic suction can be estimated from the electrical conductivity using either Figure 2.5 or empirical relationships proposed by United States Salinity Laboratory (1954) and Romero (1999) (see Equations 5.1 and 5.2) in Chapter 5.

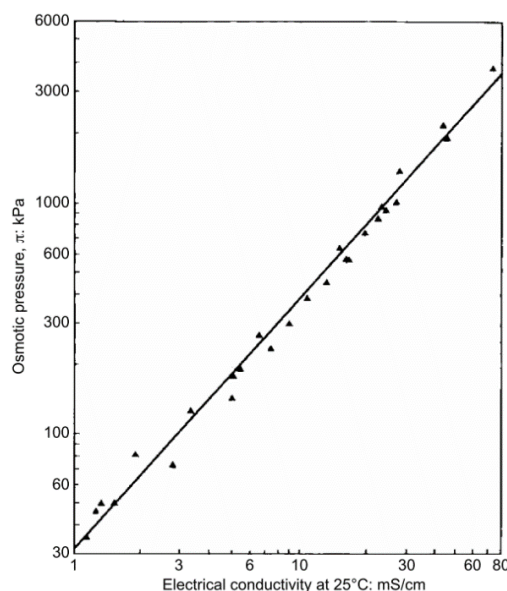


Figure 2.5 Osmotic pressure plotted against electrical conductivity for pore water containing dissolved salts (reproduced from United States Salinity Laboratory (1954), cited in (Leong et al. 2003)).

## 2.4.3 Suction control techniques

### 2.4.3.1 Pressure plate extractor

The pressure plate test is based on the axis translation technique proposed by Hilf (1956) for controlling matric suction in unsaturated soils. The technique has also been successfully used by many researchers to control the matric suction in oedometer cells (Morales 1999; Perez-Garcia et al. 2008; Lins 2009; Maleksaeedi and Nuth 2016), triaxial shear apparatus (Matyas and Radhakrishna 1968; Fredlund and Morgenstern 1977; Ho and Fredlund 1982; Wheeler and Sivakumar 1995) and direct shear apparatus (Gan et al. 1988; Miller and Hamid 2007; Nam et al. 2011). The working principle involves increasing the air pressure while maintaining the pore water pressure at a measurable reference value, typically atmospheric.

Axis translation is achieved by separating the air and water phases of the soil through the minute pores of a high-air-entry (HAE) disc. When saturated, the HAE disc has the unique capability of restricting the transfer of air, whereas it permits the free advection of water. When a specimen of soil is placed in good contact with a saturated HAE disc, positive air pressure may be imposed to the pore air on one side, while allowing the pore water to drain freely through the disc under atmospheric pressure maintained on the other side. The separation of the air and water pressure is maintained as long as the applied pressure does not exceed the air-entry pressure of the HAE material, which can be as high as 1500 kPa for sintered ceramics or 10,000 kPa for special cellulose membranes (Lu and Likos 2004). The basic principle of the ceramic disc is presented schematically in Figure 2.6.

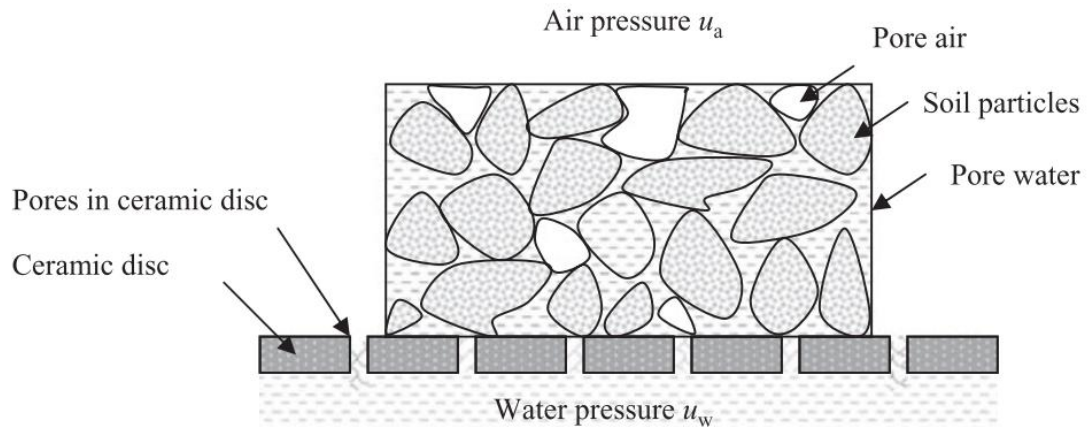


Figure 2.6 Schematic cross section of the interface between the soil specimen and high-entry-value ceramic disc (reproduced from Murray and Sivakumar 2010).

The range of suction within which the axis translation technique can be used to measure or control matric suction is limited by two factors, namely the maximum air pressure which can be imposed on the experiment system and the air entry value of the ceramic disc. One of the challenges of the axis translation technique is that it does not yield instantaneous results when used to impose matric suction. Another drawback is the long equilibrium time which make experiments particularly susceptible to the process of air diffusion (Pan et al. 2010). A good contact between the soil specimen and the saturated ceramic disc is required throughout the experiment to ensure the continuity of the air and water phases. In addition, the validity of the axis translation technique for soil samples at high degree of saturation (when the air phase is occluded) is debatable (Ng et al. 2007).

#### 2.4.3.2 Constant relative humidity desiccators

The vapour equilibrium technique (VET) can be used to measure the water content versus total suction relationship in the high-suction range (Fredlund et al. 2012). The VET for controlling total suction was originally developed by soil scientists and according to Delage et al. (1998) this technique was first applied to control total suction in geotechnical testing by Esteban et al. (1988). Relatively small containers (desiccators) can be used to establish a partial vapour pressure in the soil samples (Edlefsen and Anderson 1943; Richards 1965). The VET has also been employed for imposing total suction during the

unsaturated oedometer tests (Al-Mukhtar et al. 1999) and triaxial tests (Blatz and Graham 2000). In the laboratory, a fixed vapour pressure environment can be created by controlling relative humidity inside the desiccator.

A wide range of constant relative humidity ranging from dry to near saturation at temperatures spanning from 0 to 50°C is obtainable by the VET (ASTM E104-02 2007). Saturated or unsaturated salt solutions (or acid solutions) are employed to obtain a constant relative humidity in a closed space. A salt solution at a particular concentration and a constant temperature results in a fixed vapour pressure environment under equilibrium conditions. Saturated salt solutions provide a convenient, inexpensive, and accurate controlled relative humidity environment. As a result, the use of saturated salt solutions is preferable to the use of unsaturated salt solutions (Fredlund et al. 2012). Kelvin's equation (Eq. 2.6) can be used to convert relative humidity value to the corresponding total suction.

Figure 2.7 illustrates the schematic cross-section of the sealed system (desiccator) with a salt solution placed at the bottom and a perforated disk. The mass of the specimens is recorded periodically to infer the suction equilibration. Once the specimens are equilibrated at each imposed suction, the final measurements of water content and volume of specimens are performed for determining the WRC.

The drawback of this technique is that the suction equilibrium time may vary from several weeks to several months due to the very slow vapour transfer depending upon the soil type and size of sample. The main factors influencing the time required to establish vapour pressure equilibrium are as follows: (1) the ratio of free surface area of the solution to the chamber volume, (2) the amount of air circulation, (3) the absorption/desorption properties of the soil, and (4) the agitation of the salt solution (Fredlund et al. 2012).

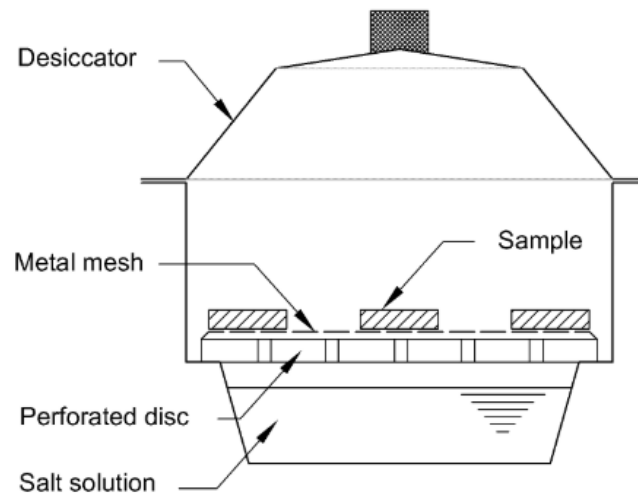


Figure 2.7 Schematic of vacuum desiccator for equilibrating small soil specimens in a constant-relative-humidity environment created by controlled salt solution (reproduced from Alabdullah 2010).

## 2.5 Water retention curve (WRC)

The water retention curve (WRC) or also known as soil – water characteristic curve (SWCC) is a fundamental constitutive relationship in unsaturated soil mechanics (Lu and Likos 2004). It constitutes the primary soil information required for the estimation and analysis of unsaturated soil property functions as many properties of an unsaturated soil such as shear strength, volume change, hydraulic behaviour, seepage, pore size distribution, particle size distribution, air flow, water content and heat flow problems at given matric suction can be related to or obtained from the WRC (Fredlund 1997; Fredlund 1999; Fredlund et al. 2012; Goh 2012). The term WRC is recommended to be used to describe the relationship between the amount of water and the matric suction of a soil (Fredlund et al. 2012). Gravimetric water content, volumetric water content, and degree of saturation are considered as variables to define the amount of water in the soil. The WRC of soils can be established by equilibrating a soil specimen to a series of different applied suctions or by using multiple specimens equilibrated at different applied suctions (Fredlund et al. 2001).

### **2.5.1 Features of WRC**

The WRC can describe either an adsorption (wetting) process or a desorption (drying) process. The drying curve represents the water desorption of soil when the matric suction increases while the wetting curve represents the water absorption of soil when the matric suction decreases. Figure 2.8 illustrates typical drying and wetting curves for a silt along with some of its key features. A significant difference between the results of drying and wetting processes can be noted in which the matric suction of soil samples undergoing a desorption process is higher than that observed for the soil experiencing an adsorption process as result of hysteresis (Klausner 1991; Feng and Fredlund 1999; Tami et al. 2004). In other words, for the same suction value, more water is retained by soil during the drying process than that adsorbed during the wetting process. The hysteresis can be due to several factors, such as geometrical effects associated with nonhomogeneous pore size distribution (referred to as ink-bottle), formation of occluded air bubbles during wetting, changes in the contact angle during drying and wetting, and change in soil structure of fine-grained soil as a result of swelling, shrinkage, ageing phenomena (Hillel 1982; Fredlund and Rahardjo 1993; Lu and Likos 2004) . For a soil, a unique WRC may not be expected due to the hysteretic behaviour associated with the drying and wetting processes (Haines 1930; Fredlund 2002; Hillel 1998). Consequently, it is not possible to determine a single stress state designation for a soil based solely on a water content measurement (Fredlund et al. 2011).

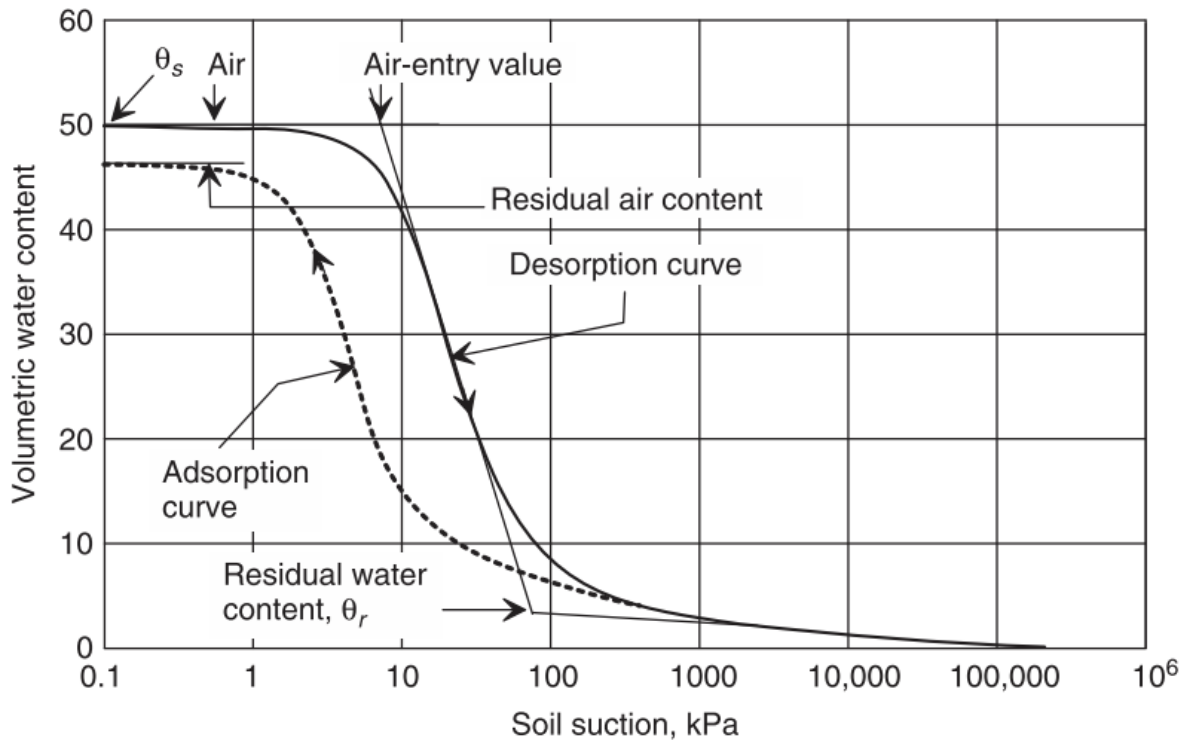


Figure 2.8 Typical WRCs for a silt under desorption and adsorption conditions (reproduced from Fredlund et al. 2012).

Figure 2.9 shows a typical desorption WRC. There are two distinct transition points that are pivotal to describing the WRC. The first point is the air-entry value (AEV) of the soil (i.e., bubbling pressure) that represents the value of suction where the air starts to enter the largest pores in the soil. The second point is the residual conditions (i.e., residual suction,  $\psi_r$ , and residual water content) at which a large suction change is required to remove water from the soil (Fredlund and Xing 1994). The AEV and residual conditions are required for the determination of all unsaturated soil properties (Fredlund 2015). These transition points divide the entire suction range (i.e. unsaturated soil behaviour) into three zones such as boundary effect or capillary (saturation) zone, transition or two phase (desaturation) zone and residual or dry zone.

Numerous approaches have been proposed for the interpretation of AEV from the experimental WRC data (Fredlund and Xing 1994; Vanapalli et al. 1998; Zhai and Rahardjo 2012). The AEV is most commonly determined graphically from the

experimental WRC data plotted in a semi-logarithmic (semi-log) plane. It is typically considered as the suction corresponding to the intersection point of two straight lines: the first line is representative of the saturated zone of WRC, i.e. the data points at which the air phase has not invaded the pores, and the second line is represented by the desaturation zone when connected pathways of air phase are formed across the pores. The second line is usually drawn as a tangent passing through the inflection point of WRC.

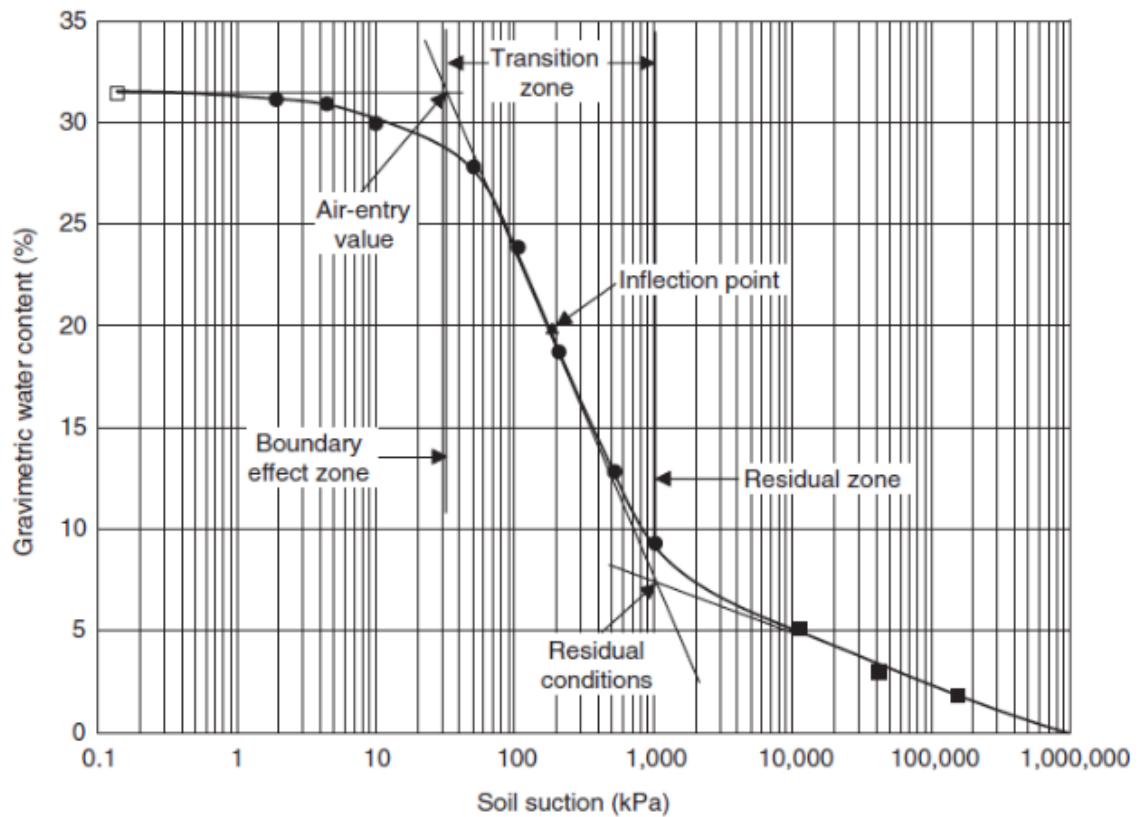


Figure 2.9 A typical WRC (reproduced from Vanapalli et al. 1999).

## 2.5.2 Factors influencing the WRC

The general shape and characteristics of the WRC are affected by many factors such as the type of soil (mineralogy and particle size), type and amount of ions present in the soil, organic material content, compaction parameters (effort, density, water content), structure and fabric of soils, addition of any admixture, applied stress, temperature, stress

history, suction history (Tinjum et al. 1997; Vanapalli et al. 1999; Lu and Likos 2004; Zhou and Yu 2005; Thu et al. 2007; Fredlund et al. 2012; Tripathy et al. 2014).

### 2.5.2.1 Influence of type of soil on WRC

Figure 2.10 presents typical desorption WRCs for sand, silt, and clay. The mineralogy and particle size of soils influence the WRC. A coarse-grained soil such as sand has higher desaturation rate controlled by the distribution of pores in the soil and has lower water content because the specific surface and surface charge properties of sand are relatively small. A lower air-entry value is also noted which is controlled by the relatively larger pore throats formed between and among the sand particles (Lu and Likos 2004). Due to the specific surface area of the silt is much larger than sand, a greater amount of water is adsorbed by the silty soil. The air-entry value is also greater because of the relatively small pores between the silt particles. On the other hand, a soil with high fines content (e.g. clay soil) has the highest ability for the water adsorption because the clay particles have charged surface and very high specific surface area as well as the clay has the highest air-entry value (Miller et al. 2002; Lu and Likos 2004; Yang et al. 2004; Nam et al. 2009).

Studies carried out on various soils under drying and wetting conditions have indicated that there is a similarity between the shapes of the WRCs and grain-size distributions of soils. The WRCs of uniform coarse grained soils have steeper slopes than those of less uniform soils. When the effective grain size ( $D_{10}$ ) of the soil is small, the residual matric suction and water-entry value tend to approach the same value (Yang et al. 2004). The effect of coarse-grained content on the drying WRC of a residual soil was explored by Indrawan et al. (2006). The air-entry value and the residual matric suction were found to decrease with an increase in the gravelly sand and medium sand contents, as well as the slopes of the drying WRCs for the soil mixtures tend to become steeper with an increase in the coarse-grained content. The influence of soil plasticity on the WRC was investigated by Lu et al. (2007) and the results showed that soil with higher plasticity index exhibits a higher ability for the water retention and a lower rate of desaturation.

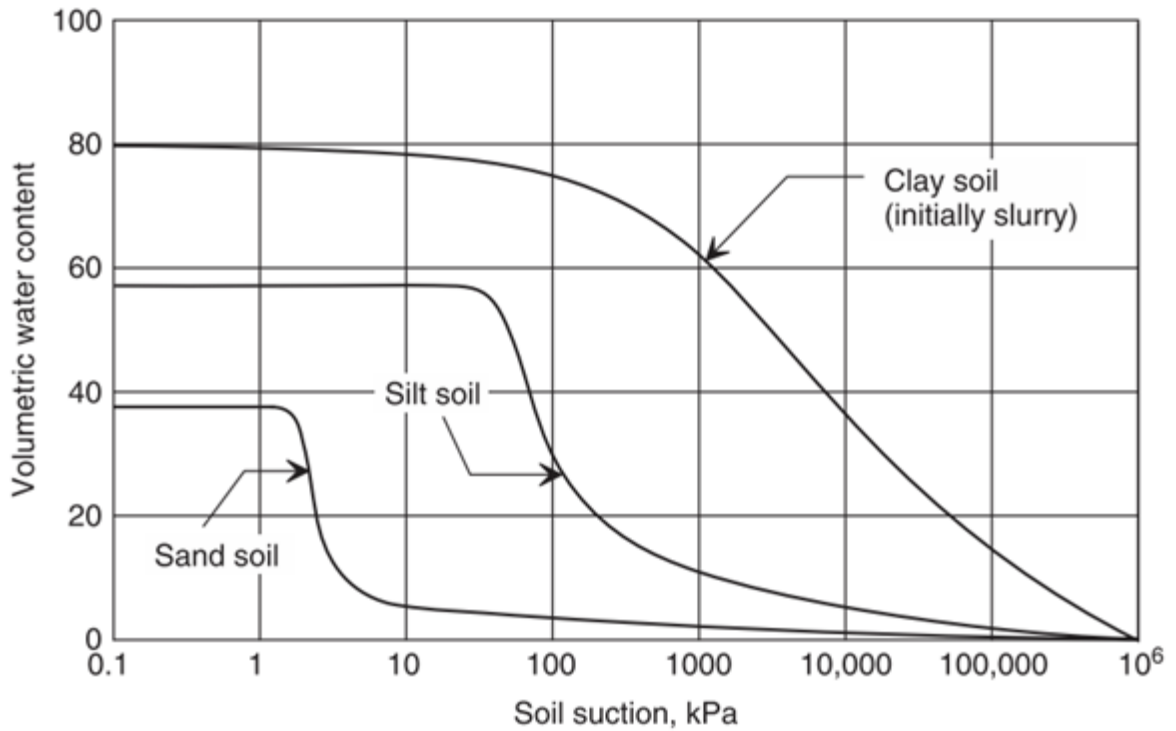


Figure 2.10 Desorption WRCs for sand, silt, and clay soils (reproduced from Fredlund and Xing 1994).

### 2.5.2.2 Influence of compaction state on WRC

Compaction of specimens to the same water content with different dry unit weights or to the same dry unit weight with various water contents using different compaction efforts results in different soils due to the different structures of these specimens (Lambe 1958). Consequently, the WRC and the various features of WRC for the same soil compacted with different compaction efforts can be affected.

Several studies have investigated the WRC of specimens compacted to the same initial water content but at different dry unit weights (e.g. Crony and Coleman 1954; Tinjum et al. 1997; and Ng and Pang 2000). The results showed that the air-entry value increased with the increase in dry unit weight. Further, the higher the initial dry density, the slower is the rate of desaturation. Yang et al. (2004) indicated that soils prepared with low compaction efforts have a lower air-entry value and residual matric suction than soils with a high dry density.

Ng and Pang (2000) explored the effect of initial water content on the WRC of volcanic soil. The specimens were compacted to be the same dry unit weight at different water contents using different compaction effort. As per Benson and Daniel (1990) and Vanapalli et al. (1999), soil specimens compacted at dry side of optimum should have relatively large pores between the clods of soil, whereas specimens compacted at the wet side of optimum should have no visible large interclod pores. The test results by these researchers inferred that the air-entry value of the specimens compacted at dry of optimum water content is lower than that of specimen compacted at wet of optimum water content. Although that the total amount of voids is assumed to be same for all specimens that have same initial dry unit weight, the difference in air-entry value can be due to the pore-size distributions. Tinjum et al. (1997) suggested that the compaction water content influences the shape of WRC of the soil because it affects the micro- and macrofabric of compacted clay and the changes in the shape are consistent with the changes in the pore structure.

### **2.5.2.3 Influence of stress state on WRC**

The stress state (confining or normal stresses) is one of the main variables most commonly experienced in the field and its impact on WRC has been investigated by several researchers (Vanapalli et al. 1996; Ng and Pang 2000; Lee et al. 2005; Thu et al. 2006; Miller et al. 2008; Tavakoli Dastjerdi et al. 2014). The stress state often influences significant parameters in the WRC, which may lead to misinterpretations in the field permeability or shear strength of the soil (Roy and Rajesh 2018).

A significant influence of applied stress can be noted on the WRC of the compacted specimens. The applied stress influences the air-entry value and degree of saturation which increased with an increase in the stress level (Vanapalli et al. 1996; Lee et al. 2005). This increase probably is due to condensed soil structure (decreased pore size) under the effect of increasing stress level (Ng and Pang 2000; Lee et al. 2005).

#### 2.5.2.4 Influence of stress history on WRC

Figure 2.11 presents WRCs corresponding to various stress histories and methods of specimen preparation. A considerable difference is observed between the WRC of an initially slurried soil specimen and a compacted (and undisturbed) specimen. Depending upon the initial water content, stress history, and nature of the clay minerals, the compressibility of clays may vary. An initially saturated slurried clay will be highly compressible, whereas the compressibility is low in case of compacted and low-activity clays. Undisturbed clay soil can have low to high deformability as well as sands are essentially nondeformable even when prepared as a slurry (Fredlund 2002; Fredlund et al. 2012). The compressibility can lead to inaccuracies in the WRCs and underestimation in the volumetric water contents / degrees of saturation if the volumetric changes are not considered (Parent et al. 2007). Consequently, the authors recommended that a suction - degree of saturation WRCs should be used rather than the WRCs in terms of gravimetric and volumetric water content for determining the air-entry value of material that exhibits a high volume change potential.

It has been reported that in deformable materials, the shape of WRC of a soil may vary depending on the volume change-suction relationship and stress history of the soil (Vanapalli et al. 1999; Ng and Pang 2000; Parent et al. 2007). Further, it has been demonstrated that methodologies which do not consider the stress history of soil may yield grossly wrong estimates of AEV (Pasha et al. 2015).

Vanapalli et al. (1999) stated that when a soil is compacted at dry side of optimum water content, the WRC is affected by the stress history, whereas the stress history has less influence on WRC when the soil compacted at the wet side of the optimum. This behaviour can be attributed to that the soils compacted dry of optimum have large pore spaces and the soil-water characteristics are governed by the aggregated macrostructure that is influenced by the prestresses. For the same soil compacted wet of optimum, the interconnected pore spaces are generally lost and the microstructure is dominant and the features of WRC are independent of the applied stress history.

At optimum water content condition, the features of WRC remains intermediately between the soils compacted at wet and dry of optimum conditions. The study has shown that the stress history or structure has no effect on the WRC at high suction ranges.

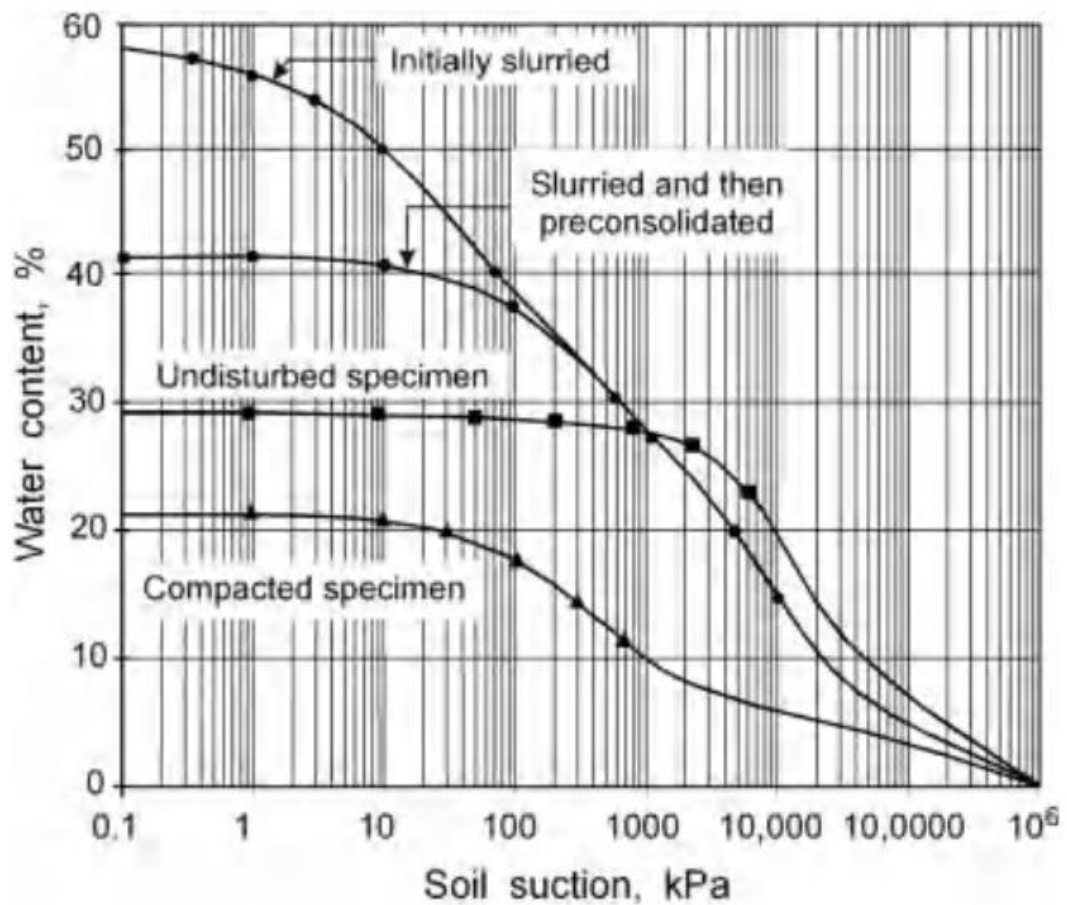


Figure 2.11 Effect of stress history and method of specimen preparation on measured SWCC (reproduced from Fredlund et al. 2012).

## 2.6 Modelling of WRC

WRCs contain the fundamental information required for describing the mechanical behaviour of unsaturated soil. Some parameters such as air-entry value, slope at the inflection point, residual water content and residual suction are commonly used to describe the WRC and other associated properties, such as shear strength and permeability. Direct or indirect measurements of the WRC and use of the graphical procedure for determining the WRC parameters can be time consuming and cumbersome (Zhai and Rahardjo 2012; Ye et al. 2019). Various empirical models/equations have been proposed by different researchers (e.g. Gardner 1958; Brooks and Corey 1964; Campbell 1974; van Genuchten 1980; Fredlund and Xing 1994; Pereira and Fredlund 2000;

Gallipoli et al. 2003; Zhou et al. 2012; Cuomo et al. 2018). The proposed empirical equations for the WRC expressed in terms of the water content can be rearranged in terms of volumetric water content or degree of saturation. It can be also best fit to either the drying or wetting curves (Fredlund et al. 2012).

The equations can be divided into categories of two parameter equations and three parameter equations (Fredlund 2006). The empirical equation has one variable that is related to the air-entry value of the soil and a second variable that is mainly related to the rate of desaturation of the soil as suction exceeds the air-entry value. In some cases, a third variable is used to give greater flexibility in best fitting the WRC data (Fredlund 2006; Fredlund et al. 2011). A least square regression technique can be used to best fit the empirical equations to the laboratory data (Fredlund and Xing 1994).

From the reviewed information, van Genuchten (1980) and Fredlund and Xing (1994) equations (Equations 5.5, 5.6, 5.7 and 5.8 in Chapter 5) have been frequently adopted to describe WRC of soils. Studies have been carried out by Leong and Rahardjo (1997), Zapata (2000), and Sillers et al. (2001) and the findings suggest that Fredlund and Xing (1994) equations (Equations 5.7 and 5.8) performed best among the available equations for best fitting the WRC data. Zapata (2000) also suggested that van Genuchten (1980) equations (Equations 5.5 and 5.6) performed well in best-fitting WRCs of fine-grained soils.

The van Genuchten (1980) equation (Equations 5.5 in Chapter 5) is a continuous best-fit WRC equation and it can be referred to as a two-parameter equation. These parameters have a particular physical meaning and the effect of one soil parameter can be distinguished from the effect of the others. The equation also provides a wide range of flexibility in fitting WRC data from a variety of soil types. In contrast, the use of this equation is restricted to the range between the air-entry value and the residual suction of soil because of the asymptotic nature of the equation (Fredlund et al. 2011).

Fredlund and Xing (1994) proposed a continuous SWCC best-fit equation (Equation 5.7 in Chapter 5) by adopting the concept of pore-size distribution and integrating the pore-size distribution function. This equation has a similar form as van Genuchten (1980) equation. Fredlund and Xing (1994) introduced a correction factor to direct the SWCC equation to a soil suction of  $10^6$  kPa at zero water content. Fredlund and

Xing (1994) equation requires fewer iterations for convergence of the curve fitting parameters than the van Genuchten model (Sillers et al. 2001).

## 2.7 Stress state variables

Stress state variables can be defined as nonmaterial variables required for the characterization of the stress condition (Fredlund and Rahardjo, 1993). The volume change and shear strength behaviour of soils can be described in terms of the state of stress in the soil. The state of stress in soil consists of certain combinations of stress variables that can be referred to as stress state variables. These variables should be independent of the physical properties of the soil. The number of stress state variables required for the description of the stress state of soil is governed by the number of phases involved.

For saturated soil, the mechanical behaviour of two phases (solid and fluid) of soil mass can be described by one stress state variable, namely the effective stress,  $\sigma'$ , defined as:  $\sigma' = \sigma - u_w$ , where  $\sigma$  is the total stress, and  $u_w$  is the pore-water pressure (Terzaghi 1936). The effective stress variable is independent of soil properties and applicable to sands, silts and clays (Fredlund and Rahardjo 1993a).

Unsaturated soil is normally considered as a three-phase system, i.e., solid, air, and water. Fredlund and Morgenstern (1977) proposed three possible combinations of stress state variables namely,  $(\sigma - u_a)$  and  $(u_a - u_w)$ ,  $(\sigma - u_w)$  and  $(u_a - u_w)$ ,  $(\sigma - u_a)$  and  $(\sigma - u_w)$  which can be utilised to describe the stress state of an unsaturated soil. The proposed stress state variables have been experimentally tested and these variables can then be employed to describe the shear strength and volume change behaviour of unsaturated soils (Fredlund and Rahardjo 1993b). Among the three combinations, the  $(\sigma - u_a)$  and  $(u_a - u_w)$  is commonly used in engineering applications. This combination is advantageous because the influences of total stress changes and pore-water pressure changes can be separated (Fredlund 1979; Fredlund and Rahardjo 1987). In 1977, Fredlund and Morgenstern introduced the contractile skin (i.e., the air- water interface) as a fourth phase. The stress states were used in the stress analysis of unsaturated soil on the basis of continuum mechanics.

## 2.8 Volume change behaviour of unsaturated soils

The volume change of unsaturated soils is governed by two stress state variables which are net normal stress ( $\sigma - u_a$ ) and matric suction ( $u_a - u_w$ ). The volume change phenomenon due to a change in matric suction or water content can be either shrinkage, swelling or collapse, and depends upon the level of net normal stress and the initial void ratio of the soil (Wijaya and Leong 2016).

Several types of volume change tests are available to investigate the volume change of the unsaturated soils and can be categorised into two primary types; the constant net vertical stress-suction controlled test and the constant suction-net vertical stress controlled test for one-dimensional and isotropic compression (Al-obaidi 2014).

Compacted soils wetted under load can exhibit both swelling and collapse behaviour depending on their condition (e.g. initial water content, dry density, and compaction method) and the level of the vertical overburden stress (Lawton et al. 1989). Different stress paths and values of the stress state variables can be applied to the soil sample depending on its initial conditions (saturated or unsaturated) and initial suction. Increasing the suction value starting from the initial low values (from unsaturated or saturated conditions) to high values leads to the drying path. In contrast, upon wetting (decrease in suction) swelling and collapse behaviour can be studied (Lawton et al. 1992; Al-Badran 2001).

The one-dimensional volume change behaviour can be investigated using the suction-controlled oedometer cells. The tests can be performed under a drained condition where the pore-air and pore-water pressures are allowed to drain during the test or under the undrained condition in which the total stress is applied to the specimen resulting in excess of pore-water and pore-air pressure (Rahardjo and Fredlund 2003). Several researchers have developed oedometer cells for investigating the volume change in unsaturated soils (Kassiff and Shalom 1971; Morales 1999; Rampino et al. 1999; Rahardjo and Fredlund 2003).

The isotropic compression tests for the investigation of the total volume change of unsaturated soil can be conducted using the suction-controlled triaxial cells. Several measurement techniques are available for monitoring the volume change of unsaturated

soils during the triaxial tests. These techniques can be categorised into three main methods (Geiser et al. 2000; Laloui et al. 2006; Sharma et al. 2006): (1) Measurement of the effect of sample volume change on the surrounding cell fluid, (2) measurement of the air and water volumes separately, and (3) direct measurement of volume of the soil specimen.

The overall volume change is commonly investigated by monitoring the changes in the volume of cell liquid using a special triaxial cell that was developed by Bishop and Donald (1961). The cell comprises two cylindrical containers made out of acrylic. The inner container is partially filled with mercury, to a level above the top of the sample. The outer cell and the upper part of the inner cell are filled with water, and the inner cell is connected to the outer cell at the top for maintaining equal pressures in both the inner and outer cells. The volume change measurement of a sample is achieved by monitoring the movement of a steel ball over the mercury surface using a cathetometer. Wheeler (1986) developed a new double-walled triaxial cell that was similar in principle to the cell developed by Bishop and Donald (1961), but with significant improvements. The two cells were filled with water in place of mercury for safety reasons, and the accuracy of results was improved by facilitating the automatic logging of sample volume changes. Further modifications have been reported by many researchers, for example, Sivakumar (1993) increased the stiffness of the cell by reinforcing the cells with fibreglass bands.

Based on the ideas of Okochi and Tatsuoka (1984), a new technique for measuring the volume change of unsaturated soils was developed by Rampino et al. (1999). The technique includes using a high-accuracy differential pressure transducer (DPT) for recording the measurements of water level inside the open-ended bottle-shaped inner cell and the reference water level. The DPT is connected to both the inner cell and a reference tube to monitor and record the changes in differential pressures between the water-pressure change inside the inner cell due to a volume change in the specimen and the constant water pressure in the reference tube (Figure 2.12).

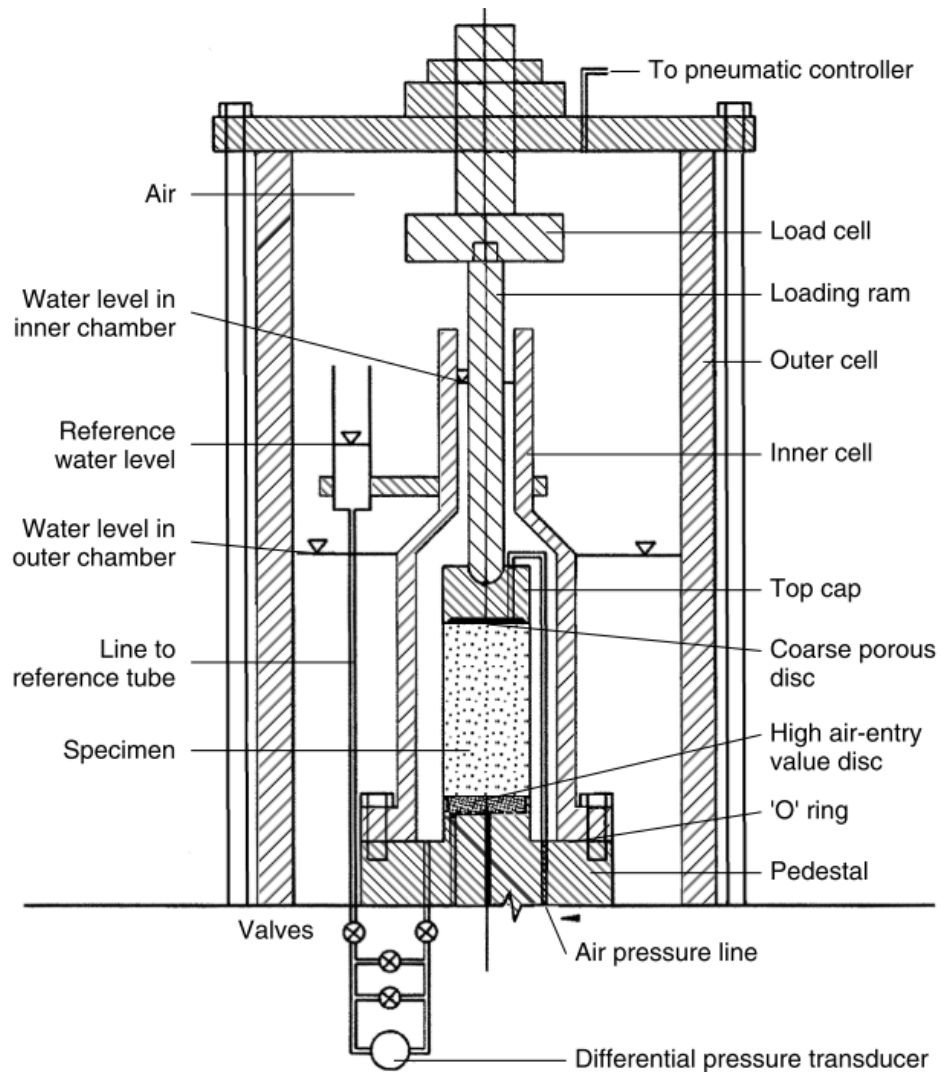


Figure 2.12 A new total volume measuring system for triaxial testing of unsaturated soils (reproduced from Ng et al., 2002).

## 2.9 Shear strength of soil

The shear strength of soils is an important aspect in many geotechnical applications such as the bearing capacity of shallow and deep foundations, the stability of the slopes of dams and embankments, soil excavation, lateral earth pressures on retaining walls, and waste containment (Fredlund et al. 2012; Das 2019). The shear strength of soil can be defined as the maximum internal resistance per unit area the soil is capable of sustaining along the failure plane under external or internal stress loading (Lu and Likos 2004). Soils gain this capacity from the internal forces where shear strength is related to internal friction for coarse-grained soils and cohesion for fine-grained soils, respectively. The shear strength of the fine-grained soils can be also affected by various factors such as effective stress, plasticity, cementation, moisture content, anisotropy and loading rate (Onur et al. 2014).

### 2.9.1 Saturated shear strength

For saturated soil, shear strength is commonly described by the Mohr-Coulomb failure criterion (Figure 2.13), which defines shear strength in terms of the material variables  $\phi'$  and  $c'$  and the effective stress state variables (Terzaghi 1936).

$$\tau_{ff} = c' + (\sigma_f - u_w)_f \tan \phi' \quad (2.8)$$

where  $\tau_{ff}$  is the shear stress on the failure plane at failure,  $c'$  is the effective cohesion, which is the shear strength intercept when effective normal stress is equal to zero,  $(\sigma_f - u_w)_f$  is the effective normal stress on the failure plane at failure,  $\sigma_{ff}$  is the total normal stress on the failure plane at failure,  $u_{wf}$  is the pore-water pressure at failure, and  $\phi'$  is the effective internal friction angle.

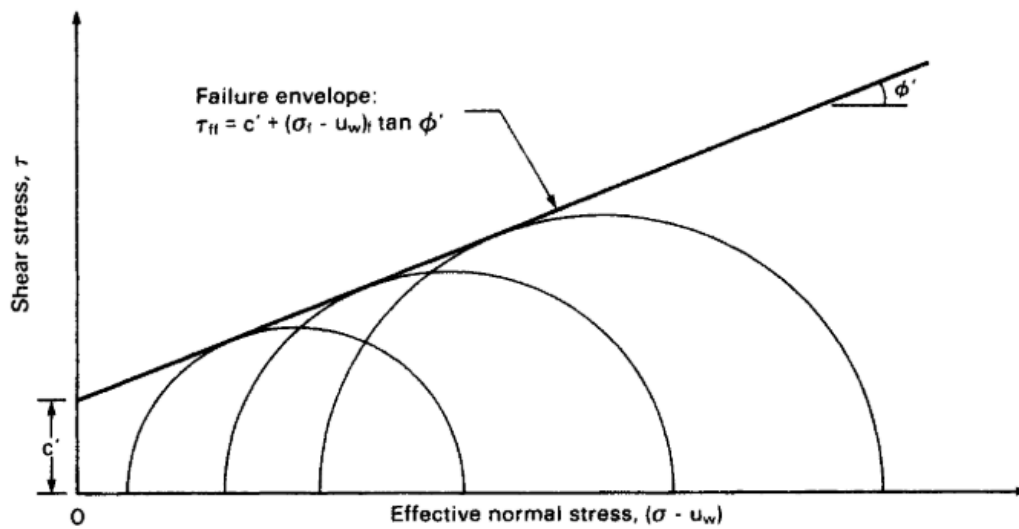


Figure 2.13 Mohr-Coulomb failure envelope for saturated soil (reproduced from Fredlund and Rahardjo 1993).

The saturated shear strength can be determined in the laboratory using various tests such as triaxial shear tests (unconsolidated undrained (UU), consolidated undrained with pore water pressure measurement (CU), and consolidated drained (CD)), direct shear tests, unconfined compression test, and vane shear test. Standard penetration test, cone penetration test, and pressuremeter test are applicable for measuring the in-situ shear strength.

## 2.9.2 Unsaturated shear strength

The soils used for the construction of engineered structures are often unsaturated (Cui et al. 2008; Fredlund et al. 2012). In the case of unsaturated soil, two independent stress state variables, i.e. net normal stress ( $\sigma - u_a$ ) and matric suction ( $\sigma - u_a$ ) are required to define the stress state and consequently the shear strength of an unsaturated soil (Fredlund et al. 1977). Theories of shear strength for unsaturated soils have been proposed as extensions to the concepts and mathematical equations that have been used for shear strength theories for saturated soils. Fredlund et al. (1978) proposed an equation to describe the shear strength of unsaturated soils in terms of two stress variables. Considering the  $(\sigma - u_a)$  and  $(u_a - u_w)$  as the stress state variables, the linear form of the shear strength equation can be written as follows:

$$\tau_{ff} = c' + (\sigma_f - u_a)_f \tan \phi' + (u_a - u_w)_f \tan \phi^b \quad (2.9)$$

where  $c'$  = intercept of the extended Mohr-Coulomb failure envelope on the shear stress axis where the net normal stress and the matric suction at failure are equal to zero, also referred to as effective cohesion,  $(\sigma_f - u_a)_f$  is the net normal stress state on the failure plane at failure,  $u_{af}$  is the pore-air pressure on the failure plane at failure,  $\phi'$  is the internal friction angle associated with the net normal stress state variable,  $(\sigma_f - u_a)_f$ ,  $(u_a - u_w)_f$  is the matric suction on the failure plane at failure, and  $\phi^b$  is the angle indicating the rate of increase in shear strength with respect to a change in matric suction,  $(u_a - u_w)_f$ .

Mohr circles in three-dimensional, that is, shear stress ( $\tau$ ),  $(\sigma - u_a)$ , and  $(u_a - u_w)$ , can be plotted to describe the failure envelope for unsaturated soil as shown in Figure 2.14. The mechanical behaviour of unsaturated soil is influenced differently by changes in net normal stress than by changes in matric suction (Jennings and Burland 1962). The envelope has slope angles of  $\phi'$  and  $\phi^b$  with respect to  $(\sigma - u_a)$  and  $(u_a - u_w)$  axes, respectively. The increase in shear strength due to an increase in net normal stress is characterized by the friction angle  $\phi'$ . The increase in shear strength caused by an increase in matric suction is characterized by the angle  $\phi^b$ . Intersecting the failure envelope with the shear stress give a cohesion intercept  $c'$ . The shear strength parameters ( $c'$ ,  $\phi'$ , and  $\phi^b$ ) are affected by several factors, such as the dry density or void ratio, degree of saturation, mineral composition, stress history, and strain rate (Fredlund et al. 2012).

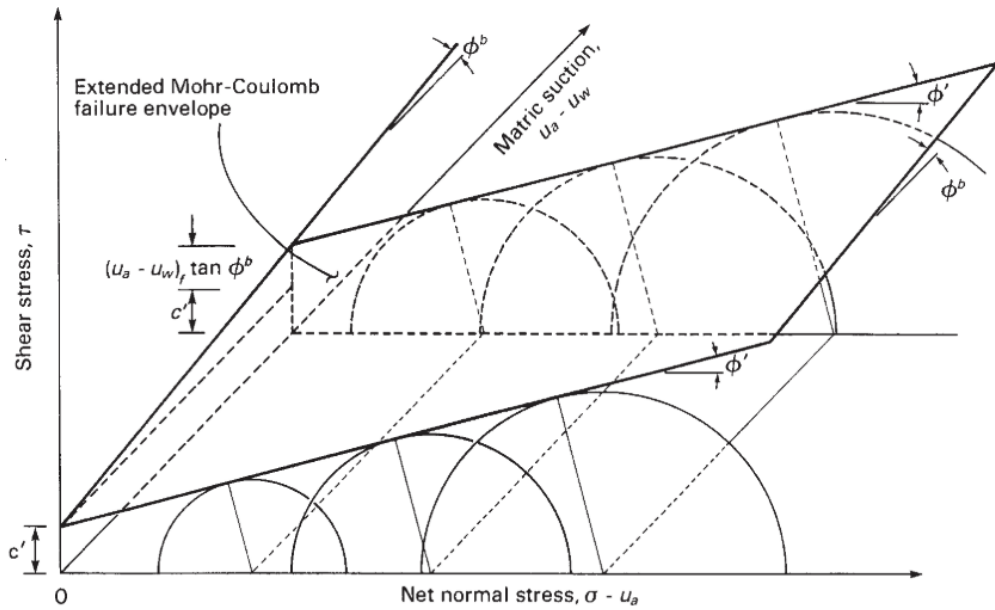


Figure 2.14 Extended Mohr-Coulomb failure envelope for unsaturated soils (reproduced from Fredlund et al. 2012).

The equation for the line of intercept of the failure envelope of shear strength versus matric suction in the extended Mohr-Coulomb failure envelope is as follows:

$$c = c' + (u_a - u_w)_f \tan \phi^b \quad (2.10)$$

where  $c$  = intercept of the extended Mohr-Coulomb failure envelope with the shear stress axis at a specific matric suction  $(u_a - u_w)_f$  (Figure 2.15). At zero net normal stress, the intercept can be referred to as the “total cohesion intercept.”

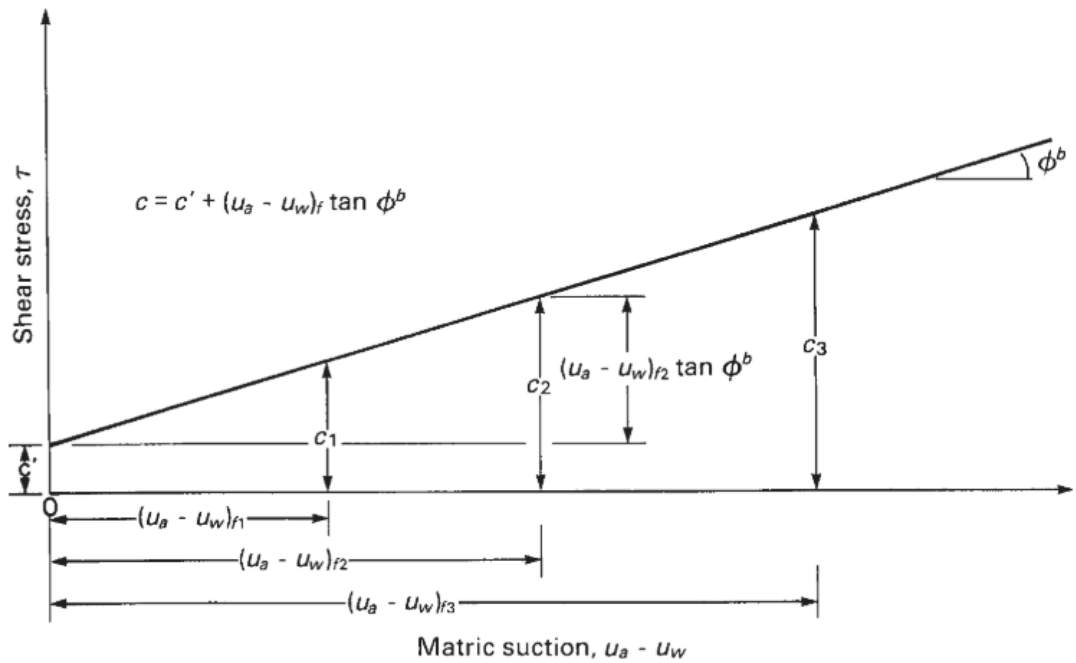


Figure 2.15 Line of intercepts along failure plane on  $\tau$  versus  $u_a - u_w$  plane (reproduced from Fredlund et al. 2012).

The linear form of the shear strength equation for the failure envelope onto the shear stress versus  $(\sigma - u_a)$  plane (Figure 2.16) can be written as follows:

$$\tau_{ff} = c + (\sigma_f - u_a)_f \tan \phi' \quad (2.11)$$

where  $c$  is the total cohesion intercept.

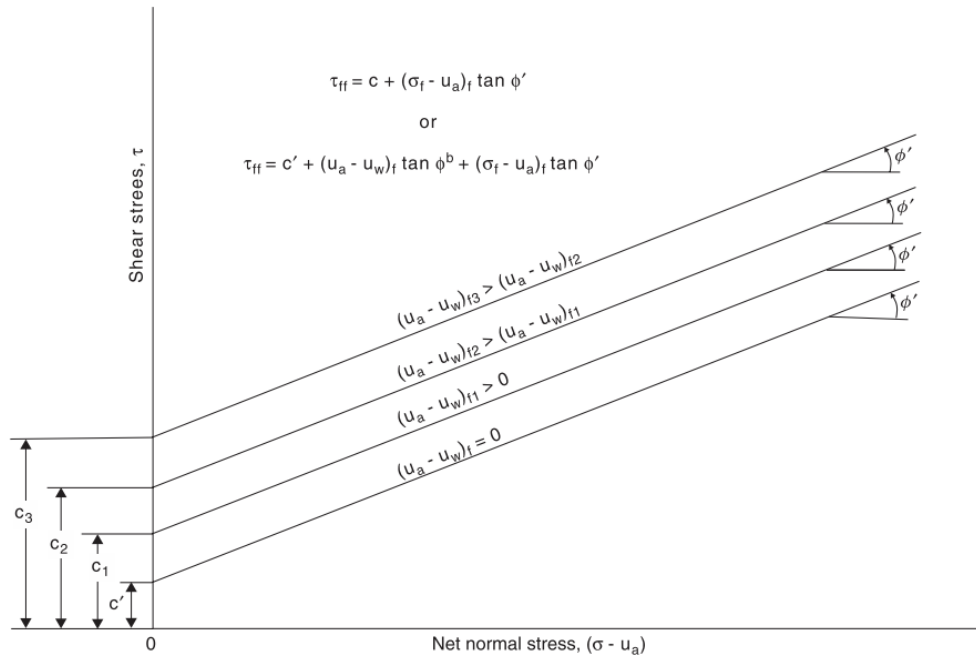


Figure 2.16 Horizontal projection of failure envelope onto  $\tau$  versus  $\sigma - u_a$  plane viewed parallel to matric suction  $(u_a - u_w)$  axis as contour lines of failure envelope on  $\sigma - u_a$  plane (reproduced from Fredlund et al. 2012).

### 2.9.2.1 The nonlinearity of Failure Envelope

Early data sets indicated that the shear strength envelopes are linear over a limited change in suction typical of what might be experienced in situ. However, recent experimental evidence using a higher range of matric suction has shown some nonlinearity in the failure envelope with respect to the matric suction axis (Escario and Saez 1986; Gan 1986; Fredlund et al. 1987; Vanapalli et al. 1996).

At low matric suctions, the value of  $\phi^b$  for a given soil can be equal or close to the internal friction angle  $\phi'$ . This condition is maintained as long as the soil is saturated (Lu and Likos 2004; Fredlund et al. 2012). A further increase in matric suction is not as effective in increasing shear strength as is an increase in net normal stress. As a result, it is necessary for the  $\phi^b$  angle to reduce to a value lower than  $\phi'$  when matric suction is increased beyond the air-entry value of the soil (Fredlund et al. 2012). In other words, the

air-entry value provides an indication of the point where the shear strength versus matric suction starts to exhibit nonlinear shear strength behaviour.

### **2.9.2.2 Determination of unsaturated shear strength**

The shear strength of unsaturated soils can be determined in the laboratory using different devices such as: a modified conventional direct shear device as described by Gallage and Uchimura (2016), a suction controlled triaxial apparatus (Handoko et al. 2013), unconsolidated undrained triaxial test (Nuntasarn and Wannakul 2012), and an unconfined compression test (Vanapalli et al. 2000). In addition, various techniques can be used for creating a suction-controlled environment during testing the unsaturated soil samples. For example, the axis translation technique (Hilf 1956; Matyas and Radhakrishna 1968; D. G. Fredlund et al. 1978; Gan et al. 1988; Toll 1988; Aversa and Nicotera 2002), osmotic and vapour equilibrium techniques (Cui and Delage 1996; Blatz and Graham 2000; Delage and Cui 2008) have been successfully used in the past. Further, the shear strength of unsaturated soil can be indirectly determined depending on the WRC and the saturated shear strength (Vanapalli et al. 1996; Vanapalli and Fredlund 2000).

## 2.10 Concluding remarks

In this chapter, the beneficial use of the CKD and/or soil-CKD mixtures in various geotechnical and geoenvironmental applications were covered. The physical and chemical characteristics of CKD and their influence on the material behaviour was reviewed. The concept of suction and water potential, suction measurement and control techniques related to the research and the methods used for determining the WRCs were reviewed. The salient features of WRC and the factors influencing WRC were presented along with some empirical equations commonly used to best-fit the experimental data. The stress state variables, volume change, and shear strength under unsaturated conditions were also reviewed.

A review of literature brought out some specific aspects related to the CKD and/or soil-CKD mixtures and their use and the conditions where the materials have been used. The important aspects of CKD that are relevant to the investigation are:

- 1- The CKD can be effectively used alone or as an admixture for stabilising problematic soils. The improvement in the engineering properties of problematic soils depends upon the physical and chemical properties of the CKD used and the properties of the treated soil. CKD and soil-CKD mixtures have been used for improving shear strength, permeability, and volume change of soils.
- 2- The behaviour of saturated CKD and soil-CKD mixtures have been studied by several researchers in the past; however, studies related to the hydro-mechanical behaviour of saturated and unsaturated CKD in terms of the following aspects have not been explored in detail:
  - (a) Volume change: the impacts of applied stress and suction
  - (b) Compressibility: the impact of initial placement conditions
  - (c) Hydraulic conductivity: the impacts of applied stress in  $K_0$  and isotropic conditions
  - (d) Water retention: both during drying and wetting processes including the applicability of various currently available methods/devices for establishing WRC, and the suitability of currently available WRC models

- (e) Shear strength: the impact of drainage conditions in case of saturated CKD and the effect of suction in case of unsaturated CKD
- (f) Hydro-mechanical behaviour of sand-CKD mixture

## **CHAPTER 3**

### **Materials and methods**

#### **3.1 Introduction**

This chapter presents the materials used and the relevant properties, the experimental techniques and the test procedures adopted in this study for achieving the main objectives of the research (water retention characteristics, unsaturated shear strength and volume change behaviour).

#### **3.2 Materials used**

The materials used in this study were a cement kiln dust (CKD) and a quartz sand. CKD is an industrial by-product generated from the cement manufacturing process. The CKD was supplied by a local cement company in Wales, UK. The sand used was procured from an aggregate industry based in the UK. The sand can be classified as poorly graded fine to medium sand. A detailed investigation was undertaken on the CKD. Additionally, a mixture of sand (85%) and CKD (15%) was used since several investigations in the past have highlighted the potential use of such mixtures for various civil engineering applications.

## 3.3 Properties of the materials used

### 3.3.1 Specific gravity

The specific gravity of the materials was determined by pycnometer method (BS 1377-2 1990). For the CKD, both kerosene and deionised water were separately used for determining the specific gravity, whereas deionised water was used for determining the specific gravity of the sand and sand-CKD mixture.

The specific gravity of the CKD was found to be similar with the use of both fluid types (2.72). Various values of specific gravity of CKDs have been reported in the past, such as 2.95 by Parsons et al. (2004), 1.90 reported by Moses and Afolayan (2011), 2.6 – 2.8 by Baghdadi (1990). For the sand and sand-CKD mixture, the specific gravity values were found to be 2.65 and 2.66 respectively.

### 3.3.2 Atterberg Limits

Atterberg limit tests are important for determining the entire range of soil state (from liquid to solid state). The liquid and plastic limits tests were carried out according to (BS 1377-2 1990). The liquid limits of the materials were determined using the cone penetrometer method. For the CKD, a sample of air-dried cement kiln dust was mixed with deionised water to form a paste. The resulting paste mixture was then divided into six equal parts. One of those parts was used for determining the liquid and plastic limits immediately after mixing. The remaining five parts were placed in sealed plastic bags and preserved in a sealed (air-tight) plastic container. The mixtures were stored in a controlled temperature room. The stored mixtures were used for subsequent determination of liquid and plastic limits after 1, 3, 7, 14 and 28 days of curing.

Figure 3.1 shows the curing time versus liquid limit, plastic limit and plasticity index of the CKD used. The liquid and plastic limits of the CKD were found to be 41% and 27% respectively. Minor variations of liquid and plastic limits were noted (about 2%) which indicates the impact of curing time on Atterberg limits was less. The liquid limit of sand-CKD mixture was found to be 19%. The sand and sand-CKD mixture behaved as non-plastic materials.

The shrinkage limit of the CKD was determined following the molten wax method (ASTM D4943 2008). For the shrinkage limit test, three identical specimens were prepared at 1.2 times the liquid limit of the CKD (41%) and placed within greased shrinkage dishes. The mass of the specimens was monitored until no further reductions in the mass was observed. The specimens were then removed for water content determination, and further volume measurements were performed using the molten wax method. The shrinkage limit of the CKD was found to be 21%.

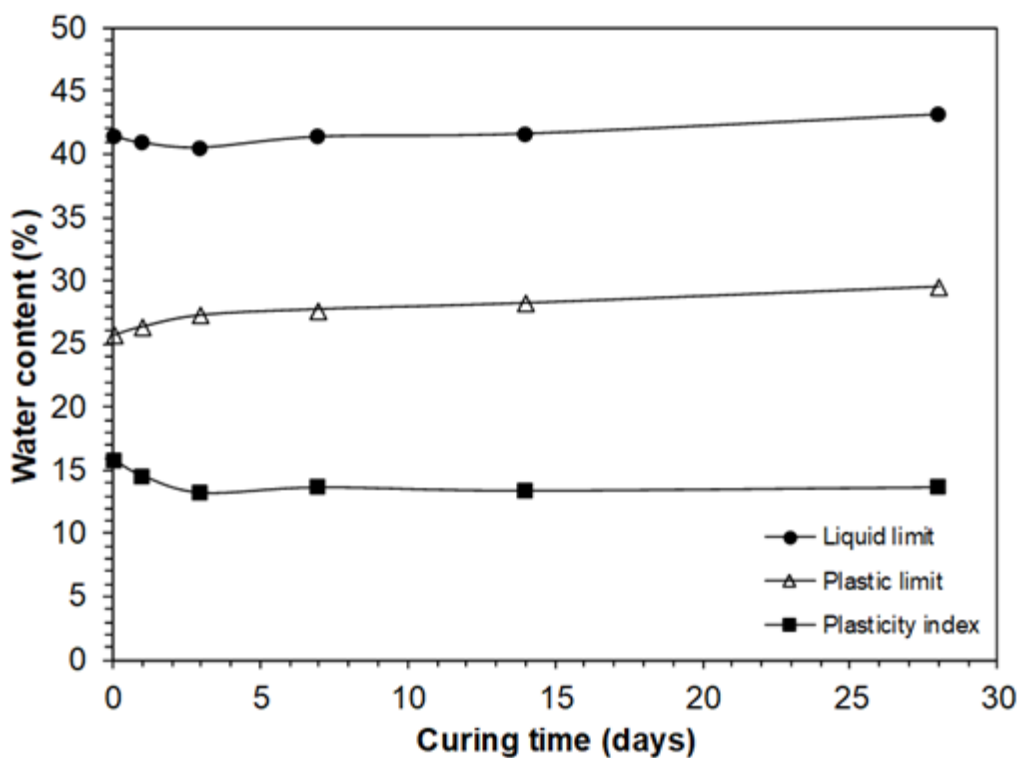


Figure 3.1 Atterberg limits – curing time relationship of cement kiln dust

### 3.3.3 Particle size distribution

Particle size distribution tests were performed on CKD, sand and sand – CKD mixture in accordance with (BS 1377-2 1990). Both dry and wet sieve methods were used. Additionally, the particle size of fine fractions of the materials was determined using sedimentation technique (hydrometer method). Figure 3.2 shows the grading curves of the materials. The grain size distribution curves of the materials indicated that the CKD used comprised 71% silt-size particles and 29% particle size finer than 2  $\mu\text{m}$ . The sand

contained about 41.3% of fine-sand, 56.8% of medium-sand, 1.4% of coarse-sand and 0.5% of silt-size fraction. The values of coefficient of uniformity ( $C_u$ ) and coefficient of curvature ( $C_c$ ) of the sand were 2.2 and 1.2, respectively. The sand-CKD mixture contained about 84.6% sand, 10.8% silt-size fraction and 4.6% clay-size particles. The fine to medium sand was used in preparing this mixture because the fine sand provides more surface area to be coated as well as results in smaller voids to be filled with the fine additives as compared to the coarse sand.

According to the Unified Soil Classification System (USCS), the CKD was classified as inorganic silt with low plasticity (ML). The sand was classified as poorly graded sand (SP), whereas the sand-CKD mixture was classified as silty sand (SM).

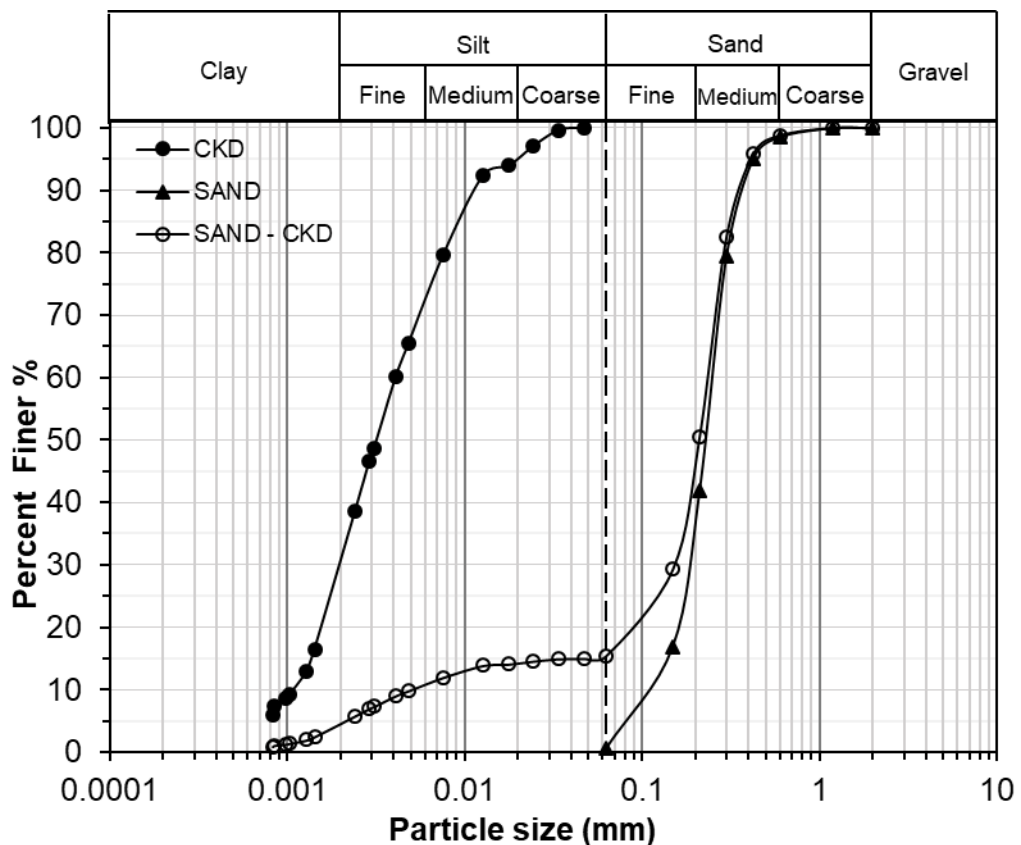


Figure 3.2 Particle size distribution curves of materials used

### 3.3.4 Compaction tests

Standard Proctor compaction test was conducted following BS 1377-4 (1990) to determine the compaction curves for the CKD, sand, and sand-CKD mixture. Each material was compacted in three layers in a compaction mould having a volume of 0.001 m<sup>3</sup> (1000 cm<sup>3</sup>) using 27 blows per layer and with a 2.5 kg hammer falling through a height of 300 mm.

The compaction curves of CKD, sand, and sand-CKD mixture are shown in Figure 3.3, Figure 3.4, and Figure 3.5, respectively. The optimum water content (OWC) for CKD remained close to the degree of saturation (*S*) of 95% (OWC = 27.6%). For the sand, the optimum water content remained close to the degree of saturation (*S*) of 50% (OWC = 13%). For the sand-CKD mixture, the optimum water content was found to be slightly below the degree of saturation (*S*) of 60% (OWC = 11%). The values of maximum dry unit weight for CKD, sand, and sand-CKD mixture were found to be 14.85, 15.53 and 17.73 kN/m<sup>3</sup> respectively. It can be seen that the addition of 15% of CKD to the sand resulted in a reduction in the optimum water content and an increase in the corresponding maximum dry unit weight.

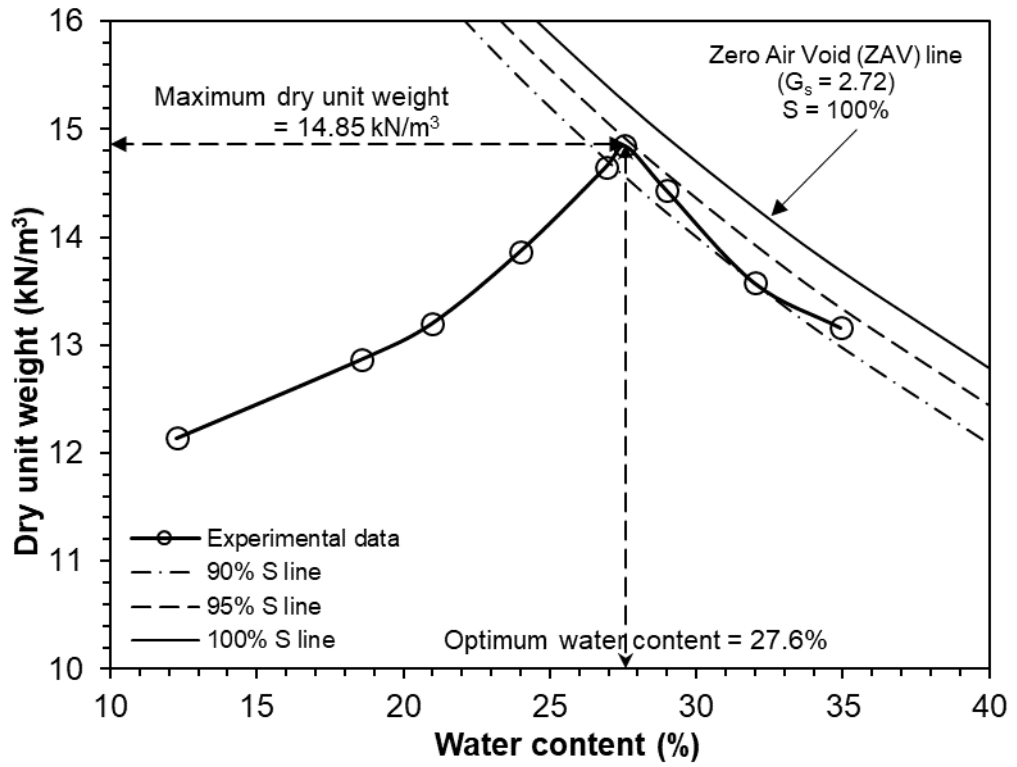


Figure 3.3 Standard Proctor compaction curve of the cement kiln dust

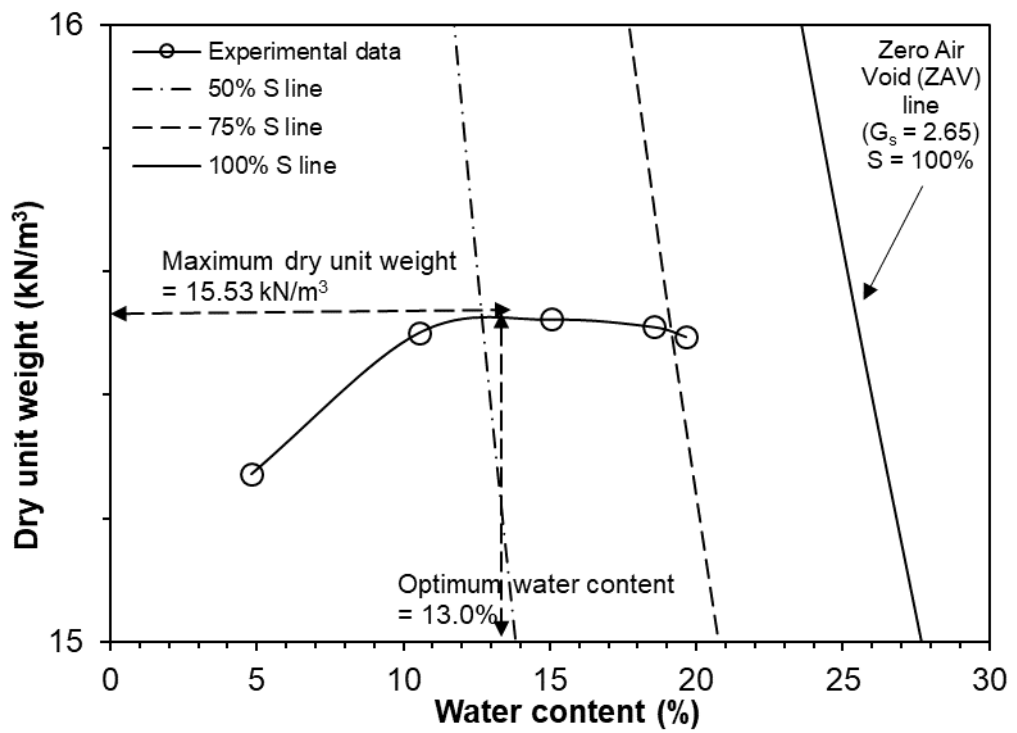


Figure 3.4 Standard Proctor compaction curve of the sand.

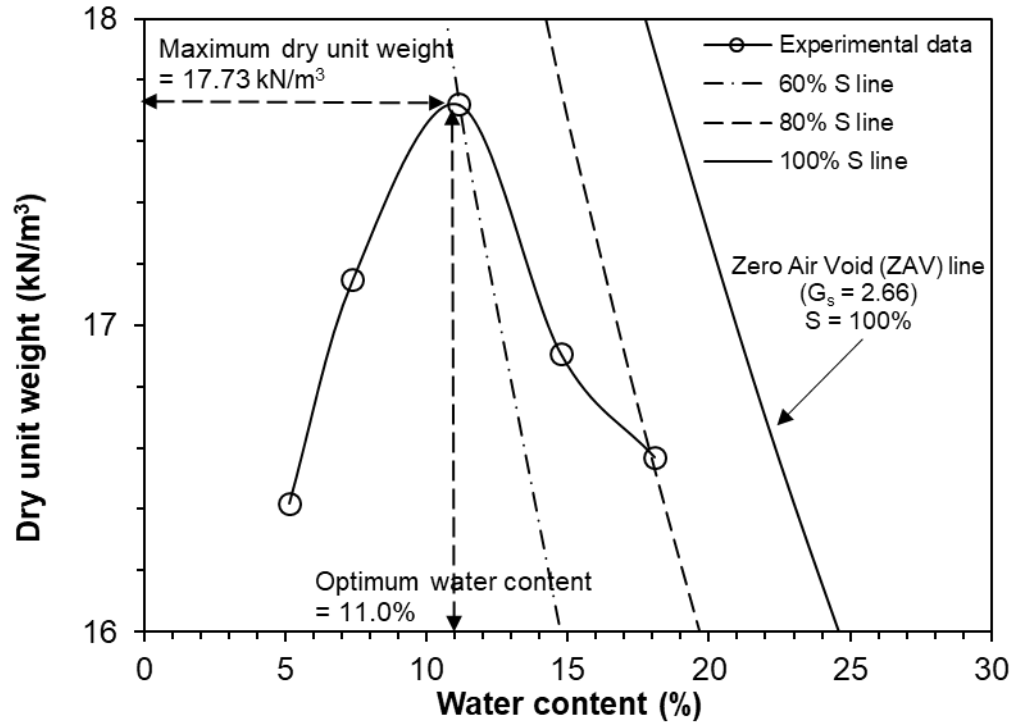


Figure 3.5 Standard Proctor compaction curve of the sand-cement kiln dust

### 3.3.5 Cation exchange capacity (CEC) of CKD

The cation exchange capacity (CEC) is the quantity of exchangeable cations required to balance the charge deficiency on the surface of the clay particles (Mitchell 1993). The rate of cation exchange depends upon the clay type, solution concentration, and temperature (Mitchell and Soga 2005). For any given soil/material, due to the environment and mineralogy conditions, the CEC is neither a fixed nor a single value. The CEC is usually expressed as milliequivalents (meq) per 100 g of dry clay (van Olphen 1977).

In this study, the CEC of the CKD was determined by the ammonium acetate method at pH 7 following a simplified method suggested by Lavkulich (1981). The fractions of cations obtained from the test indicated that the CKD mainly consists of  $\text{Ca}^{2+}$  (60.12 meq/100g) with varying percentages of other cations, such as  $\text{K}^+$ ,  $\text{Na}^+$  and  $\text{Mg}^{2+}$ . The properties of the materials used are summarised in Table 3.1.

Table 3.1 Properties of the materials used

Properties	CKD	Sand	Sand-CKD
	Value		
Specific gravity, $G_s$ <sup>1</sup>	2.72	2.65	2.66
Atterberg limits			
Liquid limit, LL (%) <sup>2</sup>	41	NP	19
Plastic limit, PL (%)	27	NP	NP
Plasticity index, PI (%)	14	NP	NP
Shrinkage limit, SL (%) <sup>3</sup>	21	.....	.....
Particle size distribution			
Sand (Coarse, medium, fine) (%)	....	1.4, 56.8, 41.3	84.6
Silt-size (%)	71	.....	10.8
Clay-size (%)	29	.....	4.6
Compaction characteristics			
Optimum water content (%)	27.6	13.0	11.0
Maximum dry unit weight (kN/m <sup>3</sup> )	14.85	15.53	17.73
Cation exchange capacity (CEC), (meq/100g)			
Na <sup>+</sup>	3.22	-	-
Ca <sup>2+</sup>	60.12	-	-
Mg <sup>2+</sup>	2.41	-	-
K <sup>+</sup>	13.46	-	-
Total Cation Exchange Capacity	79.21	-	-

1 Measured by using kerosene.

2 Determined by using Cone penetrometer method (BS 1377-2 1990)

3 Determined by using the wax method (ASTM D4943 2008)

### 3.3.6 Chemical composition

CKDs consist primarily of calcium carbonate and silicon dioxide which is similar to the cement kiln raw feed, but the amount of alkalis, chloride and sulphate is usually considerably higher in the dust (Keerthi et al. 2013). The quantity of free or available lime, as well as alkalis ( $\text{Na}_2\text{O}$ ,  $\text{K}_2\text{O}$ ), vary widely between CKDs, which render some CKDs more reactive than others. In addition to the above-mentioned factors governing the chemical and physical makeup of CKDs, their storage or disposal scenarios can have a pronounced effect on reactivity. For instance, the exposure of stockpiled CKD to moisture can lead to the hydration of free lime with a decrease in free CaO content and increase in loss on ignition (LOI) value (Button 2003; Williams 2005; Adaska and Taubert 2008).

Some researchers (Bhatty et al. 1996; Miller and Azad 2000; Adaska and Taubert 2008; Lachemi et al. 2008) indicated that the high loss on ignition (LOI) proves the fact that CKDs are high in slow-reacting calcium carbonate and low in reactive free lime available for hydration. Furthermore, Williams (2005) reported that the soil mixtures containing CKD with high LOI (> 20%) never hardened.

In this study, the X-ray fluorescence spectroscopy (XRF) was used for conducting the chemical analysis for the materials (CKD, sand, and sand-CKD mixture). The XRF results presented in Table 3.2 show that the CKD used in this study was mainly composed of the oxides of calcium, silica and aluminium and the loss on ignition (LOI) was equal to 33.8% while for the sand and sand-CKD mixture, the silica oxide was the predominant constituent.

Table 3.2 Chemical composition of materials used

Oxides	CKD		Sand	Sand-CKD
	(percentage)			
	In this study	Provided by the supplier (mean±SD)	In this study	
SiO <sub>2</sub>	13.02	14.61 ± 0.72	84.16	75.47
Al <sub>2</sub> O <sub>3</sub>	2.65	3.30 ± 0.08	0.77	0.79
Fe <sub>2</sub> O <sub>3</sub>	1.04	1.29 ± 0.08	0.25	0.44
CaO	41.46	43.04 ± 0.53	0.03	5.47
K <sub>2</sub> O	1.33	0.71 ± 0.08	0.24	0.39
Na <sub>2</sub> O	0.21	0.14 ± 0.02	0.04	0.08
MgO	1.07	1.39 ± 0.02	0.01	0.17
SO <sub>3</sub>	1.84	1.89 ± 0.05	0.07	0.31
Cl	-	0.07 ± 0.02	-	-
SrO	0.04	0.05 ± 0.00	-	0.01
P <sub>2</sub> O <sub>5</sub>	0.05	0.06 ± 0.01	0.01	0.01
Mn <sub>2</sub> O <sub>3</sub>	0.06	0.07 ± 0.02	-	0.01
TiO <sub>2</sub>	0.14	0.16 ± 0.01	0.15	0.14
ZnO	0.01	0.01 ± 0.00	-	-
Cr <sub>2</sub> O <sub>3</sub>	0.01	0.02 ± 0.01	-	-
L.O.I	33.8	33.00 ± 1.58	-	-
pH	12.07		3.6	10.1

### 3.3.7 Mineral compositions

The X-ray diffraction (XRD) technique (Grim 1968; Mitchell and Soga 2005) was used to determine the mineral composition of materials. According to Bragg's law, the XRD identifies the minerals based on the relationship between the angle of incidence of the X-rays ( $\theta$ ) to the  $c$ -axis spacing ( $d$ ). A Philips automated powder diffractometer PW 1710 (PANalytical, Cambridge, UK) was employed for the XRD analyses. The diffractometer consists of a goniometer (specimen holder), a copper X-ray generator and a controller. Specimens of CKD, sand, and sand-CKD mixture in powder form and with initial water contents were tested.

The X-ray diffraction test results of the materials are shown in Figure 3.6. Semi-quantitative analyses were conducted to determine the percentage of various minerals. The XRD test results showed that the predominant mineral in CKD is Calcite,  $\text{CaCO}_3$  (85%). The CKD also comprised Quartz,  $\text{SiO}_2$  (12%) and traces of Gypsum, Smectite-Kaolinite and Anhydrite. For the sand, the quartz (94%) is found to be the main constituent with 6% of Smectite-Kaolinite. On the other hand, the sand-CKD mixture is predominantly contained Quartz (75%) and Calcite (24%) with a trace of Anhydrite.

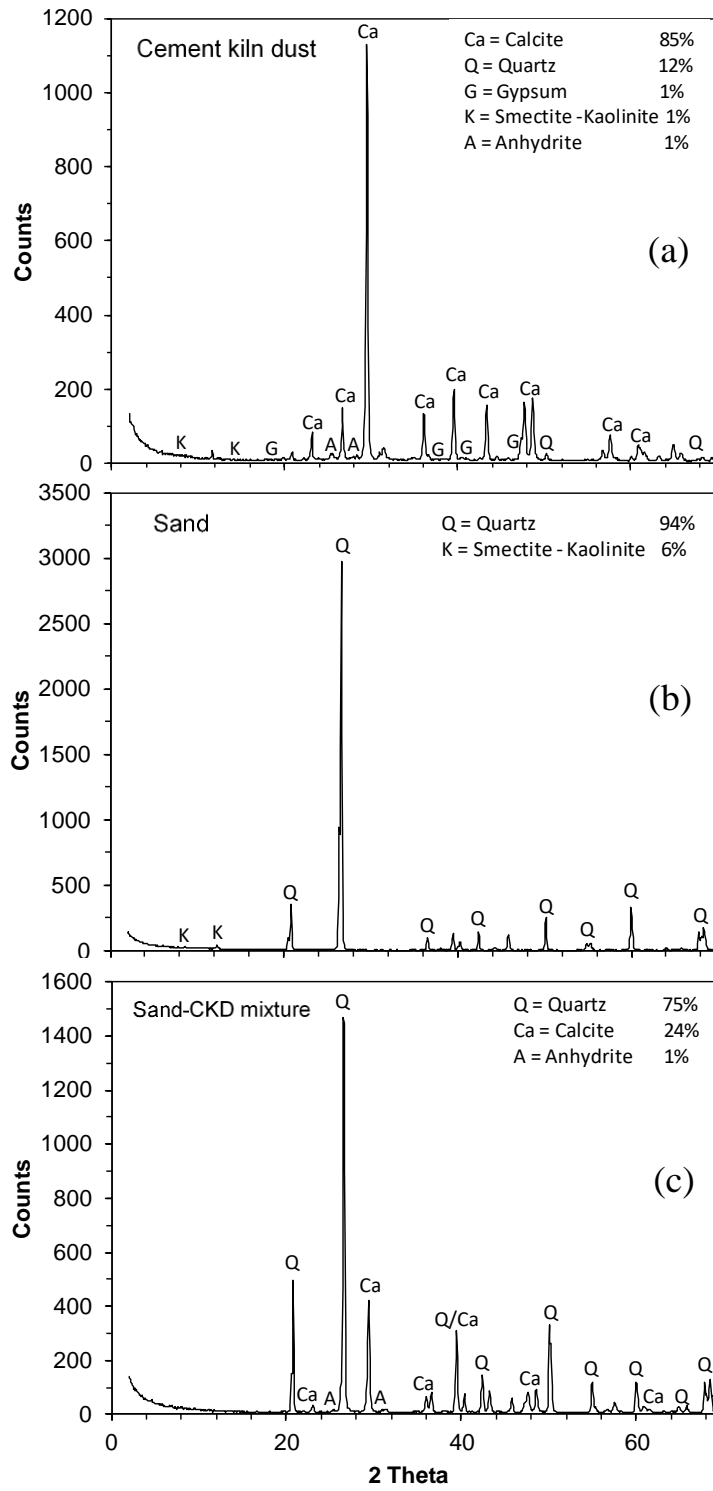


Figure 3.6 X-ray diffraction patterns of (a) Cement kiln dust (CKD); (b) Sand and (c) Sand-CKD mixture.

### 3.3.8 Microstructural analysis (SEM study)

Microstructural investigations are usually made to facilitate explanation and comparison of the micro-behaviour and physical properties of soils (Romero and Simms 2008; Solanki et al. 2009). Understanding microstructural behaviour in unsaturated soils has particular relevance to geotechnical applications in which soils undergo water content and volume changes (Romero and Simms 2008; Burton et al. 2015). In this study, Scanning Electron Microscopy (SEM) was employed to perform the microstructural analysis on specimens of the selected materials that were prepared at initial water contents. Micrographs were taken at different magnifications.

Figures 3.7, 3.8, and 3.9 show the SEM images of the CKD, sand, and sand-CKD, respectively. The microscopic appearance of the CKD powder (Figure 3.7) seemed to be predominantly composed of clusters (agglomerates) of particles with poorly defined shapes. For the sand (Figure 3.8), the largest percent of particles is close to 0.2 mm size and sub-angular to sub-rounded, and medium spherical in shape, as well as their surfaces, appeared to be rough. On the other hand, it can be seen that most of the particles of sand are covered with a large number of CKD deposits (clusters) for the sand-CKD mixture (Figure 3.9).

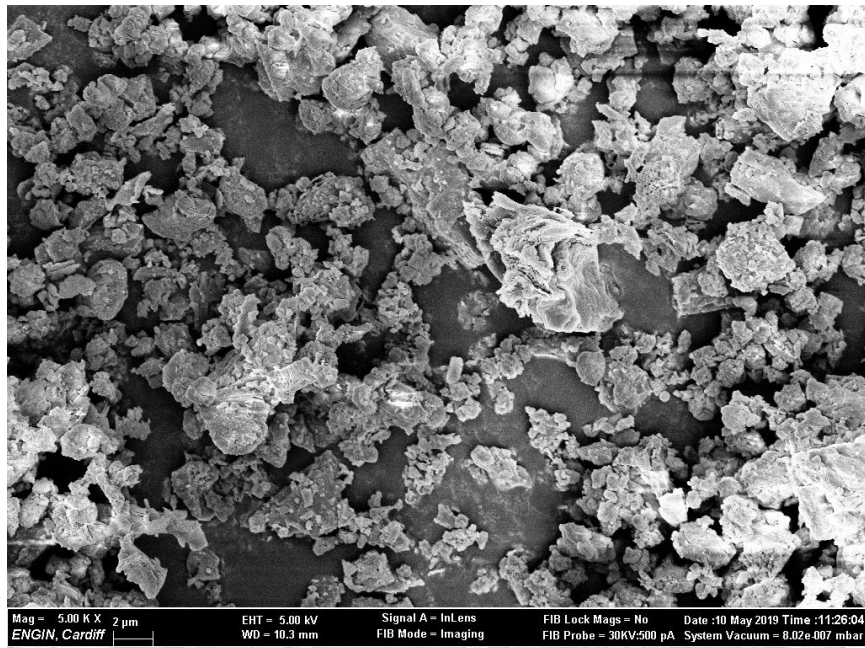


Figure 3.7 SEM photomicrograph of cement kiln dust (CKD) - 2  $\mu\text{m}$  scale

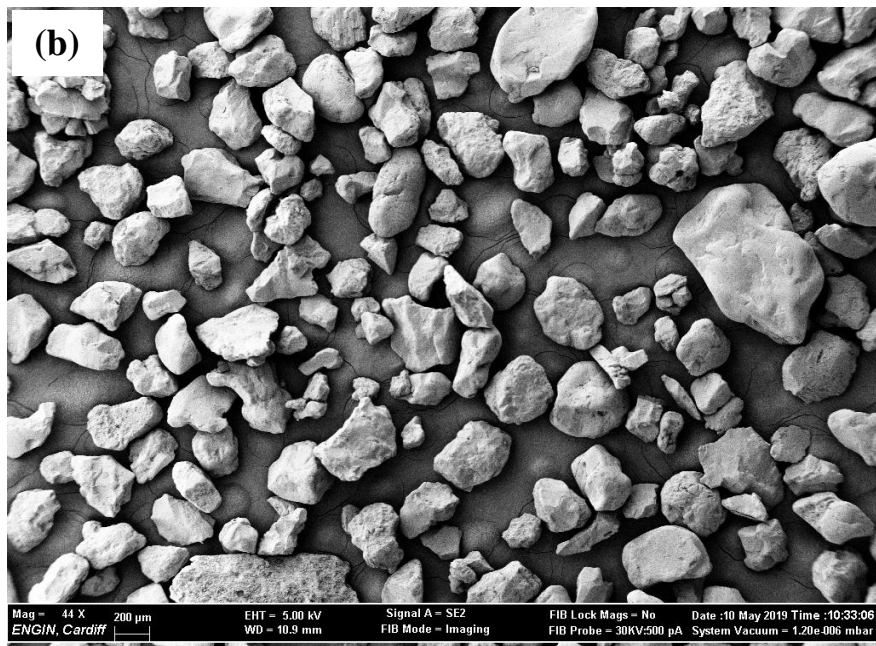
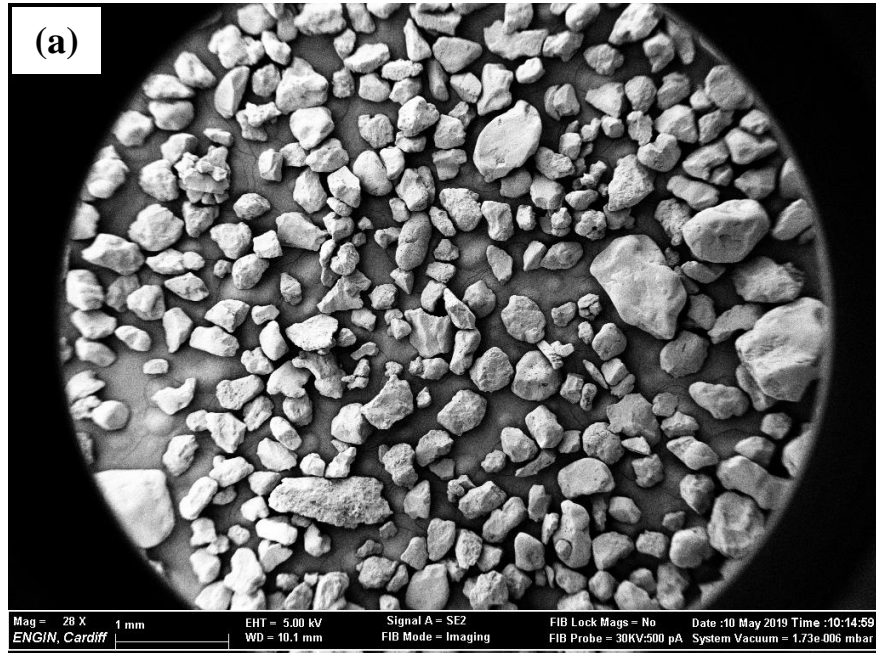


Figure 3.8 SEM photomicrographs of sand (a) 1mm scale; (b) 200 μm scale

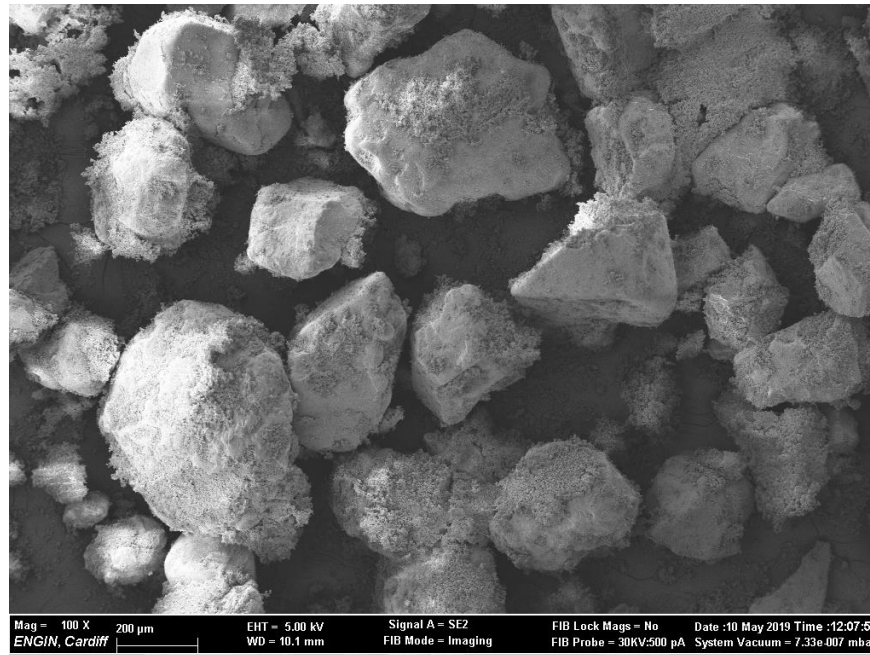


Figure 3.9 SEM photomicrographs of sand-CKD - 200  $\mu\text{m}$  scale.

### 3.4 Experimental techniques and test procedures

This section presents the various laboratory tests performed, the apparatus and techniques used for carrying out the tests and the experimental procedures adopted for preparing specimens for the tests. The laboratory experiments were conducted in four phases. In phase I, swelling and compressibility tests were performed for determining the swelling deformation, swelling pressure and consolidation characteristics of the CKD. In phase II, water retention characteristics of the materials were established by using pressure plate, salt solution, chilled-mirror dew-point potentiometer and water potential sensors. Phase III focused on shear strength tests on saturated and unsaturated specimens. For saturated specimens, UU and CU tests on the three selected materials in addition CD tests on the CKD were carried out using a conventional triaxial shear strength device. Unsaturated CD tests were conducted only on CKD specimens using an unsaturated triaxial shear strength device. Further, saturated hydraulic conductivity of all the selected materials was determined at various effective confining pressures. In phase IV, the volume change behaviour of CKD was investigated using a suction-controlled oedometer.

### **3.4.1 Preparation of the material-water mixtures**

For all tests, homogenous mixtures of CKD-water and sand–water at various selected water contents were prepared by adding predetermined quantities of distilled water. The required amount of water was added to the materials in small amount and thoroughly mixed until uniform mixtures were obtained. For the mixtures of sand and CKD, dry mixing was performed until a uniform colour was observed. Then, the required quantities of distilled water were slowly added to the mixtures while blending by hand until homogenous mixtures at different water contents were achieved. The blending process lasted for about 2 to 10 minutes depending on the amount and type of blended material in addition to the targeted water content. The mixtures were then placed in sealed plastic bags and kept in airtight containers for at least 24 hours to allow moisture equilibrium to take place.

### **3.4.2 Swelling and compressibility tests on CKD**

One-dimensional oedometer tests were conducted on CKD specimens according to (BS 1377-5 1990) for investigating the swelling deformation and consolidation parameters. A swelling pressure test was conducted at constant volume condition. For these tests compacted specimens prepared at the maximum dry density and optimum water content were used. Additionally, a consolidation test was performed on initially saturated slurried specimen with an initial water content of 1.2 times the liquid limit. This value of water content was used for ensuring the specimen is in nearly full virgin state and 100% saturation.

#### **3.4.2.1 Specimen preparation (swelling and compressibility tests on CKD)**

For both the swelling and compressibility tests, compacted specimens (70 mm dia. and 15 mm high) were prepared directly in oedometer rings (70 mm dia and 19 mm high) using the static compaction method. A compaction mould with a piston was used to obtain the desired thickness of the specimens. The components of the compaction mould and the compaction setup are shown in Figure 3.10. The dry unit weight and water content of the specimens were  $14.83 \text{ kN/m}^3$  and 27.3% respectively. Prior to preparing the specimens

the inner surfaces of the rings were lubricated with a thin layer of silicone grease to minimise the friction between the ring wall and specimens. The loading machine used applied the required static load with a constant displacement rate of 1.25 mm/min.

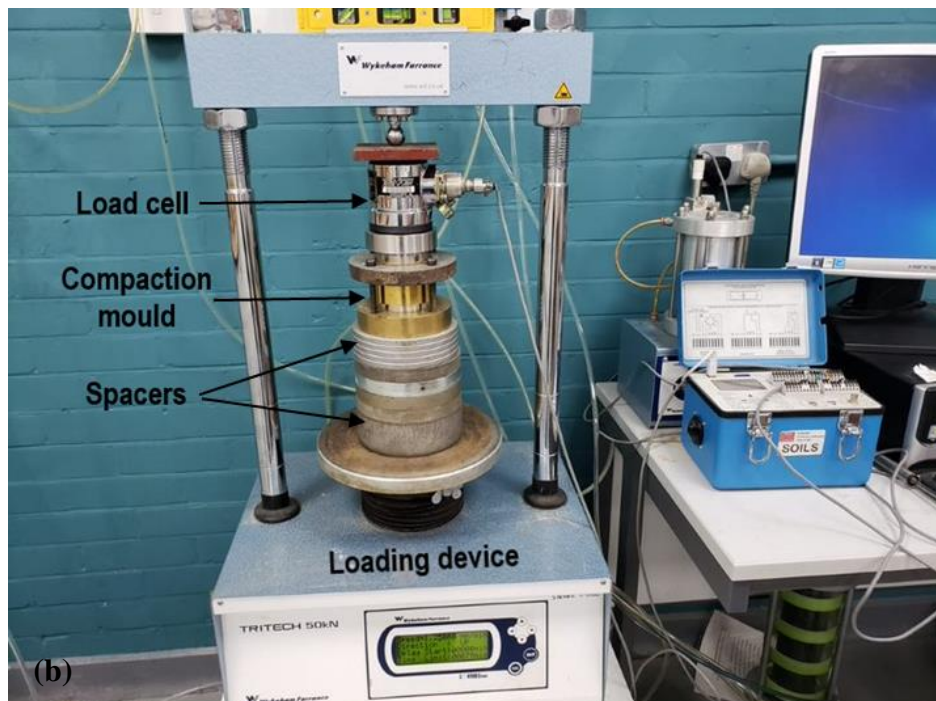


Figure 3.10 (a) A photograph of the components of compaction mould and (b) the static compaction setup used.

### **3.4.2.2 Testing procedure (one-dimensional swelling and consolidation tests on CKD)**

Two one-dimensional swelling tests were carried out in fixed ring oedometers (BS 1377-5 1990) at applied pressures of 2 kPa and 25 kPa. The choice of pressures was based on seating pressure and anticipated in situ overburden pressure. Following applications of the desired loads, the specimens were allowed to swell by filling the consolidation cell with water. The swelling deformation was measured with time by using a dial gauge until the specimens exhibited no volume change.

Consolidation tests were carried out following completion of the swelling phase. A load increment ratio of one was applied in the tests and each load was held for 24 hours. The tests were conducted up to a vertical pressure of 1600 kPa. The specimens were unloaded in a stepwise process.

A swelling pressure test was conducted at constant volume condition. An automatic computerised oedometer equipped with a load cell and a displacement transducer was used. The vertical strain of the specimen was prevented during the entire test period to keep the specimen volume constant. Development of swelling pressure was monitored until an equilibrium was reached where the specimen did not exhibit any further increase in swelling pressure, as indicated by a near constant load cell reading. Following the measurement of the swelling pressure, the specimen was consolidated by applying pressures greater than the swelling pressure. The specimen was loaded up to 1600 kPa and then unloaded. A photograph of the test set up is shown in Figure 3.11.

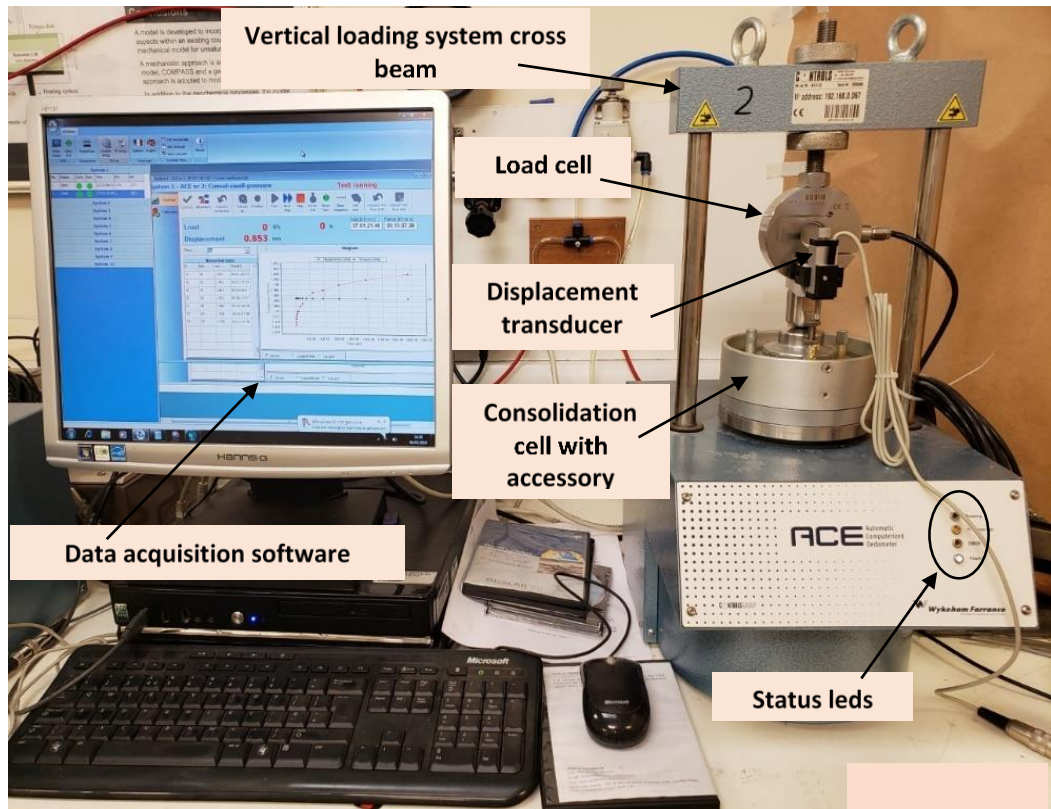


Figure 3.11 The automatic oedometer used in this study to measure swelling pressure of CKD.

A consolidation test was also conducted on an initially saturated slurried specimen using the automatic oedometer according to the procedure laid out in (BS 1377-5 1990). A CKD specimen was prepared with water content corresponding to 1.2 times the liquid limit of the material. The diameter and height of the specimens were 70 mm and 19 mm, respectively. The specimen was consolidated under loading pressure of 12 kPa up to 800 kPa with a load increment ratio equal to one. A loading duration of 24 hours was considered at each applied pressure. The specimen was then unloaded in a stepwise process.

The swelling and consolidation tests results are presented and discussed in Chapter 4.

### 3.4.3 Water retention tests on CKD

This section presents the equipment used and the test procedures adopted to obtain water retention curves (WRCs) of the CKD. Pressure plate extractor, salt solution, chilled-mirror dew-point potentiometer and fixed-matrix porous ceramic disc sensors were used for establishing the water retention curves (WRCs) of the CKD.

#### 3.4.3.1 Pressure plate tests

Pressure plate extractors utilize axis-translation concept (Hilf 1956) to control matric suction and are designed to work over a particular matric suction range. The axis translation technique allows the control of negative pore-water pressures less than zero-absolute and consists of increasing the pore-air pressure such that the desired matric suction,  $u_a - u_w$ , is obtained (Fredlund and Rahardjo 1993).

##### 3.4.3.1.1 Apparatus description

5-bar (1 bar = 100 kPa) pressure plate extractors, manufactured by Soilmoisture Equipment Corp., were used in this investigation (Figure 3.12) to establish drying WRCs up to suction of 400 kPa. The device comprises a pressure chamber, and an air supply system, drainage system and high air-entry ceramic disk. The disk is generally made of sintered kaolin soil (Fredlund and Rahardjo 1993) and the thickness and diameter of the ceramic disk are around 6.9 mm and 277 mm, respectively. The water outlet in the pressure plate apparatus was connected to a burette for flushing purpose and for collecting water that expelled out of the specimens. The air pressure required for the test is applied through an external compressed air supply line which is connected to the chamber via a regulator.

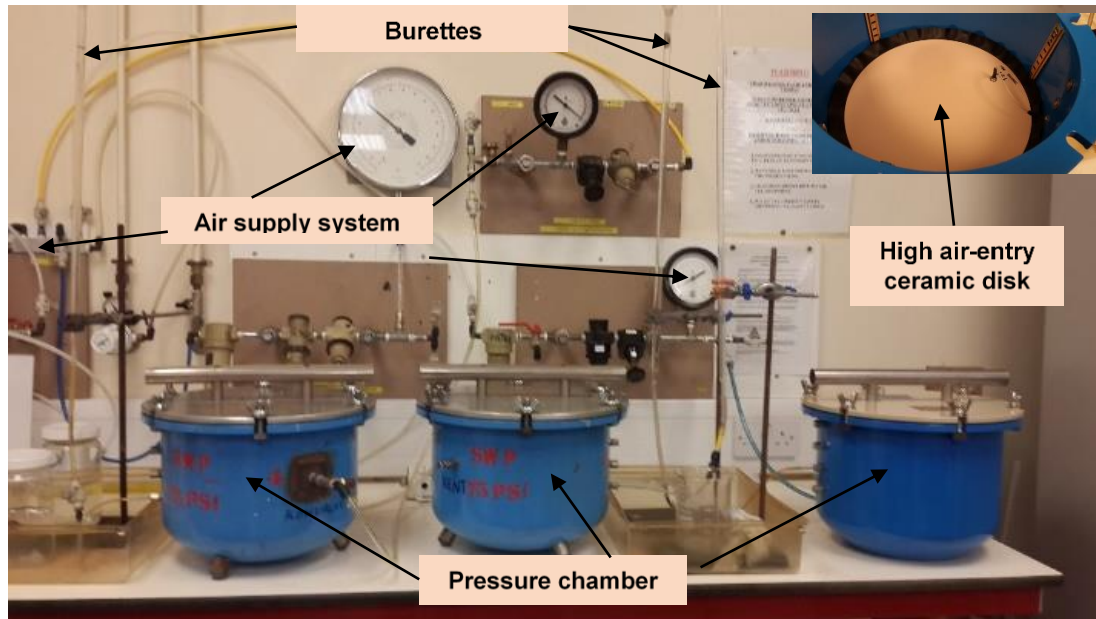


Figure 3.12 Test setup for 5-bar pressure plate extractor

#### 3.4.3.1.2 Testing procedure (pressure plate tests)

The ceramic disks of the pressure plate extractors were saturated prior to the tests. The water compartment below the disk was filled with distilled deaired water and the ceramic disk was also covered with distilled deaired water. An air pressure of 75 kPa was applied for several hours with water on the disk. The process of saturating the ceramic disk continued until no air bubbles were noticed in the burette. Fredlund and Rahardjo (1993) stated that air cannot penetrate a saturated ceramic disk due to the ability of the contractile skin that resists the flow of air. The ceramic disk acts as a membrane between the pore air and pore water.

To ensure saturation of the ceramic disk, permeability measurements were carried out following the constant head method. The outflow tube of the pressure plate extractor was connected to a digital pressure/volume controller set to zero pressure. Different hydraulic gradients were selected and applied and the volume of flowing water to the controller was monitored and recorded by GDSLAB software.

The average saturated coefficient of permeability of the ceramic disk was found to be  $1.53 \times 10^{-10}$  m/s. The saturated coefficient permeability of the ceramic disk was found to be similar to the value reported by Leong et al. (2004) and Tripathy et al. (2012) for ceramic disks with the air-entry value of 500 kPa ( $1.68 \times 10^{-10}$  m/s and  $4.7 \times 10^{-10}$  m/s, respectively).

For obtaining the drying suction-water content WRCs, saturated slurried specimens of CKD were prepared in stainless steel specimen rings and transferred onto the ceramic disks. The stainless-steel rings were coated with silicon grease to avoid the development of desiccation cracks during drying (Peron et al. 2007). Pre-wetted Whatman 3 filter papers were used as a separation material to avoid the loss of material particles and blocking the pores of the ceramic disk. A thin layer of water was left on the ceramic disc prior to the specimens being placed on the ceramic disk in order to provide good contact between the CKD specimens and the ceramic disk (Cresswell et al. 2008). The tests were performed by applying suction values of 10, 20, 30, 50, 100, 200, 300, and 400 kPa. The mass of the specimen at each imposed suction level was monitored periodically during the testing at every two days. The ceramic disk was re-saturated prior to placing the specimens back in the pressure plate. An equilibrium was achieved when there was no significant change in the mass of the specimens. After reaching the equilibrium at each suction, two specimens were removed for water content determination and for volume measurements utilizing molten wax method (ASTM D4943 2008).

### **3.4.3.2 Salt solution tests**

For establishing drying WRCs at high suctions, vapour equilibrium technique (VET) was used. This method controls total suction (Fredlund and Rahardjo 1993; Delage et al. 1998; Lloret et al. 2003; Tang et al. 2005; Blatz et al. 2008; Fredlund et al. 2011; Gao and Sun 2017). The VET uses vapour pressure of saturated salt solutions to induce total suction in a closed space.

In this study, saturated salt solutions of  $K_2SO_4$ ,  $KNO_3$ ,  $KCl$ ,  $NaCl$ ,  $K_2CO_3$ , and  $LiCl$  were used for inducing suctions of 3.4, 9.1, 21.9, 38.3, 114.1 and 277 MPa, respectively. The test setup is shown in Figure 3.13 . The tests were performed in closed-lid desiccators and in a temperature-controlled room (i.e.,  $21^\circ C \pm 0.5^\circ C$ ). The relative

humidity in the vapour space above a salt solution is related to total suction via Kelvin's equation (Eq. 2.6) (Fredlund and Rahardjo 1993). The saturated salt solutions used in this study along with the equilibrium relative humidity and suctions are shown in Table 3.3.

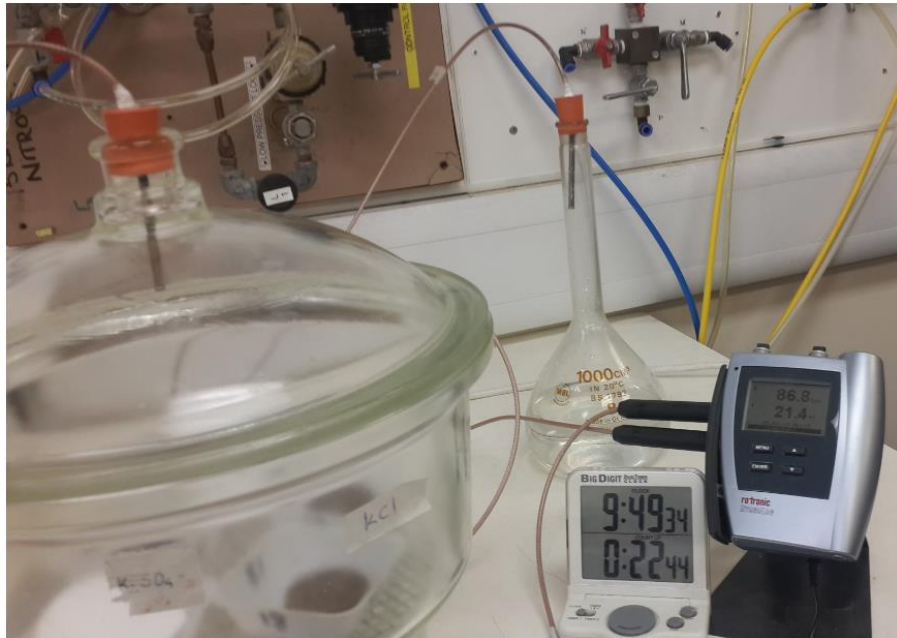


Figure 3.13 Salt solution (VET) test setup: a photograph of the desiccator used and Rotronic Hydrolog relative humidity probe arrangement

#### 3.4.3.2.1 Specimen preparation and testing procedure (vapour equilibrium technique)

Initially saturated slurried CKD specimens were first subjected to a matric suction of 400 kPa in pressure plates. The purpose of conducting this initial drying was to speed up the drying process as drying in desiccators alone generally requires a longer testing period. The specimens were placed inside plastic containers before being transferred into the test desiccators. A stainless-steel mesh was used to separate the salt solutions from being in contact with the specimens. Rotronic Hydrolog relative humidity probes (Figure 3.13) were used in order to verify the imposed suctions in the desiccator tests by measuring the relative humidity generated in the headspace of the closed-lid desiccators. The mass of the CKD specimens was recorded periodically to deduce the suction

equilibration. Once the specimens were equilibrated at each applied suction, the specimens were removed for water content determination (by oven drying method) and volume measurements using the molten wax method (ASTM D4943 2008).

Table 3.3 Relative humidity imposed by saturated salt solutions and corresponding suctions at 21°C

Saturated salt solution	Targeted RH (%)* at 21 °C	Targeted suction (MPa) (Eq.2.6)	Calculated suction based on RH probe results (MPa)	Calculated suction based on chilled-mirror device (MPa)
K <sub>2</sub> SO <sub>4</sub>	97.5	3.4	1.6	3.2
KNO <sub>3</sub>	93.5	9.1	5	9.1
KCl	84.9	21.9	19.2	22.2
NaCl	75.4	38.3	31.7	39
K <sub>2</sub> CO <sub>3</sub>	43.2	114.1	101.3	108.4
LiCl	13	277	251.3	275.9

\* After (O'brien 1948) and (ASTM E104-02 2007)

$$\text{Eq. (2.6) at 21}^\circ\text{C: } \psi = -135749 \times \ln\left(\frac{RH}{100}\right)$$

### 3.4.3.3 Chilled-mirror dew-point potentiometer tests

The WRCs of the selected materials (CKD, sand, and sand-CKD) used in this study were measured by the chilled-mirror dew-point potentiometer. The device has been utilised by several researchers to measure total suction of various materials and polyethylene glycol solutions (Leong et al. 2003; Agus and Schanz 2005; Thakur et al. 2006; Campbell et al. 2007; Tripathy et al. 2016; Karagoly et al. 2018; Jones et al. 2019). The suction measurement range of the currently available model of the potentiometer, WP4C (METER Group 2017) is 0.1 to 300 MPa. The accuracy of the potentiometer is  $\pm 0.05$  MPa for a suction range of 0 to 5 MPa and 1% for a range of suction of 5 to 300

MPa. Suction measurements using the device can be made within a selectable temperature range of 5 to 40 °C. The device measures the relative humidity of the air space above a sample and displays the equilibrium suction and temperature of the sample at which the measurement is carried out.

The device consists of a sealed chamber with a fan, a mirror, a photoelectric cell, and an infrared thermometer. A specimen fills about half the capacity of a stainless steel cup and is placed in the device in a closed chamber that comprises a mirror and a photodetector cell. Detection of the exact point at which condensation first appears on the mirror is observed by a beam of light directed onto the mirror and reflected into a photodetector cell. A thermocouple attached to the mirror records the temperature at which condensation occurs (Leong et al. 2003). The fan is used to accelerate the equilibration of the sample with the ambient air vapour within the sealed chamber. The device also equipped with a temperature controller to set the temperature of the sample at which relative humidity measurement is to be made. The device comes with a temperature equilibrium plate that utilised to bring the temperature of the specimen cup to the set-point temperature of the device (Figure 3.14). The relative humidity is calculated using the dew-point temperature of the air and the specimen temperatures, which is measured with an infrared thermometer. Kelvin's equation (Eq. 2.6) is then used to determine the total suction of the soil specimen. The calculations are carried out by software within the device and displayed on an LCD panel in MPa unit along with the specimen temperature.

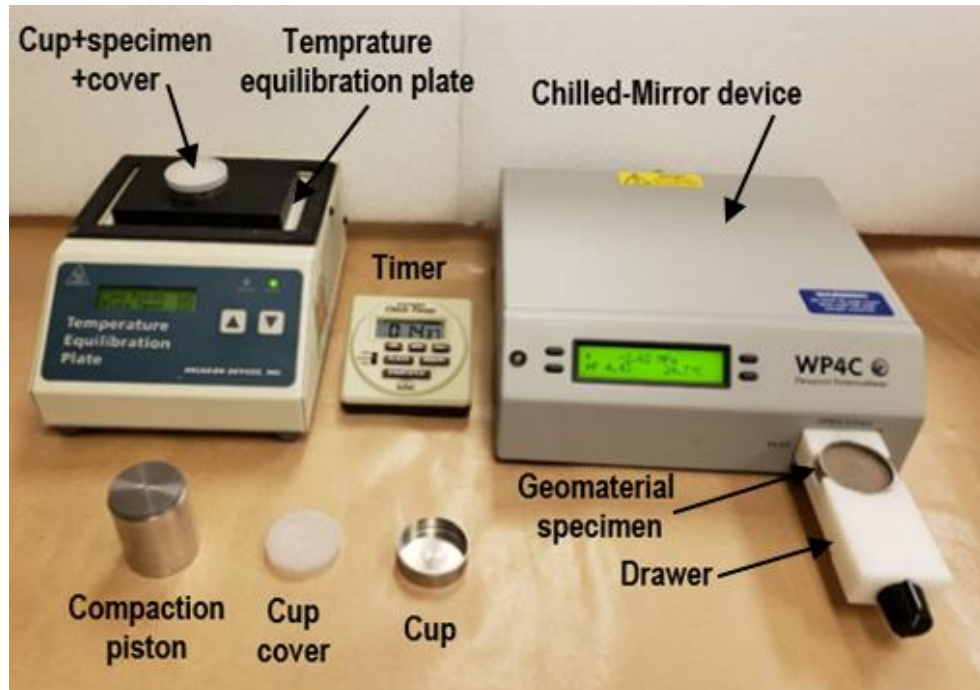


Figure 3.14 WP4-C model of chilled-mirror dew point device

Prior to the tests, calibration of the device was conducted using a standard salt solution (Potassium Chloride (KCl)) that has water potential of  $2.22 \pm 0.05$  MPa at temperature of  $25^{\circ}\text{C}$ . The solution was poured in the specimen cup and placed on a temperature equilibrium plate to bring the temperature of the specimen cup to the set-point temperature of the device. The specimen cup with the salt solution was then placed in the WP4-C's specimen drawer and the drawer knob was turned to the READ position. Once the equilibrium was reached, the total suction value was then calculated and displayed on an LCD panel in MPa unit along with the specimen temperature. After completing the calibration of the device, specimens (37.37 mm diameter and 5 mm thickness) of each material were prepared inside a stainless-steel cup. Predefined weights of the material mixtures prepared at various selected water content were placed in the specimen cup covering the bottom of the cup and fill about half of it. Similar procedures to those used for calibration of the device were followed for total suction measurements of the materials. The water contents of specimens after completion of total suction measurements were determined by oven drying method.

#### **3.4.3.4 Fixed-matrix porous ceramic disc water potential sensor tests**

Fixed-matrix porous ceramic disc water potential sensors were used for establishing the WRCs of unsaturated materials. The water potential sensor used in this study was from Decagon Devices Inc, Pullman, WA (METER Group 2017). The sensor currently known as TEROS 21 (Figure 3.15), comprises two fixed-matrix porous ceramic discs (dielectrics) separated by printed electric circuit board to form a capacitor.

The charging time of the capacitor is affected by the water content of the ceramic discs. When the sensor is brought in contact with soil/material, the water content of the ceramic disc assembly changes. The suction of the soil and the ceramic discs tend to become equal with elapsed time. The sensor measures the water content of the ceramic discs. The water content of the ceramic discs is translated into matric suction based on a predetermined relationship between water content and matric suction of the fixed-matrix ceramic discs (Figure 2.3). At equilibrium, the suction of the ceramic disc and the soil are equal. The sensor can be connected to a data acquisition system to monitor and record the measured suction. The water retention characteristic of the fixed-matrix porous ceramic discs (Figure 2.3) is established based on the mercury intrusion porosimetry data (METER Group 2017). A thermistor is located underneath the sensor overmold (resin) that enables monitoring of temperature.

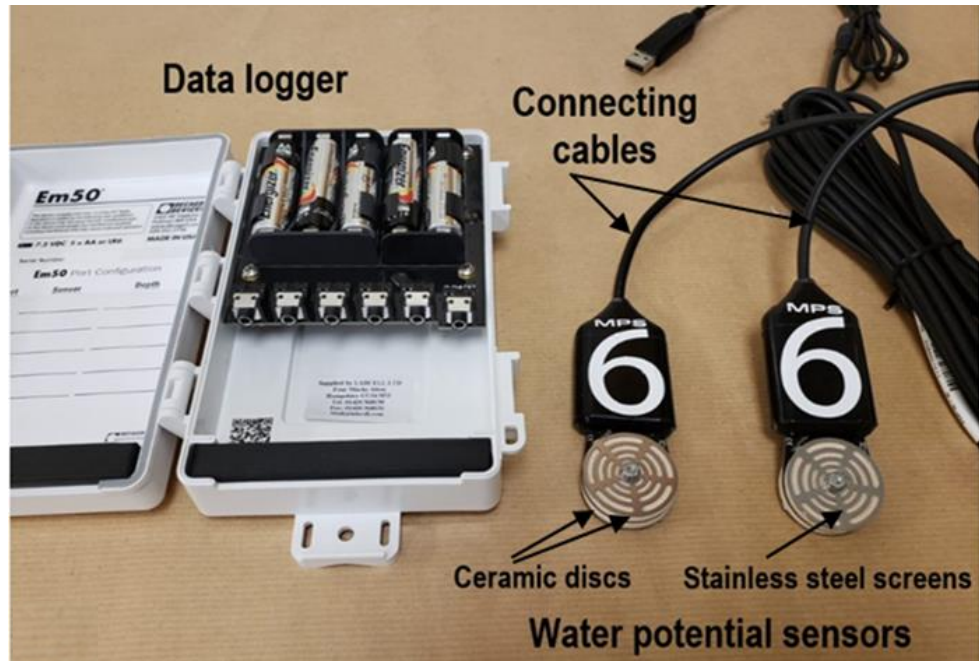


Figure 3.15 The water potential sensor and data logger used in this study

As per the manufacturer's specifications, the suction measurement range of the device is from 9 to 100,000 kPa with a resolution of 0.1 kPa. The air entry potential of the largest pores in the ceramic is about 9 kPa and this value represents the lower suction limit of the sensor. The operating temperature of the sensor is between 0 and 60 °C. The accuracy of the sensor is  $\pm (10 \% \text{ of reading} + 2 \text{ kPa})$  over a suction range of 9 – 100 kPa. At high suctions, the accuracy of the sensor depends upon the water retention characteristic of the ceramic disc (Figure 3.2).

#### 3.4.3.4.1 Specimen preparation and testing procedure (water potential sensor)

Specimens of CKD, sand and sand-CKD mixtures prepared at different water contents were placed in cylindrical plastic containers. The volume of specimen container was 150 cm<sup>3</sup> (Figure 3.16). A layer of mixture was first laid at the base of a specimen container. A sensor was positioned at the centre of the base layer and the remaining amount of the material was packed surrounding the sensor. A tamping rod was used for compacting the mixture. The dry unit weight of specimens of CKD varied between 8.93 kN/m<sup>3</sup> to 13.24 kN/m<sup>3</sup>. A better control of the dry unit weight of sand and sand-CKD

specimens was achieved. In this case, the dry unit weight of compacted specimens of sand and sand-CKD were about 12.75 and 14.81 kN/m<sup>3</sup> respectively. At the end of the compaction process, the sensor overmold (resin) remained half-buried within the specimens. Molten wax was utilised to cover the surface of the specimen for minimizing evaporation of water from the specimens. The specimen containers along with the sensors were placed in a thermocol box. The cables of the sensors were connected to a data acquisition system. The tests were terminated after about 4 days. After reaching the equilibrium condition (indicated by a steady suction value), the materials surrounding the ceramic discs were taken for measuring the final water contents.

The initial state of the fixed-matrix porous ceramic disc sensors prior to measuring suctions can be either wet or dry. The sensors can be submerged in water to attain a wet condition in which case the suction usually reads about 9 kPa. The sensors can be air-dried to read higher suctions of various magnitudes. The suction of a dry sensor may vary depending upon the duration of exposure to the ambient conditions (Karagoly et al. 2018). In this study, air dried sensors were used for measuring the suction of the materials.

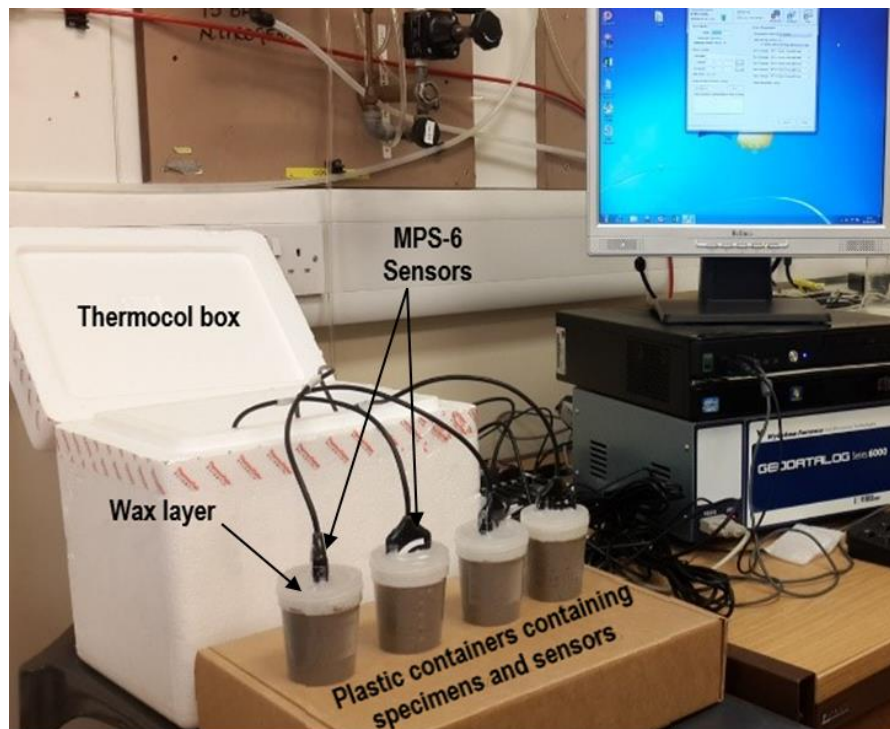


Figure 3.16 Experimental setup for measuring suction using MPS6 water potential sensors

### 3.4.3.5 Water content-void ratio relationship (shrinkage path)

The shrinkage path (the relationship between the change in water content and the void ratio) of initially saturated slurried CKD was established from clod tests. The shrinkage curve could be used in conjunction with the suction-water content WRC results to establish the suction-void ratio relationship and suction-degree of saturation WRC of the CKD.

#### 3.4.3.5.1 Clod test

Clod tests require coating specimens with an encasement glue. Initially saturated CKD specimens were firstly subjected to a suction of 50 kPa in a pressure plate. This enabled handling and coating the Clod specimens with an encasement glue. A commercially available Unibond Waterproof PVAc glue was used for coating the specimens in this study (Tadza 2011). Krosley et al. (2003) used Elmer's glue for coating soil samples. The PVAc glue used in this study was found to be a substitute for its US counterpart Elmer's glue (Tadza 2011). The glue enables water vapour to escape from the Clod during the drying process but prevents liquid water from flowing into the Clod during mass measurement in water (Krosley et al. 2003). The PVAc glue was first diluted with deionised water in order to improve the workability of the glue. A ratio of 10 part of glue to 1 part of deionised water was considered.

Figure 3.17 shows CKD specimens coated with PVAc glue. The Clod specimens were hung by threads and allowed to dry out at ambient laboratory temperature. As the glue required some time to solidify immediately after coating the specimens, measurement of the initial volume of the specimens (coated with glue) were made after about an hour after the specimens were coated with the glue.



Figure 3.17 Coated cement kiln dust specimens in clod test

To determine the volume of specimens during the drying process, the mass of the Clod in air and in water were measured. The void ratios of the specimens were calculated using volume-mass relationships (Eq. 3.1 – Eq. 3.7). Volume measurements were carried out until no further reduction in the mass of the Clod was observed.

$$M_{clod(i)} = M_{material(i)} + M_{glue(i)} \quad (3-1)$$

$$V_{clod(t)} = M_{air(t)} - M_{water(t)} \quad (3-2)$$

$$V_{material(t)} = V_{clod(t)} - V_{glue(t)} = V_{clod(t)} - M_{glue(i)} \times g_f(t) / \rho_{glue} \quad (3-3)$$

$$V_{material(t)} = V_{clod(t)} - M_{glue(t)} / \rho_{glue} \quad (3-4)$$

$$W_{material(t)} = W_{material(i)} - [(M_{material(i)} - (M_{air(t)} - M_{glue(t)})) / M_d] \times 100 \quad (3-5)$$

$$\rho_{d\ material(t)} = [(M_{air(t)} - M_{glue(t)}) / V_{material(t)}] \div (1 + W_{material(t)} / 100) \quad (3-6)$$

$$e_{material(t)} = G_s / \rho_{d\ material(t)} - 1 \quad (3-7)$$

where  $M_{\text{clod}(i)}$  = initial total mass of the Clod,  $M_{\text{material}(i)}$  = initial total mass of the specimen,  $M_{\text{glue}(i)}$  = initial mass of glue;  $V_{\text{clod}(t)}$  = total volume of the Clod,  $V_{\text{material}(t)}$  = volume of specimen,  $V_{\text{glue}(t)}$  = volume of glue,  $M_{\text{air}(t)}$  = mass of the Clod in air,  $M_{\text{water}(t)}$  = mass of Clod in water,  $g_{f(t)}$  = mass fraction of the glue at any given time during drying process from Figure 3.18,  $\rho_{\text{glue}}$  = density of the glue,  $W_{\text{material}(t)}(\%)$  = water content of the material specimen,  $W_{\text{material}(i)}(\%)$  = initial water content of the material specimen,  $M_d$  = dry mass of the specimen,  $\rho_{d \text{ material}(t)}$  = dry density of the material and  $e_{\text{material}(t)}$  = void ratio.

#### 3.4.3.5.1.1 Calibration of glue mass

The PVAc glue is a water-based material that tends to lose water during solidification. The amount of water lost from the glue during the drying process can be determined by conducting an independent test by smearing a known mass of diluted glue onto a light plastic sheet (Tadza, 2011). Measuring the changes in the mass of the glue with elapsed time was performed using sensitive 0.001g electronic balance. The change in the mass with elapsed time for three similar tests is shown in Figure 3.18. It can be seen from Figure 3.18 that the loss of water from the diluted glue was significant within about the first ten hours and the glue mass fraction reached a constant value of about 0.43 after fifty hours. A value of glue mass fraction correction of 0.43 was used for correcting the mass measurements for specimens carried out after fifty hours period, while variable glue mass fractions were used to correct the volume measurement for specimens within first fifty hours.

A reduction in the water content of glue may cause a change in the density. The variation of glue density was considered to be insignificant and a single value of density of  $1.04 \text{ Mg/m}^3$  was considered for the calculations (Eqs. 3-1 to 3-7).

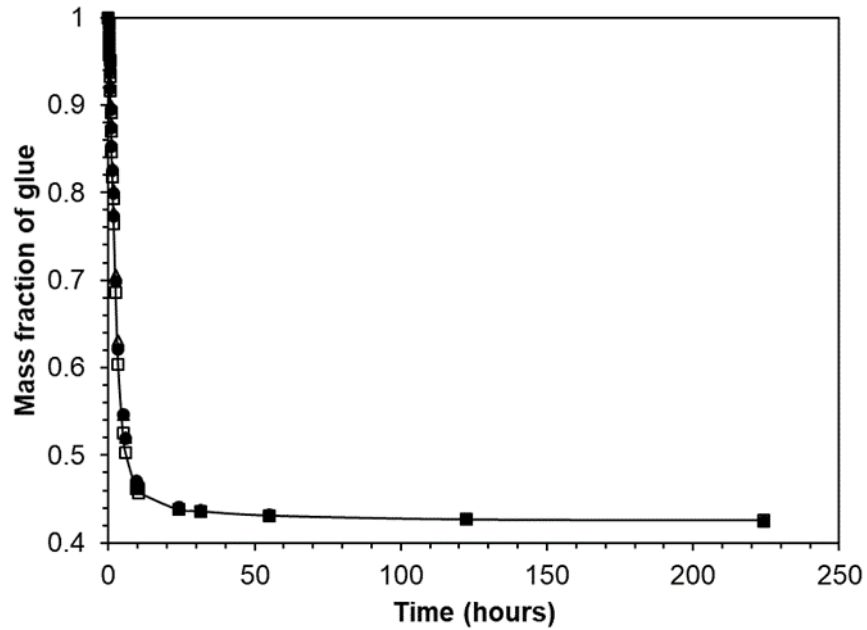


Figure 3.18 Glue mass fraction calibration curve

### 3.4.4 Saturated and unsaturated triaxial tests

Triaxial tests were carried out on all the selected materials (CKD, sand and sand-CKD mixture). The tests that were performed on CKD were Consolidated drained (CD), Unconsolidated undrained (UU), Consolidated Undrained with pore water pressure measurements (CU) and unsaturated drained shear strength tests. The triaxial tests that were carried out on sand and sand-CKD were UU and CU tests. Table 3.4 summarises the test types in this study.

Table 3.4 Summary of the triaxial tests

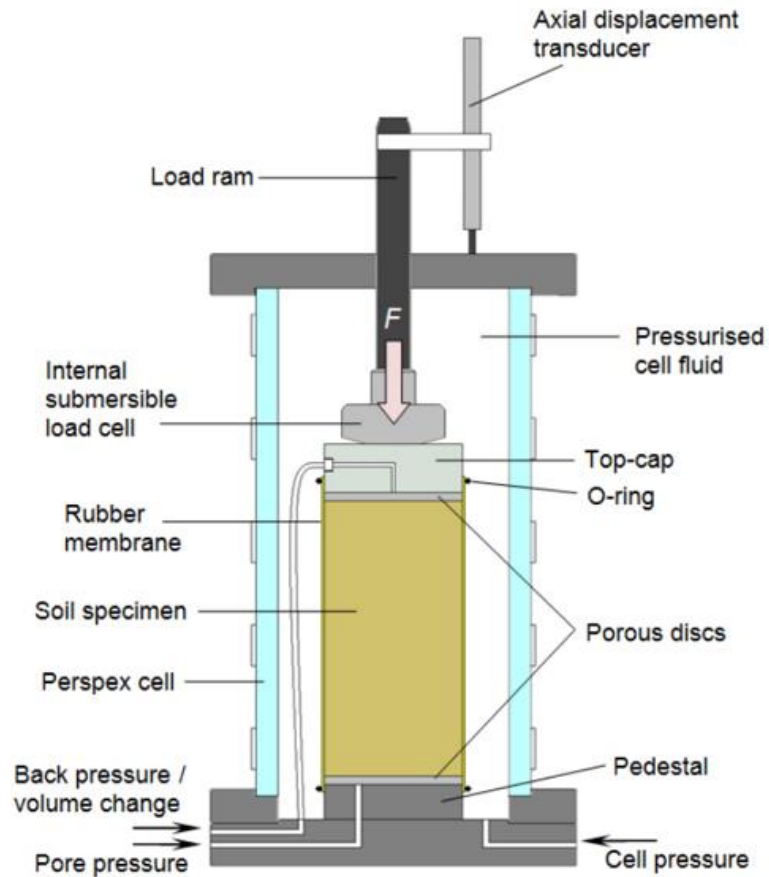
Material	Triaxial test type			
	UU	CU	CD	Unsaturated (drained)
CKD	Yes	Yes	Yes	Yes
Sand	Yes	Yes	-	-
Sand-CKD	Yes	Yes	-	-

### **3.4.4.1 Conventional Triaxial shear Tests**

All tests were conducted using conventional GDS triaxial testing apparatus. The primary components of the testing system are shown in Figure 3.19.

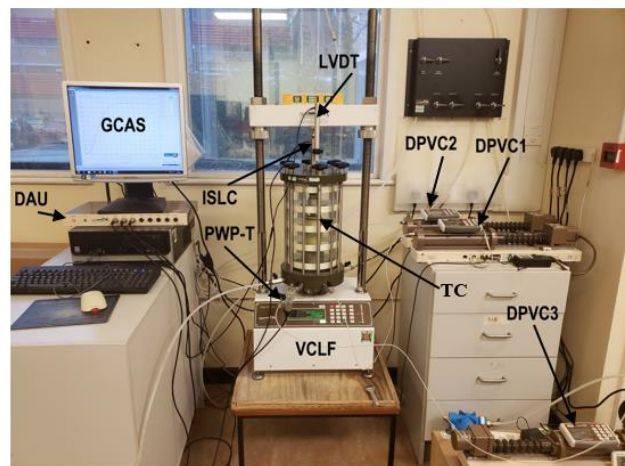
#### **3.4.4.1.1 Specimen preparation for conventional triaxial tests**

For the cement kiln dust, statically compacted specimens (50 mm dia and 100 mm high) were prepared using a triaxial sample mould. The inner surface of the mould was lubricated with silicone grease to reduce the friction between the wall and specimen during the extraction process. The samples were prepared at water contents corresponding to the optimum water contents. The material-water mixture was placed in the mould using a spoon and the surface was levelled. Static pressure was applied at a rate of 1.25 mm/min to achieve the desired density. The components of mould and compaction setup are shown in Figure 3.20.



(a)

- TC: Triaxial cell
- DPVC1: Digital pressure/volume transducer-cell pre.
- DPVC2: Digital pre. / vol. transducer-back/top pre.
- DPVC3: Digital pre. / vol. transducer-bottom pre.
- ISLC: Internal submersible load cell
- LVDT: Linear variable displacement transducer
- PWP-T: Pore water pressure transducer
- VCLF: Velocity-controlled load frame
- DAU: Data acquisition unit
- GCAS: GDSLAB control and acquisition software



(b)

Figure 3.19 Triaxial shear test set up (a) a schematic layout of the device (reproduced from Rees 2013); (b) a photograph of the experimental setup.



(a)



(b)

Figure 3.20 Triaxial compaction mould (a) a photograph of the components; (b) a compaction setup

Attempts were made to prepare sand and sand-CKD specimens by applying static compaction pressure, however the required densities of the specimens could not be achieved. Therefore, in these cases a three-split mould with an inner diameter of 50 mm (Figure 3.21) was used for preparing specimens. The specimens were prepared directly on the triaxial device starting by placing a filter paper and pre-boiled porous stone on the base pedestal. A rubber membrane was fixed on the base to accommodate the material mixture and to seal the specimen from the chamber around it and secured with O-rings. The membrane was worked onto the split mould. The upper end of membrane was folded on the mould. A predetermined quantity of material-water mixture was filled in layers inside the membrane fitted inside the mould. Each layer was compacted using a tamping rod until achieving the full height of the mould. Subsequently, a porous stone and a Perspex cap were positioned on top of the specimen and the membrane was then sealed on the top cap using rubber O-rings.

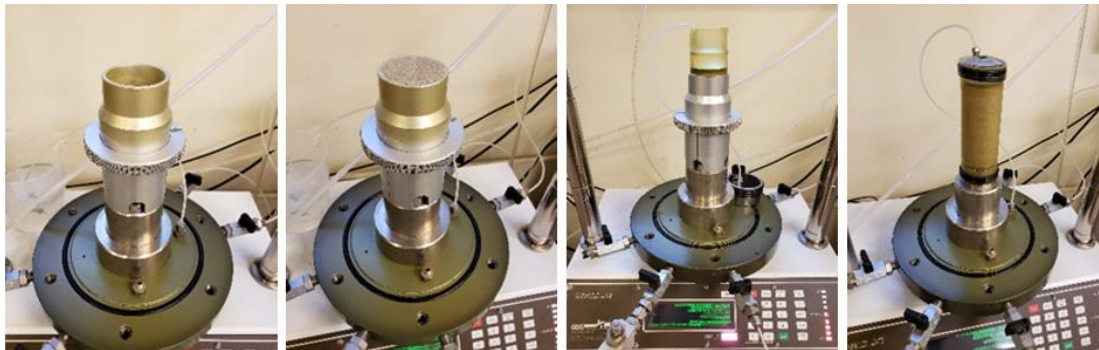


Figure 3.21 Steps for preparing sand and sand-CKD specimens

#### 3.4.4.1.2 Testing procedure (CD, UU and CU tests)

BS 1377-8 (1990) was followed for conducting the CD and CU tests that suggests four main stages, such as specimen and system preparation, saturation, consolidation and shearing. For the UU test, saturation and consolidation stages were not required (BS 1377-7 1990).

#### 3.4.4.1.2.1 Specimen and system preparation

Prior to placing the compacted specimens of CKD or preparing the sand and sand-CKD specimens on the pedestal, all the deaired water-filled pressure/volume controllers and pore pressure transducer were connected to the triaxial cell base and connections were also flushed and filled with de-aired water. For the specimens of CKD, a saturated porous stone and filter paper were then placed on the top of the pedestal of the triaxial cell base and the compacted specimens prepared according to the procedure mentioned in Section (3.4.4.1.1) were subsequently positioned on the filter paper disk. The specimen was then enclosed with a latex rubber membrane which was slid over the specimen with assistance of a membrane suction stretcher. Another porous stone and filter paper were placed between the loading cap and top of the specimen. The latex rubber membrane was secured with rubber O-rings at the cap and the base. The triaxial cell chamber was placed over the base and fixed to it and filled with de-aired water.

#### 3.4.4.1.2.2 Saturation stage

The saturation process is designed to ensure that all voids within the specimen are filled with water and this is achieved by raising the pore-water pressure in the specimen to a level high enough for the water to fill the pores (BS 1377-8 1990). In order to check the saturation level of the specimen, the pore-water pressure parameter,  $B$ , is determined periodically. The pore-water pressure parameter,  $B$ , is defined as the ratio of a change in pore-water pressure to a change in the confining pressure (Eq. 3.8).

$$B = \frac{\Delta u}{\Delta \sigma_3} \quad (3.8)$$

where  $\Delta u$  = pore-water pressure change after the increment of confining pressure and  $\Delta \sigma_3$  = increment of confining pressure.

The GDSLAB control and acquisition software used in this study allowed a selection of an automatic saturation to be applied to a test specimen. The specimens were saturated by applying increments of cell pressure,  $\sigma_3$  and back pressure,  $u_w$  maintaining a net confining pressure ( $\sigma_3 - u_w$ ) of 10 kPa to prevent significant swelling of the specimens. Saturation process was considered completed once the required pore-water

pressure parameter B value was reached. For the CKD specimens, the saturation process typically took 6 to 7 hours and back pressure of about 650 kPa were required for achieving B value of 0.95 proposed by Head and Epps (2014). While B values of 0.9 and 0.82 were attained under back pressures ranged between 950 and 1000 kPa within an elapse time ranged between 3 and 5 hours for the sand-CKD and sand, respectively.

Black and Lee (1973) carried out an extensive study to investigate the relationship between pore pressure parameter, B and degree of saturation as shown in Figure 3.22. The soils were divided into four categories (Table 3.5). It can be observed that B value of about 0.7 or higher corresponds to a degree of saturation of greater than 95% for most of soils.

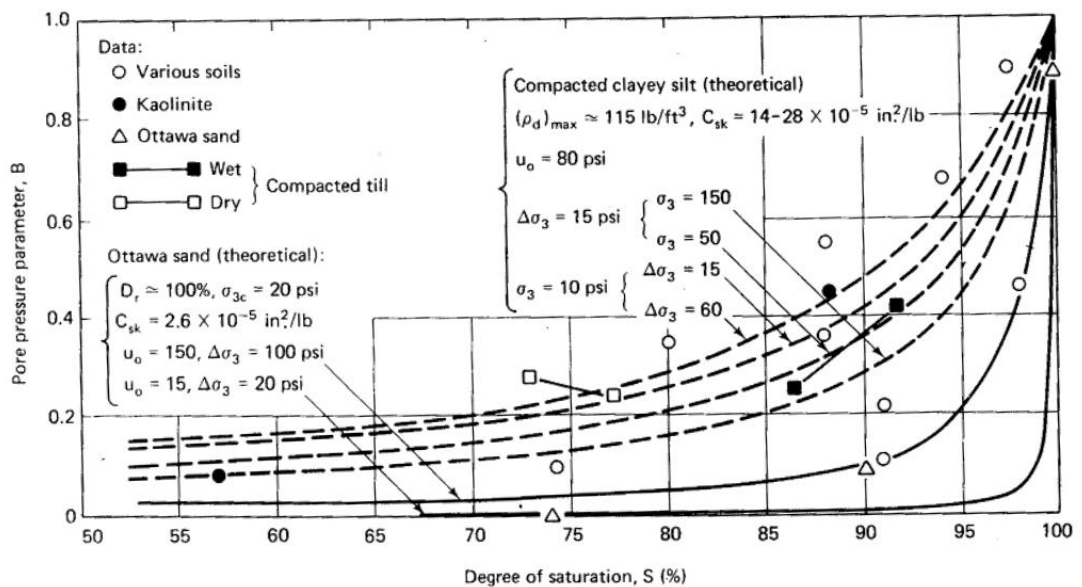


Figure 3.22 Relationship between pore pressure parameter B and degree of saturation (reproduced from Black and Lee 1973)

Table 3.5 B values for different soils at complete or nearly complete saturation  
(reproduced from Black and Lee 1973)

Soil type	Saturation		
	100%	99.5%	99%
Soft normally consolidated clays	0.9998	0.9920	0.9860
Medium (compacted clays)	0.9988	0.9630	0.9390
Stiff (Stiff clays-sands)	0.9877	0.6900	0.5100
Very stiff (very high consolidated pressure)	0.9130	0.2000	0.1000

#### 3.4.4.1.2.3 Consolidation stage

Upon completion of the saturation process, the specimens were isotropically consolidated to the designated net confining pressures,  $(\sigma_3 - u_w)$ . Saturation and consolidation stages were not applicable for UU tests. For CU and CD tests, the cell pressure was increased while maintaining a constant back pressure equal to the pore pressure reached during the final saturation stage. For each material and each test type, three tests were conducted at different confining pressures (100, 200 and 400 kPa) representing various field conditions (e.g. different fill heights). The confining pressures were applied using the pressure/volume controllers. During the consolidation process, the pore-water pressure of the specimen was monitored by the pressure transducer while the pore-water volume change of the specimen was measured by the volume controller. This process was continued until there was no longer significant pore-water volume change and the excess pore-water pressure had dissipated (Thu et al. 2006).

#### 3.4.4.1.2.4 Shearing stage

The specimens in UU and CU tests were sheared in compression at a strain rate of 1.0 mm/min (Sreekrishnavilasam and Santagata 2006; Varathungarajan et al. 2009) and these tests were continued until reaching 20% axial strain. In order to study the effect of strain rate, additional cement kiln dust specimens were sheared at a strain rate of 0.083 mm/min (Bishop and Henkel 1962; Wasemiller and Hoddinott 1997; Bensoula et al. 2015). This deformation rate was selected in order to stabilise the pore-water pressure generated throughout the specimens. All tests were continued until reaching 20% axial strain (Brandon et al. 2009).

The CD tests on CKD specimens were carried out up to an axial strain of 20% with a slow shear rate of 0.0009 mm/min in order limit the pore water pressure development to small values during the shearing process. This strain rate has been adopted by several researchers (Rahardjo et al. 1995; Rahardjo et al. 2004; Thu et al. 2006; Guan et al. 2010; Goh et al. 2015). Additionally, the properties (i.e. fine contents, saturated permeability, and plasticity index) of the CKD used were similar to those of the soils tested in the reported studies.

Following the shearing stage, all the relevant pressures were released, and the cell was disassembled. The specimens were dismantled from the pedestal and the final water contents were determined. All triaxial tests were conducted immediately after compacting the specimens (i.e., without curing) due to the limited reactivity of CKD. The test results obtained from these tests are presented in Chapter 7.

#### **3.4.4.2 Permeability tests in a triaxial test set up**

The saturated permeability of the materials was measured using triaxial compression device under a constant hydraulic gradient and under different net confining pressures (BS 1377-6 1990). The test set up (Figure 3.20) mainly consisted of a triaxial apparatus and three digital pressure/volume controllers (DPVC). These digital controllers were used for applying and maintaining the desired pressures in the cell fluid and the drainage lines to the top and bottom of the specimen. Five different net confining pressures were selected for the saturated permeability tests (Table 3.6) in order to study the effects of net confining pressure on the saturated permeability of the materials.

Compacted specimens of the materials were prepared at the maximum dry unit weight and optimum moisture content with the procedures described in Section (3.4.4.1.1). The saturation and consolidation processes remained the same as that of CD and CU triaxial tests as described in Section (3.4.4.1.2).

After consolidating the specimens to the targeted effective confining pressures, the pressures at the bottom of the specimens were maintained at specified/constant values and the pressures at the top were increased in order to obtain the desired pressure difference across the specimen. Therefore, water was made to flow downward through the specimens. The pressures at the top and bottom were applied and controlled by the

DPVCs. Various pressure differences were used for producing a reasonable rate of flow through the specimens. The pressure differences adopted for CKD, sand and sand-CKD were 20, 5, and 7 kPa respectively.

The tests were terminated when the flow rates were constant for a given period of time. The specimens were then consolidated to a higher effective confining pressure and the same the procedures were repeated several times in order measuring the permeability of the materials under higher effective confining pressures.

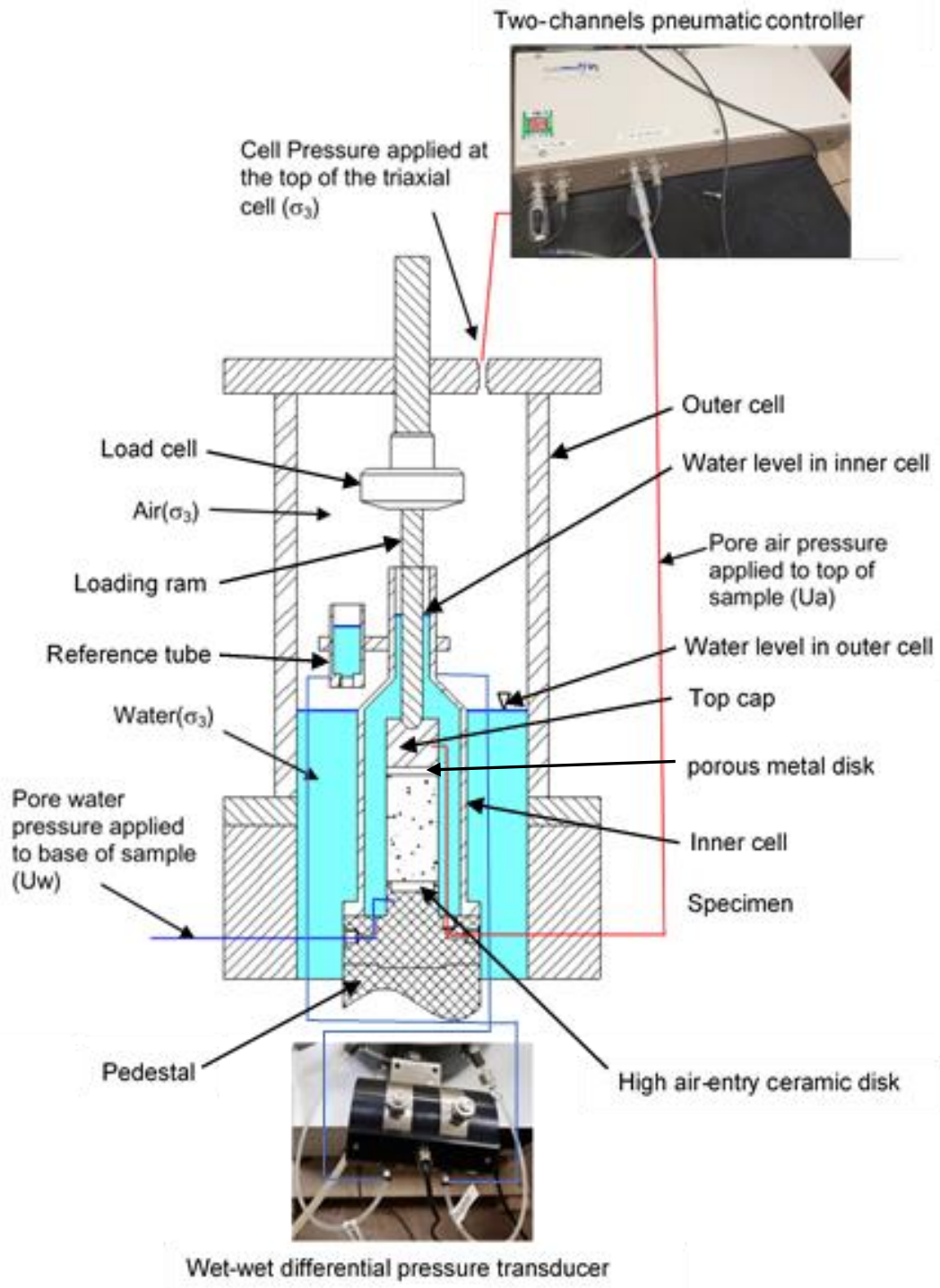
Table 3.6 The confining pressures and hydraulic gradients used for determining the coefficient of permeability of CKD, sand, and sand-CKD.

Material	Cell pressure (kPa)	Top pressure (kPa)	Bottom pressure (kPa)	Effective cell pressure (kPa)	Pressure difference (kPa)	Hydraulic gradient
Cement kiln dust	45			25		
	70			50		
	120	20	0.0	100	20	20.6
	220			200		
	420			400		
Sand	27			25		
	52			50		
	102	2	0.0	100	2	2
	202			200		
	402			400		
Sand-CKD	32			25		
	57			50		
	107	7	0.0	100	7	7.2
	207			200		
	407			400		

### **3.4.4.3 Unsaturated triaxial shear tests on CKD**

Suction-controlled unsaturated triaxial tests were carried out on compacted specimens of CKD at a net confining pressure of 25 kPa using an automatic GDS triaxial apparatus. The main unsaturated testing module used in this study was the 4-dimensional stress/strain path. In this module, the stress path provides simultaneous control of the axial stress, radial stress, pore air pressure and pore water pressure while the strain path allows independent linear control of the axial strain, radial stress, pore air pressure and pore water pressure (GDS Instruments Ltd 2013).

Figure 3.23 shows the GDS triaxial testing system. The system comprises a triaxial cell (outer cell), two pressure controllers, six transducers, a digital transducer interface, an inner cell, base pedestal containing a high air-entry ceramic disk, a load frame and a computer. Descriptions of various components are presented in Table 3.7.



(a)



(b)

Figure 3.23 Unsaturated triaxial test set up (a) A schematic of the test system (Adapted from GDS Instruments Ltd 2012) and (b) a photograph of the experimental setup

Table 3.7 Descriptions of the main components of GDS triaxial testing apparatus.

Component No.	Component	Description/Function
1	Outer triaxial cell	Is a Bishop & Wesley stress-path cell (Bishop and Wesley 1975).
2 & 3	Two independent GDS pressure controllers	One of them (No.2) is an automatic pneumatic regulator with two channels for controlling the cell pressure in both the inner and outer cell cavities and for controlling the pore air pressure in the specimen, while the other one (No.3) is a digital hydraulic pressure/volume controller
4, 5, 6, 7, 8 & 9	Six transducers	<ul style="list-style-type: none"> <li>• A load cell (No.4) to measure the axial force,</li> <li>• A linear variable displacement transducer (LVDT) (No.5) to measure the axial displacement,</li> <li>• A wet-wet differential pressure transducer (DPT) (No.6) (a component of the total volume change measuring system).</li> <li>• And three other pressure transducers for monitoring the cell pressure (No.7), the pore air pressure (No.8) and the pore water pressure (No.9).</li> </ul>
10	Digital transducer interface (DTI)	For data acquisition from the six transducers
11	Inner cell	In which the specimen is placed. This enables the cell volume change to be measured from just the inner chamber minimising the error due to temperature and pressure changes.
12	Base pedestal with high air-entry ceramic disk	The ceramic disk is used to separate the pore-air and the pore water pressures and to support a maximum air/water pressure difference equal to the air-entry value
13	A triaxial load frame	Used to apply axial loads to the triaxial cell piston with a constant strain rate.
14	GDSLAB software	Used to log the data from all the GDS units and control tests

#### **3.4.4.3.1 Control of matric suction**

The axial translation technique (Hilf 1956) is used in the GDS unsaturated triaxial testing apparatus for imposing matric suction in specimens. The pore-air pressure was applied through a coarse low air-entry disk placed on top of the specimen. The porous metal has a low AEV to allow air to go through and fill up the entire pores in the porous metal once the AEV is exceeded. The porous metal was connected with the air pressure line through the top cap and pedestal and subsequently were connected to the pore-air pressure control line. The pore-water pressure was applied through a saturated high air-entry ceramic disk sealed to the base pedestal of the triaxial apparatus. The ceramic disk was 50 mm in diameter, 6.9 mm in thickness and with air entry value of 500 kPa. When the matric suction of specimen is less than the air entry value, the free air cannot penetrate the saturated ceramic disk but the dissolved air can pass through the ceramic disk with water. The dissolved air may accumulate underneath the high air-entry ceramic disk, leading to the formation of air bubbles during a long period of testing.

#### **3.4.4.3.2 Saturating a high air-entry value ceramic disk**

In testing unsaturated soils, the high-air entry ceramic disk plays an important role and represents a basic mean in separating pore-air and pore-water pressures (Fredlund et al. 2012). Higher air pressure will be maintained than water pressure when the ceramic disk is saturated. Therefore, before conducting any unsaturated test, the high air-entry value ceramic disk must be well saturated for minimising the amount of air bubbles trapped inside the disk and to support a maximum air/water pressure difference equal to the air-entry value. The saturation procedure suggested by Fredlund and Rahardjo (1993) was adopted to saturate the ceramic disk in this study.

The saturation process commenced with applying a small positive water pressure of 30 kPa to the underside of the ceramic disk and this step continued until the top surface of the ceramic disk was pooled. This stage has normally been completed in two to four hours. Then, the cell was filled with de-aired water and high air pressure of 500 kPa was applied in normal direction whereas leaving the pore water pressure connector close. Applying high air pressure assisted in expelling the air in the ceramic disk with water flowing with a high gradient and dissolving any air bubbles left in the water. The high

pressure was maintained for one hour and then the valve connecting the pore pressure connector was then opened to the atmosphere for removing air bubbles collected under the ceramic disk (water compartment) and the water containing the dissolved air. Removal of air bubbles and diffusive air was achieved by flushing the compartment by applying 30 kPa of water pressure using a pressure/ volume controller. The valves connected to the water compartment were then closed, and the pressure in the ceramic disk was built up to the pressure in the cell. The above procedure should be repeated for at least five times if the ceramic disk was newly installed. After saturation was completed, the cell pressure was dissipated to zero and the ceramic disk was left covered with water until a specimen was ready to be placed on the disk. After each test, the high air entry ceramic disk was saturated, and it normally took twenty-four hours to accomplish the task compared to a few days for a newly mounted disk.

Prior to each new test, the measurement of saturated water permeability of ceramic disk was carried out to check any possible cracking of the ceramic disk that might have occurred during the previous tests (any cracking will lead to a significant increase in the water permeability of the disk) or to check the saturation of the ceramic disk. The procedure to that described in Section (3.4.3.1.2) was followed to measure the permeability of ceramic disk. The average saturated water permeability of ceramic disk in this part was around  $3.8 \times 10^{-10}$  m/sec. This value was similar to that of pressure plates with 5-bar ceramic disks (Section 3.4.3.1.2).

#### **3.4.4.3.3 Measurement of total volume change**

For measuring accurately the total volumetric changes of the unsaturated soil specimens that occur during the testing, a special device developed by Ng et al. (2002) was used. The basic aim of the measuring device is that the total volume change in an unsaturated specimen is measured by recording the differential pressures between the water inside an open-ended, bottle-shaped inner cell and the water inside a reference tube employing a high-accuracy wet-wet differential pressure transducer (DPT). The inner cell is fixed onto the base pedestal of the outer cell in the triaxial apparatus. The high-accuracy DPT is connected to the inner cell and to a reference tube for recording changes in the differential pressure between the water pressure change inside the inner cell due to a volume change in the specimen and the constant water pressure in the reference tube.

#### **3.4.4.3.4 Testing procedure (Unsaturated triaxial tests)**

Prior to setting up the compacted specimen for conducting the unsaturated drained triaxial testing, the digital hydraulic pressure controller was flushed and then filled with fresh de-aired water. The high air entry value disk was saturated, and any excess water left on it was removed. Furthermore, all the water lines associated with the measurement of water volume were flushed with fresh de-aired water.

Compacted specimens of the CKD were prepared with the same procedure as mentioned in Section (3.4.4.1.1). The initial dimensions and weight of the specimen were measured just before placing it on the pedestal. A rubber membrane was slid over the specimen by using a membrane stretcher. The low air entry a coarse metal disk and the top cap was then positioned on the top of the specimen. Subsequently, the membrane was then sealed at the top cap and the base pedestal by rubber O-rings. The air pressure line was then connected to the top loading cap for applying matric suction on the specimens (Figure 3.24).

On completion of the specimen installation on the base pedestal, the bottle-shaped inner cell was then placed on the base pedestal and all connections were fitted. Thereafter, the inner cell and reference tube were filled with de-aired water to an appropriate water level within the necked part and all the tubes and fittings between the inner cell and the differential pressure transducer were flushed concurrently to prevent any air entrapment in the system that could affect the results. The outer cell with the loading ram was then placed in position, and it was partially filled with de-aired water (see Figure 3.24). A contact between the loading ram and the specimen cap was then achieved.

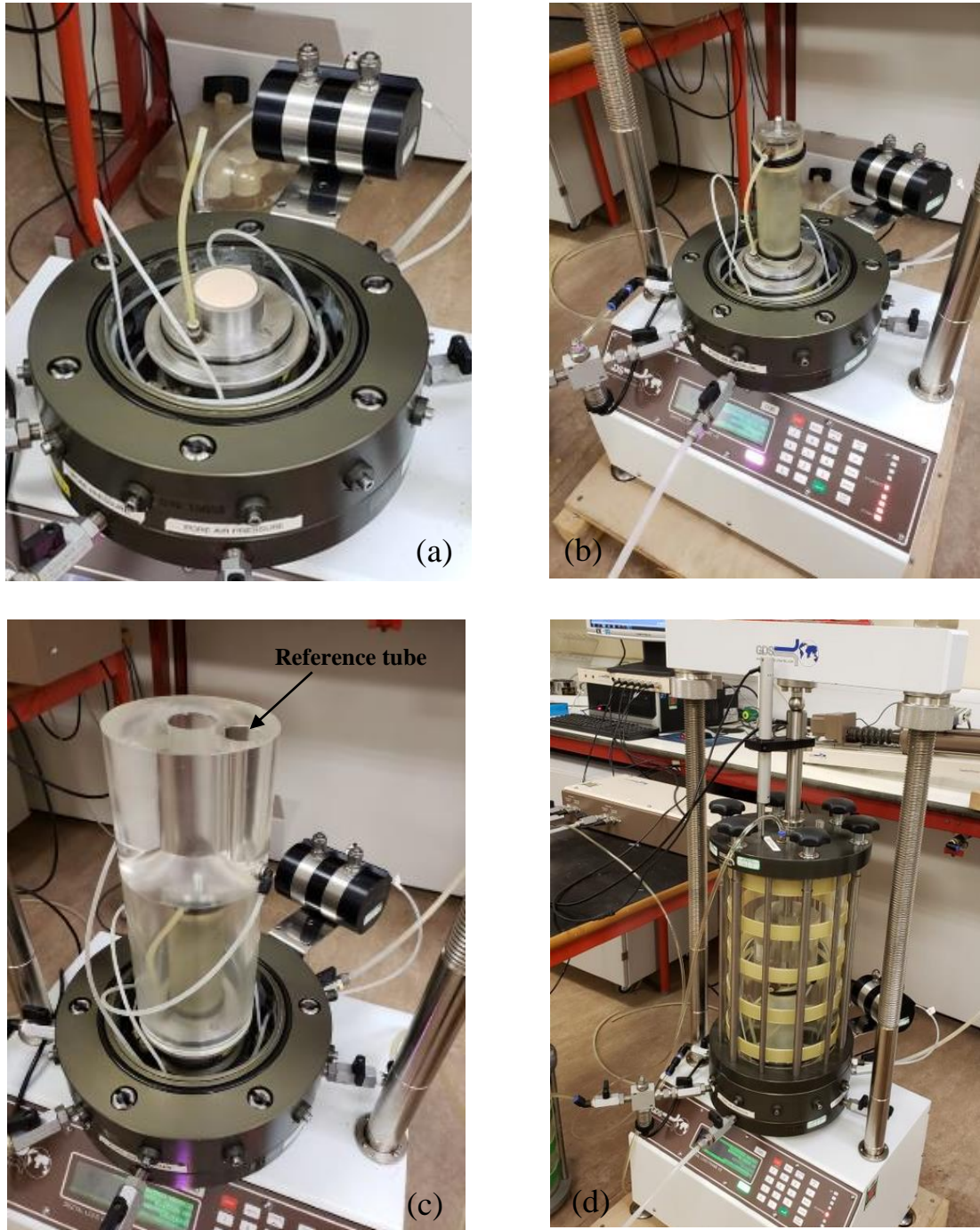


Figure 3.24 A photograph showing a CKD specimen in unsaturated triaxial test and the inner cell.

#### 3.4.4.3.4.1 Matric Suction equalisation stage

On completion of placing the specimen and installations of the inner and outer cells assemblies, the matric suction equalisation stage was undertaken. The axis-translation technique was used during the test in order to control the matric suction of specimens. A net confining pressure (25 kPa), pore air pressure and pore water pressure were applied to the specimen. Based on the WP4-C measurement, the average initial total suction of CKD specimens was about 2040 kPa, whereas the average matric suction measured using MPS-6 sensor was about 100 kPa.

The specimens were wetted by reducing the initial suction to various matric suction values ranging from 150 to 0 kPa. The amount of water inflow/outflow from the specimen during suction equalisation was recorded by the DPVC. The suction equalisation was considered to be completed when the rate of change of water volume and the change in the specimen volume was less than 0.1 cm<sup>3</sup>/day (Sivakumar 1993; Sharma 1998; Estabragh and Javadi 2008; Jie 2011; Ng et al. 2012; Qian et al. 2012; Zhang et al. 2015; Ma et al. 2016).

#### 3.4.4.3.4.2 Shearing stage

When an equilibrium condition was achieved under the applied net confining stress, ( $\sigma_3 - u_a$ ) of 25 kPa and matric suction ( $u_a - u_w$ ) of various values, the specimen was sheared by increasing the axial load at a constant strain rate. The shear rate should be sufficiently slow to avoid nonuniformity in the pore-water pressure distribution within the specimen throughout the shearing process (Ho and Fredlund 1982; Sun et al. 2016). Both pore-air and pore-water phases were in a drained condition and were maintained at the same pressures as the pressures before the shearing started. A strain rate of 0.0009 mm/min was used as adopted in the CD tests Section (3.4.4.1.2). The maximum axial strain was limited to 20 %. This rate is equivalent to shear time about 22200 mins in the GDSLAB software. Observations during testing confirmed that the shear rate chosen was slow enough to avoid generating excess pore-water pressure in the specimens.

The shearing stage was terminated when the maximum axial strain was reached, which took approximately 15 days. Subsequently, the specimens were unloaded and all the pressures were released. The specimens were dismantled from the triaxial cell, and

the final water content of the specimens were obtained. All the measurements, e.g. pore-air pressure, pore-water pressure, total and water volume changes, applied load, and displacement were automatically recorded using the acquisition programme via the connected PC.

#### **3.4.4.4 Suction-controlled oedometer tests**

Figure 3.25 shows photographs of the suction-controlled oedometer used in this study. The layout is designed for the axis translation technique. The main components of the set up are the unsaturated consolidation cell developed by Wille Geotechnik, Germany, a digital pressure/volume controller, a pressurised air panel, a load cell and a linear variable displacement transducer. The oedometer cell consists of two cylindrical parts, the lower cylinder is fitted with a 500 kPa high air-entry value ceramic disk, a grooved water compartment and a flushing system comprised of inlet and outlet connections equipped with needle valves. The water compartment under the ceramic disk serves to keep the disk saturated and to facilitate the flushing of diffused air. A stainless-steel specimen ring (71.4 mm diameter and height of 20 mm) can be assembled on the top of the ceramic disk. The upper part of the cell is designed to facilitate the application of desired vertical pressures. It consists of two external ports (with needle valves), a low friction stainless steel load piston equipped with a bracket for strain transducer and a porous metal disk fitted to the end of load piston.

The suction-controlled oedometer enables the determination of water retention characteristics curves in the wetting and drying processes as well as scanning drainage and scanning imbibition cycles. The effect of net stress on the behaviour of the WRC can be determined for simulating the overburden pressure. Additionally, the vertical deformation of the specimen can be tracked and several points along the water retention characteristic curve can also be obtained without dismantling the cell (Lins et al. 2009).

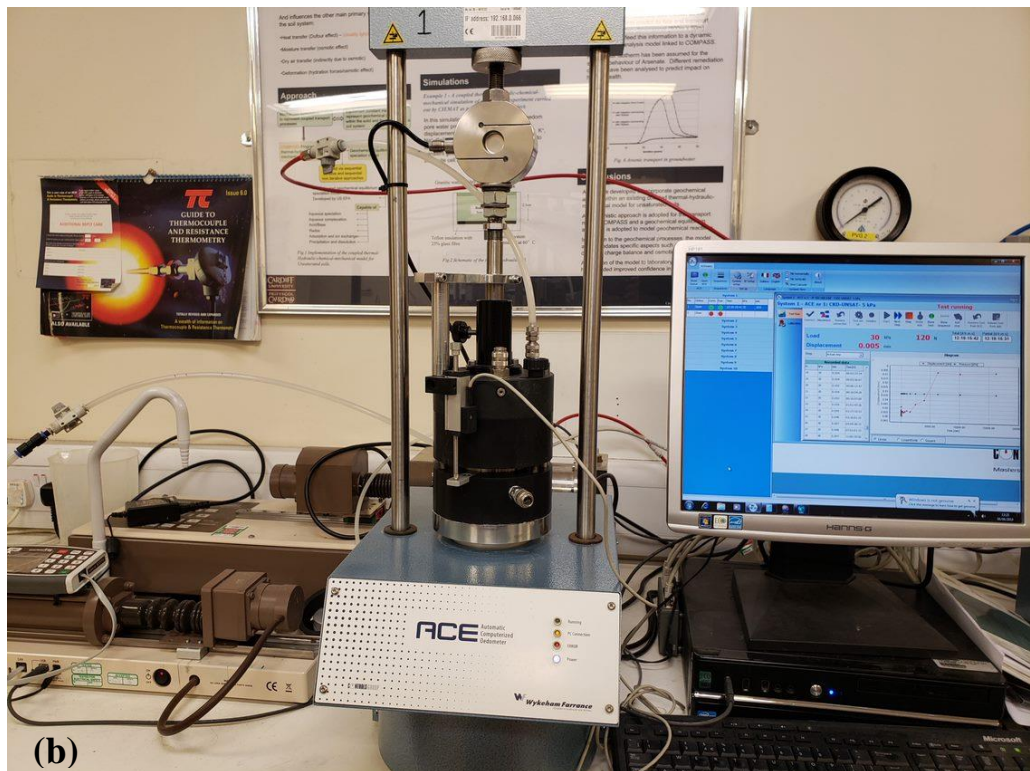
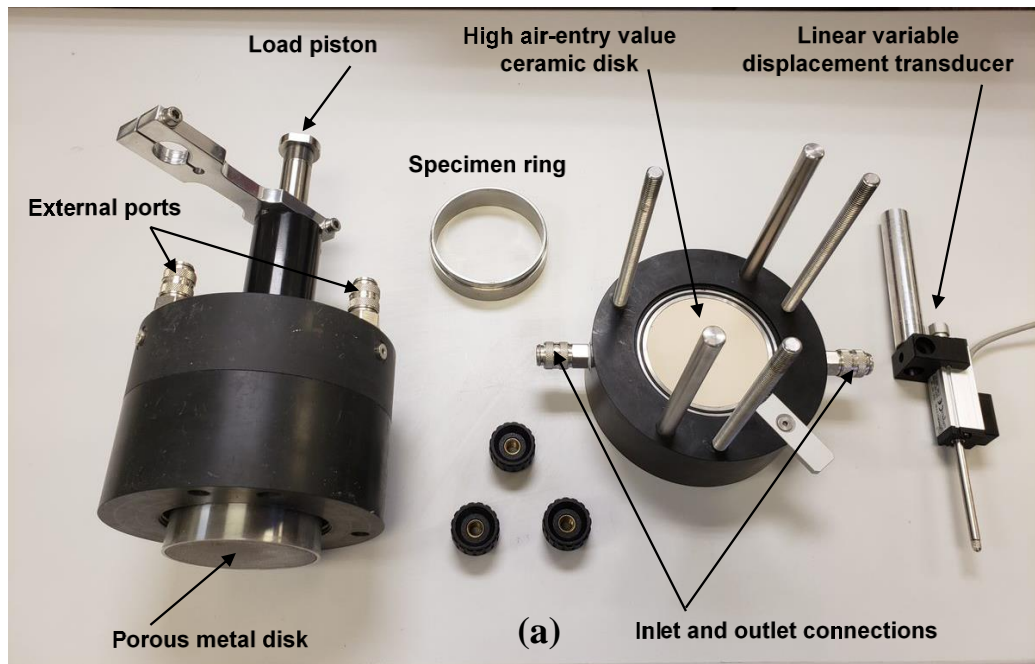


Figure 3.25 Suction-controlled oedometer test: (a) components of the unsaturated consolidation cell; (b) experimental setup of test.

#### **3.4.4.4.1 Testing procedure (suction control oedometer tests)**

Suction-controlled oedometer tests were conducted on specimens of the CKD. The specimens (71.4 mm diameter and 15 mm thick) were compacted inside the stainless-steel specimen ring. The specimens were prepared by following the procedure described in Section (3.4.2.1) at initial conditions corresponding to the optimum water content and maximum dry unit weight of 27.3% and 14.83 kN/m<sup>3</sup>, respectively.

For achieving the water phase continuity between the specimen bottom and the compartment water and supporting a maximum air/water pressure difference, the ceramic disk must be saturated. Different procedures were suggested in the literature for saturating ceramic disks (Fredlund and Rahardjo 1993; Leong et al. 2004; Tripathy et al. 2012; Sivakumar 2014). In this study, the saturation process of the ceramic disk was conducted by pressurising the ceramic disk covered with water. This process started with applying small positive pressure of 30 kPa to the underside of the ceramic disk for few hours and then, the cell ring was fitted above the ceramic disk and filled with de-aired distilled water. Afterwards, air pressure of 50 kPa was applied for several days and the water compartment beneath the ceramic disk was regularly flushed with the de-aired distilled water.

For ensuring saturation of ceramic disk and checking for no cracks, permeability measurement of the disk was carried out following the procedure described in Section (3.4.3.1.1). The average saturated coefficient of permeability was found to be  $2.98 \times 10^{-10}$  m/s. This value was found to be similar to that of pressure plates with 5-bar ceramic disks (Section 3.4.3.1.2).

On completion of the saturation process and permeability measurement, the ceramic disk was first wiped by a wet towel to provide water phase continuity and the compacted specimen was then placed on the saturated ceramic disk. A filter paper was used in the bottom of the specimen to avoid fine material particles being trapped inside the pores of the ceramic disk. Both the two cylindrical parts (the upper and lower parts) were assembled and positioned in the automatic loading frame (used to apply the vertical stress directly to the loading ram) and a linear variable displacement transducer (LVDT) was fitted by a mounting bracket fixed on the loading ram. The lid of the LVDT was placed in contact with the bottom base to measure the vertical displacement. Subsequently, the regulated compressed air system was connected to the top of the cell.

Wetting tests were performed on specimens of the CKD by imposing different suctions ranging from 150 to 0 kPa at constant net stress of 25 kPa. The initial suction was reduced directly to a target suction level, while the water in the compartment beneath the ceramic disk was kept at zero pressure by digital pressure/volume controller. The piston rod was directly loaded via the ACE automatic loading frame to achieve the constant net normal stress. Multiple specimens were required for covering the range of suctions considered in this study. During the test, deformation and water volume change were measured by the LVDT and DPVC and recorded using the ACE and GDSLAB softwares, respectively. An equilibrium was assumed to be reached under the desired suction when no more water moves out of or into the specimen for a period of at least 24 hours. After the completion of the test, the cell was dismantled and the specimen was removed from the device and oven dried to measure the final water content.

### **3.5 Concluding remarks**

In this chapter, the physical properties, chemical composition and mineralogy of the materials used were presented (Tables 3.1 and 3.2). The microstructural investigations enabled visualising the particle sizes. The procedures for preparing specimens, various devices and test set ups that were used for testing the specimens and the techniques along with the working principles of various devices and the operating procedures of equipment were described in detail.

An extensive experimental programme was considered to study the hydro-mechanical behaviour of cement kiln dust, sand and sand-cement kiln dust mixture. One-dimensional oedometer tests were conducted to explore the swelling and compressibility behaviour of the cement kiln dust. The water retention tests were carried out on all the chosen materials using various devices. The clod tests on cement kiln dust were carried out to explore the volume change during the drying process. A series of saturated shear strength and triaxial permeability tests on the materials were carried out. Unsaturated shear strength triaxial tests were also carried out on the cement kiln dust at several suctions. Suction-controlled oedometer tests were conducted to investigate the volume change behaviour of cement kiln dust under a predetermined net stress.

## **CHAPTER 4**

# **One-dimensional swelling and compressibility behaviour of cement kiln dust**

### **4.1 Introduction**

Determination of swelling and compressibility behaviour of particulate systems (soils, admixed soils, industrial wastes) are necessary due to their use in various geotechnical and geoenvironmental applications (Sridharan and Nagaraj 2000; Sridharan and Gurtug 2005; Nagaraj et al. 2010). Volumetric changes may cause undesirable effects on the stability of the civil engineering structures. The swelling behaviour of expansive materials is affected by several factors, such as the type and amount of expansive minerals and exchangeable cations, dry density, water content, soil structure, and loading conditions (Seed et al. 1962; Sridharan et al. 1986). Similarly, the compressibility behaviour is influenced by the type of material, fabric and structure, overconsolidation effects, water content, dry density and pore-size distribution (Tripathy and Schanz 2007).

Most studies in the past have used cement kiln dust (CKD) as an admixture to treat problematic soils (expansive clays, highly compressible and collapsible soils) (Miller et al. 1997; Keerthi et al. 2013; Nasr 2015). The collapse potential of soils was found to decrease upon using CKD as a stabiliser additive (Miller et al. 1997; Al-Refeai and Al-Karni 1999; Noorzad and Pakniat 2016). Similarly, an addition of CKD to expansive soils was found to decrease the swelling potential (Sayah 1993; Parsons, Kneebone and Milburn 2004; Iorliam et al. 2012; Sabat and Pati 2014; Salahudeen et al. 2014). An attempt has also been made to explore the one-dimensional compression behaviour of specimens of the dry landfilled and fresh CKD powders. The results indicated that the compressibility of the dry landfilled CKD was over two times greater than that of the fresh CKD even at low stresses (Sreekrishnavilasam and Santagata 2006).

A review of the literature indicated that research associated with the volume change behaviour of compacted CKD is very limited. Similarly, the compressibility

characteristics of CKD influenced by the initial conditions (saturated and compacted) are not very well understood. Unsaturated compacted CKD may exhibit swelling upon imbibition of water due to the presence of various cations and significant percentages of fine-size fractions. Similarly, due to the presence of fine particles, saturated CKD may exhibit significant settlement. These aspects need further investigations.

The objectives of this chapter are:

1. To experimentally determine the one-dimensional swelling behaviour of the CKD used at various applied pressures and the swelling pressure under constant volume condition.
2. To study the influence of initial conditions of the CKD (saturated slurried and compacted saturated) on the compressibility characteristics and permeability for a range of applied vertical pressures in  $K_0$ -condition.

## **4.2 Experimental programme**

One-dimensional swelling and compression tests were conducted on compacted saturated and initially saturated slurried CKD specimens. The saturated slurried specimen was prepared at an initial water content of 1.2 times the liquid limit of the CKD. The specimen was stepwise loaded to 800 kPa and then unloaded (Section 3.4). Consolidating the specimen under pressure increments up to 800 kPa was performed in order to explore the consolidation behaviour of slurried cement kiln dust under a wide range of loading conditions. The compacted CKD specimens were prepared at dry unit weight and water content of 14.83 kN/m<sup>3</sup> and 27.3% respectively. The compaction conditions were corresponding to the standard Proctor optimum conditions (Section 3.4).

For the one-dimensional swelling tests on compacted CKD specimens, the specimens were firstly hydrated with water at an initial pressure of either 2 kPa or 25 kPa. Once the swelling strains attained an equilibrium, the saturated specimens were then loaded in a stepwise manner up to a vertical pressure of 1600 kPa and then unloaded. The choice of initial pressures at the time of inundation with water was based on the potential engineering applications of CKDs (e.g. as landfill cover, and as subgrade material) and the possible average in-situ overburden pressure. Similar applied pressures have been

considered by Al-Rawas et al. (2002). For the constant volume swelling pressure test (Section 3.4), a compacted specimen was hydrated at constant volume condition.

## **4.3 Results and discussion**

### **4.3.1 Swelling strain**

Figure 4.1 presents the elapsed time versus swelling strain results of the compacted CKD specimens at two different initial pressures. The swelling strains were calculated based on the change in height and the initial height of the specimens prior to the hydration process.

It can be noticed in Figure 4.1 that an increase in the swelling strain was rapid during the initial stage for the specimen with an applied pressure of 2 kPa as compared to the specimen with an applied pressure of 25 kPa. The swelling strains attained equilibrium in both cases with an elapsed time (about 23 days and 16 days under 2 kPa and 25 kPa, respectively). The swelling strains at equilibrium were found to be about 18.8 and 1.47% at applied pressures of 2 and 25 kPa respectively.

Swelling of clays occurs due to the hydration of exchangeable cations and minerals (crystalline swelling), and physico-chemical interaction between mineral, ions and water (osmotic swelling) (Van Olphen 1977; Tripathy et al. 2004; Schanz and Tripathy 2009). By considering the mineralogy and cations present in the CKD (Sections 3.3.5 and 3.3.7; Table 3.1; Figure 3.6), the swelling strains exhibited by the CKD specimens are due to the hydration of cations and physico-chemical interaction between the minerals (calcite, gypsum, smectite and kaolinite) and water. In addition, the volume change behaviour is influenced/governed by the changes in effective stress (Sridharan et al. 1974). The effective stress is defined as the sum of all the vertical components of the forces at the contact points between the solid particles in addition to the electrical attractive and repulsive forces (particularly in the highly plastic clays) per unit cross-sectional area of soil mass. The effective stress decreases due to swelling of soils (Baille et al. 2014). The applied pressure dictates the magnitude of swelling strain. A reduction in the swelling strain of the specimen at an applied pressure of 25 kPa as compared to that of the specimen with 2 kPa is attributed to an increase in the effective stress.

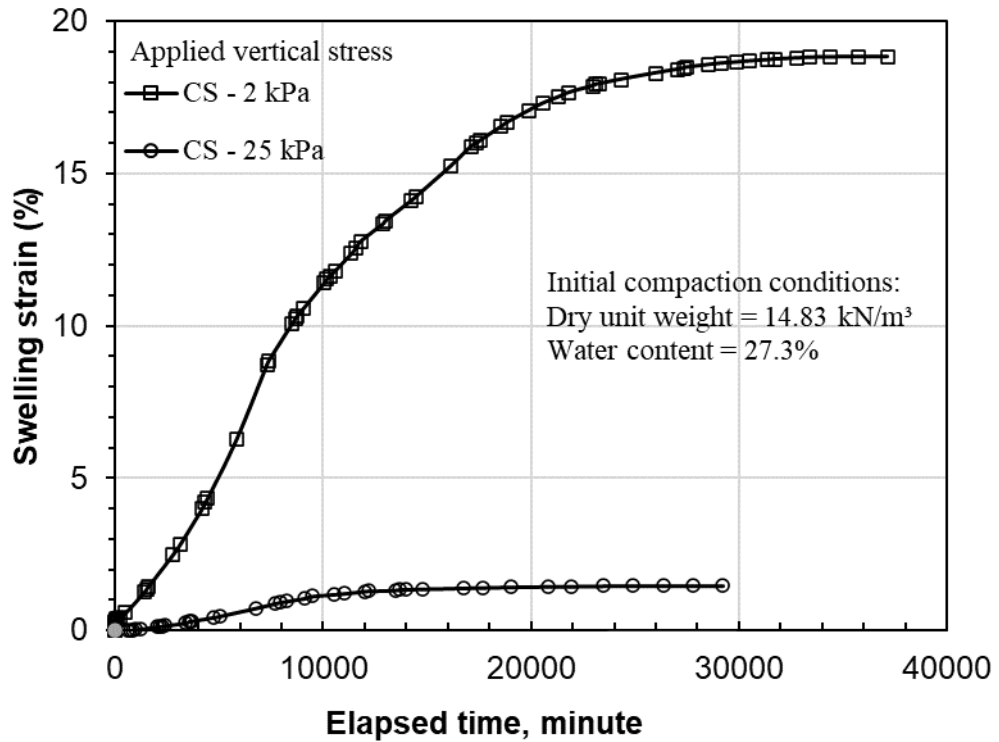


Figure 4.1 One-dimensional swelling strain of compacted CKD specimens at various applied vertical pressures.

### 4.3.2 Swelling pressure

Figure 4.2 presents the development of swelling pressure with elapsed time during the saturation process of the compacted CKD specimen. The test was conducted in constant volume condition (Section 3.4.2) for a duration of about 24 days. The test results show that the swelling pressure increased and attain a maximum value of about 67 kPa at the end of 15 days and then decreased to reach a near constant value of about 60 kPa.

The phenomena responsible for the development of swelling strain (i.e., crystalline and osmotic swelling) are also held responsible for development of pressure. The swelling pressure is defined as the pressure required to keep the volume of the material constant when it absorbs water and tends to swell. A drop in swelling pressure for compacted bentonites has been noted by several researchers in the past (Pusch 1982;

Baille et al. 2010). An expansion of micropores and a contraction of macropores is reflected in the development of swelling pressure (Baille et al. 2010).

Based on the swelling strain and swelling pressure results presented, it can be stated that a vertical pressure greater than 67 kPa would cause a collapse of the compacted CKD considered in this study. It should be noted that swelling pressure increases with an increase in the compaction dry density and decreases with an increase in the compaction water content (Baille et al. 2010). The compaction conditions considered in this study were corresponding to the maximum dry unit weight and optimum water content. Therefore, the magnitude of measured swelling pressure (67 kPa) may be considered as the maximum swelling pressure for the CKD studied.

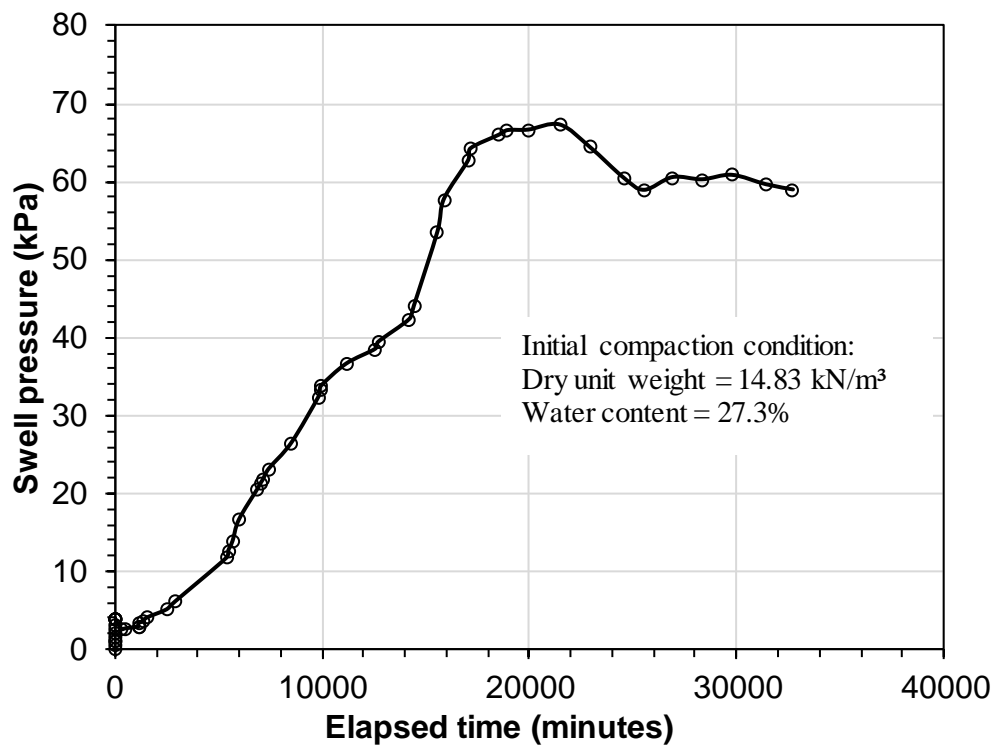


Figure 4.2 Constant volume-swelling pressure test results for compacted CKD specimen.

## 4.4 Compressibility characteristics

In this section, the consolidation test results of the CKD specimens are presented. Sections 3.4.2.1 and 3.4.2.2 presented the testing procedure for these tests. The consolidation tests were conducted on an initially saturated slurried specimen (denoted as SS) and compacted specimens. The tests on compacted CKD specimens were carried out following the swelling strain measurements at 2 and 25 kPa denoted as CS-2 kPa and CS-25 kPa, respectively and the swelling pressure measurement, denoted as CS-CV.

### 4.4.1 Time-deformation behaviour

Figures 4.3 a and b show the square root of time versus % strain plots for the saturated slurried (SS) and compacted CKD specimens (CS-2 kPa, CS-25 kPa and CS-CV) at total applied vertical pressures of 100 and 800 kPa respectively. The test results presented in Figure 4.3 are only typical results. For the test results presented in Figure 4.3 a, the previous step applied total vertical pressure on specimens SS, CS-2 kPa, and CS-25 kPa was 50 kPa, whereas that for specimen CS-CV it was 67 kPa. For the test results presented in Figure 4.3 b, the previous step applied vertical pressures was 400 kPa for all the specimens. Therefore, the test results are for a variable increase in the applied vertical pressures in Figure 4.3 a, whereas an increase in the vertical pressure was 400 kPa for the results presented in Figure 4.3 b.

It can be seen in Figure 4.3 that an increase in the applied vertical pressure caused compression deformation of all the specimens at both applied vertical pressure levels. The compression strains were greater in case of specimens SS and CS-2 kPa as compared to that occurred for specimens CS-25 kPa and CS-CV. Higher compression strains of specimens SS and CS-2 kPa are due to the stress history of the specimens during the saturation process. The time-deformation trend in all the plots in Figure 4.3 is found to be similar. The experimental data were analysed to determine the changes in the void ratio, compression index ( $C_c$ ), swelling index ( $C_s$ ), coefficient of consolidation ( $C_v$ ), coefficient of volume compressibility ( $m_v$ ) and saturated coefficient of permeability ( $k$ ) which are discussed in the following sections.

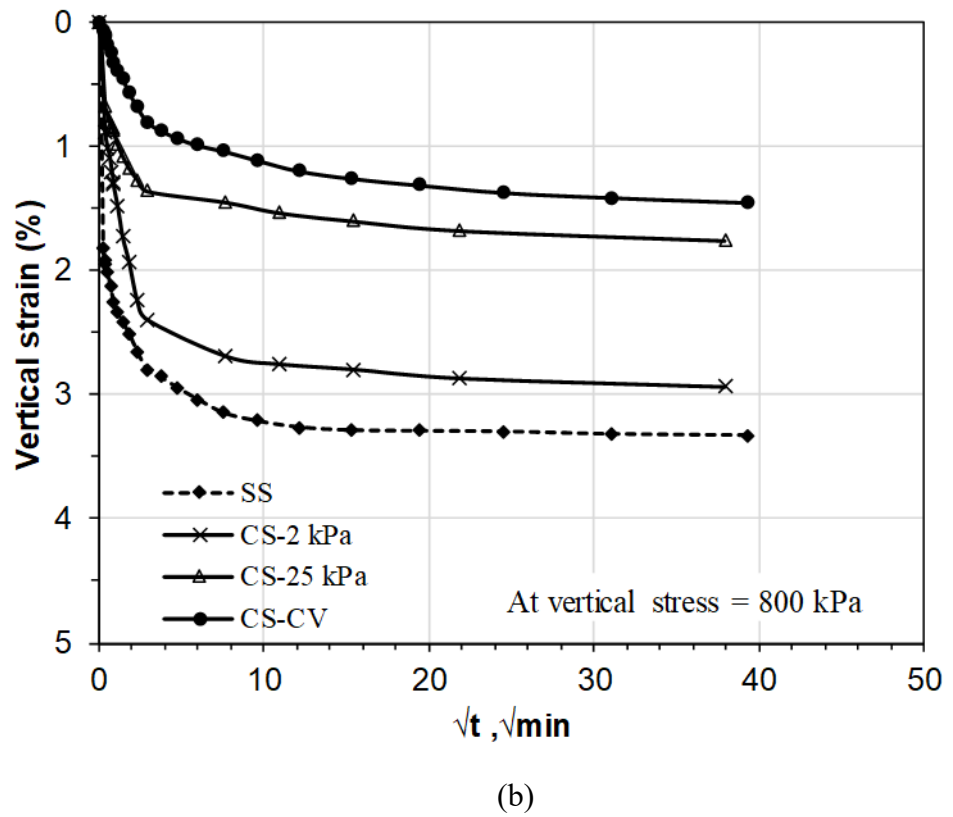
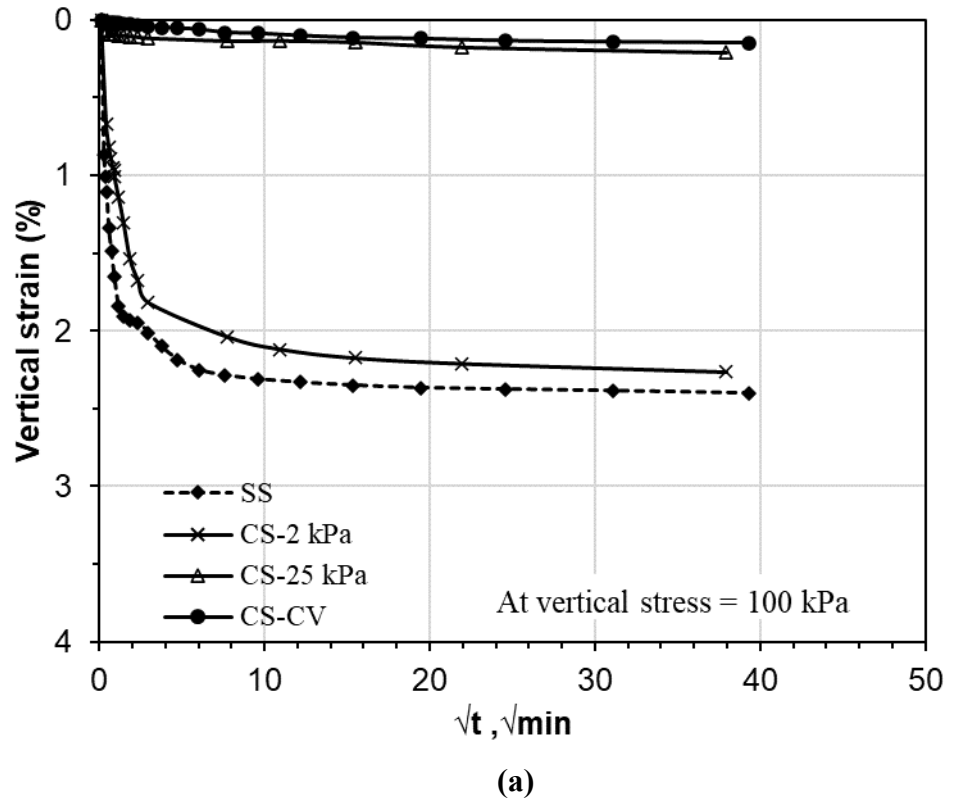


Figure 4.3 Typical time-compression plots of CKD specimens at applied vertical pressures of (a) 100 kPa and (b) 800 kPa.

#### 4.4.2 Compression index ( $C_c$ ) and swell index ( $C_s$ )

Figure 4.4 shows the applied vertical pressure (in *log*-scale) versus void ratio plots of the CKD specimens tested. The initial void ratios of specimens SS and CS-2 kPa prior to the consolidation tests were 1.34 and 1.15, respectively. Similarly, the void ratio of specimens CS-25 kPa and CS-CV prior to the tests were about 0.81 and 0.80 respectively.

The test results presented in Figure 4.4 show that at any applied vertical pressure, the void ratio remains in decreasing order for specimens SS, CS-2 kPa, CS-25 kPa and CS-CV. The ordering of the pressure-void ratio plots also remained similar to that of the void ratio trend. The elastic zone for specimens SS and CS-2 kPa remained up to about 20 to 25 kPa during the loading stage. A pre-consolidation stress of about 25 kPa for specimen SS possibly originated from the specimen preparation stage. The applied stress for preparing the compacted specimens was far higher (1200 kPa) than that observed as pre-consolidation stress for specimens CS-2 kPa, CS-25 kPa and CS-CV. This suggests that swelling erases the compaction stress effects to a great extent (Monroy 2005).

Table 4.1 shows the compression and swell indices of the CKD specimens tested. The applied vertical pressure ranges considered for determining the compression index ( $C_c$ ) and the swelling index ( $C_s$ ) are shown in Table 4.1. The  $C_c$  values for all specimens remain between 0.08 and 0.22. Specimen SS exhibited the largest value of  $C_c$ , whereas the least value was noted for specimen CS-CV. The void ratio of specimens CS-25 kPa and CS-CV were very similar prior to the loading stage. Specimen CS-25 kPa exhibited a slightly higher value of  $C_c$  as compared to that of specimen CS-CV. The swelling index ( $C_s$ ) is the slope of the void ratio-vertical pressure plot during unloading or decompression. The  $C_s$  values (Table 4.1) of all specimens tested ranged between 0.007 and 0.019. The lowest value was noted for the specimen CS-CV.

The compression index of the CKD calculated using Skempton's correlation,  $C_c = 0.007 (\text{Liquid limit} - 10)$  was found to be 0.22. Again, from a relationship with plasticity index ( $C_c = I_p/74$ , where  $I_p$  is the plasticity index) (Mitchell 1993),  $C_c$  was found to be 0.19. Although these values are close to the value obtained from experimental results for the specimen SS, the test results of compacted specimens showed lower values of  $C_c$ .

Following the relationship  $C_s = I_p/370$  (Mitchell 1993), a decompression index of 0.038 was obtained. The experimental  $C_s$  values (Table 4.1) are found to be lesser than the calculated value.

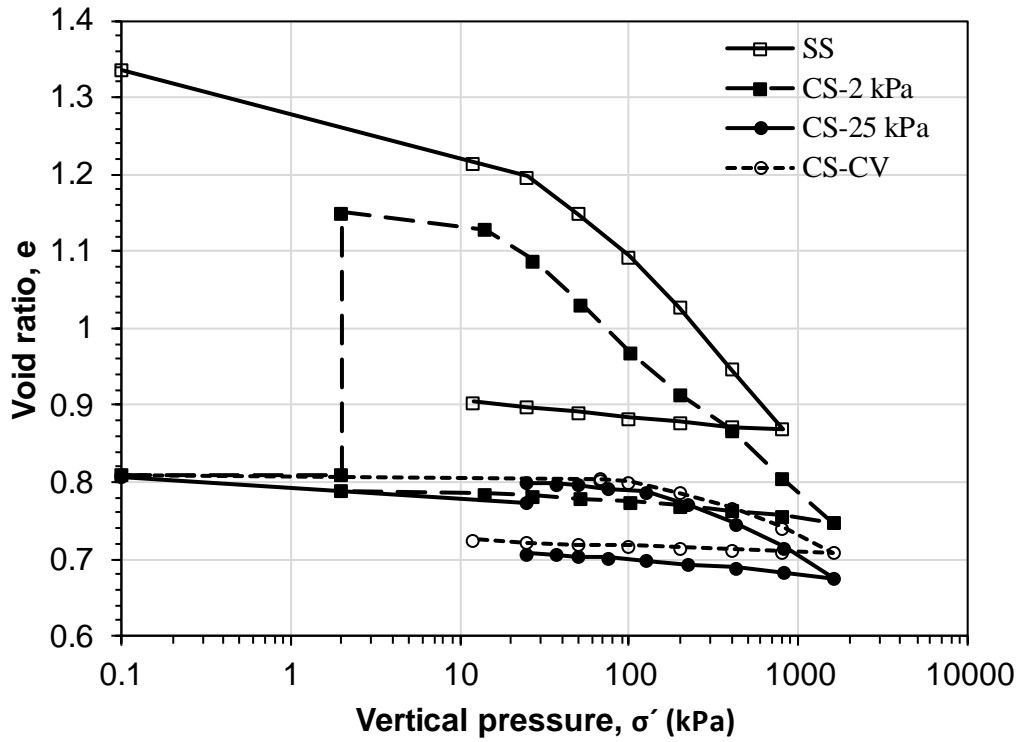


Figure 4.4 e-log p plots of compacted and slurried cement kiln dust specimens.

Table 4.1 Compression and swell indices of the cement kiln dust specimens tested.

Initial condition of specimen prior to loading	Vertical stress range for determining $C_c$ and $C_s$ (kPa)	Compression index, $C_c$	Swelling index, $C_s$
Saturated-slurried	25 - 800	0.22	0.019
Saturated at an applied pressure of 2 kPa	14 - 1602	0.18	0.018
Saturated at an applied pressure of 25 kPa	125 - 1625	0.10	0.017
Saturated in constant volume condition	100 - 1600	0.08	0.007

#### 4.4.3 Coefficient of consolidation ( $C_v$ )

For determining the  $C_v$  values of the CKD, the time-compression data were considered. Taylor's square root time fitting method was used for determining the values of  $C_v$  for each loading step. The value of  $C_v$  depends upon the mineralogy and soil type (Olson 1986; Robinson and Allam 1998). Figure 4.5 presents the average vertical pressure versus  $C_v$  plots of the CKD specimens. A variation of  $C_v$  with an increase in the vertical pressure was noted for all specimens. The  $C_v$  value generally remained between 1 to 10  $m^2/year$  ( $3.2 \times 10^{-4}$  to  $3.2 \times 10^{-3} cm^2/s$ ) for all specimens tested. A tendency of the specimens to exhibit a  $C_v$  value of about 3  $m^2/year$  ( $9.5 \times 10^{-4} cm^2/s$ ) at high applied pressures can be noted.

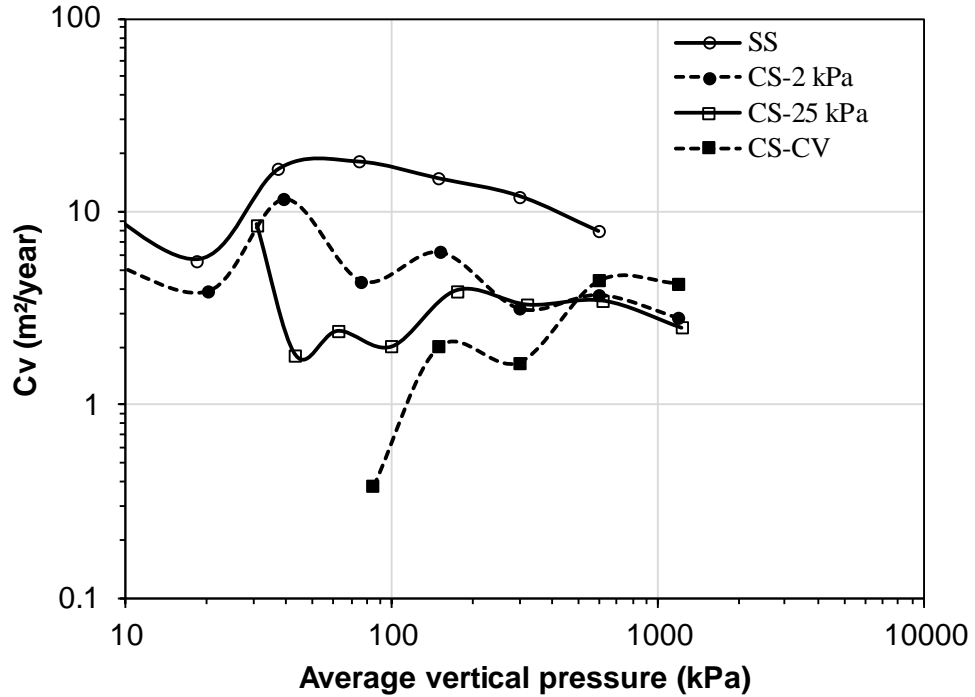


Figure 4.5 Effect of vertical pressure on the coefficient of consolidation.

Table 4.2 presents the typical values for the coefficient of consolidation of different soils (Lambe and Whitman 1969). The  $C_v$  values ( $3.2 \times 10^{-4}$  to  $3.2 \times 10^{-3}$   $\text{cm}^2/\text{s}$ ) of cement kiln dust specimens (liquid limit = 41%) that have been obtained in this study were found to be similar to that ( $1.2 \times 10^{-3}$  to  $3 \times 10^{-4}$   $\text{cm}^2/\text{s}$ ) reported for the remoulded soils with liquid limits between 30 and 60%.

Table 4.2 Typical values for Coefficient of consolidation,  $C_v$  (reproduced from Lambe and Whitman 1969).

Liquid limit (%)	Lower limit for recompression ( $\text{cm}^2/\text{s}$ )	Undisturbed virgin compression ( $\text{cm}^2/\text{s}$ )	Upper limit remoulded ( $\text{cm}^2/\text{s}$ )
30	$3.5 \times 10^{-2}$	$5 \times 10^{-3}$	$1.2 \times 10^{-3}$
60	$3.5 \times 10^{-3}$	$1 \times 10^{-3}$	$3 \times 10^{-4}$
100	$4 \times 10^{-4}$	$2 \times 10^{-4}$	$1 \times 10^{-4}$

#### 4.4.4 Coefficient of volume compressibility ( $m_v$ )

The coefficient of volume compressibility ( $m_v$ ) values of the CKD specimens were calculated based on consecutive applied vertical pressures and the corresponding void ratios. Figure 4.6 illustrates the variation of  $m_v$  of CKD specimens with an increase in the vertical pressure. In general,  $m_v$  decreased with an increase in the applied pressure.

Up to the average vertical stress of about 600 kPa, the  $m_v$  values ranged between 0.1  $m^2/MN$  and 1.0  $m^2/MN$  for the specimen SS and CS-2 kPa and between 0.03  $m^2/MN$  and 0.1  $m^2/MN$  for the compacted specimens CS-25 kPa and CS-CV. Considering the typical  $m_v$  values and descriptive terms of different types of clay reported by Carter (1983) (Table 4.3), the compressibility of the specimens SS and CS-2 kPa for the range of vertical stress in this study can be described as medium to high, whereas for the two other compacted specimens can be described as low to very low.

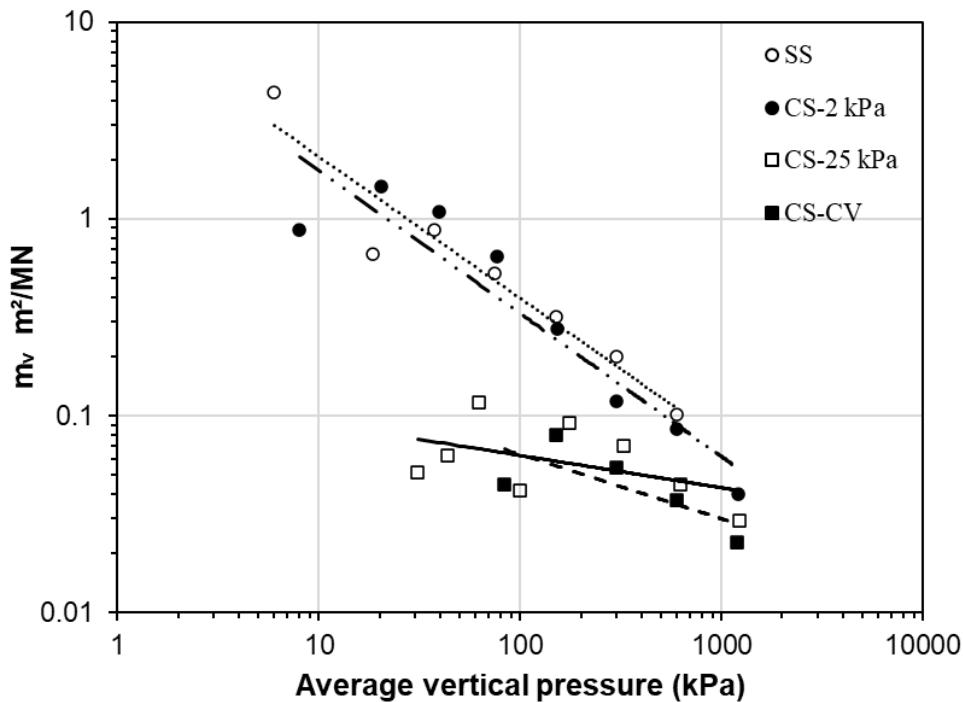


Figure 4.6 Effect of vertical pressure on the coefficient of volume compressibility of CKD.

Table 4.3 Typical values of the coefficient of volume compressibility and descriptive terms used (reproduced from Carter 1983).

Type of clay	Descriptive term	$m_v$ ( $m^2/MN$ )
Heavy over-consolidated boulder clays, stiff weathered rocks (e.g. weathered mudstone) and hard clays	Very low compressibility	< 0.05
Boulder clays, marls, very stiff tropical red clays	Low compressibility	0.05 – 0.1
Firm clays, glacial outwash clays, lake deposits, weathered marls, firm boulder clays, normally consolidated clays at depth and firm tropical red clays	Medium compressibility	0.1 – 0.3
Normally consolidated alluvial clays such as estuarine and delta deposits, and sensitive clays	High compressibility	0.3 – 1.5
Highly organic alluvial clays and peats	Very high compressibility	>1.5

#### 4.4.5 Coefficient of permeability ( $k$ )

The saturated coefficient of permeability ( $k$ ) of CKD specimens was calculated based on the values of  $m_v$  and  $C_v$  (Lambe and Whitman 1969). Figure 4.7 presents the variation of  $k$  of CKD specimens as affected by the applied vertical pressures. In general,  $k$  decreased with an increase in the applied vertical pressure. For the specimen SS,  $k$  decreased from about  $1.9 \times 10^{-8}$  m/s to  $2.5 \times 10^{-10}$  m/s for average vertical stress range of 6 to 600 kPa. The  $k$  value of specimen CS-2 kPa varied between about  $3.9 \times 10^{-9}$  and  $3.5 \times 10^{-11}$  m/s for an increase in average vertical pressure from 8 to 1202 kPa. An increase in the vertical pressure, the  $k$  value of CS-25 kPa decreased from  $1.4 \times 10^{-10}$  to  $2.3 \times 10^{-11}$  m/s. A variation of  $k$  from  $5.8 \times 10^{-12}$  to  $3.0 \times 10^{-11}$  m/s was noted for specimen CS-CV. At high vertical pressures, the  $k$  values of all specimens tend to be similar ( $5 \times 10^{-10}$  m/s). A decrease in  $k$  is attributed to a decrease in the void ratio of the specimens.

Permeability measurements of different types of cement kiln dust have been conducted by Todres et al. (1992) and Sreekrishnavilasam and Santagata (2005) on specimens compacted inside permeameter moulds with different densities and under falling and constant head. The reported values of  $k$  were found to be between  $1.5 \times 10^{-5}$  and  $1.5 \times 10^{-12}$  m/s. It can be noted that the  $k$  values obtained from one-dimensional oedometer tests in this study were within the range of  $k$  values reported in the past.

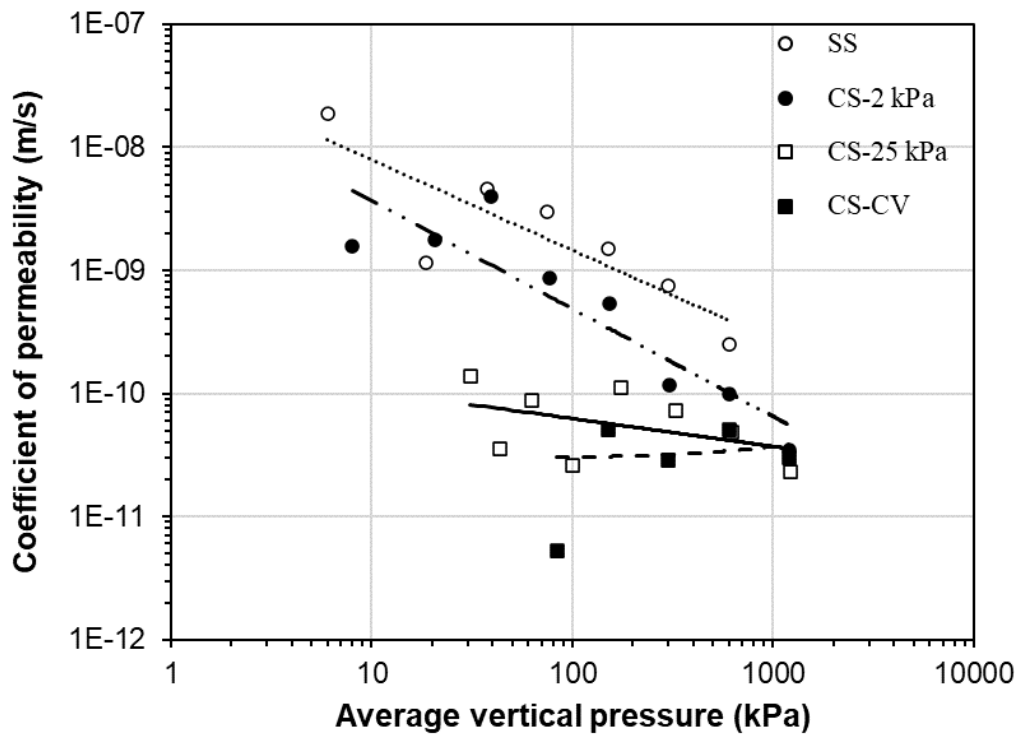


Figure 4.7 Effect of vertical pressure on the coefficient of permeability of CKD.

## **4.5 Concluding Remarks**

In this chapter, the one-dimensional swelling and consolidation test results of cement kiln dust for different initial conditions are presented. The swelling strain of compacted specimens was determined at applied pressures of 2 and 25 kPa. The swelling pressure of compacted specimen was measured under constant volume condition. The compressibility characteristics (compression index, coefficient of consolidation, and coefficient of volume compressibility) of initially saturated slurried and compacted specimens were studied for an applied pressure range of 2 to 1600 kPa. The effects of initial conditions of the specimens and vertical pressure on the swelling and compressibility characteristics of CKD are discussed. The main findings from the laboratory tests can be summarised as:

- (1) The CKD considered in this study exhibited swelling upon saturation from unsaturated condition. Similarly, swelling pressure developed when an unsaturated specimen was wetted under constant volume condition. The swelling strain of compacted CKD decreased with an increase in the applied vertical pressure prior to the saturation process. The swelling strain decreased from 18.8 to about 1.5% with an increase in applied pressure from 2 to 25 kPa. The measured swelling pressure of the CKD was 67 kPa.
- (2) Upon loading, the volume decrease in the cases of initially saturated slurried specimen and compacted-saturated specimen hydrated at 2 kPa was higher as compared to the compacted specimens that were saturated either at a higher stress or at constant volume condition.

The applied pressure and initial compaction conditions of CKD influenced the compressibility characteristics and coefficient of permeability. For an applied pressure range of 2 to 1600 kPa, the range of variation of various compressibility parameters and permeability are as follows:

Compression index ( $C_c$ ): 0.22 and 0.08,

Coefficient of volume compressibility ( $m_v$ ): 0.03 to 3 m<sup>2</sup>/MN,

Coefficient of consolidation ( $c_v$ ): 1.0 to 20 m<sup>2</sup>/yr,

Swelling index ( $C_s$ ): 0.007 to 0.019, and

Coefficient of permeability ( $k$ ): 10<sup>-8</sup> to 10<sup>-11</sup> m/s.

These parameters are useful information towards assessing the settlement and rate of settlement of CKD. Some of the reported correlations between the various parameters and the plasticity properties of soil were found to be valid in case of the CKD used in this study.

## **CHAPTER 5**

# **Water retention characteristics of CKD, sand, and sand-CKD**

### **5.1 Introduction**

The water retention curve (WRC), which is a graphical relationship between water content (either gravimetric or volumetric) or degree of saturation and soil suction plays a key role in understanding the behaviour of unsaturated soil (Fredlund 2006). Unsaturated soils are encountered in many geotechnical and geoenvironmental engineering problems/applications. The WRC contains the fundamental information, such as air-entry value, slope at the inflection point, residual water content/degree of saturation and residual suction that are often needed for determining unsaturated shear strength, hydraulic conductivity, compressibility and swelling potential (Vanapalli et al. 1996; Delage et al. 1998; Zhai and Rahardjo 2012; Fredlund and Houston 2013).

Several devices are currently available to measure and control suction in unsaturated soils (Nam et al. 2009; Fredlund et al. 2012; Tripathy et al. 2016). Similarly, several parametric models have been proposed to analytically describe the WRC (e.g. Brooks and Corey 1964; van Genuchten 1980; Fredlund and Xing 1994).

Previous studies have reported that CKDs (particularly, high free lime-fresh CKDs) can be successfully used in modification/stabilisation of both fine- and coarse-grained soils (McCoy and Kriner 1971; Baghdadi and Rahman 1990; Zaman 1992; Miller and Azad 2000; Miller and Zaman 2000; Parsons et al. 2004; Sreekrishnavilasam et al. 2007; Peethamparan et al. 2008; Moses and Afolayan 2013). In addition, low free lime-CKDs (e.g. landfilled CKDs) with limited cementing properties and high water absorption capacity (due to the fineness) can be used as an ideal material for low-strength backfill, sanitary and municipal landfills covers (Bhatty 1995; Sreekrishnavilasam et al. 2006; Adaska and Taubert 2008). Further, the investigations carried out on CKD landfills in the United States and according to the Subtitle D landfill regulations, CKD has been approved to be used as alternative to soil for daily or intermediate cover at CKD landfills

and proposed or used as a CKD liner or cap at several locations in the United States (USEPA 1998).

In many cases, local soils are undesirable to be used in infrastructure construction, particularly so when the water holding capacity plays an important role. Sands possess high permeability and low water retention capability compared to the finer soils. One of the most effective ways to improve the hydraulic characteristic of sand is to add other materials that contribute in decreasing the permeability and improving the water-holding capacity. Previous studies have reported that addition of CKD to sand resulted in reduction in permeability (Mohamed 2002; Moses and Afolayan 2011) and enhancement of the water retention ability (Oriola et al. 2012).

Studies associated with WRC of CKD are very limited. Oriola et al. (2012) have determined the water retention curves (WRCs) of foundry sand treated with CKD using pressure plate extractor. Further, Brooks-Corey and van Genuchten models have been used to best-fit the experimental data. The WRCs of CKD and sand-CKD mixture for a large range of suction have not been explored in detail.

The objective of this chapter is to establish water retention curves of CKD and sand-CKD mixture for a large range of suction by using various laboratory techniques. A mixture of 85% sand and 15% CKD (by dry mass) was considered in this study. The WRC of sand was also established for comparison. van Genuchten (1980) and Fredlund and Xing (1994) parametric models were used to identify and compare various salient features in WRCs for the materials considered.

## **5.2 Experimental programme**

Laboratory tests were conducted on initially saturated slurried specimens of the CKD for establishing the drying WRC. Initially saturated slurried CKD specimens were prepared in stainless steel specimen rings at an initial water content corresponding to 1.2 times the liquid limit. The specimens were then transferred onto the ceramic disks of pressure plates (sections 3.4.3.1.1). The pressure plate tests were carried out for a suction range of 10 to 400 kPa.

After the pressure plate tests, selected specimens were transferred to desiccators containing salt solutions. The vapour equilibrium tests were conducted for a suction range

of 3 to 300 MPa (section 3.4.3.2.1). The changes in specimen volume during the drying process in pressure plate and desiccator tests, and at each applied suction, were measured using molten wax method. Therefore, suction-water content and suction-degree of saturation WRCs and suction-void ratio and water content-void ratio plots could be obtained. Additionally, clod tests (Section 3.4.3.5.1) were carried out on initially saturated slurried CKD specimens for establishing the relationship between the change in water content and void ratio.

The suctions of compacted CKD, sand-CKD mixture and sand were measured using the chilled-mirror dew-point potentiometer (WP4-C) and a fixed matrix porous ceramic disk water potential sensor (MPS-6). Compacted specimens were prepared at several initial water contents for suction measurements using WP4-C and MPS-6.

For the WP4-C tests, compacted specimens were prepared in stainless-steel cups of the WP4-C device (Section 3.4.3.3). In the WP4-C tests, the dry unit weight of compacted CKD was varied between 7.3 to 13.83 kN/m<sup>3</sup>, whereas that of sand-CKD specimens was about 14.81 kN/m<sup>3</sup>. The sand specimens were compacted at two different dry unit weights, such as 12.75 kN/m<sup>3</sup> for the washed and unwashed sand, and 14.81 kN/m<sup>3</sup> for unwashed sand. Washing of the sand was done with distilled water for removing any undesired impurities.

For the MPS-6 tests, compacted specimens were prepared in cylindrical plastic containers (Section 3.4.3.4.1). In this case, the compaction dry unit weights of specimens of CKD, sand, sand-CKD were 8.93 to 13.2, 12.75, and 14.81 kN/m<sup>3</sup>, respectively.

For some engineering applications (e.g. landfill covers), soils are usually compacted at a dry unit weight corresponding to 80-90% of standard Proctor maximum dry unit weight (Albright et al. 2010). Due to difficulty in achieving the maximum dry unit weight in the specimen cup of WP4-C and in order to protect the ceramic disk of MPS-6 sensor from damage during the compaction process, the specimens of the materials were compacted at dry unit weights less than the respective maximum unit weights.

For determining the osmotic suction of the CKD, electrical conductivity measurements of the pore liquid extracted from saturated samples were made. The samples in this case were prepared at various water contents, such as at the liquid limit (LL),  $2 \times LL$ ,  $2.5 \times LL$ , and  $3 \times LL$ .

## **5.3 Results and discussion**

In the following sections, the suction equilibrium times in pressure plate, desiccator, WP4-C and MPS-6 tests are presented followed by the influence of material type and testing technique on the WRCs. Further, the best-fit WRCs of the materials were established using the parametric models proposed by van Genuchten (1980) and Fredlund and Xing (1994).

### **5.3.1 Suction equilibrium time**

The suction equilibrium time depends upon several factors such as the type of soil, suction level, technique used, temperature, and the size of the soil specimen (Tang and Cui 2005a; Oliveira and Marinho 2008; Li et al. 2018).

#### **5.3.1.1 Suction equilibration time in pressure plate tests**

Figure 5.1 shows the change in water content versus elapsed time for specimens of CKD upon subjected to various suctions (10 kPa to 400 kPa). A rapid decrease in the water content within the first two days can be seen under an applied suction of 10 kPa. Thereafter, the water content decrease was less until the equilibrium was reached. A significant decrease in the water content for this specimen within first two days can be attributed to the high initial water content of the specimen (1.2 times liquid limit). For suctions greater than 10 kPa, a gradual decrease in the water content was observed. A duration of 6 to 21 days was required for achieving equilibrium conditions for the specimens at suctions greater than 10 kPa.

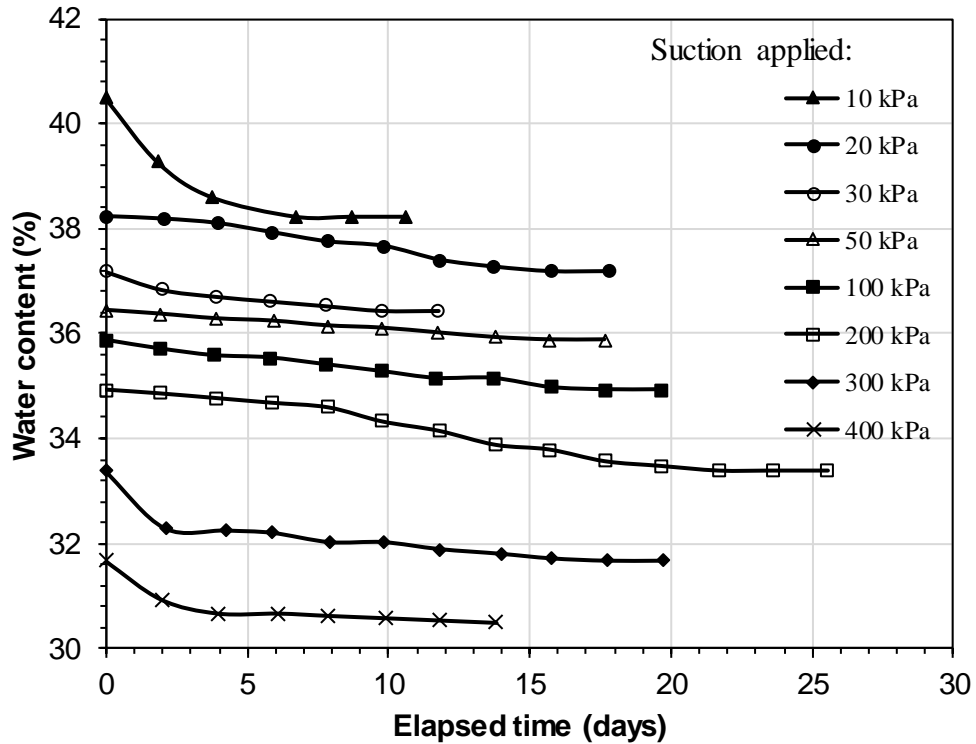


Figure 5.1 Elapsed time versus water content in pressure plate tests for CKD specimens

### 5.3.1.2 Suction equilibration time in vapour equilibrium tests

Figure 5.2 presents the variations of water content versus elapsed time for the CKD specimens and for six salt solutions considered. The rate of decrease in the water content was high for the specimens that were placed inside the desiccators containing salt solutions  $\text{KNO}_3$ ,  $\text{KCl}$ ,  $\text{NaCl}$ ,  $\text{K}_2\text{CO}_3$ , and  $\text{LiCl}$  for inducing total suctions of 9.1, 21.9, 38.3, 114.1, and 277 MPa, respectively. Thereafter, the reduction in the water content decreased until the equilibrium was reached. The water content varied from initial value of about 30% to final values of about 3, 2, 1.6, 1.3 and 0.9% at the above stated suctions. The rate of decrease in the water content at an applied suction of 3.4 MPa ( $\text{K}_2\text{SO}_4$ ) was less as compared to other applied suctions.

It can be seen that 3 to 4 weeks was required for attaining an equilibrium at suctions of 21.9, 38.3, 114.1, and 277 MPa, whereas the specimens that were subjected to a suction of 9.1 MPa reached an equilibrium after about 10 weeks. A significant time

of about 6 months was required for the specimen to attain an equilibrium at suction of 3.4 MPa ( $K_2SO_4$ ).

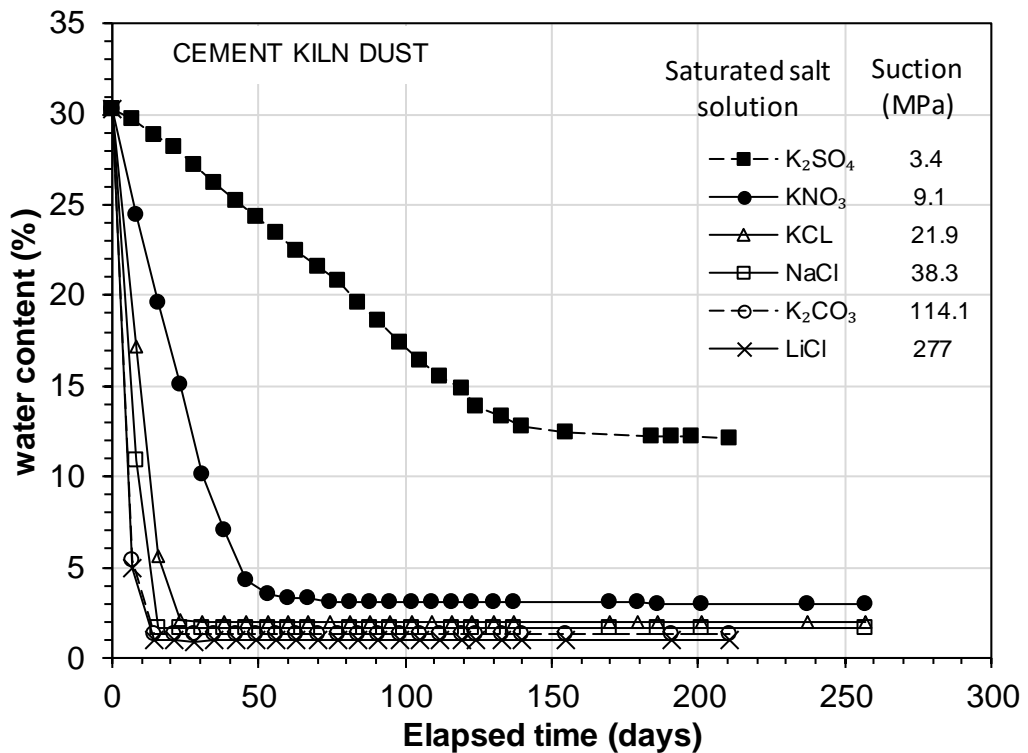


Figure 5.2 Elapsed time versus water content plot of CKD in desiccator tests

### 5.3.1.3 Suction equilibration in chilled-mirror dew-point potentiometer (WP4-C) tests

Figure 5.3 shows the suction measurement times for CKD, sand, and sand-CKD specimens using the WP4-C device. It can be noted that the measurement time increased dramatically as the water content of materials decreased except for the sand-CKD mixture specimens. For the sand-CKD specimens, the measurement time ranged between about 7 and 23 minutes for the range of water content considered in this study. In general, the suction measurement time was less than about 15 minutes for most of the specimens of

the CKD and less than about 25 minutes for all specimens of the sand-CKD mixture. For sand specimens, the suction measurement time varied between 15 to about 65 minutes.

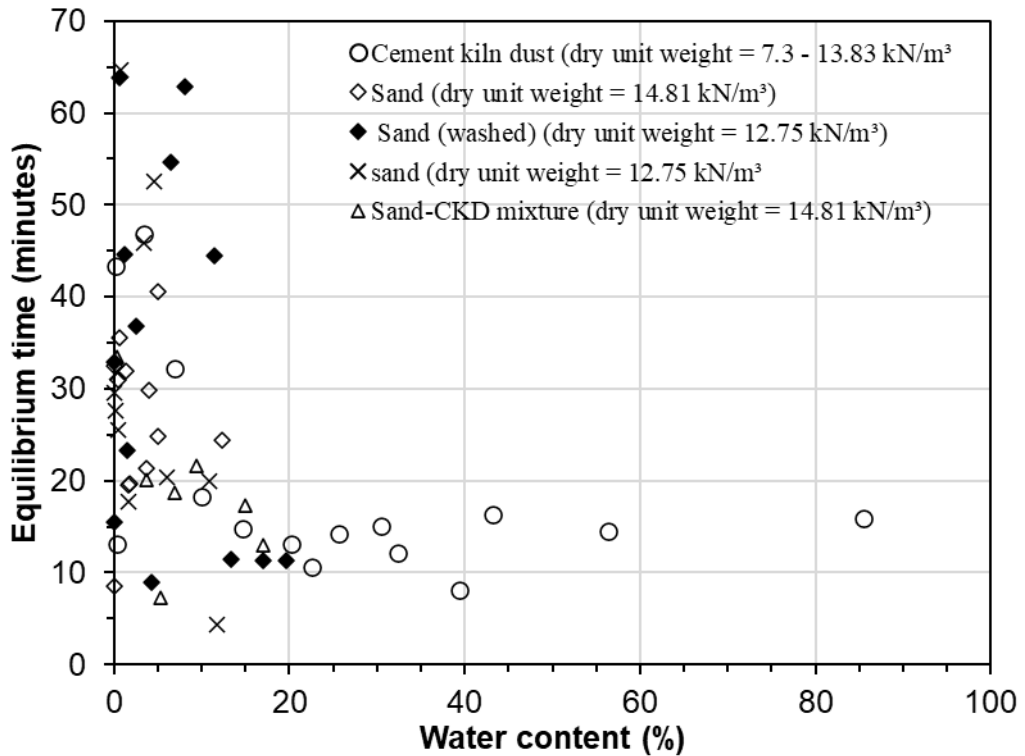


Figure 5.3 Suction measurement time in chilled-mirror dewpoint potentiometer.

#### 5.3.1.4 Suction equilibration in MPS-6 tests

Figures 5.4, 5.5 and 5.6 show the elapsed time versus measured suction plots for CKD, sand, and sand-CKD specimens. In all cases, air-dried sensors with initial suctions ranged between about 6 and 20 kPa were used. According to the water retention characteristic of the fixed-matrix porous ceramic discs (Figure 2.3), the corresponding initial water content of the ceramic discs was between about 40 and 85%. For the specimens with higher water contents, the measured suctions decreased with an elapsed time prior to attaining an equilibrium, whereas for the specimens with low water contents, the measured suctions decreased, increased and further decreased before attaining an equilibrium.

The suction equilibrium time for higher water content specimens was generally varied between about 5 and 24 h, whereas much higher equilibrium times were noted for specimens with low water contents (Figure 5.4), particularly for the sand and sand-CKD specimens (Figures 5.5 and 5.6). A longer equilibrium time in case of the sand specimens is attributed to a lack of good water phase continuity between the specimens and the ceramic disks of the sensors.

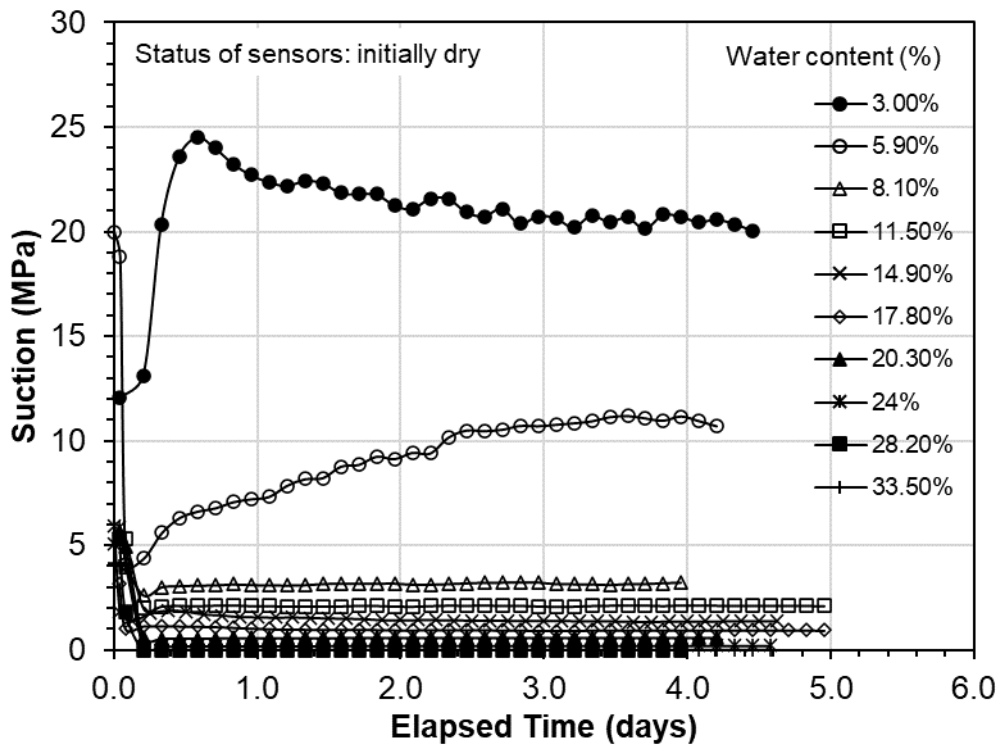


Figure 5.4 Suction measurement time for CKD specimens in MPS-6 sensors.

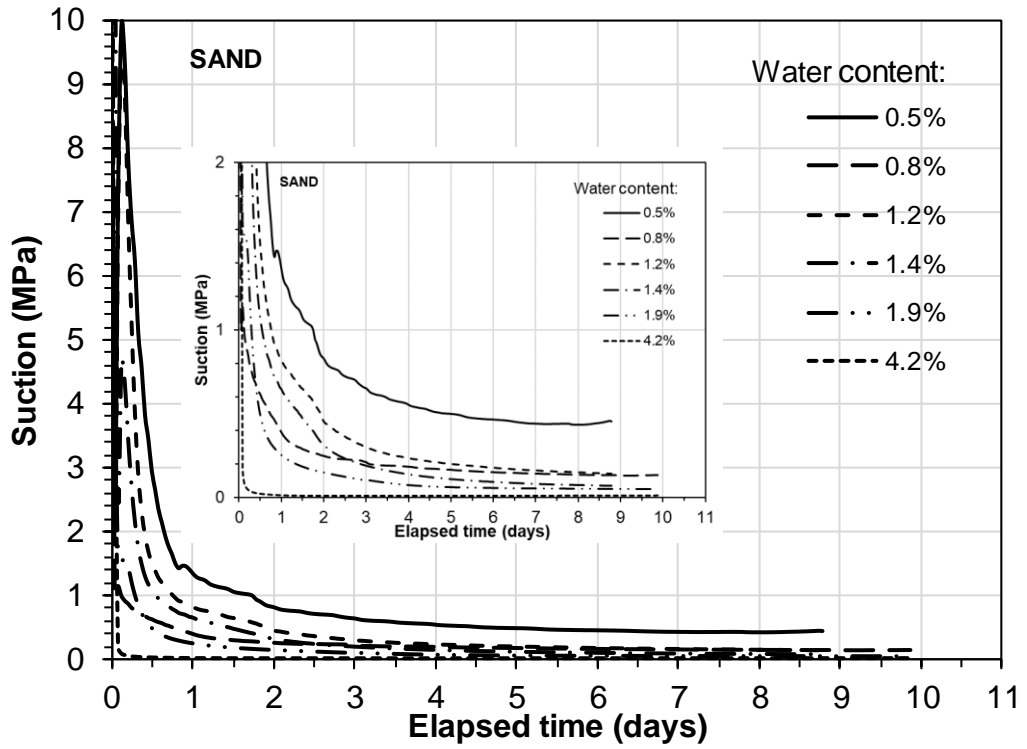


Figure 5.5 Suction measurement time for sand specimens in MPS-6 sensors.

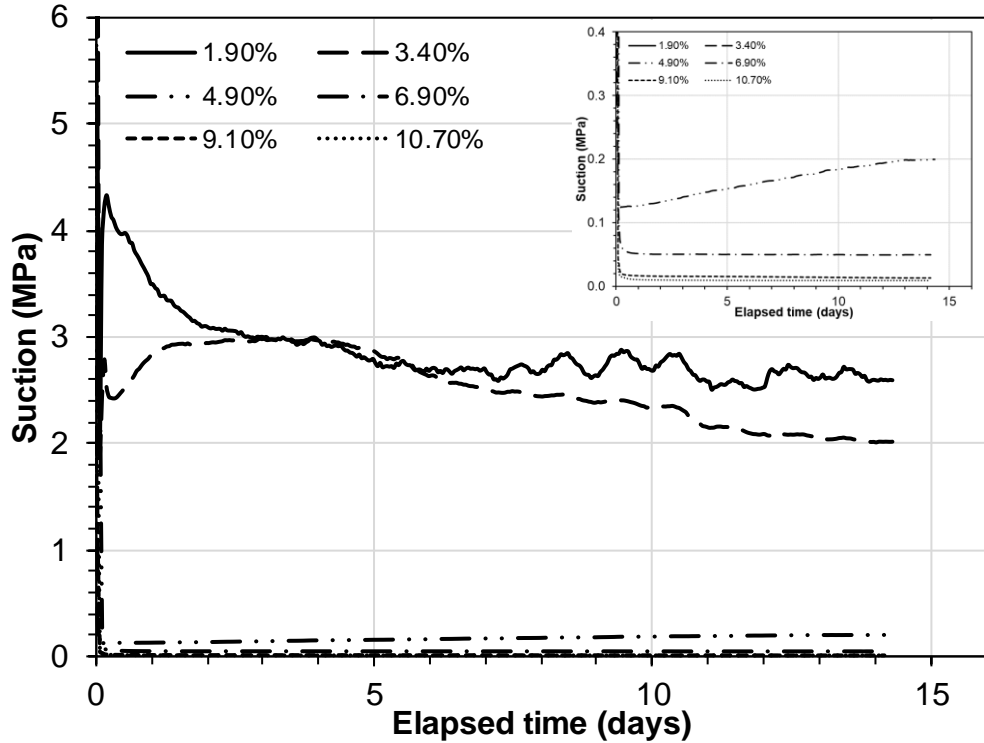


Figure 5.6 Suction measurement time for sand-CKD specimens in MPS-6 sensors.

### 5.3.2 Osmotic suction of CKD

The presence of exchangeable cations in the CKD may influence the total suction of the material. This in turn, may affect the differences in the WRCs measured using various techniques that either measure the matric suction or the total suction. Therefore, osmotic suction measurements are required for the CKD.

Several electrical conductivity tests were carried out on pore water extracted from the saturated CKD samples. The osmotic suctions were determined from the electrical conductivity measurements using two equations. Equation 5.1 is from the United States Salinity Laboratory (1954), whereas Equation 5.2 is from Romero (1999) (Nam et al. 2009).

$$\psi_o = 0.36EC \quad (5.1)$$

where  $\psi_o$  = osmotic suction in atm unit and EC = electrical conductivity in mS/cm.

$$\psi_o = 0.024EC^{1.065} \quad (5.2)$$

where  $\psi_o$  = osmotic suction in kPa, and EC = electrical conductivity in  $\mu\text{S}/\text{cm}$ .

The results from Equations 5.1 and 5.2 yield the reference values of osmotic suctions (Nam et al. 2009).

Table 5.1 shows the osmotic suction estimated from the measured electrical conductivities for the CKD at various water contents. It can be seen that the osmotic suction decreased with an increase in water content and this reduction can be attributed to the decreased salt concentration in the pore water resulting lower electrical conductivity of the extracted pore water. The osmotic suction ranged between 44.2 kPa and 127.7 kPa corresponding to the electrical conductivity of 1226.8  $\mu\text{S}/\text{cm}$  to 3150.8  $\mu\text{S}/\text{cm}$  at water contents ranged between the liquid limit (LL) and  $3 \times \text{LL}$ , respectively. The values of osmotic suction were used in interpreting and analysing the suction results obtained from various techniques.

Table 5.1 Electrical conductivity and osmotic suction of cement kiln dust.

Water content of sample (%)	Electrical conductivity	$\psi_o$ (kPa) (Eq. 6.1)	$\psi_o$ (kPa) (Eq. 6.2)
LL	3150.8	113.43	127.70
2 × LL	1873.7	67.50	73.4
2.5 × LL	1314.7	47.33	50.32
3 × LL	1226.8	44.16	46.75

### 5.3.3 Water retention curves (WRCs)

The accuracy of WRCs is largely based on the techniques used and procedures adopted for establishing WRCs (Peranić et al. 2018). Further, there are several factors, such as the type of soil, initial water content, dry density, soil structure, stress history and mineralogy that have significant effects on the features of WRCs (Zhou and Yu 2005). Tripathy et al. (2016) stated that test results from the devices that measure or induce total suction via vapour equilibrium and matric suction via water phase continuity should be considered separately for comparisons of WRCs.

#### 5.3.3.1 Suction-water content WRCs of CKD

Figure 5.7 presents the experimental results of the CKD obtained from pressure plate and desiccator tests in term of the water content. The test results represent the drying WRC. For the WP4-C and MPS-6 tests, the specimens were prepared by adding predetermined quantities of water. Therefore, the test results may be considered as wetting WRCs. The experimental data from pressure plate and desiccator tests were best-fitted using van Genuchten (1980) and Fredlund & Xing (1994) parametric models. For clarity, only the Fredlund & Xing model is included in Figure 5.7, whereas the parameters from the model results are compared in Section (5.4.5). The results from WP4-C and MPS-6 tests are shown in Figure 5.7 for comparison. The model results are shown separately for WP4-C and MPS-6 tests.

It can be seen in Figure 5.7 that at low suctions (up to about 1000 kPa), the results from the MPS-6 tests are below the drying curve, whereas that from the WP4-C tests remained above with a significant difference even at high water contents.

From MPS-6 and WP4-C test results, the influence of dry unit weight on the WRC is found to be insignificant. Further, considering the values of osmotic suction, the differences between measured suction are still significant. Therefore, the differences between the WRCs established from various tests can be attributed to the osmotic suction of CKD and the accuracies of the measuring devices.

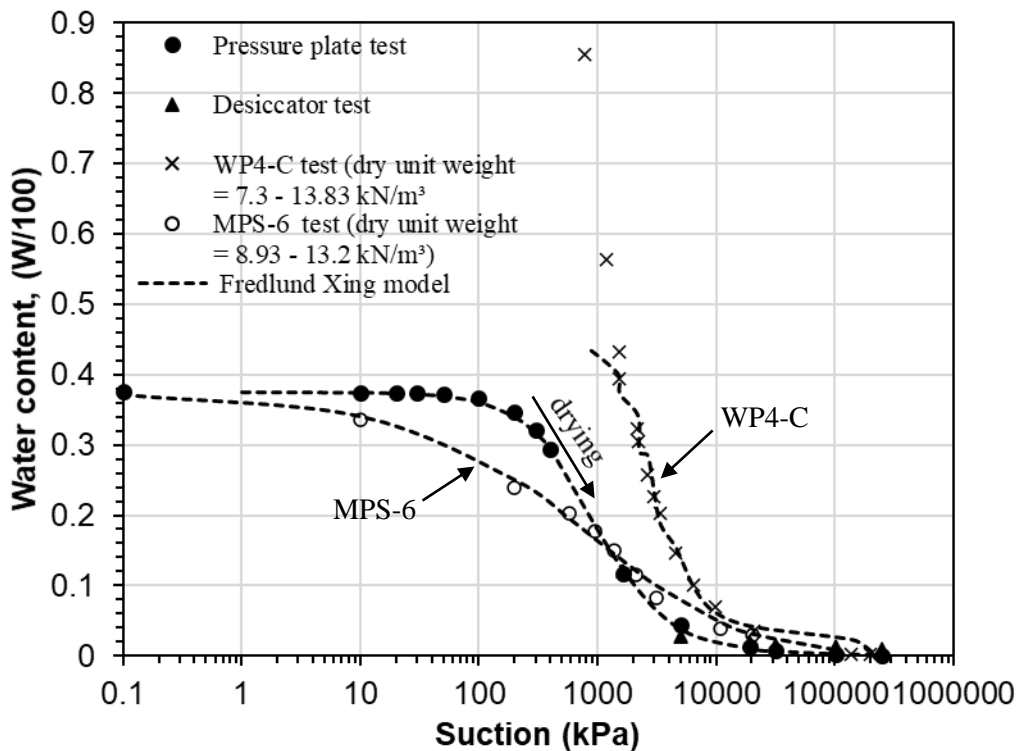


Figure 5.7 Suction–water content WRC test results of CKD using various techniques.

### 5.3.3.2 Suction-degree of saturation WRCs of CKD

Figure 5.8 shows the suction-degree of saturation WRCs of the CKD based on the four suction control and measurement tests (pressure plate, desiccator, chilled-mirror, and

water potential sensor). Again, a smooth curve joining the data points of the pressure plate and desiccator tests has been considered. Significant differences can be noted between the WRC and the results from WP4-C and MPS-6 tests particularly, at low suctions (less than 2000 kPa). The results of the pressure plate and desiccator tests remained below those of the WP4-C test results and above those of the results from MPS-6 tests. At higher suctions (> 2000 kPa), the differences decreased and the results from all tests/techniques tend to converge.

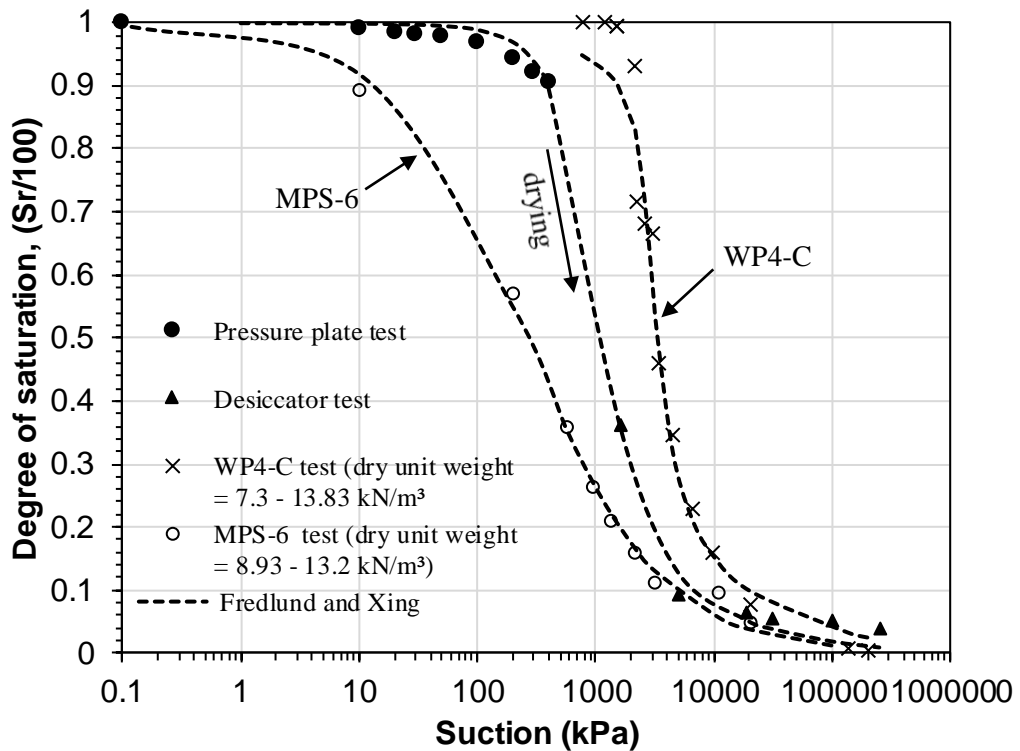


Figure 5.8 Suction – degree of saturation WRC test results of CKD using various techniques.

### 5.3.3.3 Shrinkage curve of CKD

During the drying process, fine soils often exhibit volume change (i.e void ratio change) due to a reduction in the water content. The relationship between the water content and the void ratio is known as the shrinkage curve. For the typical shrinkage

curve, four shrinkage phases can be described, such as the structural shrinkage, the normal shrinkage, the residual shrinkage and the zero shrinkage (Haines 1923).

In this study, clod tests were conducted on initially slurried saturated specimens of CKD for obtaining a smooth shrinkage path and to determine precisely the start of desaturation. For obtaining a smooth shrinkage path the test results were best-fitted using a parametric model. Fredlund et al. (2002) model (Eq. 5.3) was used for best-fitting the clod test results and the solver functions in Microsoft Excel were utilised to generate the best-fitted curve. The model has three curve-fitting parameters, namely  $a_{sh}$ ,  $b_{sh}$  and  $c_{sh}$ .

$$e(w) = a_{sh} \left[ \frac{w^{c_{sh}}}{b_{sh} c_{sh}} + 1 \right]^{1/c_{sh}} \quad (5.3)$$

$$\frac{a_{sh}}{b_{sh}} = \frac{G_s}{S_0} \quad (5.4)$$

where  $e$  = void ratio,  $w$  = gravimetric water content,  $a_{sh}$  = minimum void ratio,  $c_{sh}$  = curvature of the shrinkage curve,  $b_{sh}$  = slope of the line of tangency,  $G_s$  = specific gravity, and  $S_0$  = initial degree of saturation. In best-fitting the experimental data,  $b_{sh}$  can be considered as a fixed parameter in Eq. 5.4.

The results of volume change of the clod specimens with the elapsed time during the shrinkage process (under laboratory conditions of  $21 \pm 0.5$  °C and about 55% relative humidity) are illustrated in Figure 5.9. It can be seen that about 14 days was required for drying of the CKD specimen to a constant volume.

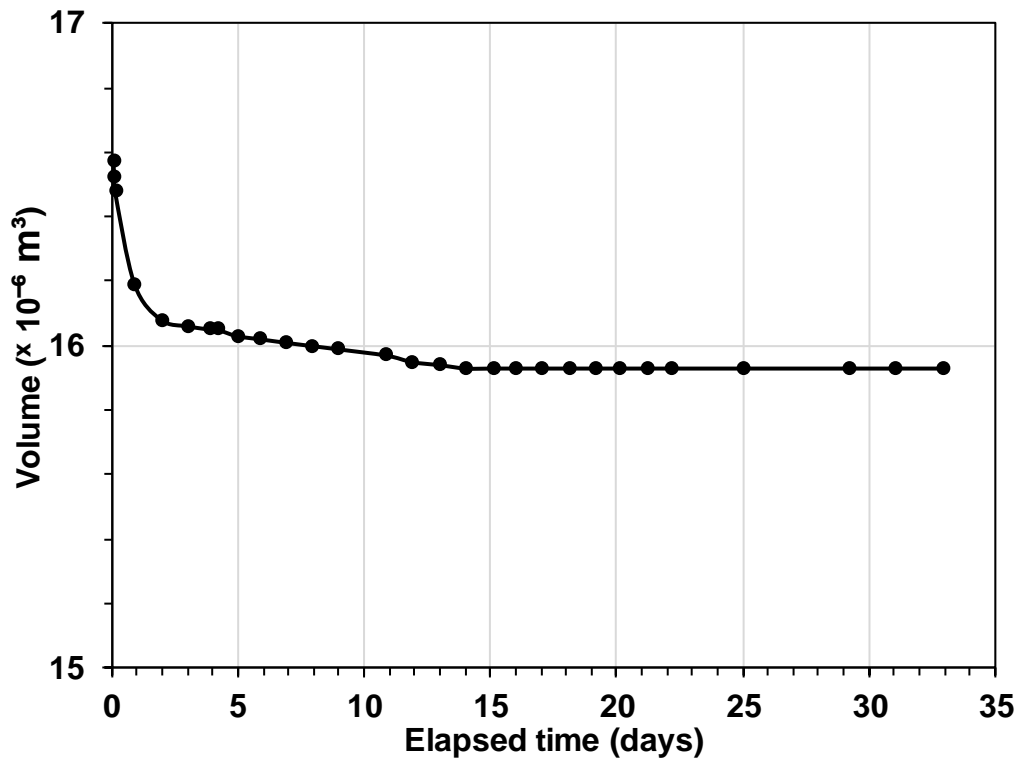


Figure 5.9 Measured volume change with elapsed time for the cement kiln dust during drying process in clod test.

Figure 5.10 shows the clod test results in terms of  $wG_s$  versus void ratio. The void ratios of the specimens in pressure plate and desiccator tests were determined by the molten wax method. The plastic and shrinkage limits of CKD are also presented in Figure (5.10).

At the end of drying process in the clod test, the void ratio of the specimen was significantly greater than that of void ratios corresponding to the shrinkage and plastic limits. Further, void ratios of specimens from the desiccator tests, particularly for the specimens under low relative humidity (i.e under high suction) were found to be considerably less than that of void ratios for the clod specimens. The low void ratios noted at low values of  $wG_s$  refer to that the specimens in desiccator tests did not exhibit no-shrinkage phase during the drying process as compared to the clod results. Similar behaviour has been reported by Tripathy et al. (2014) for some clays (MX 80 bentonite, Yellow bentonite, and Speswhite kaolin). It can be noted from the best-fitted shrinkage

curve that the specimens followed the 100% saturation line during the drying process (the normal shrinkage). The void ratio ( $e_{AEV}$ ) and water content ( $w_{AEV}$ ) at the desaturation point were found to be 0.93 and 34%, respectively. The water content was then considered on the suction-water content WRC based on the results of the pressure plate and desiccator tests (Figure 5.7) and the corresponding suction was found to be about 240 kPa. For this value of suction, a degree of saturation of about 96.5% was obtained from the suction-degree of saturation WRC (Figure 5.8).

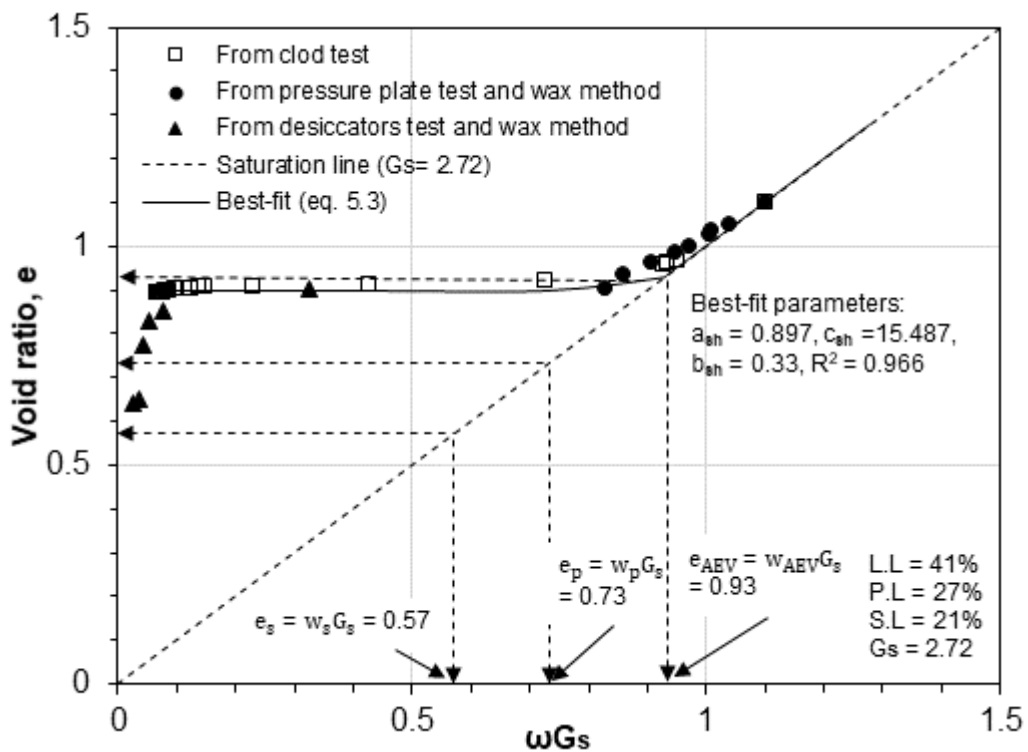


Figure 5.10 Shrinkage curve for the cement kiln dust.

### 5.3.4 WRCs of compacted sand and sand-CKD mixture

Figure 5.11 presents the suction versus water content plots based on the fixed-matrix porous ceramic disc water potential sensor (MPS-6) and chilled-mirror dew-point potentiometer (WP4-C) tests for the sand used. Specimens of unwashed sand compacted

at two dry unit weights of 14.81 and 12.75 kN/m<sup>3</sup> and other specimens of washed sand compacted at dry unit weight of 12.75 kN/m<sup>3</sup> were tested using the WP4-C device.

Differences can be noted between the WRC results of the sand specimens prepared at different conditions (washed and unwashed), particularly for suctions greater than about 100 kPa. The test results of unwashed sand with dry unit weight of 14.81 kN/m<sup>3</sup> remained above the other WRCs. Distinct differences are also observed between the test results of the sand (at dry unit weight of 12.75 kN/m<sup>3</sup>) using MPS-6 and that of all sand specimens from the WP4-C device. All suctions of the sand specimens measured by the WP4-C clearly remained above that of the measured suctions from the MPS-6 sensor. Better agreements between the test results from both devices was noted at higher suctions, especially for the washed sand specimens. The differences in the suction results from both devices cannot be solely attributed to the osmotic suction. It is because differences in the test results from the two devices were also noted in case of the washed sand specimens that had insignificant osmotic suction. Considerations of the accuracies of the measuring devices did not eliminate the differences between suctions measured by the two devices.

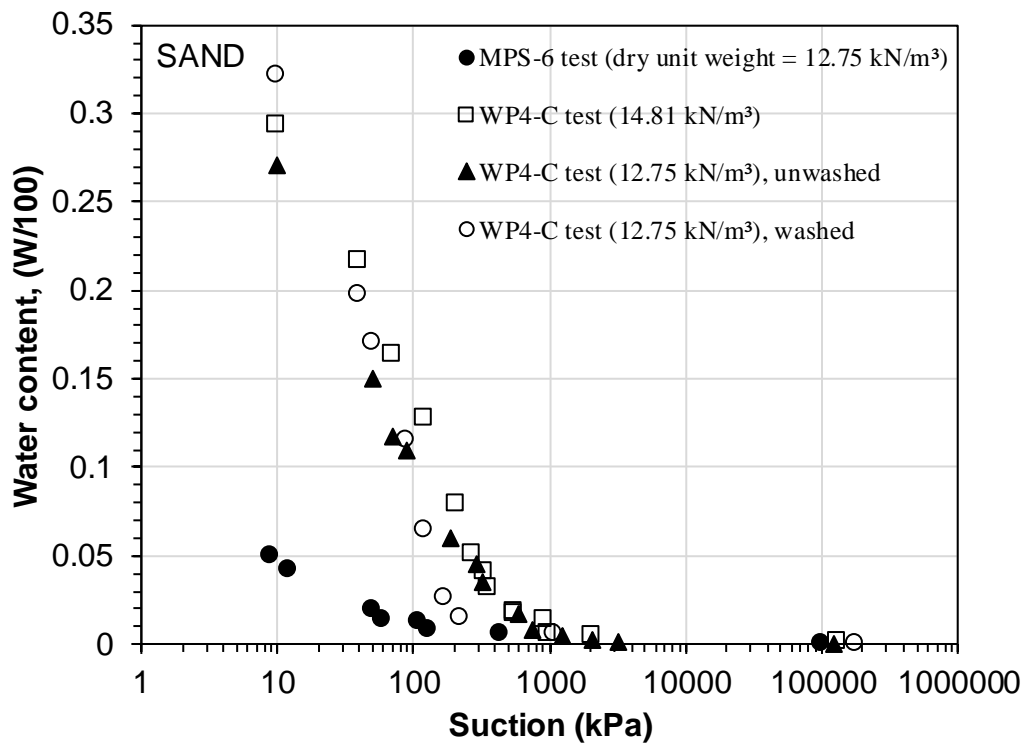


Figure 5.11 Comparisons of fixed-matrix porous ceramic disc (MPS-6) sensor and chilled-mirror dew-point potentiometer (WP4-C) test results for the sand used.

Figure 5.12 shows the suction-degree of saturation results of the sand based on the fixed-matrix porous ceramic disk water potential sensor (MPS-6) and Chilled-mirror dew-point potentiometer (WP4-C) tests. Noticeable differences were observed between test results from the two devices, particularly for values of degree of saturation greater than about 5%. It can be seen that the MPS-6 sensor tests for the unwashed sand exhibited the lowest values of suction over the range of degree of saturation considered and these results remained below that of all results from the WP4-C tests. Slight difference was noted between the WP4-C results for the unwashed and washed sand tested at same dry unit weight (12.75 kN/m<sup>3</sup>). Further, the effect of dry unit weight on the test results was obvious where the unwashed sand tested at a dry unit weight of 14.81 kN/m<sup>3</sup> has maintained the highest values of total suctions.

The model results presented in Figure 5.12 are for the MPS-6 tests and the WP4-C tests. For the latter, the model lines are drawn by ignoring the differences of the results due to dry unit weight effects and other possible effects (accuracies).

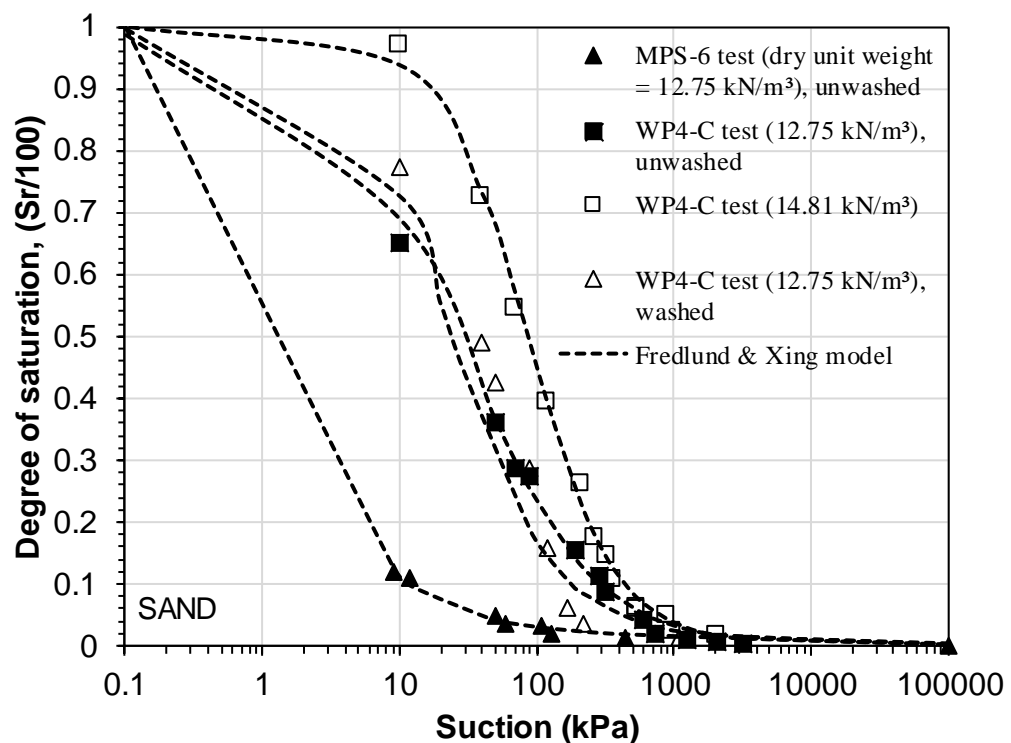


Figure 5.12 Comparisons of fixed-matrix porous ceramic disc (MPS-6) sensor and chilled-mirror dew-point potentiometer (WP4-C) test results for the sand used.

Figure 5.13 shows the suction versus water content plots for the sand-CKD mixture (15%-CKD and 85%-sand) based on the WP4-C and MPS-6 sensor tests. A considerable difference between the test results from both devices is observed. The total suctions measured by WP4-C are noticeably greater than the suction measured by the MPS-6 sensor. As the suction was increased, the difference between both the devices reduced, particularly at high suctions ( $> 1000$  kPa).

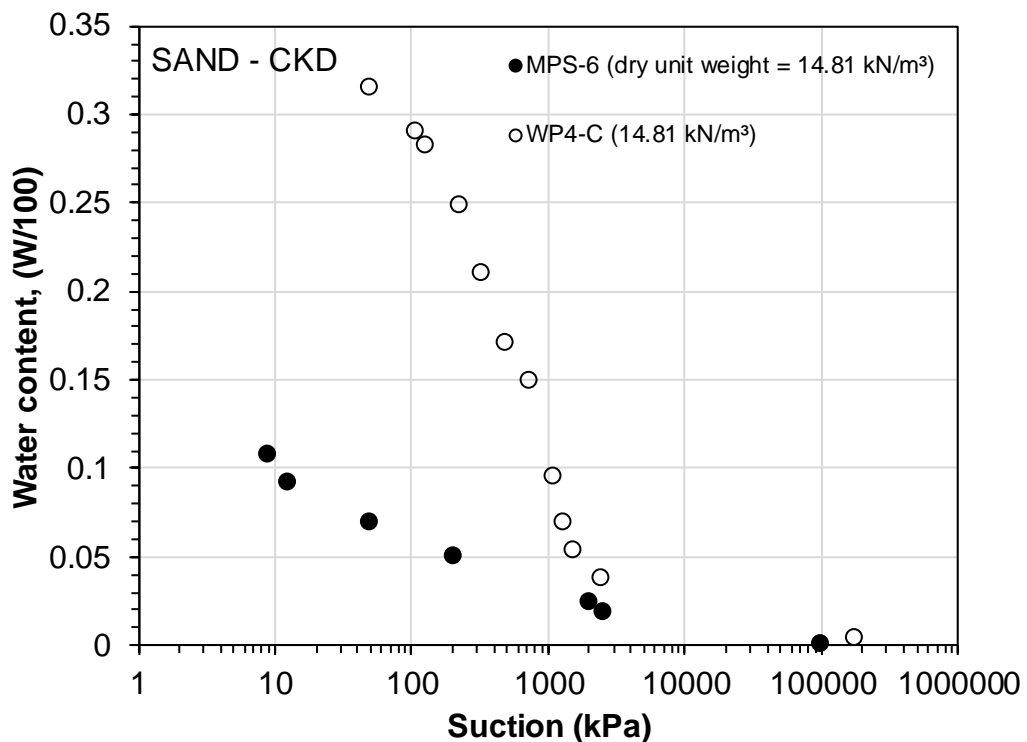


Figure 5.13 Comparisons of fixed-matrix porous ceramic disc (MPS-6) sensor and chilled-mirror dew-point potentiometer (WP4-C) test results for compacted sand-CKD mixture.

Figure 5.14 indicates the suction-degree of saturation results of the sand-CKD mixture from the MPS-6 sensor and WP4-C tests. Again, the difference between the results from both devices is remarkable, particularly at degree of saturation greater than about 10%. Further, the effect of fine material (CKD) added to the sand on the values of measured suctions and the difference between both devices results can be clearly seen as compared to the results of sand.

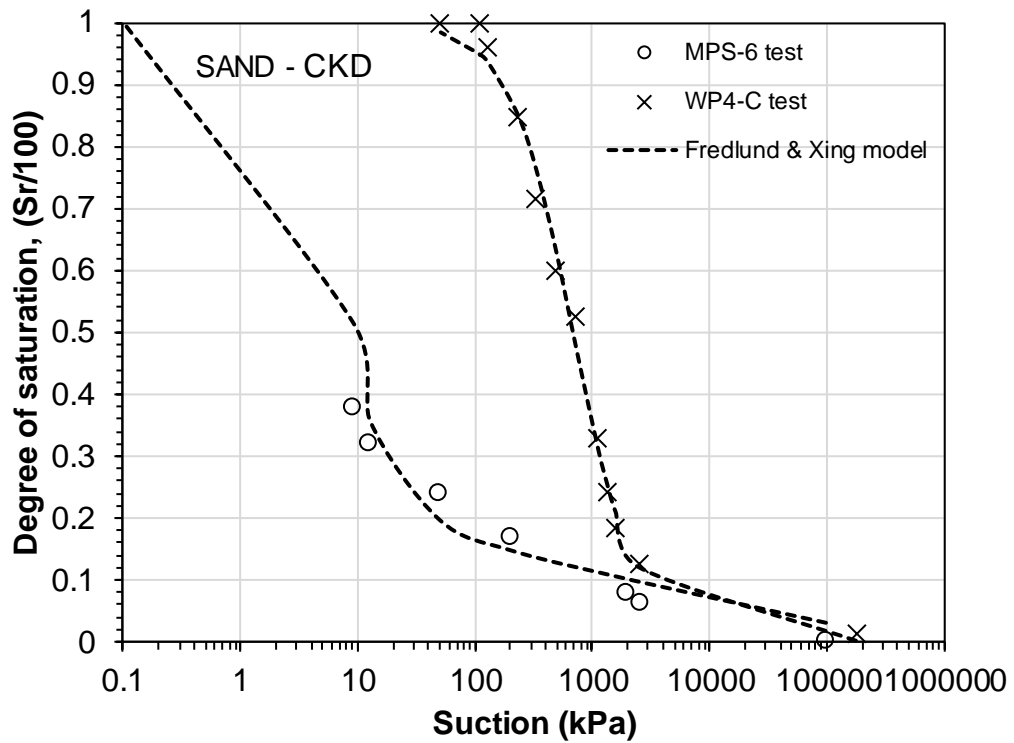


Figure 5.14 Comparisons of fixed-matrix porous ceramic disc (MPS-6) sensor and chilled-mirror dew-point potentiometer (WP4-C) test results for compacted sand-CKD mixture.

### 5.3.5 WRC parametric model results

Several empirical models have been proposed to describe the WRCs data for different types of soils (Sillers and Fredlund 2001; Yang et al. 2004). Leong and Rahardjo (1997) have reported that the van Genuchten (1980) model and the Fredlund and Xing (1994) model are the best WRC models for a variety of soils. Therefore, the experimental test results in terms of suction–water content and suction–degree of saturation for various materials using different techniques were best fitted with the models developed by van Genuchten (1980) and Fredlund & Xing (1994). A non-linear regression analysis was carried out using the “solver” addin in Microsoft Excel to determine the best-fit parameters.

The equations for WRC in terms of water content ( $w$ ) and degree of saturation ( $S_r$ ) based on van Genuchten (1980) model can be expressed as follows:

$$w = \frac{w_s}{\{1+[\alpha(\psi)]^n\}^{(1-1/n)}} \quad (5.5)$$

$$S_r = S_{res} + \frac{(1-S_{res})}{\{1+[\alpha(\psi)]^n\}^{(1-1/n)}} \quad (5.6)$$

where  $w$  = gravimetric water content at any specified suction,  $\psi$ ;  $w_s$  = saturated soil water content,  $\alpha$  = fitting parameter inversely related to the air entry suction,  $n$  = fitting parameter directly related to the slope of the WRC (reflect the pore size distribution of soil),  $S_r$  = degree of saturation, and  $S_{res}$  = residual suction. The typical values of  $\alpha$  and  $n$  falls in the range of (0.0 – 0.5)  $\text{kPa}^{-1}$  and (1.1–8.5), respectively (Lu and Likos 2004).

Based on Fredlund and Xing model (1994), the equations in terms water content and degree of saturation for best-fitting the WRCs can be expressed as follows:

$$w = \left[ 1 - \frac{\ln\left(1 + \frac{\psi}{\psi_{res}}\right)}{\ln\left(1 + \frac{10^6}{\psi_{res}}\right)} \right] * \frac{w_s}{\left\{ \ln\left[ e + \left(\frac{\psi}{a}\right)^n \right] \right\}^m} \quad (5.7)$$

$$S_r = \left[ 1 - \frac{\ln\left(1 + \frac{\psi}{\psi_{res}}\right)}{\ln\left(1 + \frac{10^6}{\psi_{res}}\right)} \right] * \frac{1}{\left\{ \ln\left[ e + \left(\frac{\psi}{a}\right)^n \right] \right\}^m} \quad (5.8)$$

where  $\psi_{res}$  = estimated residual suction for the soil,  $e$  = irrational constant equal to 2.71828 used when taking the natural logarithm,  $a$  = suction related to the inflection point and is greater than the air-entry value and  $m$  = fitting parameter related to the curvature near residual conditions.

The WRCs data of the slurried specimens of CKD and compacted specimens of all materials were best fitted using van Genuchten (1980) and Fredlund & Xing (1994) models (Figures 5.7, 5.8, 5.12, and 5.14). The best-fit parameters obtained by considering the pressure plate and desiccator test results of CKD are shown in Tables 5.2. Table 5.3

shows the fitting parameters for WP4-C and MPS-6 test results for CKD, sand-CKD and sand.

It can be observed in Figures 5.7, 5.8, 5.12 and 5.14 that Equations (5.7) and (5.8) could be well used to best-fit the experimental data. In all the cases  $R^2$  values were found to be close to 1 (Tables 5.2 and 5.3). Considering the model results presented in Tables 5.2 and 5.3, for any case, a difference in the value of  $n$  can be noted from both the models. Additionally, the  $a$  and  $\alpha$  values are found to be different for water content and degree of saturation WRCs. Similarities in the values of  $(1/\alpha)$  in the case of van Genuchten and  $a$  in the case of Fredlund and Xing can be seen in Tables 5.2 and 5.3.

The air entry values of CKD, sand-CKD and sand were obtained by following the graphical construction procedure proposed by Vanapalli et al. (1998) for both water content and degree of saturation WRCs and are presented in Table 5.4. The air entry fitting parameters obtained from van Genuchten and Fredlund and Xing models are also presented in Table 5.4 for comparison.

It can be seen in Table 5.4 that the air entry values (AEVs) obtained from the graphical construction procedure were generally lower than that obtained from the model fitting parameters. For any case, dissimilarities are noted between the air entry parameters from water content and degree of saturation WRCs. The air entry values of materials were found to be different due to the differences in the WRCs (in terms of both water content and degree of saturation). The WRC of the materials were found to be affected by the devices/techniques used. The AEVs inferred from the WP4-C test results were found to be the highest. Additionally, higher AEVs were observed for the CKD as compared to the sand and sand-CKD mixture which can be attributed to the pore-size of the materials. Materials having higher fine contents usually possess lower void ratios and smaller pore sizes (Yang et al. 2004; Nam et al. 2009) as compared to the materials with higher coarse size fractions. For the sand-CKD mixture, the AEVs remained between those of CKD and sand. The results suggest an addition of 15% CKD caused changes in the structure of the sand. Considering that CKDs undergo significant volumetric deformation, the suction – degree of saturation WRCs are more appropriate for determining the air entry value. The air entry values determined from Fredlund and Xing model were found to be higher than that of their counterparts determined from van Genuchten model and the graphical procedure.

Table 5.2 Model parameters in relation to water content and degree of saturation from both equations based on the pressure plate and desiccator for the CKD. (s = suction, w = water content, Sr = degree of saturation).

Device	Relation type	van Genuchten fitting parameters			Fredlund and Xing fitting parameters			
		$\alpha$ (kPa <sup>-1</sup> )	$n$	R <sup>2</sup>	$a$ (kPa)	$n$	$m$	R <sup>2</sup>
Pressure plate and desiccator	s-w	0.002	1.929	0.999	903.6	1.443	2.109	0.999
	s-S <sub>r</sub>	0.0014	2.259	0.999	789.2	2.457	1.205	0.999

Table 5.3 model parameters in relation to water content and degree of saturation from both equations based on the MPS-6 and WP4-C tests for CKD, sand, and sand-CKD. (s = suction, w = water content, Sr = degree of saturation).

Device	Material	Relation type	van Genuchten fitting parameters			Fredlund and Xing fitting parameters			
			$\alpha$ (kPa <sup>-1</sup> )	$n$	R <sup>2</sup>	$a$ (kPa)	$n$	$m$	R <sup>2</sup>
MPS-6	CKD	s-w	0.009	1.396	0.999	1357.6	0.503	3.151	0.999
		s-S <sub>r</sub>	0.011	1.616	0.999	228.67	0.729	2.30	0.999
	Sand-CKD	s-w	0.575	1.497	0.999	2.586	3.499	0.681	0.999
		s-S <sub>r</sub>	0.497	1.563	0.997	6.601	10.74	0.523	0.998
	Sand	s-w	0.301	2.772	0.999	2.990	4.729	1.244	0.999
		s-S <sub>r</sub>	0.281	3.180	0.999	2.555	3.820	1.304	0.999
WP4-C	CKD	s-w	0.00036	3.323	0.986	2181.8	4.48	1.075	0.987
		s-S <sub>r</sub>	0.00033	3.231	0.997	2641.2	7.04	0.684	0.996
	Sand-CKD	s-w	0.0025	2.094	0.999	492.61	1.876	1.633	0.999
		s-S <sub>r</sub>	0.0026	2.127	0.999	633.31	1.617	2.178	0.999
	Sand (12.75 kN/m <sup>3</sup> )	s-w	0.053	1.891	0.999	47.95	0.772	3.621	0.999
		s-S <sub>r</sub>	0.106	1.659	0.996	53.06	0.737	3.83	0.999
	Sand (14.81 kN/m <sup>3</sup> )	s-w	0.022	1.969	0.999	131.58	1.157	3.605	0.999
		s-S <sub>r</sub>	0.022	2.073	0.999	106.98	1.205	3.085	0.999
Washed sand	s-w	0.098	1.727	0.999	17.95	1.273	2.018	0.999	
	s-S <sub>r</sub>	0.085	1.832	0.997	25.919	1.057	2.679	0.998	

Table 5.4 Air entry values for the materials used. (s = suction, w = water content, Sr = degree of saturation)

Device	Material	Relation type	Air entry value (kPa)		
			Graphical method	van Genuchten (1980)	Fredlund and Xing (1994)
Pressure plate and desiccator	CKD	s-w	112	500	903.60
		s-S <sub>r</sub>	325	714.30	789.20
MPS-6	CKD	s-w	32	111.11	1357.6
		s-S <sub>r</sub>	24	90.91	228.67
	Sand-CKD	s-w	---	1.74	2.586
		s-S <sub>r</sub>	---	2.01	6.601
	Sand	s-w	---	3.32	2.990
		s-S <sub>r</sub>	---	3.56	2.555
WP4-C	CKD	s-w	1550	2777.8	2181.8
		s-S <sub>r</sub>	1600	3030.3	2641.2
	Sand-CKD	s-w	175	400	492.61
		s-S <sub>r</sub>	180	384.6	633.31
	Sand (12.75 kN/m <sup>3</sup> )	s-w	12	18.87	47.95
		s-S <sub>r</sub>	7.0	9.43	53.06
	Sand (14.81 kN/m <sup>3</sup> )	s-w	17.5	45.45	131.58
		s-S <sub>r</sub>	20	24.45	106.98
	Washed sand	s-w	3.0	10.20	17.95
		s-S <sub>r</sub>	5.5	11.76	25.919

## **5.4 Concluding remarks**

In this chapter, the water retention curves (WRCs) of CKD, sand-CKD, and sand are presented. The WRCs were experimentally determined using various devices (pressure plate extractor, desiccator, chilled-mirror dew-point potentiometer, and fixed-matrix porous ceramic disk water potential sensor). The parametric analysis of the WRCs was performed using van Genuchten (1980) and Fredlund & Xing (1994) models. Clod tests were carried out to study the shrinkage behaviour of the CKD. Electrical conductivity tests were also carried out on the cement kiln dust specimens to determine the osmotic suction. The main findings of this study can be summarised as follows:

(1) The suction equilibration time was influenced by the suction measurement and control techniques used in the study. Several days to weeks were required to attain equilibrium in pressure plate and desiccator tests, whereas a much lower equilibrium time was noted for the WP4-C and MPS-6 tests. For the MPS-6 tests, a longer equilibrium time was required for the sand and sand-CKD, particularly at low water contents that can be attributed to a lack of good water phase continuity between the specimens and the ceramic disks of the sensors.

(2) For any material in this study, the WRCs in terms of the water content and the degree of saturation were affected by the device used to establish the WRCs. At high water contents or at lower suctions distinct differences were noted in the WRCs even after applying corrections for the osmotic suction and compaction dry density. The differences in the WRCs were found to be lesser at high suctions.

(3) Parametric models, such as van Genuchten and Fredlund and Xing enabled best-fitting the WRCs and in each case the  $R^2$  value was found to be close to 1. The fitting parameters obtained for the water content and degree of saturation WRCs were found to be dissimilar. The Clod test results suggested that CKDs exhibit significant shrinkage characteristic and hence the suction – degree of saturation WRCs are more relevant for the determination of air entry value of CKDs. The air entry fitting parameters from both van Genuchten and Fredlund and Xing models were found to be different. Comparisons of the air entry value from graphical construction procedure and the models showed that Fredlund and Xing equation provided higher values of the air entry.

## **CHAPTER 6**

# **Effects of suction and net stress on the one dimensional volume change behaviour of cement kiln dust**

### **6.1 Introduction**

Volumetric behaviour of unsaturated soils and industrial wastes can have a significant influence on foundations, landfill cover systems, embankments, and earth dams (Mitchell and Soga 2005; Lins 2009; Dixit 2016; Ng et al. 2016). Volume change in soils is manifested in swell and collapse and are directly influenced by a variation of the stress acting on the soil. Both the effects of external total stress and pore water pressure depend upon the soil/material type (Sridharan et al. 1986; Mitchell and Soga 2005). In recent years, the importance of considering the volume change of soils during suction change has been recognized by a number of researchers (Peron et al. 2007; Perez-Garcia et al. 2008; Lins 2009; Nuth and Laloui 2011; Fredlund and Houston 2013). Several laboratory tests are available to determine the deformation characteristics of unsaturated soils, such as the one-dimensional compression test, isotropic compression test, and wetting and drying tests under various stress conditions in triaxial and direct shear tests.

Previous studies on CKDs have demonstrated that an addition of CKD with free lime controls the volume change in fine-grained soils (Parsons et al. 2004; Sreekrishnavilasam and Santagata 2006; Andrew 2012; Moses and Afolayan 2013; Yilmaz 2014). A significant volumetric expansion was also reported when CKD with high sulfate content was added to some soils (Parsons et al. 2004; Sreekrishnavilasam and Santagata 2006). Swelling of CKD and mixture of sand and CKD also have been reported in the past (Tuncer et al. 2012). Previous studies have not explored the effects of suction and net stress on the volume change behaviour of compacted unsaturated CKD. Such studies are crucial for determining the unsaturated property functions.

The main objective of this chapter is to investigate the volume change behaviour of compacted CKD during the wetting processes at constant net normal stress. The testing device used in this study was a suction-controlled oedometer which allows simultaneous application and control of the matric suction ( $u_a - u_w$ ) and the net normal stress ( $\sigma - u_a$ ) during a test. The volume change of specimens can be monitored during a test.

## **6.2 Experimental programme**

Suction-controlled oedometer tests (Figure 3.26 and Section 3.4.4.4.1) were performed on compacted unsaturated CKD specimens. Suction was applied using the axis-translation technique. The initial water content and dry unit weight of the compacted specimens were 27.3% and 14.83 kN/m<sup>3</sup>, respectively (Section 3.4.2.1). The initial total suction of the specimens measured by chilled-mirror dew-point potentiometer was about 2040 kPa, whereas a much lower suction was measured using other devices (Chapter 5). The wetting tests were carried out by applying various suctions at a constant net normal stress of 25 kPa. The initial suction was directly reduced to the target values of 150, 100, 50, 5, 0 kPa. For this purpose, five specimens with identical compaction conditions were used.

During the test, the water volume change and vertical deformation were monitored. The vertical deformation was measured by a linear variable displacement transducer and the water volume change was recorded by a pressure/volume controller which maintained a pore water pressure of 0 kPa during the test.

## **6.3 Results and discussion**

The following sections present the results of suction-controlled oedometer tests in terms of water volume/water content and vertical deformation. The pressure plate test results (drying tests) are also considered for comparison.

### **6.3.1 Water volume and vertical deformation**

Figures 6.1 a and b show the elapsed time versus the water volume change and vertical deformation at various applied and at a net vertical stress of 25 kPa. The test results for zero suction were from conventional oedometer device and therefore no water volume change was obtained. Difficulties were encountered in determining the water volume change for the specimen subjected to matric suction of 150 kPa due to the diffusion of air during the test. Diffused air accumulated over time in the water compartment and volume/pressure controller and hence the results were unreliable.

The water volume change in specimens were found to be significant during the first week after the tests were commenced which remained nearly constant thereafter until the end of the tests. The total duration of tests varied between 15 to 21 days at which the water volume attained equilibrium.

Figure 6.1 b shows that all specimens demonstrated collapse behaviour at all the imposed suctions during the initial testing period. A negative sign has been used to refer to the collapse deformation whereas a positive sign has been utilised for the swelling deformation. The magnitudes of vertical deformation remained less than 0.05 mm and hence can be considered insignificant. The calculated collapse strain at applied suctions of 150 and 100 kPa was found to be about 0.03%. With an elapsed time, the specimens at applied suctions of 50, 5, and 0 kPa exhibited minor swelling deformations. The vertical deformation at applied suctions of 50, 5 and 0 kPa were found to be about 0, 0.1, and 0.2 mm respectively, and hence can be considered insignificant. Development of swelling strain following the collapse of the CKD specimen can be attributed to (i) compression of macropores due to a decrease in suction that caused a collapse and (ii) absorption of water by the aggregates over time due to expansion of the microstructure within the aggregates. Several studies in the past have reported that the swelling and collapse behaviour can be attributed to the changes in structure and stress state of material upon wetting (Jennings and Burland 1962; Gallipoli et al. 2003; François and Laloui 2008).

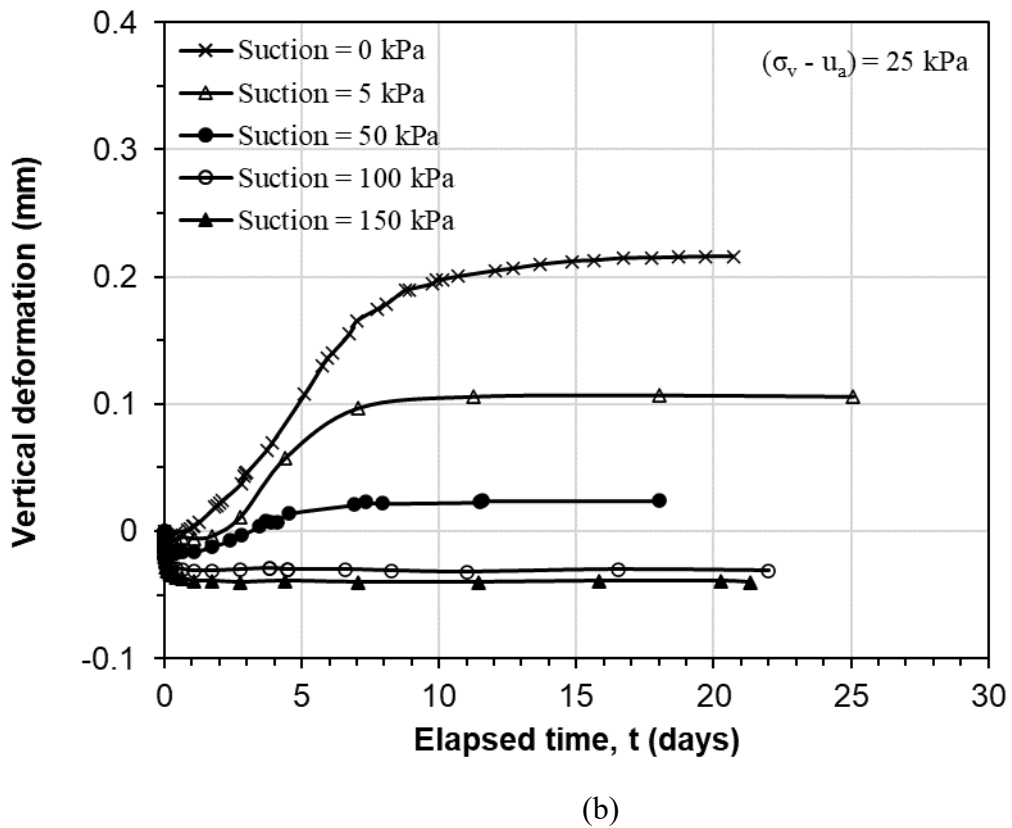
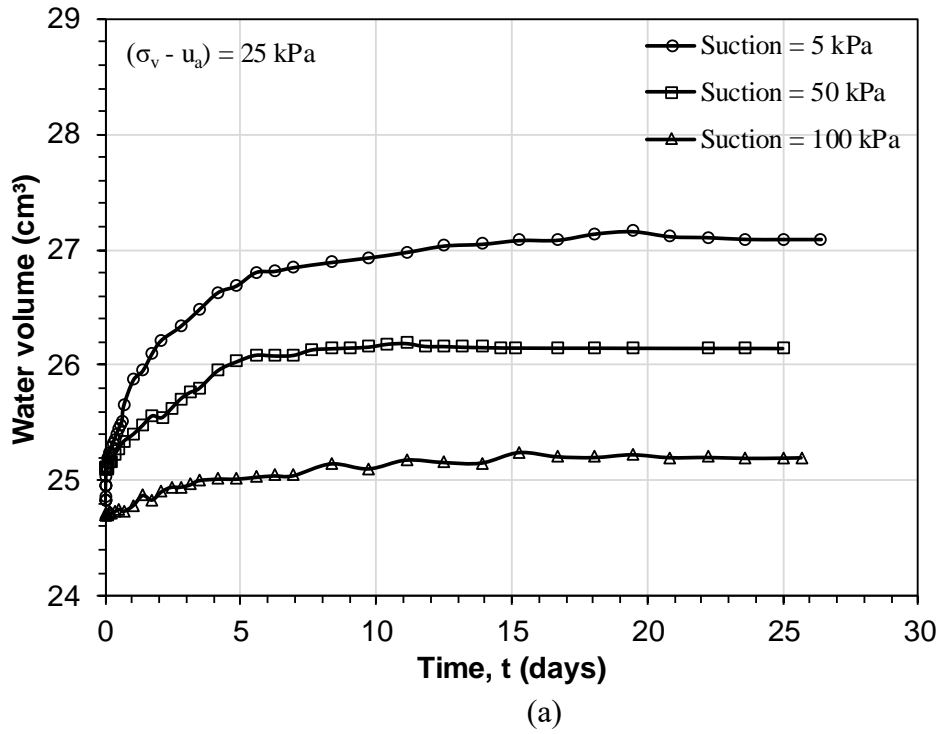


Figure 6.1 Elapsed time versus (a) water volume change and (b) vertical deformation at various applied suctions and a constant net stress of 25 kPa.

The overall behaviour of soil depends upon the magnitude of the applied loads and the change of water content (Jennings and Burland 1962; Sivakumar 1993). At low suctions, it is expected that much water is absorbed by the CKD. At high suction, the absorbed amount of water was lesser as can be evidenced from the water volume change data (Figure 6.1 a). The test results show that an application of surcharge significantly reduces the swelling of the CKD, whereas the collapse deformation can be considered insignificant. The effects of vertical deformation due to suction changes on the void ratio and WRC is presented in the following sections.

### **6.3.2 Void ratio change during wetting and drying**

The void ratio of the specimens at each applied suction in the suction-controlled oedometer tests were calculated based on measured vertical deformations. Figure 6.2 shows the applied suction versus void ratio plot for the CKD. The initial void ratio and initial suction of the specimens were 0.79 and 2040 kPa, respectively. The suction-void ratio results from the pressure plate tests (drying tests) at zero net stress are also included in Figure 6.2 for comparison.

The test results presented in Figure 6.2 show that wetting of the CKD caused a minor change (increase) in the void ratio, particularly at smaller suctions, whereas a decrease in the void ratio was noted at higher suctions. The increase in the void ratio is due to the swelling of the material at smaller applied suctions. The resulting increase in the void ratio (swelling) could be explained as the change in microstructure of the CKD specimen, whereas the rearrangement of the particles (macrostructure) is responsible for the reduction in void ratio (collapse).

Comparing the suction-controlled oedometer test results with the pressure plate test results showed two distinct aspects, such as (i) the void ratios of the CKD from the suction-controlled oedometer tests remained below that of the results from the pressure plate tests (drying tests) and (ii) for any suction change, the change in the void ratio in case of pressure plate tests (drying tests) was greater as compared to that occurred in wetting tests in suction control oedometer. A higher void ratio attained by the specimen in pressure plate tests is due to the initial conditions of the specimen (water content greater than the liquid limit) that underwent the drying process under a zero external load. In the

suction-controlled oedometer tests, the compacted specimens underwent wetting process at an applied vertical pressure of 25 kPa.

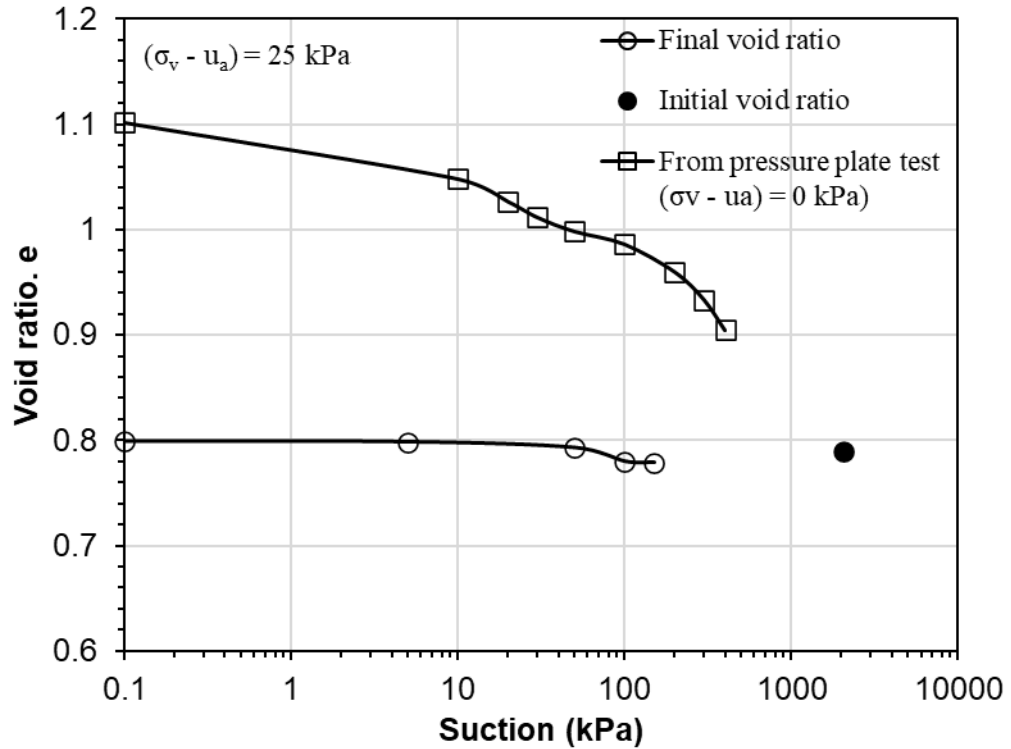


Figure 6.2 Effect of the applied suction on the void ratio of cement kiln dust.

### 6.3.3 Water retention behaviour of CKD during the wetting process

Figure 6.3 presents the measured water contents of CKD at various applied suctions and at a constant net stress of 25 kPa. The water contents were also calculated based on the initial water content (27.3%) of the specimen and the water volume changes during the tests that were measured by the pressure/volume controller. The water retention data (suction versus water content) from the pressure plate tests are also included in Figure 6.3 for comparison.

It can be seen in Figure 6.3 that the water content of CKD increased from 27.3 to about 30% for a suction decrease from 2040 to 0 kPa. That is an increase in the water content of only about 2.5%. At an applied suction of 150 kPa, the water content of the

specimen was found to be less than the initial water content. The differences between the measured water contents and calculated water contents based on initial water content and water volume change measurements remained less than about 0.5%. This difference between the measured and calculated values may be attributed to the evaporation and condensation of water inside the cell because of the fluctuation in the room temperature (Perez-Garcia et al. 2008) as well as the presence of the filter paper between the specimen bottom and the ceramic disk.

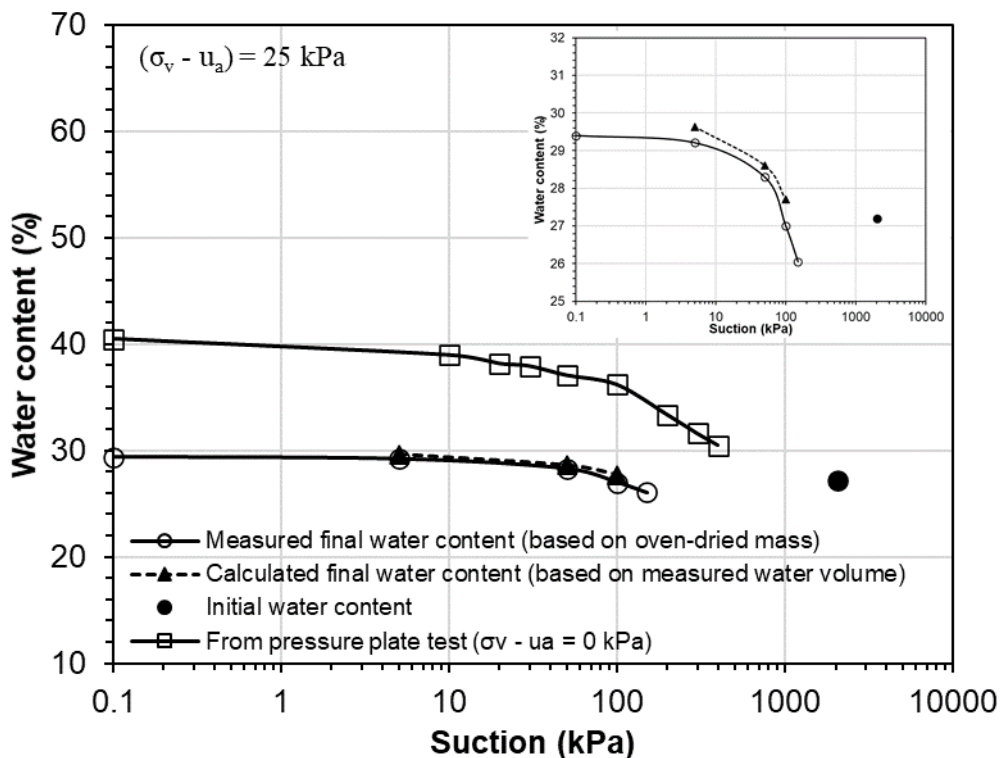


Figure 6.3 Effect of the applied suction on the water content of cement kiln dust specimens at a constant net normal stress of 25 kPa.

Figure 6.4 illustrates the water retention behaviour of CKD in terms of the degree of saturation. The degree of saturation of the specimens at various applied suctions were calculated based on (i) the final measured water contents and the void ratios after swelling and collapse processes and (ii) on the initial degree of saturation, vertical deformation and water volume changes.

The results presented in Figure 6.4 show that a decrease in the degree of saturation of the specimen occurred at an applied suction of 150 kPa, whereas at all other applied

suctions, the degree of saturation increased. Differences were noted between degree of saturation calculated based on the measured water contents and vertical deformation and the calculated degree of saturation based on the water volume measurements. As expected, the degree of saturation of CKD during the drying process (from the pressure plate test results) were greater than that during the wetting process (suction-controlled oedometer tests).

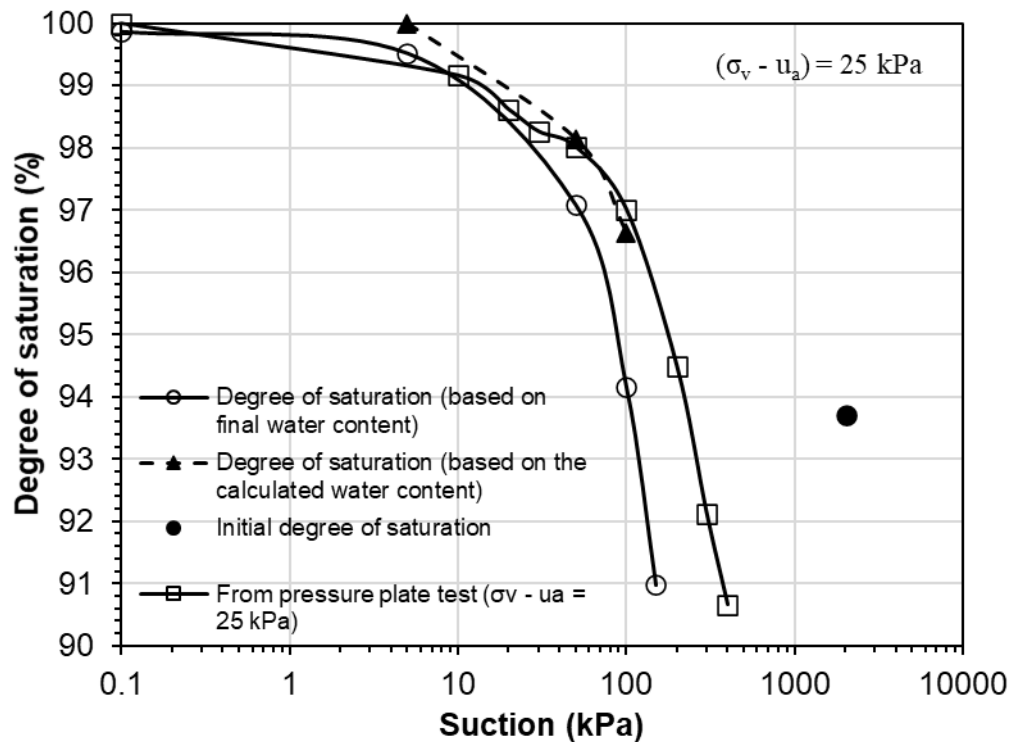


Figure 6.4 Effect of the applied suction on the degree of saturation of cement kiln dust specimens at constant net normal stress of 25 kPa.

## **6.4 Concluding Remarks**

In this chapter, the one-dimensional volume change behaviour of compacted cement kiln dust during the wetting process was studied. A suction-controlled oedometer was used for this purpose. The tests were carried out at a net normal stress of 25 kPa. The test results from the suction-controlled oedometer tests (wetting tests) were compared with the results from the pressure plate tests (drying tests). The test results revealed the following:

(1) Wetted under a constant net stress of 25 kPa, compacted unsaturated CKD exhibited minor swelling deformation at low suctions ( $< 50$  kPa), whereas very minor collapse deformations were noted at high suctions (100 and 150 kPa). The vertical deformation influenced the water content and degree of saturation. As compared to the initial compaction water content, an increase in the water content and degree of saturation was observed at low applied suctions, whereas the water content and degree of saturation decreased at high applied suctions. A decrease in the water content is attributed to a slight decrease in the void ratio due to collapse compression of the CKD.

(2) The impact of applied net stress of 25 kPa was distinct on the void ratio, water content and degree of saturation of the CKD. The wetting suction - degree of saturation and suction – water content WRCs were found to remain below that of the WRC established from the results of pressure plate tests (drying WRC).

## **CHAPTER 7**

# **Shear strength, volume change, and permeability behaviour under saturated and unsaturated conditions**

### **7.1 Introduction**

Compacted soils are used in various geotechnical and geoenvironmental structures, such as earth dams, landfill liners and covers for waste containment, embankments, foundations, pavement subgrades, soil barriers, backfill, engineered slopes and earth retaining walls (Vanapalli et al. 1997; Sheng et al. 2011; Goh et al. 2015; Saffari et al. 2015). Depending upon the availability of specific soil types and cost-effectiveness, in some cases alternative materials can also be selected to satisfy the engineering properties required in the design of these structures. Shear strength and hydraulic conductivity are two of the most important engineering properties that are required to be evaluated under saturated and unsaturated conditions (Vanapalli et al. 1997).

The internal shear resistance is a result of friction and the interlocking of particles and possibly cementation or bonding at the particle contacts (Onur et al. 2014; Roy and Kumar 2017). The shear strength of soils is influenced by the confining pressure, drainage conditions, water content, soil structure, rate of strain, plasticity, cementation, void ratio, type of minerals, and the size, shape, and gradation of the particles (Lambe and Whitman 1969; Poulos 1988; Onur et al. 2014).

In the saturated soil, the shear strength is commonly described by the Mohr-Coulomb failure criterion, which defines shear strength in terms of the material variables ( $\phi'$ ) and  $c'$  and the effective stress variable controlling the behaviour of saturated soils (Terzaghi 1936). For unsaturated soils, the shear strength is controlled by two stress states variables which are the net normal stress and the matric suction (Fredlund et al. 2012). The suction component of shear strength is referred to as the apparent or total cohesion

(Taylor 1948). The rate of change in shear strength relative to changes in matric suction is defined by the angle  $\phi^b$ . This angle was assumed to be constant and a linear relationship between the shear strength and matric suction has been presented for the unsaturated soils. However, as a wider variety of soil types have been tested over a wider range of soil suctions, it has become increasingly obvious that the shear strength versus matric suction relationship should not be limited to a linear relationship (Escario and Saez 1986; Fredlund et al. 1987; Gan et al. 1988; Vanapalli et al. 1996; Farouk et al. 2004; Fredlund et al. 2012; Chowdhury and Azam 2016). The air-entry value provides an indication of the point where the shear strength versus matric suction starts to exhibit nonlinear shear strength behaviour (Sivakumar 1993; Fredlund et al. 2012).

The contribution of matric suction to the shear strength of unsaturated soils has been studied by many researchers (Fredlund et al. 1978; Fredlund et al. 1996; Vanapalli et al. 1996; Taha et al. 2000; Vanapalli and Fredlund 2000; Farouk et al. 2004; Estabragh and Javadi 2012; Goh 2012; Gui and Wu 2014; Elsharief and Abdelaziz 2015; Chowdhury and Azam 2016; Pujiastuti et al. 2018).

The saturated hydraulic conductivity is influenced by several factors such as the void ratio, shape and roughness of particles, confining pressure, initial water content and dry density, fine content, mineralogical composition, the ionic concentration and the thickness of layers of water held to the clay particles, and soil skeleton structure (Mitchell and Soga 2005; Das 2010). Saturated hydraulic conductivity is a function of void ratio only, whereas for unsaturated soils, the hydraulic conductivity with respect to water is a function of both void ratio and degree of saturation (Leong and Rahardjo 1997; Cai et al. 2014). The value of unsaturated hydraulic conductivity of water phase is influenced by types of soil, properties of porous medium (e.g., density), degree of saturation, water-air interfacial tension, and viscosity of water (Fredlund and Rahardjo 1993). Hydraulic conductivity measurements of unsaturated soils in the laboratory (steady-state and unsteady-state methods) is usually considered a time-consuming process, particularly for low water content conditions (Leong and Rahardjo 1997). The unsaturated hydraulic conductivity can be estimated from the soil-water retention curve by establishing hydraulic conductivity functions (empirical, macroscopic, and statistical models). In this study, only saturated hydraulic conductivity of the selected materials has been measured.

From the information reviewed on the shear strength and permeability of cement kiln dust (CKD) and/or CKD-treated soils (admixtures) it was found that, most of the previous studies performed the direct shear tests and unconfined compression tests to investigate the shear strength behaviour under saturated conditions. However, a few studies were performed on such materials using triaxial compression tests under different drainage conditions and with different strain rates. In addition, the saturated hydraulic conductivity of such materials has been explored using the constant and falling head methods using the rigid and flexible wall (at constant effective confining pressure) permeameters. However, studies on the saturated hydraulic conductivity under different confining pressures are limited and studies on the unsaturated shear strength of cement kiln dust under various matric suctions are still scarce.

Previous studies have shown that CKD-treated soils exhibited an improvement in shear strength and distinct changes in coefficient of permeability depending on the type of treated soils and amount and type of CKD used as an additive (Baghdadi and Rahman 1990; Baghdadi et al. 1995; USEPA 1998; Mohamed 2002; Sariosseiri and Muhunthan 2008; Moses and Afolayan 2011; Andrew 2012; Elmashad and Hashad 2013; Al-hassani et al. 2015; Ata et al. 2015; Osinubi et al. 2015; Upma and Kumar 2015; Lake 2016). Baghdadi et al. (1995) reported that CKD and CKD-mixture specimens exhibited relatively high strengths, but the specimens of 75% and 100% CKD did not satisfy the durability requirement under cycles of freeze - thaw.

The objectives of this chapter are:

- 1- To determine the shear strength parameters of compacted CKD, sand, and sand-CKD under saturated condition and at drained and undrained conditions to explore the impact of drainage conditions on the shear strength parameters.
- 2- To study effect of confining pressure on the saturated hydraulic conductivity of compacted CKD, sand, and sand-CKD.
- 3- To investigate the shear strength and volume change behaviour of the unsaturated compacted CKD during the wetting process at matric suctions and at a constant net confining pressure of 25 kPa in triaxial testing conditions.

## **7.2 Experimental program**

The experimental program consisted of three series of triaxial tests - UU, CU and CD shear tests on compacted-saturated materials, permeability tests on compacted-saturated materials in triaxial test set up, and unsaturated shear strength tests. All compacted specimens used in this investigation were 50 mm in diameter and 100 mm in height and prepared following the procedure described in Section 3.4.4.1.1.

Firstly, saturated shear strength tests (UU and CU-Tests) were carried out on the compacted specimens of CKD, sand, and sand-CKD under different confining pressures (100, 200, 400 kPa). These specimens were prepared at an average compaction water content of 27.5, 13.0, and 11.1% and an average dry unit weight of 14.83, 15.48, and 17.76 kN/m<sup>3</sup> for the CKD, sand, and sand-CKD, respectively. The specimen and measuring system preparation and testing stages were according to the procedures described in Section 3.4.4.1.2. The sand and sand-CKD specimens were sheared with a strain rate of 1 mm/min in the UU and CU-tests while the CKD specimens were tested with a strain rate of 1 mm/min in the UU tests and two strain rates of 1 and 0.083 mm/min were used in the CU tests. Similar strain rates have been adopted by Bishop and Henkel (1962), Wasemiller and Hoddinott (1997), Sreekrishnavilasam and Santagata (2006), Varathungarajan et al. (2009), Bensoula et al. (2015).

The consolidated drained (CD) tests were conducted on compacted-saturated CKD specimens under confining pressures of 25, 100, 200, and 400 kPa in order to obtain the cohesion intercept ( $c'$ ) at full saturation condition (suction = 0 kPa) and the angle of internal friction ( $\phi'$ ) to be adopted for the development of the extended Mohr-Coulomb failure envelope for unsaturated specimens. The system preparation, saturation, consolidation, and shearing stages were conducted according to the procedures described in Section 3.4.4.1.2. The specimens were sheared at a constant strain rate of 0.0009 mm/min until the maximum axial strain was reached. This strain rate was used in order to limit the pore water pressure development to small values during the shearing process. This strain rate has been adopted by several researchers (Rahardjo et al. 1995; Rahardjo et al. 2004; Thu et al. 2006; Guan et al. 2010; Goh et al. 2015). Additionally, the properties (i.e. fine contents, saturated permeability, and plasticity index) of the CKD used were similar to the soils used in the reported studies.

In the second series of tests, saturated permeability of compacted CKD, sand, and sand-CKD specimens was determined using a triaxial test set up. Section 3.4.4.1.1 presents the test procedure. The initial water contents of CKD, sand and sand-CKD specimens were 27.3, 13.2, and 11.2% respectively. The initial dry unit weights of CKD, sand and sand-CKD were 14.85, 15.43, and 17.73 kN/m<sup>3</sup>, respectively. The saturation and consolidation stages were carried out following the procedures similar to that of the CD and CU triaxial tests (Section 3.4.4.1.2). Five different net confining pressures (25, 50, 100, 200, and 400 kPa) were selected and the pressure difference between the bottom and top of the specimens during the permeability tests were 20, 2, and 7 kPa. The corresponding hydraulic gradients for the CKD, sand, and sand-CKD, were 20.61, 2.02, and 7.14 respectively.

In the third series of tests, unsaturated consolidated drained (CD) tests were conducted on the compacted CKD specimens under various imposed matric suctions (150, 100, 50, and 5 kPa) at a net confining pressure of 25 kPa. The compacted specimens were prepared following the procedure described in Section 3.4.4.1.1 at average initial water content 27.3% and average dry unit weight 14.95 kN/m<sup>3</sup>. The initial total suction of the specimens measured by chilled-mirror dew-point potentiometer was about 2040 kPa. Therefore, the specimens were taken through the wetting process. During the tests, the pore-air pressure was controlled using the axis translation technique and the pore water pressure was set to zero via volume/pressure controller. Each specimen was equalised to the targeted suction during wetting process and was then sheared at a constant strain rate (0.0009 mm/min) until attaining the specified maximum axial strain. During the suction equalisation and shearing processes, water volume change and total volume change were measured by a volume/pressure controller and a differential pressure transducer.

In following sections, the results from UU, CU and CD tests on compacted-saturated materials are presented first followed by the results from the permeability tests on compacted saturated materials and unsaturated consolidated drained tests on compacted CKD.

## 7.3 Results and discussion

### 7.3.1 UU and CU triaxial test results

#### 7.3.1.1 UU and CU-test results of compacted-saturated cement kiln dust (CKD)

Figure 7.1 a and b show the deviator stress versus axial strain plots from UU and CU triaxial tests on compacted-saturated specimens of CKD. Figure 7.1 c presents the variations of pore water pressure during the shearing process in case of the CU tests. The confining pressures and shearing rates (1 mm/min and 0.083 mm/min) are indicated in Figures 7.1 b and c. The UU tests were conducted with a strain rate of 1 mm/min (Figure 7.1 a).

The UU test results (Figure 7.1 a) show that compacted-saturated specimens of CKD exhibited brittle behaviour at confining pressures of 200 and 400 kPa. In these cases, the deviator stress increased and attained peak values (530 kPa and 865 kPa at axial strains of about 14.3% and 15.7%, for applied confining pressures of 200 and 400 kPa, respectively and further decreased. Unexpected behaviour was observed under the applied confining pressure of 100 kPa, where the specimen exhibited ductile and strain hardening behaviour (showing no distinct peak stress) instead of strain softening and brittle failure. This behaviour can be due to the potential differences between the specimens in terms of the stress state and fabric during the preparation process in addition to the effect of the maximum stress ratio that depends on the confining pressure.

The CU test results (Figures 7.1 b and c) showed some distinct trends, such as (i) most specimens, except the specimen tested with a confining pressure of 400 kPa and sheared under 1 mm/min, exhibited ductile and strain hardening behaviour with no distinct peaks and (ii) the maximum deviator stresses obtained for specimens sheared at a rate of 0.083 mm/min were less as compared to the specimens sheared at 1 mm/min, whereas at any applied confining pressure, the impact of strain rate on the deviator stress was insignificant at 20% strain. Evolution of shear and pore water pressure of fine soils can be considerably controlled by arrangement of fine particles within the soil mass which is influenced by the applied strain rate (Sachan and Penumadu 2007). When a low loading rate is applied, the specimen may show contractive nature and variation in the microfabric

accompanied by an increase in pore water pressure. Consequently, the specimens exhibit lower effective stress and shear strength as compared to that tested at higher strain rate. Similar response of cohesive soils during the shearing process has been reported by Svoboda and McCartney (2014).

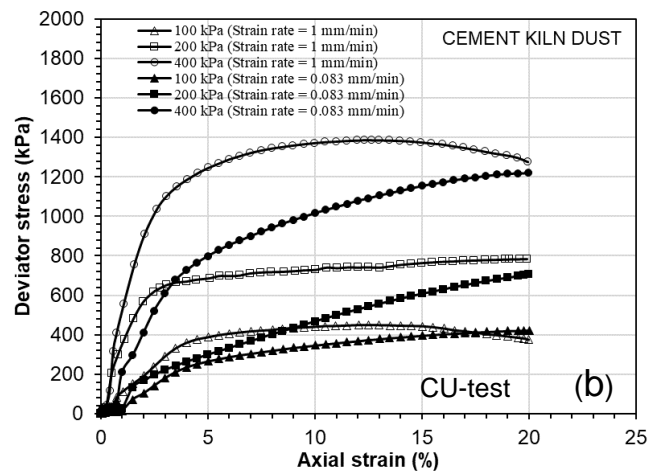
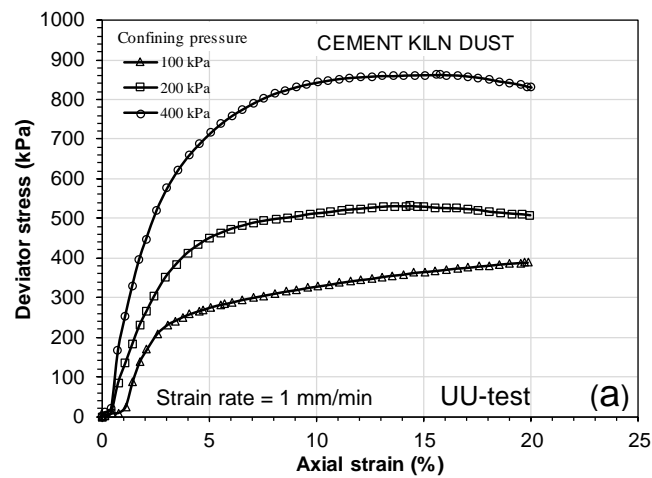
Comparisons of the peak deviator stresses (particularly under confining pressures of 200 and 400 kPa) obtained under both shearing rates for CU tests were found to be significantly higher than that of the specimens tested in UU tests. Higher maximum deviator stresses obtained in CU tests can be attributed to the densification of the specimens (decrease in void ratio) that occurred during the consolidation process under the effect of confining pressures.

The excess pore water pressure development in CU tests showed similar trend at all confining pressures (Figure 7.1 c). The pore water pressure increased with an increase in the axial strain and further decreased to attain negative values at high axial strain. The peak values of the pore water pressure were attained at an axial strain of about 2.5% or even less. The maximum value of the pore water pressure increased with an increase in the confining stress. The specimens behaved similar to overconsolidated soils that usually tend to exhibit dilatancy behaviour (Horpibulsuk et al. 2004; Head and Epps 2014). The peak deviator stresses from UU and CU tests on CKD specimens are presented in Table 7.1.

Figure 7.2 illustrates the Mohr-Coulomb failure envelopes for the CKD specimens from UU tests at a strain rate of 1 mm/min (Figure 7.2 a), and from CU tests at a strain rate of 1 and 0.083 mm/min (Figures 7.2 b and c).

From the UU tests, the undrained cohesion ( $c_u$ ) and angle of internal friction ( $\phi_u$ ) were found to be about 70 kPa and 27°, respectively. For the CU tests at shearing rate of 1 mm/min, the values of effective cohesion ( $c'$ ) and angle of internal friction ( $\phi'$ ) were found to be about 7 kPa, and 33.7°, respectively. Similarly, for the specimens sheared at strain rate of 0.083 mm/min, the values of  $c'$  and ( $\phi'$ ) were about 0 kPa and 34° respectively. It can be seen that the results showed nearly no cohesion under shearing rate of 0.083 mm/min and the shear strength was mainly controlled by the frictional interaction between the particles. This behaviour may be attributed to that the specimens tested at lower strain rate underwent variations in their structure which in turn affected

the interparticle bonding properties leading to an elimination of the cohesion effect. The test results show that the effect of shearing rate on the shear strength parameters from the CU tests is insignificant, whereas significant differences were noted between the shear strength parameters from UU and CU tests. The differences may be attributed to the change in fabric and the densification achieved during the consolidation process (Horpibulsuk et al. 2004; Bushra and Robinson 2012).



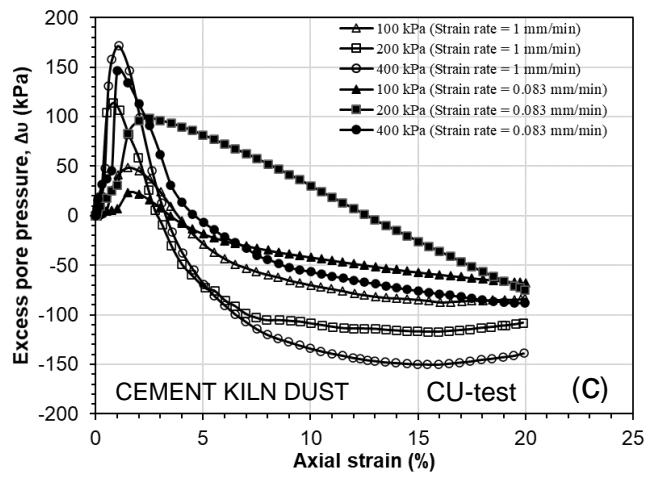


Figure 7.1 Results of the triaxial compression tests for the cement kiln dust specimens: (a) deviator stress from UU-tests; (b) deviator stress from CU-tests and (c) excess pore water pressure from CU-tests.

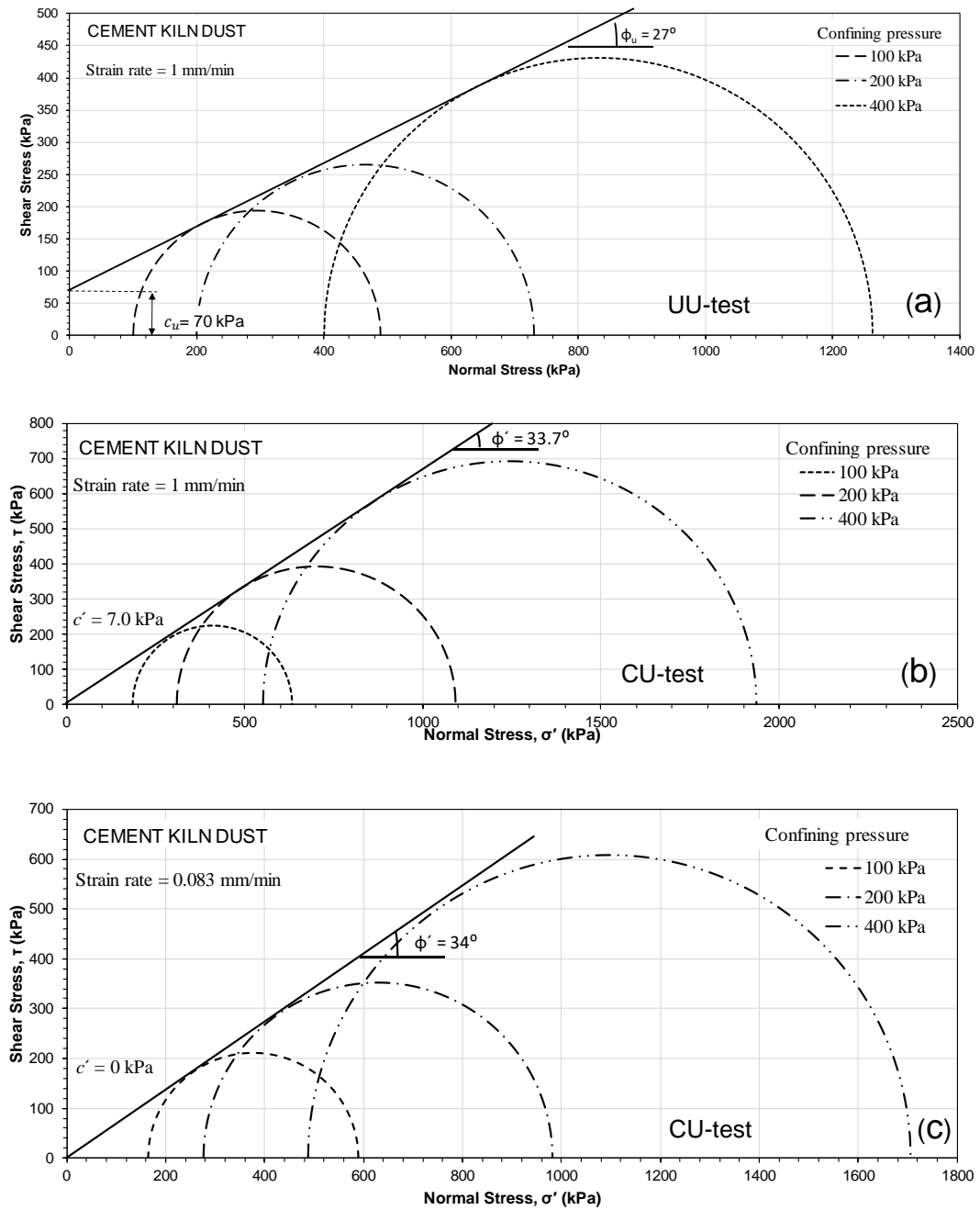


Figure 7.2 Mohr-Coulomb failure envelopes for the cement kiln dust specimens: (a) UU-tests with strain rate of 1 mm/min; (b) CU-tests with strain rate of 1 mm/min and (c) CU-tests with strain rate of 0.083 mm/min.

### **7.3.1.2 UU and CU-Test results of sand**

Figure 7.3 a presents the deviator stress versus axial strain plots from the UU triaxial tests of the sand tested. Figures 7.3 b and c show the deviator stress versus axial strain and axial strain versus excess pore water pressure plots from the CU triaxial tests for the sand specimens. The confining pressures are shown in Figure 7.3. A shearing rate of 1 mm/min was adopted in all these tests. The test results of the CKD and sand-CKD materials are also presented in Figure 7.3 a for comparison.

For the UU tests (Figure 7.3 a), an increase in the deviator stress was significant at low axial strain. The peak stresses were noted at an axial strain of about 5% or less. The deviator stress gradually decreased thereafter. The specimens exhibited brittle and strain softening behaviour, particularly at high confining pressures.

Comparing with the CKD and sand-CKD specimens, the sand specimens showed a different stress-strain response and greater peak deviator stress as compared to the CKD material whereas, the behaviour was similar to that of the sand-CKD mixture (Figure 7.5 a) with lower values of deviator stresses and axial strains at the peak.

For the CU tests (Figure 7.3 b), the specimens exhibited significantly higher peak deviator stresses as compared to that of the specimens in UU tests. The values of excess pore water pressure (Figure 7.3 c) showed an increasing trend until a peak value was reached and then decreased gradually to attain constant values, particularly under confining pressures of 100 kPa and 400 kPa.

The Mohr-Coulomb failure envelopes for UU and CU tests are presented in Figures 7.4 a and b, respectively. The values of deviator stresses and the axial strains corresponding to the peak stresses are presented in Table 7.1. The shear strength parameters are presented in Table 7.2.

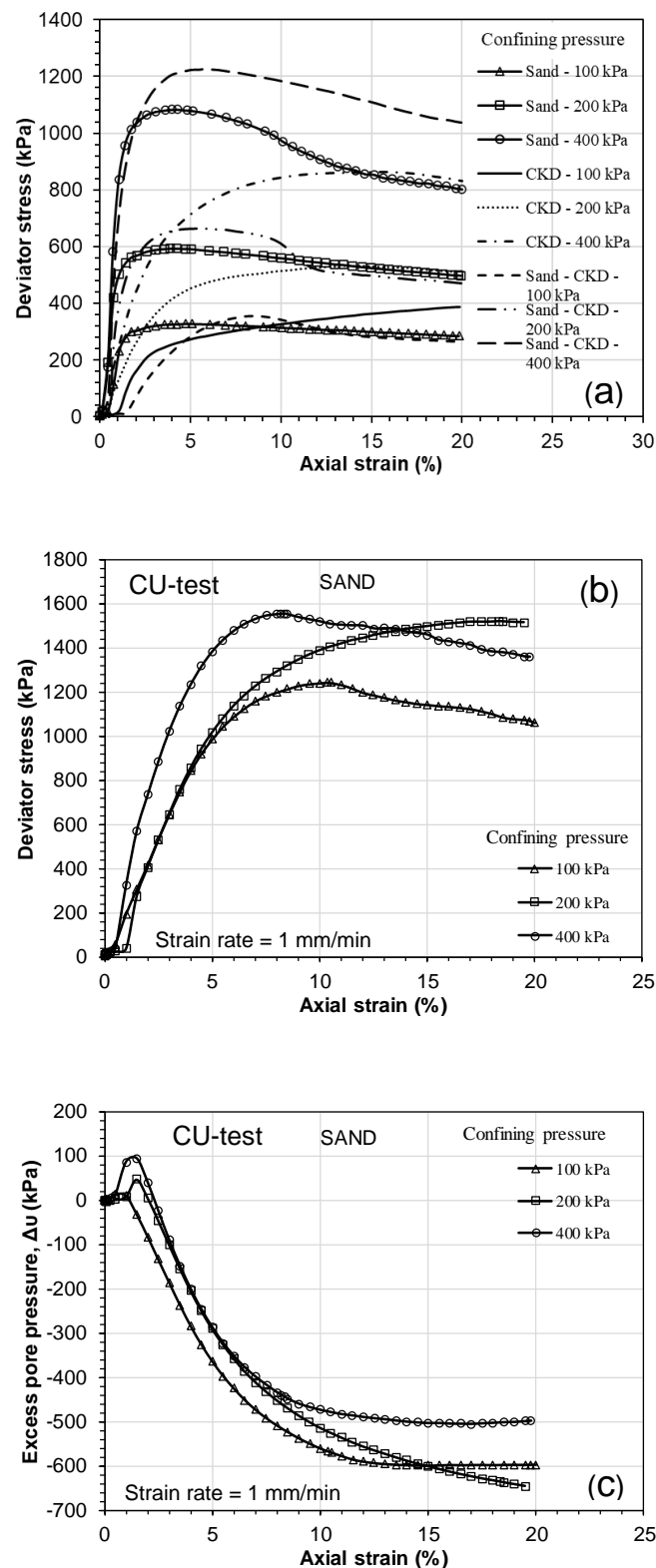


Figure 7.3 Results of the triaxial compression tests for the sand specimens: (a) axial strain versus deviator stress from UU-tests; (b) axial strain versus deviator stress from CU-tests and (c) axial strain versus excess pore water pressure from CU-tests.

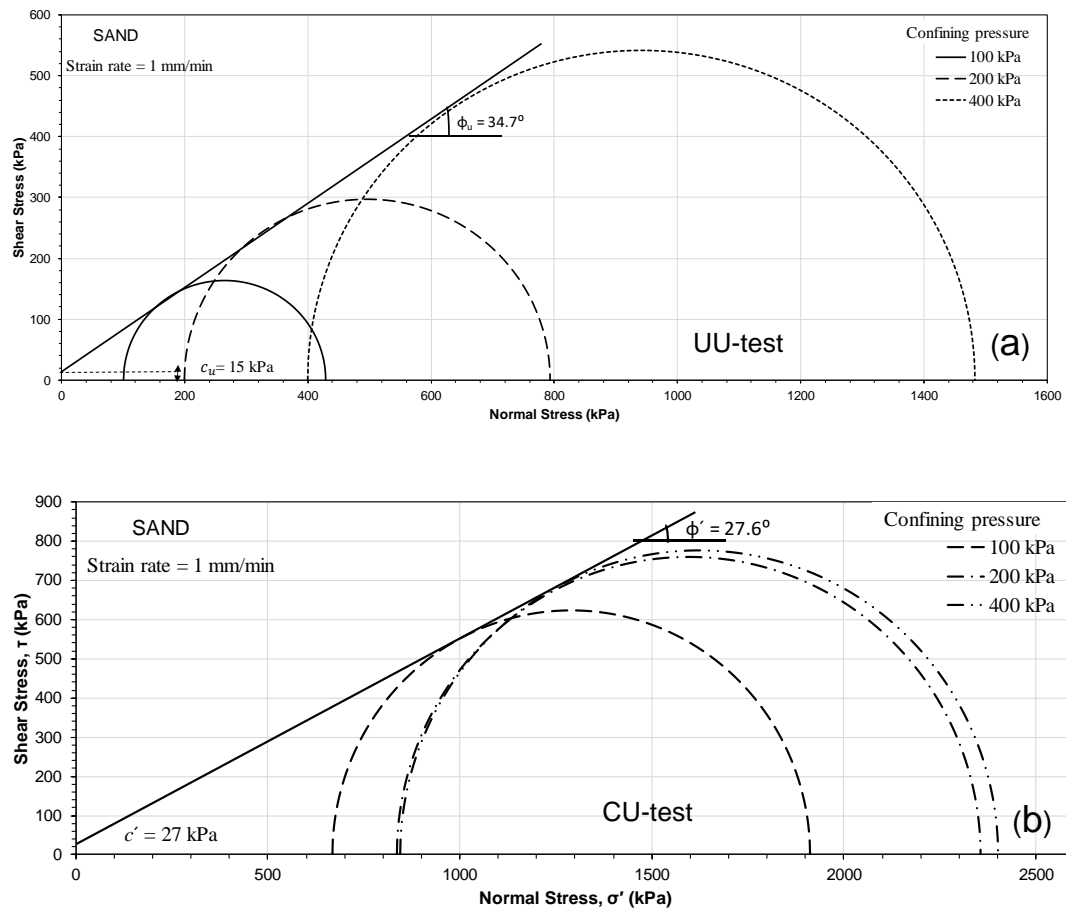


Figure 7.4 Mohr-Coulomb failure envelopes for the sand specimens: (a) UU-tests and (b) CU-tests.

### 7.3.1.3 UU and CU-Test results of the compacted sand-CKD mixture

Figure 7.5 illustrates the results of the UU and CU tests for the sand-CKD mixture. The stress-strain response of compacted-saturated sand (85%)-CKD (15%) specimens was found to be similar to that of sand specimens. The peak stress was higher in CU tests than in UU tests. However, higher values of peak deviator stresses at higher axial strains were observed as compared to that exhibited by the sand specimens. This may be attributed to the effect of addition of the CKD filling partially void of sand matrix and causing increase in the density of the mixture and change in sand structure influenced by grain size distribution and associated pores and interparticle forces such as cementation, electrostatic, and electromagnetic attractions (Lambe and Whitman 1969; Mitchell 1993).

It has been reported that the strength and deformation characteristics are mainly governed by the soil structure (Horpibulsuk et al. 2004; Hong et al. 2007). Previous studies conducted on mixtures of dune sand-CKD and foundry sand-CKD using the unconfined compression tests reported that results exhibited an improvement in strength as a result of the addition of the CKD (Baghdadi and Rahman 1990; Baghdadi et al. 1995; Moses and Afolayan 2011).

A brittle and strain-softening mode of failure was observed for the sand-CKD in a way similar to that noted for the sand specimens. In addition, results of the excess pore water pressure of specimens exhibit a behaviour nearly similar to that of the CKD specimens tested with a strain rate of 1 mm/min.

The Mohr-Coulomb envelopes for both UU and CU tests on sand-CKD mixture are plotted in Figure 7.6. The angle of internal friction was found to be higher and the apparent cohesion was lower in UU tests as compared to that in CU tests. The peak deviator stresses are presented in Table 7.1, whereas the shear strength parameters are presented in Table 7.2.

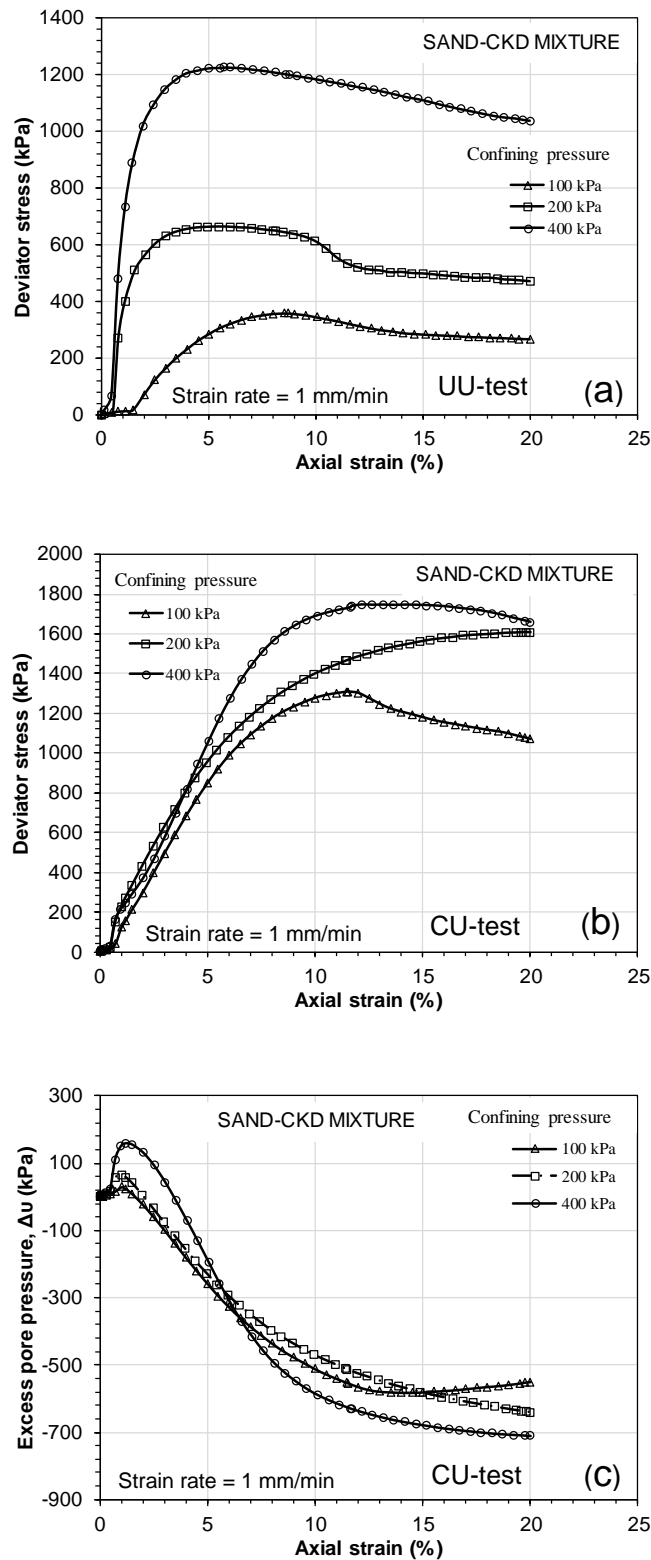


Figure 7.5 Results of the triaxial compression tests for the sand-CKD specimens: (a) axial strain versus deviator stress from UU-tests; (b) axial strain versus deviator stress from CU-tests and (c) axial strain versus excess pore water pressure from CU-tests.

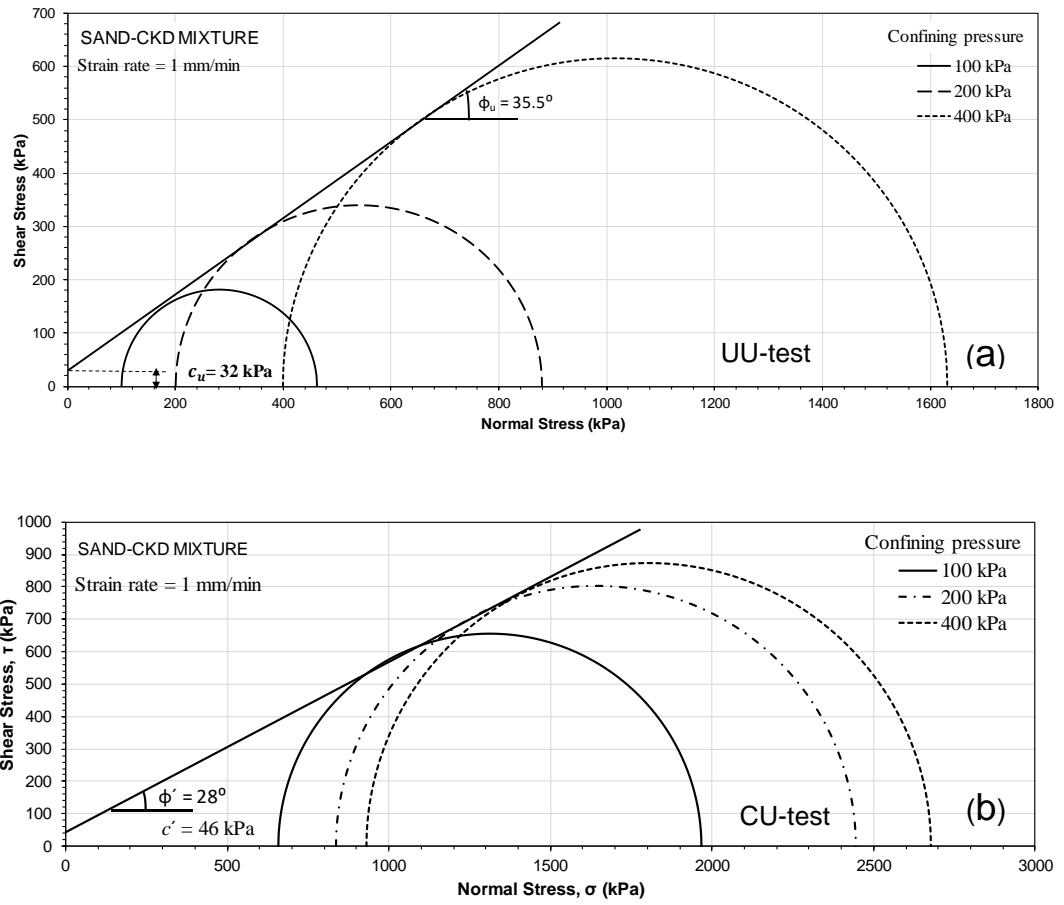


Figure 7.6 Mohr-Coulomb failure envelopes for the sand-CKD specimens: (a) UU-tests and (b) CU-tests.

#### **7.3.1.4 Peak deviator stress and axial strain under various conditions**

Figure 7.7 illustrates the peak deviator stress and axial strain plots of the CKD, sand, and sand-CKD under different confining pressures, test conditions, and strain rates. In general, regardless of the type of material and test, the peak deviator stress (Figure 7.7 a) increased with an increase in the confining pressure. The highest values of peak were observed for the sand-CKD specimens, whereas the lowest values were achieved by the CKD specimens. Further, the maximum deviator stresses of all materials from the CU tests were greater than those obtained from the UU tests. On the other hand, higher axial strain (Figure 7.7 b) was required to mobilise the maximum deviator stress for the CKD under both the test conditions (UU and CU tests), whereas lower values were noted for the other materials. Moreover, at strain rate of 0.083 mm/min, larger axial strain was required to mobilise the peak stresses of the CKD specimens as compared to the specimens sheared at 1 mm/min.

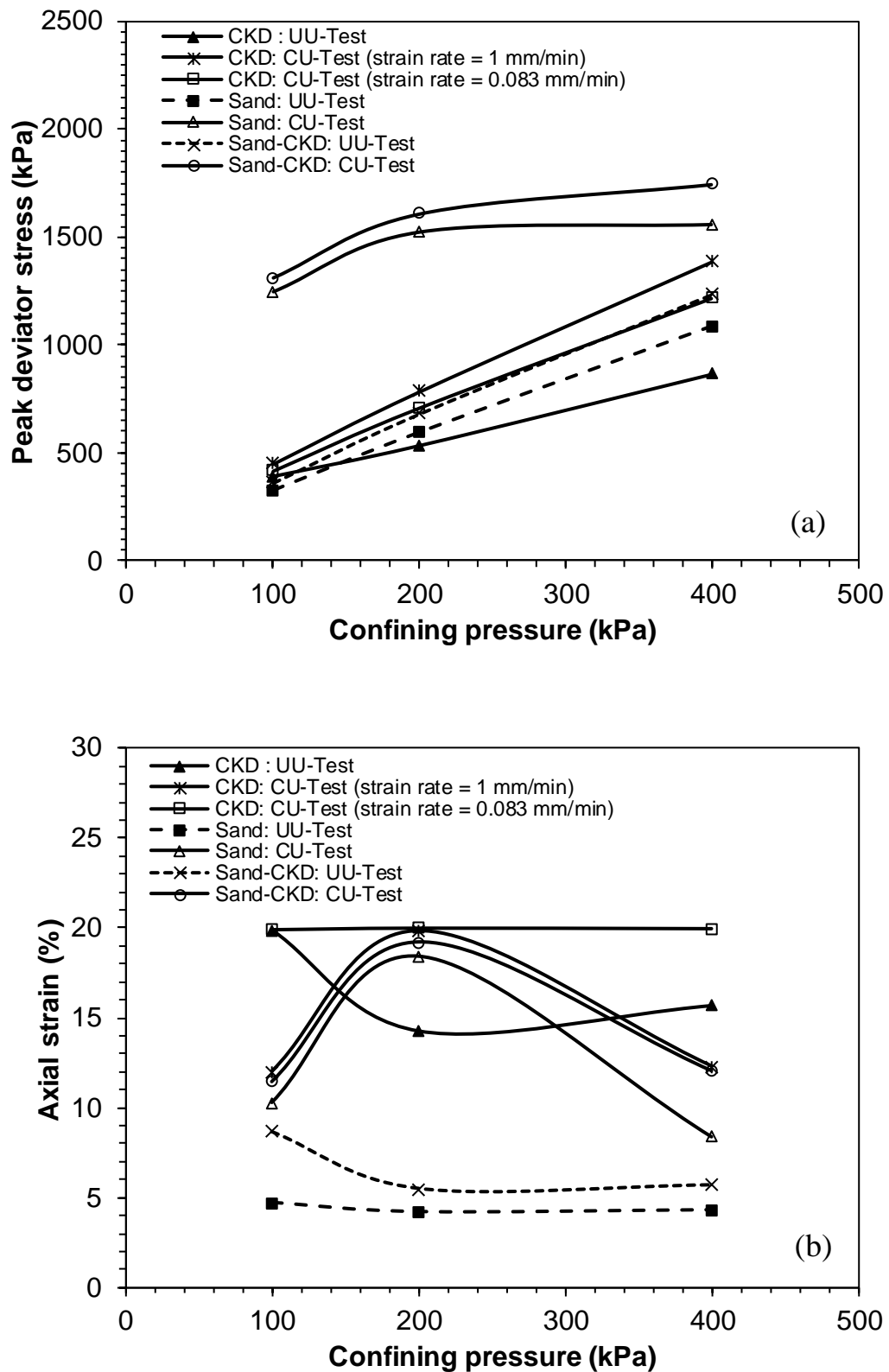


Figure 7.7 Results of saturated triaxial compression tests (UU and CU-Tests) for the selected materials: (a) confining pressure versus peak deviator stress, and (b) confining pressure versus axial strain.

Table 7.1 Summary of saturated shear strength test results of the materials.

Material	Type of test	Water content (%)		Dry unit weight (kN/m <sup>3</sup> )	Confining pressure (kPa)	Peak deviator stress (kPa)	Axial strain (%) at Peak deviator stress
		Initial	Final				
CKD	UU	27.5	27.2	14.75	100	388	19.9
		27.4	27.3	14.85	200	530	14.3
		27.6	27.3	14.85	400	863	15.7
	CU	27.4	29.2	14.85	100	450	12
		27.5	29.4	14.85	100	417	20*
		27.7	28.9	14.95	200	785	20
		27.5	29.0	14.95	200	710	20*
		27.4	28.6	14.75	400	1385	12.6
		27.7	28.7	14.75	400	1218	20*
	CD	27.4	31.0	14.95	25	155	3
		27.3	29.6	14.95	100	357	3
		27.3	29.3	14.75	200	640	10
27.4		28.4	14.85	400	1303	6	
Sand	UU	13.1	12.9	15.53	100	328	4.7
		12.7	12.9	15.53	200	593	4.2
		13.3	13.0	15.43	400	1083	4.3
	CU	13.2	20.7	15.43	100	1245	10.3
		12.8	20.2	15.43	200	1520	18.4
		13.0	19.9	15.53	400	1555	8.4
Sand-CKD	UU	11.1	10.8	17.83	100	362	8.7
		11.3	11.1	17.73	200	680	5.5
		10.9	10.7	17.83	400	1232	5.7
	CU	11	15.7	17.73	100	1308	11.5
		11.2	15.4	17.63	200	1607	19.2
		11.2	15.2	17.83	400	1745	13.7

\* Strain rate is 0.083 mm/min

### **7.3.1.5 CD triaxial test results of CKD**

Figure 7.8 presents the CD triaxial test results (axial strain versus deviator stress, axial strain versus volumetric strain and Mohr-Coulomb failure envelope) of compacted-saturated CKD specimens.

The specimens attained peak deviator stresses at an axial strain between about 3 to 5%. The peak deviator stress was more prominent for specimens tested at higher confining pressures. The deviator stress further decreased and remained nearly constant. A brittle failure and strain-softening behaviour were observed in all cases.

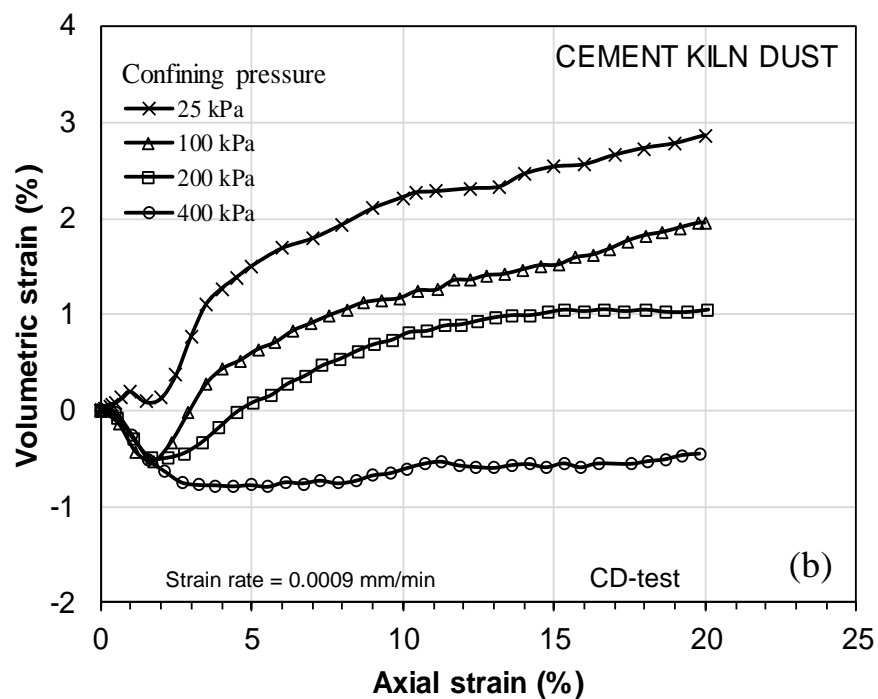
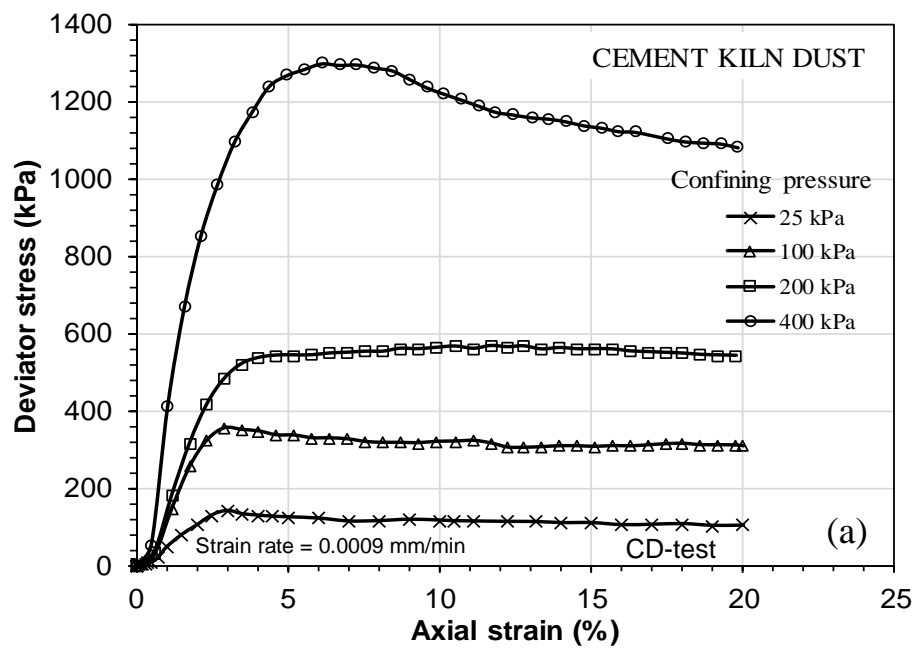
The volumetric strain versus axial strain results (Figure 7.8 b) showed that at a confining pressure of 25 kPa, the specimen exhibited the highest dilative volumetric strain and behaved similar to overconsolidated soils, whereas the highest contractive and then slight dilative volumetric strains were observed for the specimens at a confining pressure of 400 kPa in which case the specimen behaved as normally consolidated soil. Under the confining pressures of 100 and 200 kPa, the specimens exhibited lower contractive behaviour at relatively small strain and then high dilative volumetric strain and also behaved as overconsolidated soil. This behaviour can be attributed to that the volumetric strain becomes more dilative with increasing the maximum stress ratio (deviator stress/mean effective stress) depending on the confining pressure (Lackenby et al. 2007).

The effective cohesion intercept ( $c'$ ) and angle of internal friction ( $\phi'$ ) were found to be about 18.7 kPa and 36.9°, respectively. The shear strength parameters from CD tests will be further considered in unsaturated shear strength analysis.

Table 7.2 summaries the shear strength parameters of the CKD, sand, and sand-CKD obtained from the UU, CU, and CD tests. For the CKD in UU tests, the cohesion was higher and internal friction angle was lower than those obtained from the CU tests. Similar behaviour was reported by Xu et al. (2018) from tests conducted on compacted clay. Additionally, the internal friction angle obtained from the CD tests was the highest as compared to those from the UU and CU tests. The effect of shearing rate on the shear strength parameters of the CKD under CU condition was not significant.

For the sand and sand-CKD, it can be seen that the angle of internal friction obtained from the UU tests were found to be higher than that obtained under CU

conditions. Similarly, the undrained cohesion of the both sand and sand-CKD were lower than those under CU conditions. The apparent cohesion of sand may be due to interlocking shear resistance and the capillary forces arising from the air present (Lu and Likos 2013). A significant increase in cohesion of sand was observed due to the replacement of 15% of sand with the CKD while the internal friction angle slightly increased.



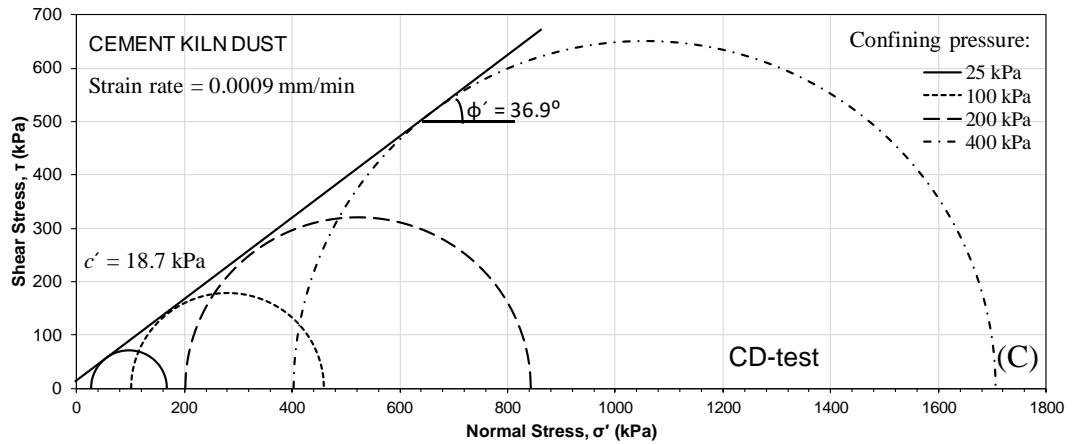


Figure 7.8 Results of saturated CD-triaxial tests of cement kiln dust specimens under different confining pressures: (a) axial strain versus deviator stress, (b) axial strain versus volumetric strain, and (c) normal stress versus shear stress.

Table 7.2 Effective and total shear strength parameters of CKD, sand and sand-CKD based on Mohr-Coulomb failure criterion. (UU, CU, and CD - Triaxial Tests).

Test type	Parameter	Strain rate (mm/min)	CKD	sand	Sand-CKD
UU	$c_u$ (kPa)	1	70	15	32
	$(\phi_u)$ (°)		27	34.7	35.5
CU	$c'$ (kPa)	1	7.0	27	46
	$(\phi')$ (°)		33.7	27.6	28
	$c'$ (kPa)	0.083	0	---	---
	$(\phi')$ (°)		34	---	---
CD	$c'$ (kPa)	0.0009	18.7	---	---
	$(\phi')$ (°)		36.9	---	---

### **7.3.2 Saturated permeability from triaxial tests**

Figure 7.9 and Table 7.3 present the permeability test results for CKD, sand, and sand-CKD mixture. The applied confining pressures during the tests were 25, 50, 100, 200, and 400 kPa. The hydraulic gradients adopted for the tests on CKD, sand and sand-CKD were of 20.6, 2, and 7 respectively.

The permeability decreased with an increase in the confining pressure and this reduction can be attributed to the decrease in void ratio or an increase in the density due to an increase in the effective stress during the consolidation process prior to conducting the permeability tests. Further, the permeability values of sand and sand-CKD specimens were of similar order indicating that addition of 15% CKD to sand had very marginal effect on the permeability.

The value of permeability ranged between  $9.50 \times 10^{-9}$  and  $1.22 \times 10^{-8}$  m/s for the CKD,  $3.24 \times 10^{-6}$  and  $4.91 \times 10^{-6}$  m/s for the sand and  $2.95 \times 10^{-6}$  m/s, and  $4.75 \times 10^{-6}$  m/s for the sand-CKD mixture. The permeability for the CKD was found to be about 1 to 3 order higher than that obtained from the indirect measurements of the compacted specimens (oedometer tests – Section 4.4.5). Similar observations have been reported by (Dafalla et al. 2015) for sand-clay mixtures in which case the results of oedometer tests were less by 2 to 3 orders of magnitude from those obtained from the direct measurements at different effective stresses. Previous studies conducted on various types of cement kiln dust using flexible wall permeameter tests showed a wide range of permeability which varied from  $3.8 \times 10^{-12}$  to  $1.1 \times 10^{-6}$  m/sec (USEPA 1998).

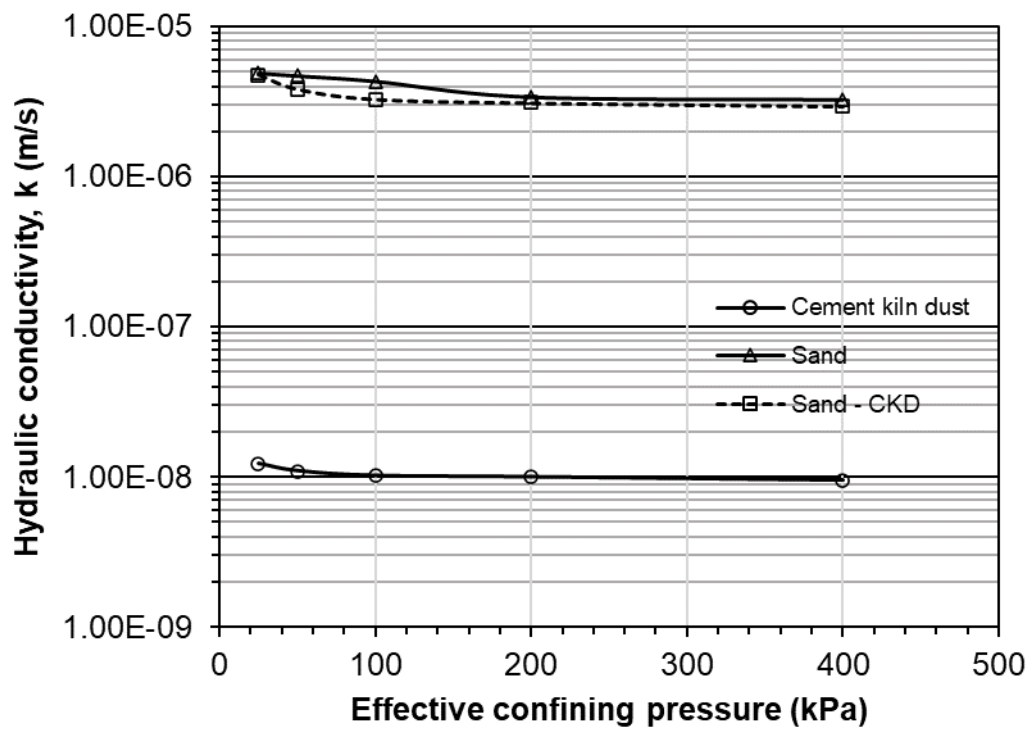


Figure 7.9 Hydraulic conductivity of the selected material (CKD, Sand, and Sand-CKD) under various confining pressures.

Table 7.3 Summary of the saturated permeability tests results.

Material	Effective confining pressure (kPa)	Pressure difference (kPa)	Hydraulic gradient ( $\Delta h/L$ )	k (m/s)
CKD	25	20	20.61	$1.22 \times 10^{-8}$
	50	20	20.61	$1.10 \times 10^{-8}$
	100	20	20.61	$1.02 \times 10^{-8}$
	200	20	20.61	$9.97 \times 10^{-9}$
	400	20	20.61	$9.50 \times 10^{-9}$
Sand	25	2	2.02	$4.91 \times 10^{-6}$
	50	2	2.02	$4.71 \times 10^{-6}$
	100	2	2.02	$4.33 \times 10^{-6}$
	200	2	2.02	$3.38 \times 10^{-6}$
	400	2	2.02	$3.24 \times 10^{-6}$
Sand-CKD	25	7	7.14	$4.75 \times 10^{-6}$
	50	7	7.14	$3.82 \times 10^{-6}$
	100	7	7.14	$3.28 \times 10^{-6}$
	200	7	7.14	$3.11 \times 10^{-6}$
	400	7	7.14	$2.95 \times 10^{-6}$

### **7.3.3 Unsaturated Consolidated Drained triaxial test results of CKD**

Compacted specimens of CKD (average initial water content 27.3% and average dry unit weight  $14.95 \text{ kN/m}^3$ ) were taken through wetting process at a predetermined confined pressure of 25 kPa to targeted applied suctions of 150, 100, 50, and 5 kPa. The initial suction of the compacted specimen was 2040 kPa. Duplicate specimens with identical compaction conditions were tested. Details of specimen preparation and testing details are presented in Sections 3.4.4.1.1 and 3.4.4.3.4.

#### **7.3.3.1 Matric suction equalisation**

Figure 7.10 shows the change in water volume and total volume change with the elapsed time during the suction equalisation under a constant net confining pressure of 25 kPa. The specimens absorbed water during the wetting process when the suction was reduced from 2040 kPa to 100, 50 and 5 kPa (Figure 7.10 a). In these cases, the amount of water absorbed increased with a decrease in suction. Wetting of the specimen at matric suction of 150 kPa caused an expulsion of water from the specimen indicating that there was a collapse/compression of the specimen. The overall volume changes are controlled by the void ratio within the packet of particles and the resistance of each packet available to prevent breakdown (Sivakumar 1993b). On wetting, the inter-aggregate/packet forces are removed and the aggregate/packet structure is collapsed into the inter-aggregate/packet voids. Therefore, the compression of specimen could be explained as collapse of the microstructural arrangement of aggregates/packets which is accompanied by reduction in void spaces and consequently, expulsion of water from the specimen. Similar behaviour was also noted in suction-controlled oedometer test (Chapter 6). A duration of about 20 to 24 days was required for attaining matric suction equalisation in each case.

The water volume change in the specimens during the wetting process was accompanied by changes in the total volume (Figure 7.10 b). At early stages of the equalisation process (up to about 2 days), all specimens exhibited a contractive behaviour and the total volume decreased and then increased, particularly under matric suction of 5 and 50 kPa and the specimens exhibited swelling until equilibrium was reached. For the specimens subjected to matric suction of 100 kPa and 150 kPa, after initial compression,

the total volume of the specimens slightly increased and then decreased before attaining a constant volume.

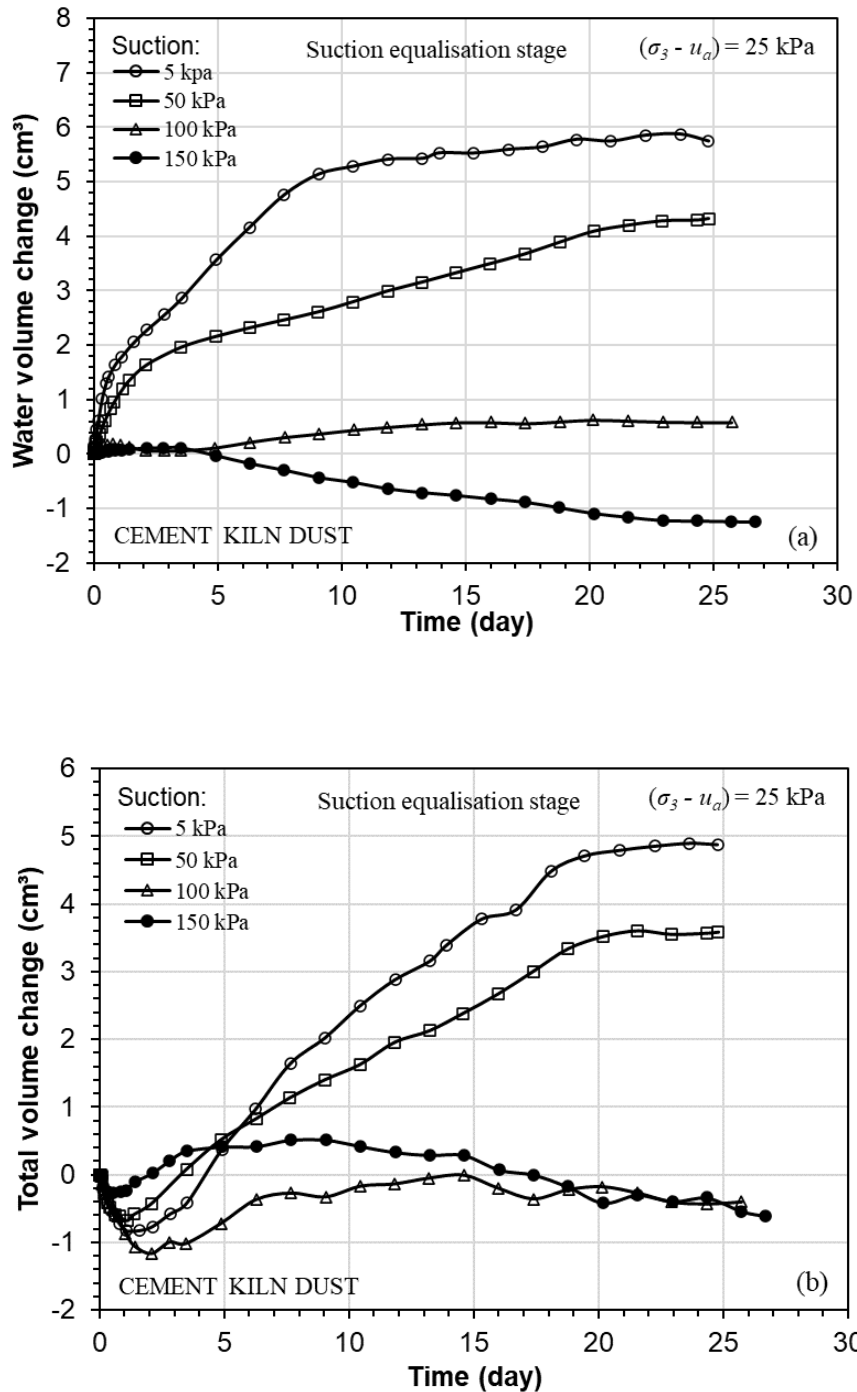


Figure 7.10 Test results of unsaturated triaxial tests for the cement kiln dust specimens during the equalisation process under different suctions at constant net confining pressure: (a) water volume change, (b) total volume change

### **7.3.3.2 Water content, void ratio, and degree of saturation at various imposed matric suctions**

Figures 7.11 a, b and c show the applied suction versus water content, void ratio and degree of saturation of compacted CKD specimens at the end of suction equalisation process. The test results from suction-controlled oedometer (wetting tests) and pressure plate (drying tests) are also presented in Figure 7.11 for comparison.

The initial suction of the specimens prior to the tests was 2040 kPa (Section 7.2). The water contents of the specimens at applied suctions 100, 50 and 5 kPa were found to be greater than the average initial water content (27.3%) (Figure 7.11 a). At an applied suction of 150 kPa, the water content of the specimen (26.8%) was found to be lower than the initial value.

The initial and final water contents are shown in Table 7.4. The final water contents from the unsaturated triaxial shear strength tests were similar to those obtained from suction-controlled oedometer tests at low suctions, whereas slightly lower water contents were noted at higher suctions (50 kPa, 100 kPa, and 150 kPa). A direct comparison of the observed volume changes between the triaxial and the oedometer test results is not possible because the radial stress in the oedometer is unknown (Rampino et al. 2000). The water content values obtained from the wetting process were significantly lower than that measured in pressure plate tests.

From Figure 7.11 b and Table 7.4, it can be noted that the initial void ratio of the specimens was influenced by the wetting and drying processes. The average initial void ratio (0.796) slightly decreased under the imposed matric suction of 100 and 150 kPa, whereas a significant increase in void ratio was noted for the specimens subjected to the suction of 5 and 50 kPa. The decrease in void ratio can be attributed to the change in volume of the macropores resulting from the collapse of the aggregates structure on wetting, whereas the expansion of microstructure of aggregates due to absorption of water caused an increase in the void ratio of the specimens.

Figure 7.11 c illustrates the final degree of saturation of the specimens. The average initial degree of saturation of compacted specimens was 93.6% that increased when the suction was reduced from 2040 kPa to various suctions (100, 50, 5, and 0 kPa).

The degree of saturation of the specimen at an imposed suction of 150 kPa was lower than the initial degree of saturation.

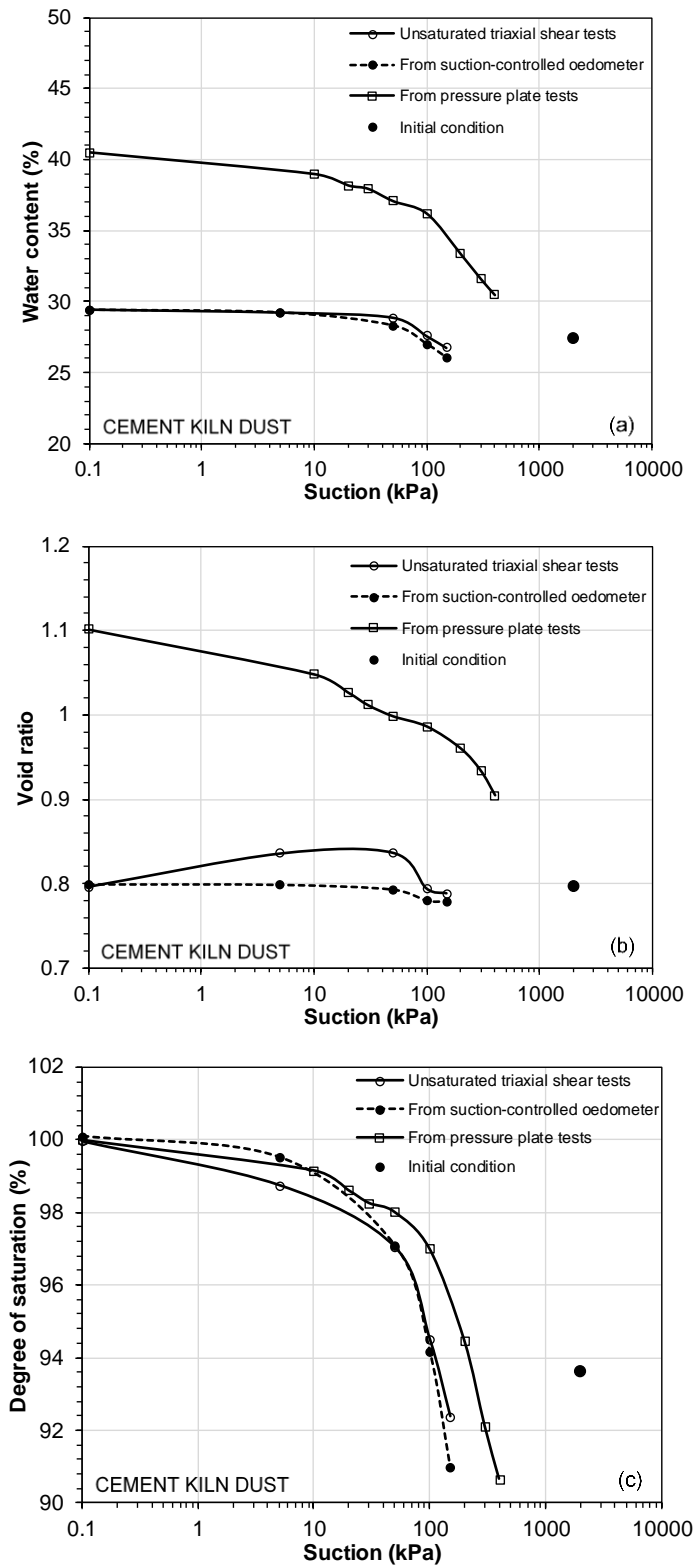


Figure 7.11 Test results of equalisation process under various suction at constant net confining pressure: (a) water content; (b) void ratio; (c) degree of saturation.

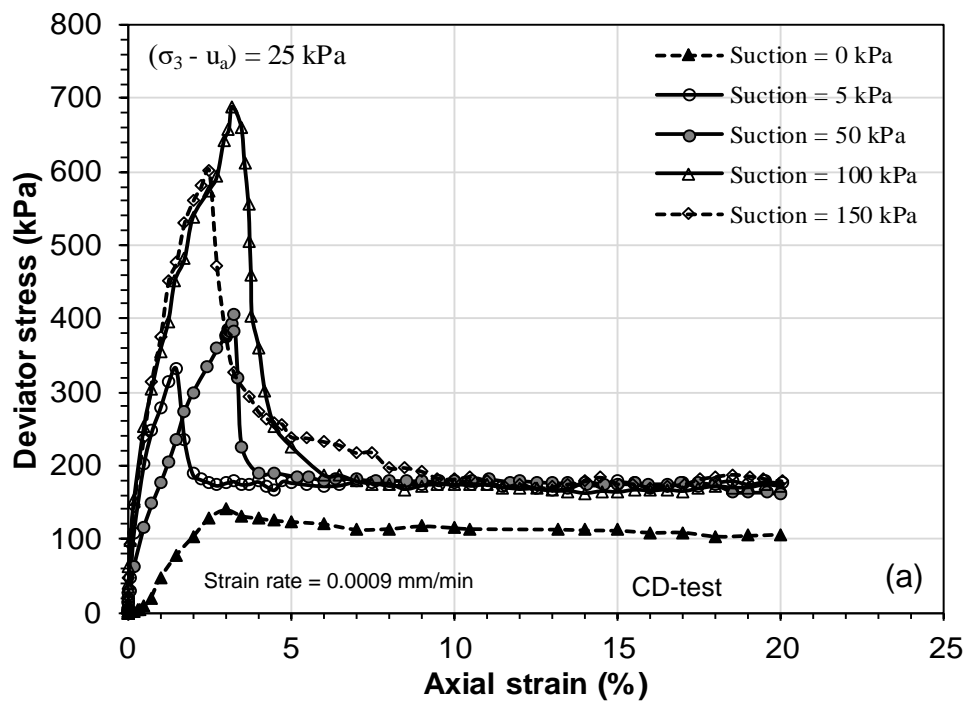
Considering results of the suction-controlled oedometer and the pressure plate tests, good agreements were observed between the final degree of saturation results from both the suction-controlled triaxial and oedometer tests performed under matric suctions of 50, 100, and 150 kPa, whereas under suction of 5 kPa the final degree of saturation was found to be lesser than that of oedometer tests. This can be attributed to a higher increase in void ratio during the wetting process in triaxial setting. The values of the degree of saturation from triaxial and oedometer tests (wetting from compacted unsaturated condition) remained below that of the pressure plate test (drying from initially saturated slurried condition) results.

### **7.3.3.3 Shear strength at various matric suctions**

Figure 7.12 a and b show the axial strain versus deviator stress and axial strain versus volumetric strain plots for CKD at matric suctions of 5, 50, 100 and 150 kPa. The test results were obtained at a net confining pressure of 25 kPa. The CD results for compacted-saturated specimen (suction = 0 kPa) at confining pressure of 25 kPa is shown for comparison.

It can be seen in Figure 7.12 a that the peak deviator stress values were attained at axial strains ranging between 1.7 and 3.2%. It can be seen in Figure 7.12 a that the peak deviator stress values were attained at axial strains ranging between 1.7 and 3.2%. In general, for the unsaturated soils, it is observed that the axial strain at failure decreases with an increase in suction at shearing under a constant net confining pressure (Farouk et al. 2004; Kasangaki 2012; Zhang et al. 2015b). However, the aforementioned values of the axial strain did not show any specific trend with the imposed matric suctions considered in this study. This behaviour can be attributed to that the specimens are probably undergone dissimilar changes on the microstructure and macrostructure levels due to the hydration reactions, the changes in dissolution and ion concentrations, the electrical attractive and repulsive forces and the potential thixotropy effects. Consequently, the brittleness of the specimens and axial strain at failure are affected by these variations. Further, the deviator stress decreased and remained nearly constant at high axial strains. The specimens exhibited a brittle and strain-softening mode of failure.

The peak deviator stresses of unsaturated CKD specimens were greater than that of the saturated specimen. A higher peak deviator stress of unsaturated CKD is on account of matric suction effect. The capillary action arising from suction at the contractile skin increases the normal forces at the interparticle contacts (Fredlund and Rahardjo 1993). These additional normal forces may increase the friction and the cohesion at the interparticle contacts.



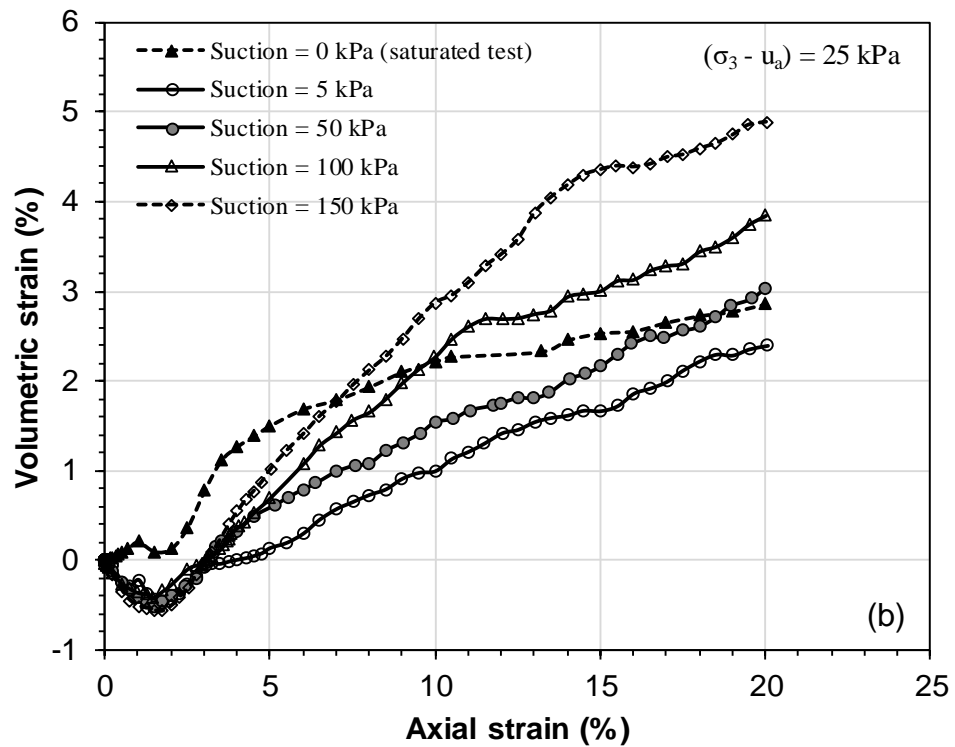


Figure 7.12 Results of the unsaturated CD-triaxial compression tests of the cement kiln dust specimens under different suctions at constant net confining pressure of 25 kPa: (a) deviator stress and (b) volumetric strain.

The peak deviator stress of specimen at suction of 150 kPa was found to be lower than that obtained under suction of 100 kPa. Similar behaviour has been reported by Farouk et al. (2004) for specimens of unsaturated sand. The shear strength of soil is affected by the area of the pore water in contact with soil particles which in turn is governed by the degree of saturation of soil (Rahardjo et al. 2004). At lower degree of saturation, the number of soil particles-water contact points (which act as bond forces) is smaller leading to lower shear strength. Therefore, the drop in the peak deviator stress value can be due to the reduction in degree of saturation of the specimen as compared to the specimen subjected to matric suction of 100 kPa that showed higher degree of saturation.

At the early stage of shearing, all the unsaturated specimens exhibited a slight contractive behaviour and further a dilative trend was observed (Figure 7.12 b). The total volumetric strain increased with the increase in the applied suction and values ranged between about 2.4 and 4.9%. On the other hand, the saturated specimen (suction = 0 kPa) generally showed the dilation behaviour with a total volumetric strain of 2.8% at the end of the test.

Table 7.4 shows the water content, void ratio and degree of saturation of CKD specimens at various suctions after suction equalisation and after the shearing stage. It can be seen that during the suction equalisation process, the specimens subjected to matric suctions of 5, 50, and 100 kPa showed an increase in the water content and degree of saturation. Except for the specimen under suction of 100 kPa, the void ratios were also increased. Under suction of 150 kPa, as compared to the initial values, the water content, void ratio, and degree of saturation were slightly decreased.

During the shearing process, an increase in void ratio and a decrease in degree of saturation were observed for all imposed matric suctions. In addition, a slight increase in water content was noted for specimens sheared under matric suction of 5 and 50 kPa, whereas the water content decreased for the specimens subjected to suctions of 100 and 150 kPa.

Table 7.4 Summary of water content ( $w$ ), void ratio ( $e$ ), and degree of saturation ( $S_r$ ) of saturated and unsaturated cement kiln dust specimens from triaxial tests.

Suction (kPa)	Parameters	Initial conditions	After saturation	After suction equalisation	After shearing
0	$w$ (%)	27.4	29.4	---	31.0
	$e$	0.796	0.796	---	0.843
	$S$ (%)	93.6	99.9	---	100.0
5	$w$ (%)	27.3	---	29.2	29.5
	$e$	0.792	---	0.836	0.88
	$S$ (%)	93.8	---	98.8	91.1
50	$w$ (%)	27.4	---	28.9	29.0
	$e$	0.80	---	0.837	0.892
	$S$ (%)	93.9	---	97.0	88.5
100	$w$ (%)	27.4	---	27.6	27.3
	$e$	0.798	---	0.794	0.862
	$S$ (%)	93.4	---	94.5	87.2
150	$w$ (%)	27.2	---	26.8	26.3
	$e$	0.794	---	0.788	0.879
	$S$ (%)	93.2	---	92.4	81.4

### 7.3.3.4 Unsaturated shear strength parameters

Figure 7.13 presents the Mohr-Coulomb failure envelopes and cohesion intercepts for the saturated and unsaturated compacted CKD specimens under various imposed matric suctions and at constant net confining pressure of 25 kPa. The cohesion intercepts for unsaturated specimens were determined by drawing Mohr-Coulomb failure envelopes. Tangents were drawn to the Mohr circles for unsaturated specimens (Figure 7.13). These tangents were kept parallel to the failure envelope for saturated specimen with a slope angle equal to the angle of internal friction ( $36.9^\circ$ ). It is commonly observed that the Mohr circles at failure become progressively larger (showing increasing levels of shearing) with an increase in the matric suction. However, at the imposed matric suction of 150 kPa, the Mohr circle was found to be smaller than that at 100 kPa. The lower

contribution of the imposed matric suction of 150 kPa to the shear strength manifested in the reduced value of the peak deviator stress as compared to the suction of 100 kPa is behind this behaviour.

Figure 7.14 presents the suction versus cohesion for saturated and unsaturated specimens. It can be observed that the cohesion intercept increased with an increasing of matric suction up to 100 kPa and then decreased at suction of 150 kPa. The cohesion intercept for saturated specimen (18.7 kPa) was found to be lower than that for unsaturated specimen. It is clear from the test results that the suction-cohesion relationship was nonlinear, particularly at high matric suctions and this is due to the volumetric changes noted at high suctions (Figure 7. 11 c and Table 7.4).

The cohesion results in Fig. 7.14 were best-fitted to determine the  $\phi^b$  value. The  $\phi^b$  for the CKD was found to be about  $36^\circ$  which was slightly smaller than the effective angle of internal friction for saturated specimens ( $36.9^\circ$ ).

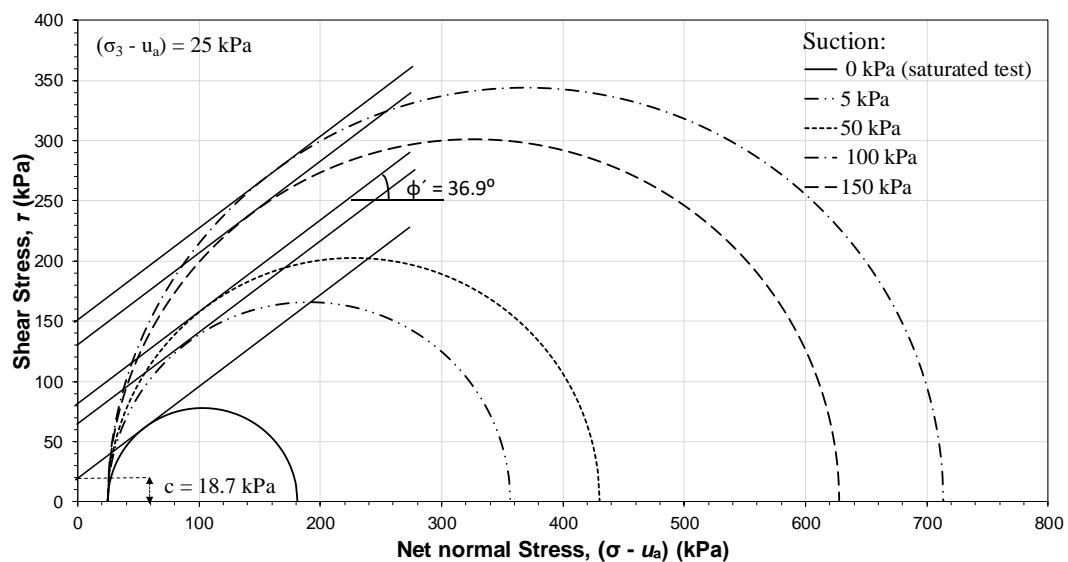


Figure 7.13 Mohr circles and cohesion intercepts of the saturated and unsaturated cement kiln dust specimens under different suctions at constant net confining pressure of 25 kPa.

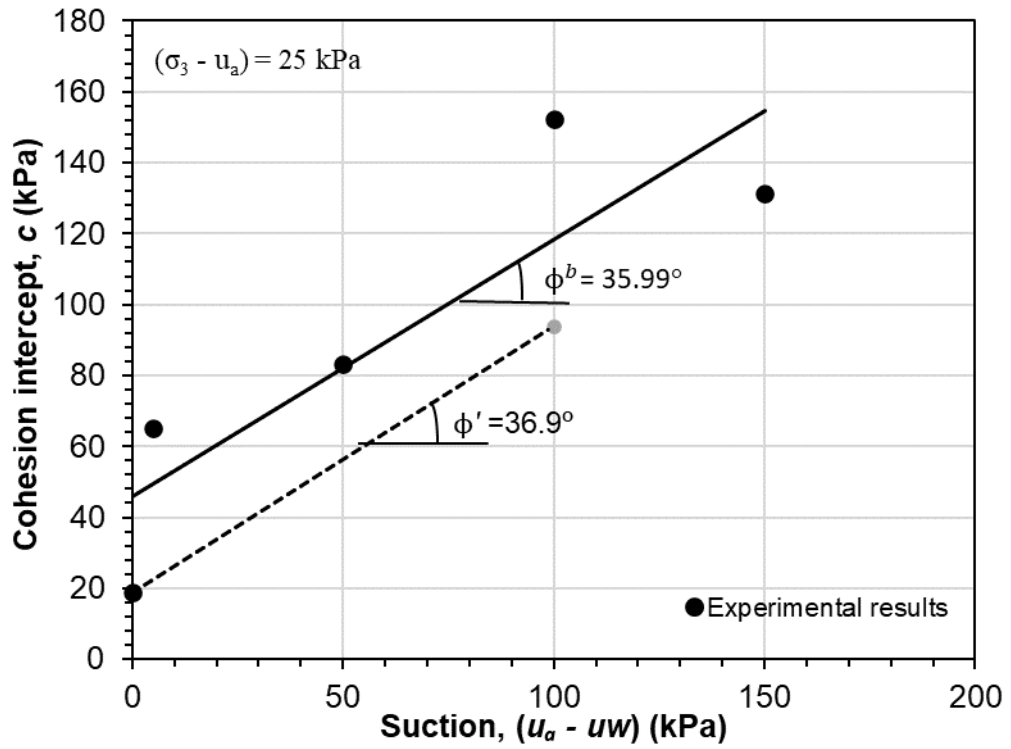


Figure 7.14 Suction versus cohesion intercept of the saturated and unsaturated cement kiln dust specimens under different suctions at constant net confining pressure of 25 kPa.

## **7.4 Concluding Remarks**

Triaxial UU and CU tests were performed on compacted-saturated specimens of CKD, sand, and sand-CKD mixture at various confining pressures. The effect of the strain rate on the shear strength of the CKD in CU test was studied. Permeability measurements were carried out on saturated specimens of the materials in triaxial tests. Saturated and unsaturated triaxial tests (CD tests) were carried out on compacted CKD specimens. The applied suctions in unsaturated triaxial tests were 150, 100, 50 and 5 kPa. The net stress in unsaturated triaxial tests was 25 kPa. The test results in terms of stress-strain, Mohr-Coulomb failure envelopes, time-volume change, suction-degree of saturation, and suction-cohesion intercept were analysed. The main findings emerged from tests results are as follows:

### Triaxial tests and permeability on compacted-saturated materials

- (1) The test results from UU and CU tests on compacted-saturated CKD, sand and sand-CKD showed that, at any applied confining pressure, the peak deviator stress in CU test was greater than that occurred in the UU test. A higher peak deviator stress in CU tests can be attributed to an increase in the dry density of the materials during the consolidation phase. The magnitude of peak deviator stress at any confining pressure remained in the decreasing order for sand-CKD, sand and CKD.
- (2) Both ductile and brittle behaviour with strain hardening and softening, were noted during the shearing process depending upon type of material, drainage condition and stress level. The materials exhibited dilative behaviour when sheared under undrained condition with development of negative pore water pressures. A higher axial strain was required for the mobilisation of peak deviator stress in case of the CKD than in sand and sand-CKD.
- (3) For both sand and sand-CKD, the value of  $c$  was lower and  $\phi$  was higher in UU tests than in CU tests, whereas for the CKD,  $c$  was higher and  $\phi$  was lower in UU tests than in CU tests. An addition of CKD to sand increased the cohesion, whereas the angle of internal friction remained almost unaltered. For the CKD, the highest value of  $\phi$  ( $37^\circ$ ) was in the CD tests.

- (4) In the CU tests for the CKD, the applied strain rate during the shearing process affected the rate of development of deviator stress and the peak deviator stress, but the effect of strain rate had negligible influence on the deviator stress and pore water pressure response at large axial strains. The impact of strain rate during shearing on both  $c$  and  $\phi$  was negligible.
- (5) The saturated coefficient of permeability of CKD was found to be in the order of  $10^{-8}$  to  $10^{-9}$  m/s. The values of permeability determined from the triaxial tests were found to be higher (about 2 to 3 order) than that calculated from the one dimensional consolidation test results. An addition of 15% of CKD to sand did not affect the permeability which remained at  $10^{-6}$  m/s.

#### Unsaturated Triaxial tests on CKD

- (6) Upon wetting at low applied suctions, unsaturated CKD specimens exhibited swelling behaviour accompanied by an increase in the water content and degree of saturation, whereas when wetted at high suctions collapse of the specimen occurred accompanied by an expulsion of water from the specimen. The compression behaviour and the expulsion of water can be attributed to the decrease in void spaces resulted from the microstructure reorganisation of the compacted specimen.
- (7) Good agreements were noted between the suction - water content, suction - void ratio and suction - degree of saturation results of the CKD from the wetting tests at a constant net stress of 25 kPa in both oedometer and triaxial test set ups. The results from the wetting tests remained distinctly below that of the results from the drying tests from pressure plate.
- (8) Strain softening and brittle behaviour accompanied by dilation of specimens was noted in case of unsaturated specimens during the shearing process. Failure usually occurred at low axial strains of 1.7 to 3.2%. The impact of matric suction on stress-strain response of CKD was found to be distinct. The peak deviator stress was greater in compacted unsaturated specimen than in compacted-saturated specimens and which decreased with a decrease in matric suction.
- (9) Cohesion decreased with a decrease in the matric suction. The suction – cohesion relationship was found to be non-linear, particularly at high suctions, whereas

ignoring the non-linear relationship, the values of  $\phi$  and  $\phi^b$  were found to be similar (36 – 37°).

## **CHAPTER 8**

# **Conclusions and Recommendations**

### **8.1 Conclusions**

A variety of solid wastes are generated in many parts of the world due to various industrial activities. Disposal and storage of these large quantities of solid wastes have become a challenging issue due to significant financial implications, their impacts on the environment and land use. Therefore, use of industrial wastes in various civil engineering construction practices have received increasing attention. Cement kiln dust (CKD) is an industrial by-product that has been considered (either CKD alone or as admixture) in various geotechnical and geoenvironmental applications. Prior to use of CKD in various geoinfrastructures (pavement, railway formation, shallow foundation, backfill), the engineering properties are required to be evaluated. The main aim of this study is to investigate the hydro-mechanical behaviour. The objectives are to study in detail the volume change, compressibility, water retention, and shear strength of saturated and unsaturated CKD using various conventional and advanced laboratory experimental techniques.

A CKD collected from a local cement company was used in this investigation to study the hydro-mechanical behaviour. Additionally, a mixture of sand (85%) and CKD (15%) was used to explore the effect of admixture on the hydro-mechanical behaviour. The physical and chemical properties of the materials along with the mineralogy and microscopic features were determined using the standard testing methods. The swelling and compressibility properties of the CKD were investigated using the conventional one-dimensional oedometer cell. The specimens were tested under various initial conditions (initially saturated slurried, compacted). The consolidation characteristics of initially saturated slurried CKD was studied by step-wise loading the specimen to a vertical pressure of 800 kPa which was then unloaded. Compacted CKD specimens were hydrated at applied vertical pressures of 2 and 25 kPa to study the one-dimensional volume change. Further, these specimens were loaded to a vertical pressure of 1600 kPa in a step-wise

manner and then unloaded. These tests provided information on: compression index, swelling index, coefficient of volume compressibility, coefficient of consolidation, swelling/collapse strain). The swelling pressure of compacted CKD was determined by hydrating a specimen at constant volume condition.

The water retention curves (WRCs) of the CKD, sand, and sand-CKD were determined based on the test results from pressure plate extractor, desiccator, chilled-mirror dew-point potentiometer (WP4-C), and fixed-matrix porous ceramic disk water potential sensor (MPS-6). The results from these tests in conjunction with clod tests (shrinkage tests) on CKD provided WRCs in terms of water content and degree of saturation and the impact of addition of CKD to sand on WRC. Osmotic suction of CKD was determined from electrical conductivity measurements for interpreting the test results of CKD from various tests. Additionally, compacted CKD was taken through the wetting process by step-wise decreasing suction in a suction-control oedometer at a constant applied net stress of 25 kPa. The test results from suction-control oedometer yielded suction – water content and suction – degree of saturation WRCs. The test results from suction-control oedometer and other tests allowed comparing the WRCs of the CKD. The van Genuchten (1980) and Fredlund and Xing (1994) parametric models were used to best-fit the WRCs and obtaining the model parameters.

The shear strength of compacted-saturated CKD, sand and sand-CKD mixture was determined from unconsolidated-undrained (UU) and consolidated-undrained test with pore water pressure measurements (CU) tests. CD tests were carried out on compacted-saturated CKD. The UU, CU and CD tests were carried out using a conventional triaxial device at various confining pressure which provided the cohesion and angle of internal friction of the materials in this study. The tests results allowed comparing the peak deviator stress in various drainage conditions and the impact of strain rate on shear strength. The effect of confining pressure on the permeability of all the materials was also investigated in triaxial test set up at various hydraulic gradients. Unsaturated consolidated drained (CD) shear strength tests were carried out on compacted CKD in a suction-control triaxial device. Compacted CKD specimens were taken through the wetting process at a constant confining pressure of 25 kPa by decreasing suction to different predetermined values. The test results provided information on the volume change, WRC, peak stress and shear strength parameters ( $c'$ ,  $\phi$  and  $\phi^b$ ) and

further enabled comparing the shear strength parameters and peak deviator stresses from saturated and unsaturated shear strength tests.

The main conclusions derived from the detailed experimental investigations on the CKD, sand and sand-CKD mixture in this thesis are as follows:

### Reactivity of CKD

1. The dominant mineral in the CKD studied was found to be calcite which is often found in Portland cement. A high loss on ignition (LOI) of 33.8% suggested that the CKD used in this study was a low reactivity CKD. The plasticity properties (liquid limit, plastic limit and plasticity index) of the CKD did not change significantly with the curing time up to 28 days.

### One-dimensional swelling and compressibility behaviour

2. The CKD considered in this study exhibited swelling upon saturation from unsaturated condition. Similarly, swelling pressure developed when an unsaturated specimen was wetted under constant volume condition. The swelling strain of compacted CKD decreased with an increase in the applied vertical pressure prior to the saturation process. The swelling strain decreased from 18.8 to about 1.5% with an increase in applied pressure from 2 to 25 kPa. The measured swelling pressure of the CKD was 67 kPa. (Upon saturation, the CKD exhibited swelling strain that decreased with an increase in the applied vertical pressure prior to the saturation process. Swelling pressure of 67 kPa was developed under constant volume condition.
3. Upon loading, the initially saturated slurried specimen and compacted-saturated specimen wetted at 2 kPa, exhibited higher compression strain as compared to the compacted specimens that were hydrated either at a higher stress or at constant volume condition. It was also noted that the compressibility characteristics and coefficient of permeability were affected by the applied pressure and initial compaction conditions. Over a range of the applied pressures of 2 to 1600 kPa,

the range of variation of various compressibility parameters and permeability are as follows:

Compression index ( $C_c$ ): 0.22 and 0.08,

Coefficient of volume compressibility ( $m_v$ ): 0.03 to 3 m<sup>2</sup>/MN,

Coefficient of consolidation ( $C_v$ ): 1.0 to 20 m<sup>2</sup>/year,

Swelling index ( $C_s$ ): 0.007 to 0.019, and

Coefficient of permeability ( $k$ ): 10<sup>-8</sup> to 10<sup>-11</sup> m/s.

These parameters are useful information towards assessing the settlement and rate of settlement of CKD. Some of the reported correlations between the various parameters and the plasticity properties of soil were found to be valid in case of the CKD used in this study.

#### Water retention characteristics

4. The suction equilibration time was influenced by the suction measurement and control techniques used in the study. Several days to weeks were required to attain equilibrium in pressure plate and desiccator tests, whereas a much lower equilibrium time was noted for the WP4-C and MPS-6 tests. For the MPS-6 tests, a longer equilibrium time was required for the sand and sand-CKD, particularly at low water contents that can be attributed to a lack of good water phase continuity between the specimens and the ceramic disks of the sensors.
5. For any material in this study, the WRCs in terms of the water content and the degree of saturation were affected by the device used to establish the WRCs. At high water contents or at lower suctions distinct differences were noted in the WRCs even after applying corrections for the osmotic suction and compaction dry density. The differences in the WRCs were found to be lesser at high suctions.
6. The best-fit results in term of water content and degree of saturation obtained using van Genuchten and Fredlund and Xing models showed good compatibility

with the experimental data with  $R^2$  close to 1. The fitting parameters obtained for the water content and degree of saturation WRCs were found to be dissimilar. The Clod test results suggested that CKDs exhibit significant shrinkage characteristic and hence the suction – degree of saturation WRCs are more relevant for the determination of air entry value of CKDs. The air entry fitting parameters from both van Genuchten and Fredlund and Xing models were found to be different. Comparisons of the air entry value from graphical construction procedure and the models showed that Fredlund and Xing equation provided higher values of the air entry.

### Suction-controlled one-dimensional volume change

7. Wetted under a constant net stress of 25 kPa, compacted unsaturated CKD exhibited minor swelling deformation at low suctions ( $\leq 50$  kPa), whereas very minor collapse deformations were noted at high suctions (100 and 150 kPa). The vertical deformation influenced the water content and degree of saturation. As compared to the initial compaction water content, an increase in the water content and degree of saturation was observed at low applied suctions, whereas the water content and degree of saturation decreased at high applied suctions. A decrease in the water content is attributed to a slight decrease in the void ratio due to collapse compression of the CKD.
8. The impact of applied net stress of 25 kPa was distinct on the void ratio, water content and degree of saturation of the CKD. The wetting suction - degree of saturation and suction – water content WRCs were found to remain below that of the WRC established from the results of pressure plate tests (drying WRC).

### Triaxial tests and permeability on compacted-saturated materials

9. The test results from UU and CU tests on compacted-saturated CKD, sand and sand-CKD showed that, at any applied confining pressure, the peak deviator stress in CU test was greater than that occurred in the UU test. A higher peak deviator stress in CU tests can be attributed to an increase in the dry unit weight of the

materials during the consolidation phase. The magnitude of peak deviator stress at any confining pressure remained in the decreasing order for sand-CKD, sand and CKD.

10. Both ductile and brittle behaviour with strain hardening and softening, were noted during the shearing process depending upon type of material, drainage condition and stress level. The materials exhibited dilative behaviour when sheared under undrained condition with development of negative pore water pressures. A higher axial strain was required for the mobilisation of peak deviator stress in case of the CKD than in sand and sand-CKD.
11. For both sand and sand-CKD, the value of  $c$  was lower and  $\phi$  was higher in UU tests than in CU tests, whereas for the CKD,  $c$  was higher and  $\phi$  was lower in UU tests than in CU tests. An addition of CKD to sand increased the cohesion, whereas the angle of internal friction remained almost unaltered. For the CKD, the highest value of  $\phi$  ( $37^\circ$ ) was found in the CD tests.
12. In the CU tests for the CKD, the applied strain rate during the shearing process affected the rate of development of deviator stress and the peak deviator stress, but the effect of strain rate had negligible influence on the deviator stress and pore water pressure response at large axial strains. The impact of strain rate during shearing on both  $c$  and  $\phi$  was negligible.
13. The saturated coefficient of permeability of CKD was found to be in the order of  $10^{-8}$  to  $10^{-9}$  m/s. The values of permeability determined from the triaxial tests were found to be higher (about 2 to 3 order) than that calculated from the one-dimensional consolidation test results. An addition of 15% of CKD to sand did not affect the permeability which remained at  $10^{-6}$  m/s.

#### Unsaturated Triaxial tests on CKD

14. Upon wetting at low applied suctions, unsaturated CKD specimens exhibited swelling behaviour accompanied by an increase in the water content and degree

of saturation, whereas when wetted at high suctions collapse of the specimen occurred accompanied by an expulsion of water from the specimen.

15. Good agreements were noted between the suction - water content, suction - void ratio and suction - degree of saturation results of the CKD from the wetting tests at a constant net stress of 25 kPa in both oedometer and triaxial test set ups. The results from the wetting tests remained distinctly below that of the results from the drying tests from pressure plate.
16. Strain softening and brittle behaviour accompanied by dilation of specimens was noted in case of unsaturated specimens during the shearing process. Failure usually occurred at low axial strains of 1.7 to 3.2%. The impact of matric suction on stress-strain response of CKD was found to be distinct. The peak deviator stress was greater in compacted unsaturated specimen than in compacted-saturated specimens and which decreased with a decrease in matric suction.
17. Cohesion decreased with a decrease in the matric suction. The suction - cohesion relationship was found to be non-linear, particularly at high suctions, whereas ignoring the non-linear relationship, the values of  $\phi$  and  $\phi^b$  of the CKD were found to be similar (36 - 37°).

## **8.2 Recommended further studies**

Cement kiln dust (CKD) and CKD - amended soils have been considered as alternative materials in various geotechnical and geoenvironmental applications. These materials are commonly used in unsaturated state and are anticipated to be affected by climate change. There is a strong motivation to extend the present study to include the following:

1. Studying the hydro-mechanical behaviour of sand-CKD mixtures with different CKD contents.

2. Investigating the unsaturated hydraulic conductivity of CKD and sand-CKD mixtures under a range of matric suctions and net confining pressures under cycles of wetting-drying process.
3. To study the effect of cycles of wetting and drying processes on the volume change behaviour, permeability and shear strength of CKD and sand-CKD mixtures for a range of matric suctions and net confining pressures.
4. Developing a test apparatus consisting of instrumented columns (simulate the capillary barrier system) to assess the store - release capacity and effectiveness of the CKD and/or sand-CKD mixtures as water retention layer to limit water infiltration into the underling layers.
5. Developing artificial neural networks (ANNs) models utilising the available literature data for evaluating suitability of using the CKD in various applications and for predicting the engineering behaviour of the CKD and/or CKD-treated soils under saturated and unsaturated conditions depending on easily measurable data.

## References

- Adaska, W.S. and Taubert, D.H. 2008. Beneficial uses of cement kiln dust. In: *2008 IEEE Cement Industry Technical Conference Record*. pp. 210–228.
- Agus, S.S. and Schanz, T. 2005. Comparison of four methods for measuring total suction. *Vadose Zone Journal* 4(4), pp. 1087–1095.
- Aitchison, G.D. 1965. Moisture equilibria and moisture changes in soils beneath covered areas. In: *A symposium in print. Butterworths, Sydney, Australia*. pp. 7–22.
- Al-Badran, Y. 2001. Collapse behavior of Al-Tharthar gypseous soil. *M. Sc. theses, Civil Engineering Department, University of Baghdad*.
- Al-hassani, A.M.J., Kadhim, S.M. and Fattah, A.A. 2015. Characteristics of Cohesive Soils Stabilized by Cement Kiln Dust. 6(4), pp. 2032–2038.
- Al-Mukhtar, M., Qi, Y., Alcover, J.F. and Bergaya, F. 1999. Oedometric and water-retention behavior of highly compacted unsaturated smectites. *Canadian Geotechnical Journal* 36(4), pp. 675–684.
- Al-obaidi, Q.A.J. 2014. Hydro-Mechanical Behaviour of Collapsible Soils Dissertation. Dissertation, Ruhr-Universität at Bochum.
- Al-Rawas, A.A., Taha, R., Nelson, J.D., Al-Shab, T.B. and Al-Siyabi, H. 2002. A comparative evaluation of various additives used in the stabilization of expansive soils. *Geotechnical Testing Journal* 25(2), pp. 199–209.
- Al-Rawas, A.A., Hago, A.W. and Al-Sarmi, H. 2005. Effect of lime, cement and Sarooj (artificial pozzolan) on the swelling potential of an expansive soil from Oman. *Building and Environment* 40(5), pp. 681–687.
- Al-Refeai, T.O. and Al-Karni, A.A. 1999. Experimental Study on the Utilization of Cement Kiln Dust for Ground Modification. *Journal of King Saud University* 11(Engineering Sciences 2), pp. 217–232.
- Alabdullah, J. 2010. Testing Unsaturated Soil for Plane Strain Conditions: A New Double Wall Biaxial Device. Dissertation, Bauhaus-University Weimar.

## References

---

- Albright, W.H., Benson, C.H. and Stoller, S.M. 2010. Water Balance Covers for Waste Containment : Principles and Practice. *ASCE Press: Reston, VA, USA, 2010*.
- Alonso, E.E., Gens, A. and Hight, D.W. 1987. General report. Special problem soils. In: *Proceedings of the 9th European Conference on soil mechanics and foundation engineering, Dublin*. pp. 1087–1146.
- Andrew, E.E. 2012. Potentials of Cement Kiln Dust in Subgrade Improvement. Thesis, University of Nigeria, Nsukka.
- ASTM D4943 2008. Standard Test Method for Shrinkage Factors of Soils by the Wax Method 1. (July), pp. 1–6.
- ASTM D5050 – 08 2015. Standard Guide for Commercial Use of Lime Kiln Dusts and Portland Cement Kiln Dusts.
- ASTM E104-02 2007. Standard Practice for Maintaining Constant Relative Humidity by Means of Aqueous Solutions. *WWW.Astm.Org* 02(Reapproved 2012), pp. 1–5.
- Ata, A.A., Salem, T.N. and Elkhawas, N.M. 2015. Properties of soil-bentonite-cement bypass mixture for cutoff walls. *Construction and Building Materials* 93, pp. 950–956.
- Aversa, R. and Nicotera, S. 2002. A Triaxial and Oedometer Apparatus for Testing Unsaturated Soils. *Geotechnical Testing Journal, GTJODJ* 25(1), pp. 3–15.
- Baghdad, Z.A., Fatani, M.N. and Sabban, N.A. 1995. Soil modification by cement kiln dust. *Journal of Materials in Civil Engineering* 7(4), pp. 218–222.
- Baghdadi, Z.A. 1990. Utilization of Kiln Dust in Clay Stabilization. *JKAU: Engineering Science* 2, pp. 153–163.
- Baghdadi, Z.A. and Rahman, M.A. 1990. The potential of cement kiln dust for the stabilization of dune sand in highway construction. *Building and Environment* 25(4), pp. 285–289.

- Baille, W., Tripathy, S. and Schanz, T. 2010. Swelling pressures and one-dimensional compressibility behaviour of bentonite at large pressures. *Applied Clay Science* 48(3), pp. 324–333.
- Baille, W., Tripathy, S. and Schanz, T. 2014. Effective stress in clays of various mineralogy. *Vadose Zone Journal* 13(5), p. 10.
- Bandara, N. and Grazioli, M.J. 2009. Cement Kiln Dust Stabilized Test Section on I-96/I-75 in Wayne County--Construction Report.
- Benson, C.H. and Daniel, D.E. 1990. Influence of Clods on Hydraulic Conductivity of Compacted Clay. *Journal of Geotechnical Engineering*, 116(8), pp. 1231–1248.
- Bensoula, M., Missoum, H. and Bendani, K. 2015. Critical Undrained Shear Strength of Loose-Medium Sand-Silt Mixtures Under Monotonic Loadings. *Journal of Theoretical and Applied Mechanics* 53(2), pp. 331–344.
- Bhatty, J.I. 1995. Alternative uses of cement kiln dust. *Report RP 327. Skokie, IL: Portland Cement Association.*
- Bhatty, J.I., Bhattacharja, S. and Todres, H.A. 1996. Use of cement kiln dust in stabilizing clay soils. *Portland Cement Association, Washington, DC, USA, PR343.*
- Bishop, A.W. and Donald, I.B. 1961. The experimental study of partly saturated soil in the triaxial apparatus. *5th International Conference on Soil Mechanics and Foundation Engineering*, pp. 13–21.
- Bishop, A.W. and Henkel, D.J. 1962. The measurement of soil properties in the triaxial test. *2nd ed., Edward Arnold, London.*
- Bishop, A.W. and Wesley, L.D. 1975. A hydraulic triaxial apparatus for controlled stress path testing. *Géotechnique* 25(4), pp. 657–670.
- Black, D.K. and Lee, K.L. 1973. Saturating laboratory samples by back pressure. *Journal of the soil mechanics and foundations division* 99(1), pp. 75–93.

## References

---

- Blatz, J. and Graham, J. 2000. A system for controlled suction in triaxial tests. *Geotechnique* 50(4), pp. 465–469.
- Blatz, J.A., Cui, Y.-J. and Oldecop, L. 2008. Vapour equilibrium and osmotic technique for suction control. In: *Laboratory and Field Testing of Unsaturated Soils*. Springer, pp. 49–61.
- Brandon, T., Brown, J., Daniels, W., DeFazio, T., Filz, G., Musselman, J., Forshaand, C. and Mitchell, J. 2009. Rapid Stabilization/Polymerization of Wet Clay Soils; Literature Review. *Air Force Research Laboratory, Blacksburg*.
- Brooks, R. and Corey, A. 1964. Hydraulic properties of porous media. *Hydrology Papers, Colorado State University* 3(March), p. 37 pp.
- BS 1377-2 1990. Soils for civil engineering purposes. *Part 2* :, pp. 1–64.
- BS 1377-4 1990. Soils for civil engineering purposes. *Part 4*, pp. 1–63.
- BS 1377-5 1990. Soils for civil engineering purposes. *Part 5*, pp. 1–34.
- BS 1377-6 1990. Soils for civil engineering purposes. *Part 6* (1), pp. 1–64.
- BS 1377-7 1990. Soils for civil engineering purposes. *Part 7*, pp. 1–48.
- BS 1377-8 1990. Soils for civil engineering purposes. *Part 8*, pp. 1–30.
- BS 1377-9 1990. Soils for civil engineering purposes. *Part 9*, pp. 1–62.
- Buckingham, E. 1907. Studies on the movement of soil moisture. *US Dept. Agric. Bur. Soils Bull.* 38.
- Bulut, R. and Leong, E.C. 2008. Indirect Measurement of Suction. *Geotech Geol Eng.*
- Burton, G.J., Pineda, J. a., Sheng, D. and Airey, D. 2015. Microstructural changes of an undisturbed, reconstituted and compacted high plasticity clay subjected to wetting and drying. *Engineering Geology* 193, pp. 363–373.
- Bushra, I. and Robinson, R. 2012. Shear strength behavior of cement treated marine clay. *International Journal of Geotechnical Engineering* 6(4), pp. 455–466.

- Button, J.W. 2003. Kiln Dust for Stabilization of Pavement Base and Subgrade Materials. *Texas Transportation Institute, College Station, Texas, TTI2003-1, June.*
- Cai, G., Zhou, A. and Sheng, D. 2014. Permeability function for unsaturated soils with different initial densities. *Canadian Geotechnical Journal* 51(12), pp. 1456–1467.
- Campbell, G.S. 1974. A simple method for determining unsaturated conductivity from moisture retention data. *Soil science* 117(6), pp. 311–314.
- Campbell, G.S., Smith, D.M. and Teare, B.L. 2007. Application of a Dew Point Method to Obtain the Soil Water Characteristic. *Experimental Unsaturated Soil Mechanics*, pp. 71–77.
- Carter, M. 1983. Geotechnical engineering handbook. *Pentech Press. London,(SW/266), 1983, 226.*
- Chowdhury, Rashedul H. and Azam, S. 2016. Unsaturated shear strength properties of a compacted expansive soil from Regina, Canada. *Innovative Infrastructure Solutions* 1(1), pp. 1–11.
- Cresswell, H.P., Green, T.W. and McKenzie, N.J. 2008. The adequacy of pressure plate apparatus for determining soil water retention. *Soil Science Society of America Journal* 72(1), pp. 41–49.
- Crone, D. and Coleman, J.D. 1954. Soil structure in relation to soil suction (pF). *Journal of Soil Science* 5(1), pp. 75–84.
- Cui, Y.J., Tang, A.M., Mantho, A.T. and De Laure, E. 2008. Monitoring field soil suction using a miniature tensiometer. *Geotechnical Testing Journal* 31(1), pp. 95–100.
- Cui, Y.J. and Delage, P. 1996. Yielding and plastic behaviour of an unsaturated compacted silt. *Géotechnique* 46(2), pp. 291–311.
- Cuomo, S., Moscariello, M., Manzanal, D., Pastor, M. and Foresta, V. 2018. Modelling the mechanical behaviour of a natural unsaturated pyroclastic soil within

- Generalized Plasticity framework. *Computers and Geotechnics* 99(January), pp. 191–202.
- Dafalla, M., Shaker, A.A., Elkady, T., Al-Shamrani, M. and Dhowian, A. 2015. Effects of confining pressure and effective stress on hydraulic conductivity of sand-clay mixtures. *Arabian Journal of Geosciences* 8(11), pp. 9993–10001.
- Das, B. 2010. *Principles of geotechnical engineering (Seven edition)*. Stamford, CT: Thomson Learning, USA.
- Das, B.M. 2019. *Advanced Soil Mechanics*. 5th edition. | Boca Raton : Taylor & Francis.
- Day, P.R., Bolt, G.H. and Anderson, D.M. 1967. Nature of soil water. *Irrigation of Agricultural Lands* 11, pp. 191–208.
- Degré, A., van der Ploeg, M.J., Caldwell, T. and Gooren, H.P.A. 2017. Comparison of soil water potential sensors: A drying experiment. *Vadose Zone Journal* 16(4).
- Delage, P., Howat, M.D. and Cui, Y.J. 1998. The relationship between suction and swelling properties in a heavily compacted unsaturated clay. *Engineering Geology* 50(1–2), pp. 31–48.
- Delage, P. and Cui, Y.J. 2008. An evaluation of the osmotic method of controlling suction. *Geomechanics and Geoengineering* 3(1), pp. 1–11.
- Dismuke, T.D., Coburn, S.K. and Hirsch, C.M. 1981. Handbook of corrosion protection for steel pile structures in marine environments. *American Iron and Steel Institute*, p. 245.
- Dixit, M.S. 2016. Damage mechanism in problematic soils. *International Journal of Civil Engineering and Technology* 7(5), pp. 232–241.
- Ebrahimi, A., Edil, Tuncer B. and Son, Y.-H. 2012. Effectiveness of Cement Kiln Dust in Stabilizing Recycled Base Materials. *Journal of Materials in Civil Engineering* 24(8), pp. 1059–1066.

- Edlefsen, N.E. and Anderson 1943. Thermodynamics of soil moisture. *A Journal of Agricultural Science Published by the California Agricultural Experiment Station* 15(2).
- Elgabou, H.M. 2013. Critical Evaluation of Some Suction Measurement Techniques. PhD thesis, Cardiff University.
- Elmashad, M. and Hashad, A. 2013. Improving the Strength of Sandy Silt soils by Mixing with Cement Kiln Dust. *International Journal of Scientific & Engineering Research* 4(12), pp. 78–85.
- Elsharief, A.M. and Abdelaziz, O.A. 2015. Effects of Matric Suction on the Shear Strength of Highly Plastic Compacted Clay. *Innovative Geotechnics for Africa - Bouassida, Khemakhem & Haffoudhi (Eds.)*, pp. 97–103.
- EPA, U.S. 1993. *Report to congress on cement kiln dust*. Environmental Protection Agency. Environmental Protection Agency.
- Escario, V. and Saez, J. 1986. The shear strength of partly saturated soils. *Geotechnique* 36(3), pp. 453–456.
- Estabragh, A.R. and Javadi, A.A. 2008. Critical state for overconsolidated unsaturated silty soil. *Canadian Geotechnical Journal* 45(3), pp. 408–420.
- Estabragh, A.R. and Javadi, A.A. 2012. Effect of suction on compressibility and shear behaviour of unsaturated silty soil. *Geomechanics and Engineering* 4(1), pp. 55–65.
- Esteban, V., Saez, J. and Romana, M. 1988. A device to measure the swelling characteristics of rock samples with control of the suction up to very high values. In: *Proc. ISRM Symposium on Rock Mechanics and Power Plants*.
- Farouk, A., Lamboj, L. and Kos, J. 2004. Influence of Matric Suction on the Shear Strength Behaviour of Unsaturated Sand. *Acta Polytechnica* 44(4), pp. 11–17.
- Feng, M. and Fredlund, D.G. 1999. Hysteretic influence associated with thermal conductivity sensor measurements. *52nd Canadian Geotechnical Conf. and Unsaturated Soil Group, Proceeding from Theory to the Practice of*

- Unsaturated Soil Mechanics, Canadian Geotechnical Society, Richmond, BC, Canada*, pp. 651–657.
- François, B. and Laloui, L. 2008. *Thermo-plasticity in unsaturated soils, a constitutive approach*.
- Fredlund, D.G., Bergan, A.T. and Wong, P.K. 1977. Relation between resilient modulus and stress conditions for cohesive subgrade soils. *Transportation Research Record* (642).
- Fredlund, D. G., Morgenstern, N.R. and Widger, R.A. 1978. The shear strength of unsaturated soils. *Canadian Geotechnical Journal* 15(3), pp. 313–321.
- Fredlund, D.G. 1979. Second Canadian Geotechnical Colloquium: Appropriate Concepts and Technology for Unsaturated Soils. *Canadian Geotechnical Journal* 16(1), pp. 121–139.
- Fredlund, D.G., Rahardjo, H. and Gan, J.K.. 1987. Non-linearity of strength envelope for unsaturated soils. In: *Proceedings, 6th International Conference of Expansive Soils*. pp. 49–54.
- Fredlund, D.G., Xing, A., Fredlund, M.D. and Barbour, S.L. 1996. The relationship of the unsaturated soil shear strength to the soil-water characteristic curve. *Canadian Geotechnical Journal* 33(3), pp. 440–448.
- Fredlund, D.G. 1997. From theory to the practice of unsaturated soil mechanics. *NSAT'97 - 3rd Brazilian Symposium on Unsaturated Soil*, pp. 1–20.
- Fredlund, D.G., Harianto Rahardjo, Leong, E.C. and Ng, C.W.W. 2001. Suggestions and recommendations for the interpretation of soil-water characteristic curves. *Proceedings of the 14th Southeast Asian Geotechnical Conference, Hong Kong* 1, pp. 503–508.
- Fredlund, D.G. 2002. Use of soil-water characteristic curves in the implementation of unsaturated soil mechanics. *Proceedings of the 3rd International Conference on Unsaturated Soils, Recife, Brazil*.

- Fredlund, D.G. 2006. Unsaturated Soil Mechanics in Engineering Practice. *Journal of Geotechnical and Geoenvironmental Engineering* 132(3), pp. 286–321.
- Fredlund, D.G., Sheng, D. and Zhao, J. 2011. Estimation of soil suction from the soil-water characteristic curve. *Canadian Geotechnical Journal* 48(2), pp. 186–198.
- Fredlund, D.G., Rahardjo, H. and Fredlund, M.D. 2012. *Unsaturated Soil Mechanics in Engineering Practice*. John Wiley & Sons, Inc., Hoboken, New Jersey, USA.
- Fredlund, D.G. 2015. Relationship between the laboratory SWCCs and field stress state. In: *Sixth Asia-Pacific Conference on Unsaturated Soil*. pp. 3–14.
- Fredlund, D.G. and Houston, S.L. 2013. Interpretation of soil-water characteristic curves when volume change occurs as soil suction is changed. *Advances in Unsaturated Soils c*, pp. 15–31.
- Fredlund, D.G. and Morgenstern, N.R. 1977. Stress state variables for unsaturated soils. *Journal of Geotechnical and Geoenvironmental Engineering* 103(ASCE 12919).
- Fredlund, D.G. and Rahardjo, H. 1987. Soil Mechanics Principles for Highway Engineering in Arid Regions. *Transportation Research Record* 0(1137), pp. 1–11.
- Fredlund, D.G. and Rahardjo, H. 1993. *Soil mechanics for unsaturated soils*. John Wiley & Sons, Inc., Hoboken, New Jersey, USA.
- Fredlund, D.G. and Xing, A. 1994. Equations for the soil-water characteristic curve. *Canadian Geotechnical Journal* 31(6), pp. 1026–1026.
- Fredlund, M.D. 1999. The Role of Unsaturated Soil Property Functions in the Practice of Unsaturated Soil Mechanics.
- Fredlund, M.D., Wilson, G.W. and Fredlund, D.G. 2002. Representation and estimation of the shrinkage curve. In: *Proc., 3rd Int. Conf. on Unsaturated Soils, UNSAT 2002*. pp. 145–149.

- Freer-Hewish, R.J., Ghataora, G.S. and Niazi, Y. 1999. Stabilization of desert sand with cement kiln dust plus chemical additives in desert road construction. *Proceedings of the Institution of Civil Engineers-Transport* 135(1), pp. 29–36.
- Gallage, C. and Uchimura, T. 2016. Direct shear testing on unsaturated silty soils to investigate the effects of drying and wetting on shear strength parameters at low suction. *Journal of Geotechnical and Geoenvironmental Engineering* 142(3), pp. 1–9.
- Gallipoli, D., Wheeler, S.J. and Karstunen, M. 2003. Modelling the variation of degree of saturation in a deformable unsaturated soil. *Geotechnique* 53(1), pp. 105–112.
- Gan, J.K.M., Fredlund, D.G. and Rahardjo, D.H. 1988. Determination of the shear strength parameters of an unsaturated soil using the direct shear test. *Can Geotech* 25, pp. 500–510.
- Gan, K.-M.J. 1986. Direct shear strength testing of unsaturated soils. Thesis, University of Saskatchewan, Saskatoon, Canada.
- Gardner, W.R. 1958. Mathematics of Isothermal in Water Conduction Unsaturated Soil. *Highway research board special report*, pp. 78–87.
- GDS Instruments Ltd 2012. *GDS Unsaturated Triaxial Testing Systems Handbook*.
- GDS Instruments Ltd 2013. *The GDS Laboratory Users Handbook: GDSLAB v2.5.4*.
- Geiser, F., Laloui, L., Vulliet, L. and others 2000. On the volume measurement in unsaturated triaxial test. In: *Unsaturated soils for Asia. Proceedings of the Asian Conference on Unsaturated Soils, UNSAT-ASIA 2000, Singapore, 18-19 May, 2000*. pp. 669–674.
- van Genuchten, M.T. 1980. A Closed-form equation for predicting the hydraulic conductivity of unsaturated soils. *Soil Science Society of America Journal* 44(5), p. 892.
- Goh, S.G. 2012. Hysteresis effects on mechanical behaviour of unsaturated soils. PhD thesis Nanyang Technological University, Singapore.

- Goh, S.G., Rahardjo, H. and Leong, E.C. 2015. Modification of triaxial apparatus for permeability measurement of unsaturated soils. *Soils and Foundations* 55(1), pp. 63–73.
- Grim, R.E. 1968. *Clay mineralogy 2nd ed.* McGraw-hill Book Company. New York, pp.185-224.
- Guan, G.S., Rahardjo, H. and Choon, L.E. 2010. Shear Strength Equations for Unsaturated Soil under Drying and Wetting. *Journal of Geotechnical and Geoenvironmental Engineering* 136(4), pp. 594–606.
- Guan, Y. and Fredlund, D.G. 1997. Use of the tensile strength of water for the direct measurement of high soil suction. *Canadian Geotechnical Journal* 34, pp. 604–614.
- Gui, M.W. and Wu, Y.M. 2014. Failure of soil under water infiltration condition. *Engineering Geology* 181, pp. 124–141.
- Haines, W.B. 1923. The volume-changes associated with variations of water content in soil. *The Journal of Agricultural Science* 13(3), pp. 296–310.
- Haines, W.B. 1930. Studies in the Physical Properties of Soils. V. The hysteresis effect in capillary properties, and the modes of moisture distribution associated therewith. *The Journal of Agricultural Science* 20(1), pp. 97–116.
- Handoko, L., Yasufuku, N., Oomine, K. and Hazarika, H. 2013. Suction controlled triaxial apparatus for saturated-unsaturated soil test. *International Journal of GEOMATE* 4(1), pp. 466–470.
- Hashad, A. and El-Mashad, M. 2014. Assessment of soil mixing with cement kiln dust to reduce soil lateral pressure compared to other soil improvement methods. *HBRC Journal* 10(2), pp. 169–175.
- Head, K.H. and Epps, R.J. 2014. *Manual of Soil Laboratory Testing, Volume 3: Effective Stress Tests.* Whittles Publishing, Dunbeath Mill, Dunbeath, Scotland, UK.

- Hilf, J.W. 1956. *An investigation of pore-water pressure in compacted cohesive soils*. U.S. Dept. of Interior Bureau of Reclamation, Design and Construction Division, Denver, Colo. Technical Memorandum No. 654.
- Hillel, D. 1982. *Introduction to Soil Physics*. Academic Press, Inc.(London) Ltd.
- Hillel, D. 1998. *Environmental soil physics*. Academic Press, San Diego, USA.
- Ho, D. Y. F. and Fredlund, D.G. 1982. Increase in shear strength due to suction for two Hong Kong soils. In: *Proc ASCE Geotech Conf, Engineering and Construction on Tropical and residual soils. Honolulu, Hawaii, USA, January*. pp. 11–15.
- Ho, D.Y. F. and Fredlund, D.G. 1982. Strain rates for unsaturated soil shear strength testing. In: *Proceedings of the Seventh Southeast Asian Geotechnical Conference , Hong Kong*. Southeast Asian Geotechnical Society, Bangkok, pp. 787–803.
- Hong, Z., Shen, S., Deng, Y. and Negami, T. 2007. Loss of soil structure for natural sedimentary clays. *Proceedings of the Institution of Civil Engineers: Geotechnical Engineering* 160(3), pp. 153–159.
- Horpibulsuk, S., Miura, N. and Bergado, D.T. 2004. Undrained Shear Behavior of Cement Admixed Clay at High Water Content. *Journal of Geotechnical and Geoenvironmental Engineering* 130(10), pp. 1096–1105.
- Indrawan, I.G.B., Rahardjo, H. and Leong, E.C. 2006. Effects of coarse-grained materials on properties of residual soil. *Engineering Geology* 82(3), pp. 154–164.
- Iorliam, A.Y., Agbede, I.O. and Joel, M. 2012. Effect of Cement Kiln Dust (CKD) on some geotechnical properties of Black Cotton Soil (BCS). *Electronic Journal of Geotechnical Engineering* 17 H, pp. 967–977.
- Iyer, B. 1990. Pore water extraction-Comparison of saturation extract and high-pressure squeezing. *ASTM Special Technical Publication* (1095), pp. 159–170.
- Jennings, J.E.B. and Burland, J.B. 1962. Limitations to the use of effective stresses in partly saturated soils. *Geotechnique* 12(2), pp. 125–144.

- Jie, X. 2011. Experimental study of effects of suction history and wetting drying on small strain stiffness of an unsaturated soil. PhD thesis, Hong Kong University of Science and Technology, Hong Kong.
- Jones, B.R., Merwe, F.H. Van Der and Pequenino, F.P. 2019. Harvesting from agriculture: Evaluating the in-situ measurement of matric suction for geotechnical applications using a water potential sensor.
- Jury, W.A., Gardner, W.R. and Gardner, W.H. 1991. Soil Physics. *John Wiley & Sons. Inc. New York.*
- Karagoly, Y., Tripathy, S., Cleall, P.J. and Mahdi, T. 2018. Suction measurements by a fixed-matrix porous ceramic disc sensor. *Proceedings of the 7th International Conference on Unsaturated Soils* (September), pp. 703–708.
- Kasangaki, G.J. 2012. Experimental Study of Hydro-Mechanical Behaviour of Granular Materials. Heriot-Watt University.
- Kassiff, G. and Shalom, A. Ben 1971. Experimental Relationship Between Swell Pressure and Suction. *Geotechnique* 21(3), pp. 245–255.
- Keerthi, Y., Kanthi, P.D., Tejaswi, N., Chamberlin, K.S. and Satyanarayana, B. 2013. Stabilization of Clayey Soil using Cement Kiln Waste. *International Journal of Advanced Structures and Geotechnical Engineering* 02(02), pp. 77–82.
- Kim, D. and Siddiki, N. 2004. Lime kiln dust and lime--A comparative study in Indiana. In: *Transportation Research Board 83rd Annual Meeting, CD-ROM Publication, Transportation Research Board, Washington, DC.*
- Klausner, Y. 1991. *Fundamentals of Continuum Mechanics of Soils.*
- Krahn, J. and Fredlund, D.G. 1972. On total, matric and osmotic suction. *Soil Science* 114(5), pp. 339–348.
- Krosley, L., Likos, W.J. and Lu, N. 2003. Alternative Encasement Materials for Clod Test. *Geotechnical Testing Journal* 26(4), pp. 461–464.

- Kunal, P., Siddique, R. and Rajor, A. 2012. Use of cement kiln dust in cement concrete and its leachate characteristics. *Resources, Conservation and Recycling* 61, pp. 59–68.
- Lachemi, M., Hossain, K.M.A., Shehata, M. and Thaha, W. 2008. Controlled low strength materials incorporating cement kiln dust from various sources. *Cement & Concrete Composites* 30, pp. 381–392.
- Lackenby, J., Indraratna, B., McDowell, G. and Christie, D. 2007. Effect of confining pressure on ballast degradation and deformation under cyclic triaxial loading. *Geotechnique* 57(6), pp. 527–536.
- Lake, C. 2016. Manufactured aggregate from cement kiln dust. *Environmental Geotechnics* 6(2), pp. 111–122.
- Laloui, L., Peron, H., Geiser, F., Rifa, A., Vulliet, L. and Others 2006. Advances in volume measurement in unsaturated soil triaxial tests. *Soils and foundations* 46(3), pp. 341–349.
- Lambe, T.W. 1958. The structure of compacted clay. *Journal of the Soil Mechanics and Foundations Division* 84(2), pp. 1–34.
- Lambe, T.W. and Whitman, R. V 1969. *Soil Mechanics*. John Wiley, New York.
- Lavkulich, L.M. 1981. Methods manual: pedology laboratory. *Vancouver, BC, CA: University of British Columbia, Department of Soil Science*.
- Lawton, B.E.C., Frigaszy, R.J., Hetherington, M.D. and Member, A. 1992. Review of Wetting-Induced Collapse in Compacted Soil. *Journal of Geotechnical Engineering* 118(9), pp. 1376–1394.
- Lawton, E.C., Frigaszy, R.J. and Hardcastle, J.H. 1989. Collapse of Compacted Clayey Sand. *Journal of Geotechnical Engineering* 115(9), pp. 1252–1267.
- Lee, I.-M., Sung, S.-G. and Cho, G.-C. 2005. Effect of stress state on the unsaturated shear strength of a weathered granite. *Canadian Geotechnical Journal* 42(2), pp. 624–631.

- Leong, E.C., Tripathy, S. and Rahardjo, H. 2003. Total suction measurement of unsaturated soils with a device using the chilled-mirror dew-point technique. *Géotechnique* 53(2), pp. 173–182.
- Leong, E.C., Tripathy, S. and Rahardjo, and H. 2004. Technical Note. *Geotechnical Testing Journal* 27(3), pp. 322–331.
- Leong, E. C. and Rahardjo, H. 1997. Permeability functions for unsaturated soils. *Journal of Geotechnical Engineering* 123(12), pp. 1118–1126.
- Leong, Eng Choon and Rahardjo, H. 1997. Review of Soil-Water Characteristic Curve Equations. *Journal of Geotechnical and Geoenvironmental Engineering* 123(12), p. 2.
- Li, J., Hao, K. and Feng, P. 2018. Research on suction equilibrium time of unsaturated reticulate red clay. *KSCE Journal of Civil Engineering* 22(2), pp. 565–571.
- Lins, Y. 2009. Hydro-Mechanical Properties of Partially Saturated Sand. PhD Dissertaton, Faculty of Civil Engineering, University Bochum, Weibenfels, Germany.
- Lins, Y., Schanz, T. and Fredlund, D.G. 2009. Modified pressure plate apparatus and column testing device for measuring SWCC of sand. *Geotechnical Testing Journal* 32(5).
- Lloret, A., Villar, M. V., Sánchez, M., Gens, A., Pintado, X. and Alonso, E.E. 2003. Mechanical behaviour of heavily compacted bentonite under high suction changes. *Géotechnique* 53(1), pp. 27–40.
- Lu, N. and Likos, W.J. 2004. *Unsaturated soil mechanics*. John Wiley & Sons, Inc., Hoboken, New Jersey, USA:
- Lu, N. and Likos, W.J. 2013. Origin of cohesion and its dependence on saturation for granular media. *Poromechanics V - Proceedings of the 5th Biot Conference on Poromechanics*, pp. 1669–1675.

- Lu, Y., Luo, X., Wu, Y. and Cui, Y.J. 2007. Study of fundamental properties of soil--water characteristic curve. In: *Proceedings of the 3rd Asian conference on unsaturated soils*. Beijing: Science Press. pp. 243–249.
- Lynch, K., Sivakumar, V., Tripathy, S. and Hughes, D. 2019. Development of a laboratory technique for obtaining Soil Water Retention Curves under external loading in conjunction with high capacity tensiometers. *Géotechnique* 69(4), pp. 320–328.
- Ma, T., Wei, C., Wei, H. and Li, W. 2016. Hydraulic and mechanical behavior of unsaturated Silt: experimental and theoretical characterization. *International Journal of Geomechanics* 16(6), p. D4015007.
- Malazian, A., Hartsough, P., Kamai, T., Campbell, G.S., Cobos, D.R. and Hopmans, J.W. 2011. Evaluation of MPS-1 soil water potential sensor. *Journal of Hydrology* 402(1–2), pp. 126–134.
- Maleksaeedi, E. and Nuth, M. 2016. A modified oedometer apparatus for experimentally obtaining the soil-water retention curve. *Geovancouver*. Vancouver: Springer.
- Matyas, E.L. and Radhakrishna, H.S. 1968. Volume change characteristics of partially saturated soils. *Geotechnique* 18(4), pp. 432–448.
- McCoy, W.J. and Kriner, R.W. 1971. Use of waste kiln dust for soil consolidation. *Lehigh Portland Cement Co., Allentown, Penn.*
- Miller, C.J., Yesiller, N., Yaldo, K. and Merayyan, S. 2002. impact of soil type and compaction conditions on soil water characteristic. *Journal of Geotechnical and Geoenvironmental Engineering* 128(9), pp. 733–742.
- Miller, G. and Zaman, M. 2000. Field and Laboratory Evaluation of Cement Kiln Dust as a Soil Stabilizer. *Transportation Research Record* 1714(1), pp. 25–32.
- Miller, G.A., Azad, S. and Dhar, B. 1997. The effect of cement kiln dust on the collapse potential of compacted shale. *Testing Soil Mixed with Waste or Recycled Materials*, pp. 232–245.

- Miller, G.A., Khoury, C.N., Muraleetharan, K.K., Liu, C. and Kibbey, T.C.G. 2008. Effects of soil skeleton deformations on hysteretic soil water characteristic curves: Experiments and simulations. *Water Resources Research* 44(5), pp. 1–10.
- Miller, G.A. and Azad, S. 2000. Influence of soil type on stabilization with cement kiln dust. *Construction and Building Materials* 14(2), pp. 89–97.
- Miller, G.A. and Hamid, T.B. 2007. Interface direct shear testing of unsaturated soil. *Geotechnical Testing Journal* 30(3), pp. 182–191.
- Mitchell, J.K. 1993. *Fundamentals of soil behavior*. 2nd ed. New York ; Chichester: John Wiley&Sons.
- Mitchell, James Kenneth and Soga, K. 2005. *Fundamentals of soil behavior*. John Wiley & Sons Hoboken, NJ.
- Mohamed, A.M.O. 2002. Hydro-mechanical evaluation of soil stabilized with cement-kiln dust in arid lands. *Environmental Geology* 42(8), pp. 910–921.
- Monroy, R. 2005. The influence of load and suction changes on the volumetric behaviour of compacted London clay. PhD thesis, University of London (Imperial College London).
- Morales, E.R. 1999. Characterisation and thermo-hydro-mechanical behaviour of unsaturated Boom clay: an experimental study. Tesis doctoral, Universitat Politècnica de Catalunya.
- Moses, G. and Afolayan, J.O. 2011. Compacted foundry sand treated with cement kiln dust as hydraulic barrier material. *Electronic Journal of Geotechnical Engineering* 16, pp. 337–355.
- Moses, G. and Afolayan, J.O. 2013. Desiccation-Induced Volumetric Shrinkage of Compacted Foundry Sand Treated with Cement Kiln Dust. *Geotechnical and Geological Engineering* 31(1), pp. 163–172.

- Muhunthan, B. and Sariosseiri, F. 2008. *Interpretation of Geotechnical Properties of Cement Treated Soils*. Proceedings of Geocongress, Washington State University, 134.
- Mukherjee, S. and Ghosh, B. 2013. *The science of clays: Applications in industry, engineering and environment*. Springer: Dordrecht, Netherlands.
- Murray, E.J. and Sivakumar, V. 2010. *Unsaturated Soils: A fundamental interpretation of soil behaviour*.
- Nagaraj, H., Munna, M. and Sridharan, A. 2010. Swelling behavior of expansive soils. *International Journal of Geotechnical Engineering* 4(1), pp. 99–110.
- Naik, T.R., Canpolat, F. and Chun, Y. 2003. Uses of CKD other than for flue gas desulfurization. *Center for by-products utilization, A CBU Report for Holcim (US), Report No. CBU-2003-35*, pp. 1–33.
- Nam, S., Gutierrez, M., Diplas, P., Petrie, J., Wayllace, A., Lu, N. and Muñoz, J.J. 2009. Comparison of testing techniques and models for establishing the SWCC of riverbank soils. *Engineering Geology* 110, pp. 1–10.
- Nam, S., Gutierrez, M., Diplas, P. and Petrie, J. 2011. Determination of the shear strength of unsaturated soils using the multistage direct shear test. *Engineering Geology* 122(3–4), pp. 272–280.
- Napeierala, R. 1983. Stabilization of the subsoil with the dust from the kilns for Portland cement clinker burning. *Cement-Wapno-Gips XXXVI/L (4)*, pp. 127–128.
- Nasr, A.M.A. 2015. Geotechnical Characteristics of Stabilized Sabkha Soils from the Egyptian-Libyan Coast. *Geotechnical and Geological Engineering*, pp. 893–911.
- Ng, C.W., Zhan, L.T. and Cui, Y.J. 2002. A new simple system for measuring volume changes in unsaturated soils. *Canadian Geotechnical Journal* 39(3), pp. 757–764.

- Ng, C.W.W., Cui, Y., Chen, R. and Pierre, D. 2007. The axis-translation and osmotic techniques in shear testing of unsaturated soils: a comparison. *Soils and Foundations* 47(4), pp. 675–684.
- Ng, C.W.W., Lai, C.H. and Chiu, C.F. 2012. A modified triaxial apparatus for measuring the stress path-dependent water retention curve. *Geotechnical Testing Journal* 35(3), pp. 490–495.
- Ng, C.W.W., Cheng, Q., Zhou, C. and Alonso, E.E. 2016. Volume changes of an unsaturated clay during heating and cooling. *Geotechnique Letters* 6(3), pp. 192–198.
- Ng, C.W.W. and Menzies, B. 2007. *Advanced unsaturated soil mechanics and engineering*. Taylor & Francis.
- Ng, Charles W.W. and Pang, Y.W. 2000. Experimental investigations of the soil-water characteristics of a volcanic soil. *Canadian Geotechnical Journal* 37(6), pp. 1252–1264.
- Ng, Charles W. W. and Pang, Y.W. 2000. Influence of stress state on soil-water characteristics and slope stability. *Journal of Geotechnical and Geoenvironmental Engineering* 126(2), pp. 157–166.
- Nidzam, R.M. and Kinuthia, J.M. 2010. Sustainable soil stabilisation with blastfurnace slag - a review. *Proceedings of Institution of Civil Engineers: Construction Materials* 163(3), pp. 157–165.
- Noorzad, R. and Pakniat, H. 2016. Investigating the effect of sample disturbance, compaction and stabilization on the collapse index of soils. *Environmental Earth Sciences* 75(18), pp. 1–9.
- Nuntasarn, R. and Wannakul, V. 2012. The relationship between soil suction and the maximum unsaturated undrained shear strengths of compacted khon kaen soil. *International Journal of GEOMATE* 2(1), pp. 166–170.
- Nuth, M. and Laloui, L. 2011. A model for the water retention behavior of deformable soils including capillary hysteresis. *Foundations d*, pp. 56–65.

- O'Brien, F.E.M. 1948. The Control of Humidity by Saturated Salt Solutions. *Journal of Scientific Instruments* 25(3), pp. 73–76.
- Oliveira, O.M. and Marinho, F.A.M. 2008. Suction equilibration time for a high capacity tensiometer. *Geotechnical Testing Journal* 31(1), pp. 101–105.
- Van Olphen, H. 1977. *An introduction to clay colloid chemistry, for clay technologists, geologists, and soil scientists.*
- Olson, R.E. 1986. State of the art: consolidation testing. In: *Consolidation of soils: testing and evaluation.* ASTM International.
- Onur, M.I., Evirgen, B., Tuncan, A. and Tuncan, M. 2014. Modelling of shear strength parameters of saturated clayey soils. *International Journal of GEOMATE* 7(2), pp. 1107–1110.
- Or, D., Tuller, M. and Wraith, J.M. 2005. Soil water potential. *Encyclopedia of soils in the environment* 3, pp. 270–277.
- Oriola, F.O.P., Moses, G. and Afolayan, J. 2012. Soil-Water Characteristics Curves for Cement Kiln Dust Treated Foundry Sand. *IJMRS's International Journal of Engineering Sciences* 01(03).
- Osinubi, K.J., Moses, G. and Liman, A.S. 2015. The Influence of Compactive Effort on Compacted Lateritic Soil Treated with Cement Kiln Dust as Hydraulic Barrier Material. *Geotechnical and Geological Engineering* 33(3), pp. 523–535.
- Oss, H.G. van 2010. Minerals information – cement.
- Pan, H., Qing, Y. and Pei-Yong, L. 2010. Direct and indirect measurement of soil suction in the laboratory. *Electronic Journal of Geotechnical Engineering* 15 A, pp. 1–14.
- Parent, S.É., Cabral, A. and Zornberg, J.G. 2007. Water retention curve and hydraulic conductivity function of highly compressible materials. *Canadian Geotechnical Journal* 44(10), pp. 1200–1214.

- Parsons, R.L., Kneebone, E. and Milburn, Justin P. 2004. *Use of cement kiln dust for subgrade stabilization*. Final Report No. KS-04-03, Kansas Department of Transportation, Topeka, Kansas.
- Pasha, A., Khoshghalb, A. and Khalili, N. 2015. Common Mistakes in Determination of Air Entry Value from Gravimetric Water Content Based Soil-Water Characteristic Curve. In: *Unsaturated Soil Mechanics-from Theory to Practice: Proceedings of the 6th Asia Pacific Conference on Unsaturated Soils (Guilin, China, 23-26 October 2015)*. p. 335.
- Peethamparan, S., Olek, J. and Lovell, J. 2008. Influence of chemical and physical characteristics of cement kiln dusts (CKDs) on their hydration behavior and potential suitability for soil stabilization. *Cement and Concrete Research* 38(6), pp. 803–815.
- Peranić, J., Arbanas, Ž., Cuomo, S. and Maček, M. 2018. Soil-Water Characteristic Curve of Residual Soil from a Flysch Rock Mass. *Geofluids* 2018, pp. 1–15.
- Pereira, J.H. and Fredlund, D.G. 2000. Volume change behavior of collapsible compacted Gneiss soil. *Journal of Geotechnical and Geoenvironmental Engineering* 126(10), pp. 859–946.
- Perez-Garcia, N., Houston, S.L., Houston, W.N. and Padilla, J.M. 2008. An oedometer pressure plate SWCC apparatus. *Geotechnical Testing Journal* 31(2), pp. 115–123.
- Peron, H., Hueckel, T. and Laloui, L. 2007. An Improved Volume Measurement for Determining Soil Water Retention Curves. *Geotechnical Testing Journal* 30(1), pp. 1–8.
- Peroni, N. and Tarantino, A. 2005. Measurement of osmotic suction using the squeezing technique. In: *Unsaturated Soils: Experimental Studies*. pp. 159–168.
- Pinilla, J.D., Miller, G.A., Cerato, A.B. and Snethen, D.S. 2011. Influence of curing time on the resilient modulus of chemically stabilized soils. *Geotechnical Testing Journal* 34(4), pp. 1–9.

- Poulos, S.J. 1988. Liquefaction and related phenomena. *Advanced dam engineering for design, construction, and rehabilitation*.
- Pranshoo Solanki, Khoury, N. and Zaman, M. 2007. Engineering Behavior and Microstructure of Soil Stabilized with Cement Kiln Dust. *GSP 172 Soil Improvement*, pp. 1--10.
- Pujiastuti, H., Rifa'i, A., Adi, A.D. and Fathani, T.F. 2018. The effect of matric suction on the shear strength of unsaturated sandy clay. *International Journal of GEOMATE* 14(42), pp. 112–119.
- Pusch, R. 1982. Mineral–water interactions and their influence on the physical behavior of highly compacted Na bentonite. *Canadian Geotechnical Journal* 19(3), pp. 381–387.
- Qian, Y.L., Wang, F.Y. and Li, X.W. 2012. Test Study on Strength Characteristics of Unsaturated Silt. *Applied Mechanics and Materials* 204–208, pp. 446–451.
- Rahardjo, H., Lim, T.T., Chang, M.F. and Fredlund, D.G. 1995. Shear-strength characteristics of a residual soil. *Canadian Geotechnical Journal* 32(1), pp. 60–77.
- Rahardjo, H., Heng, O.B. and Choon, L.E. 2004. Shear strength of a compacted residual soil from consolidated drained and constant water content triaxial tests. *Canadian Geotechnical Journal* 41(3), pp. 421–436.
- Rahardjo, H. and Fredlund, D.G. 2003. Ko-volume change characteristics of an unsaturated soil with respect to various loading paths. *Geotechnical Testing Journal* 26(1), pp. 79–91.
- Rampino, C., Mancuso, C. and Vinale, F. 1999. Laboratory testing on an unsaturated soil: equipment, procedures, and first experimental results. *Canadian Geotechnical Journal* 36(1), pp. 1–12.
- Rampino, C., Mancuso, C. and Vinale, F. 2000. Experimental behaviour and modelling of an unsaturated compacted soil. *Canadian Geotechnical Journal* 37(4), pp. 748–763.

## References

---

- Rees, S. 2013. Part One: Introduction to the triaxial testing. *Published on the GDS website www.gdsinstruments.com* 1(Cd), pp. 1–4.
- Richards, B.G. 1965. Measurement of free energy of soil moisture by the psychrometric technique, using thermistors. *A Symposium in Print, Sydney, Australia. Edited by G.D. Aitchison. Butterworths & Co. Ltd., pp. 35-46.*
- Richards, B.G. 1974. Behaviour of unsaturated soils. *In: Lee IK (ed), Soil mechanics—new horizons. American Elsevier, New York, pp. 112–157.*
- Ridley, A.M. and Burland, J.B. 1993. A new instrument for the measurement of soil moisture suction. *Géotechnique* 43(2), pp. 321–324.
- Robinson, R.G. and Allam, M.M. 1998. Effect of clay mineralogy on coefficient of consolidation. *Clays and Clay Minerals* 46(5), pp. 596–600.
- Romero, E. and Simms, P.H. 2008. Microstructure investigation in unsaturated soils: a review with special attention to contribution of mercury intrusion porosimetry and environmental scanning electron microscopy. *In: Laboratory and Field Testing of Unsaturated Soils. Springer, pp. 93–115.*
- Roy. S & Kumar. S 2017. Role of geotechnical properties of soil on civil engineering structures. *Resources and Environment* 7(4), pp. 103–109.
- Roy, S. and Rajesh, S. 2018. Influence of Confining Pressure on Water Retention Characteristics of Compacted Soil. *Indian Geotechnical Journal* 48(2), pp. 327–341.
- Sabat, Akshay Kumar and Pati, S. 2014. A Review of Literature on Stabilization of Expansive Soil Using Solid Wastes. *Electronic Journal of Geotechnical Engineering* 19(Bund. U), pp. 6251–6267.
- Sachan, A. and Penumadu, D. 2007. Effect of Microfabric on Shear Behavior of Kaolin Clay. *Journal of Geotechnical and Geoenvironmental Engineering* 1(October), pp. 1–7.

- Saffari, P., Noor, M.J.M., Hadi, B.A. and Motamedi, S. 2015. Laboratory Test Methods for Shear Strength Behavior of Unsaturated Soils Under Suction Control, Using Triaxial Apparatus. In: *InCIEC 2014*. Springer, pp. 567–576.
- Salahudeen, A.B., Eberemu, A.O. and Osinubi, K.J. 2014. Assessment of Cement Kiln Dust-Treated Expansive Soil for the Construction of Flexible Pavements. *Geotechnical and Geological Engineering* 32(4), pp. 923–931.
- Sariosseiri, F. and Muhunthan, B. 2008. Geotechnical properties of Palouse loess modified with cement kiln dust and Portland cement. In: *GeoCongress 2008: Characterization, Monitoring, and Modeling of GeoSystems*. pp. 92–99.
- Sayah, A.I. 1993. Stabilization of expansive clay using cement dust. M. Sc. Thesis, Graduate School, University of Oklahoma, Norman, Oklahoma, USA.
- Scanlon, B.R., Andraski, B.J. and Bilskie, J. 2002. 3.2. 4 Miscellaneous methods for measuring matric or water potential. *Methods of Soil Analysis: Part 4 Physical Methods*, pp. 643–670.
- Schanz, T. and Tripathy, S. 2009. Swelling pressure of a divalent-rich bentonite: Diffuse double-layer theory revisited. *Water Resources Research* 45(2), pp. 1–9.
- Seed, H.B., Lundgren, R. and others 1962. Prediction of swelling potential for compacted clays. *Journal of the soil mechanics and foundations division* 88(3), pp. 53–88.
- Sharma, R. 1998. Mechanical behaviour on unsaturated highly expansive clays. Doctoral dissertation, University of Oxford, UK.
- Sharma, R.S., Hong, L. and Singhal, S. 2006. Developments in Measurement of Volume Change in Triaxial Testing of Unsaturated Soils. (Gsp 148), pp. 93–101.
- Sheng, D., Zhou, A. and Fredlund, D.G. 2011. Shear Strength Criteria for Unsaturated Soils. *Geotechnical and Geological Engineering* 29(2), pp. 145–159.
- Sillers, W.S., Fredlund, D.G. and Zakerzaheh, N. 2001. Mathematical attributes of some soil-water characteristic curve models. *Geotechnical and Geological Engineering*, pp. 243–283.

- Sillers, W.S. and Fredlund, D.G. 2001. Statistical assessment of soil-water characteristic curve models for geotechnical engineering. *Canadian Geotechnical Journal* 38(6), pp. 1297–1313.
- Sivakumar, V. 1993. A critical state framework for unsaturated soil. PhD thesis, University of Sheffield.
- Sivakumar, V. 2014. The influence of high air entry filter on the testing of unsaturated soils using the axis translation technique. *Environmental Geotechnics* 3(2), pp. 90–98.
- Solanki, P., Khoury, N. and Zaman, M.M. 2009. Engineering Properties and Moisture Susceptibility of Silty Clay Stabilized with Lime, Class C Fly Ash, and Cement Kiln Dust. *Journal of Materials in Civil Engineering* 21(December), pp. 749–757.
- Solanki, P. and Zaman, M. 2012. Microstructural and Mineralogical Characterization of Clay Stabilized Using Calcium-Based Stabilizers. In: *Scanning Electron Microscopy*. IntechOpen, p. pp.771-798.
- Sreekrishnavilasam, A., King, S. and Santagata, M. 2006. Characterization of fresh and landfilled cement kiln dust for reuse in construction applications. *Engineering Geology* 85(1–2), pp. 165–173.
- Sreekrishnavilasam, A., Rahardja, S., Kmetz, R. and Santagata, M. 2007. Soil treatment using fresh and landfilled cement kiln dust. *Construction and Building Materials* 21(2), pp. 318–327.
- Sreekrishnavilasam, A. and Santagata, M.C. 2006. Development of Criteria for the Utilization of Cement Kiln Dust (CKD) in Highway Infrastructures. *Joint Transportation Research Program*.
- Sridharan, A., Venkatappa Rao, G. and De, P.K. 1974. Mechanisms Controlling Volume Change Of Saturated Clays and the Role of the Effective Stress Concept. *Geotechnique* 24(3), pp. 447–449.
- Sridharan, A., Sreepada Rao, A. and Sivapullaiah, P. V. 1986. Swelling Pressure of Clays. *Geotechnical Testing Journal* 9(1), pp. 24–33.

- Sridharan, A. and Gurtug, Y. 2005. Compressibility characteristics of soils. *Geotechnical and Geological Engineering* 23(5), pp. 615–634.
- Sridharan, A. and Nagaraj, H.B. 2000. Compressibility behaviour of remoulded, fine-grained soils and correlation with index properties. *Canadian Geotechnical Journal* 37(3), pp. 712–722.
- Sun, D., Zhang, J., Gao, Y. and Sheng, D. 2016. Influence of suction history on hydraulic and stress-strain behavior of unsaturated soils. *International Journal of Geomechanics* 16(6), pp. 1–9.
- Svoboda, J.S. and McCartney, J.S. 2014. Impact of Strain Rate on the Shear Strength and Pore Water Pressure Generation of Saturated and Unsaturated Compacted Clay. In: *Geo-Congress 2014: Geo-characterization and Modeling for Sustainability*. pp. 1453–1462.
- Tadza, M. 2011. Soil-water characteristic curves and shrinkage behaviour of highly plastic clays: an experimental investigation. PhD thesis, Cardiff University, UK.
- Taha, M.R., Hossain, M.K. and Mofiz, S.A. 2000. Effect of suction on the strength of unsaturated soil. *Advances in Unsaturated Geotechnics*, pp. 210–221.
- Tami, D., Rahardjo, H. and Leong, E.-C. 2004. Effects of Hysteresis on Steady-State Infiltration in Unsaturated Slopes. *Journal of Geotechnical and Geoenvironmental Engineering* 130(9), pp. 1390–1392.
- Tang, A.M. and Cui, Y.J. 2005. Controlling suction by the vapour equilibrium technique at different temperatures and its application in determining the water retention properties of MX80 clay. *Canadian Geotechnical Journal* 42, pp. 287–296.
- Tavakoli Dastjerdi, M.H., Habibagahi, G. and Nikooee, E. 2014. Effect of confining stress on soil water retention curve and its impact on the shear strength of unsaturated soils. *Vadose Zone Journal* 13(5).
- Taylor, D.W. 1948. Fundamentals of soil mechanics. *New York, USA*.

- Terzaghi, K. von 1936. The shearing resistance of saturated soils and the angle between the planes of shear. In: *First international conference on soil Mechanics, 1936*. pp. 54–59.
- Thakur, V.K.S., Sreedeeep, S. and Singh, D.N. 2006. Laboratory investigations on extremely high suction measurements for fine-grained soils. *Geotechnical and Geological Engineering* 24(3), pp. 565–578.
- Thu, T.M., Rahardjo, H. and Leong, E.C. 2006. Shear Strength and Pore-Water Pressure Characteristics during Constant Water Content Triaxial Tests. *Journal of Geotechnical and Geoenvironmental Engineering* 132(3), pp. 411–419.
- Thu, T.M., Rahardjo, H. and Leong, E.C. 2007. Soil-water characteristic curve and consolidation behavior for a compacted silt. *Canadian Geotechnical Journal* 44(3), pp. 266–275.
- Tian, Z., Kool, D., Ren, T., Horton, R. and Heitman, J.L. 2018. Determining in-situ unsaturated soil hydraulic conductivity at a fine depth scale with heat pulse and water potential sensors. *Journal of Hydrology* 564(July), pp. 802–810.
- Tinjum, J.M., Benson, C.H. and Lisa R. Blotz 1997. Soil-water characteristic curves for compacted clays. *Journal of Geotechnical and Geoenvironmental Engineering* 123(11), pp. 1060–1069.
- Todres, H.A., Mishulovich, A. and Ahmed, J. 1992. *Cement kiln dust management: Permeability*.
- Toll, D.G., Lourenço, S.D.N. and Mendes, J. 2013. Advances in suction measurements using high suction tensiometers. *Engineering Geology* 165, pp. 29–37.
- Tripathy, S., Sridharan, A. and Schanz, T. 2004. Swelling pressures of compacted bentonites from diffuse double layer theory. *Canadian Geotechnical Journal* 41(3), pp. 437–450.
- Tripathy, S., Elgabu, H. and Thomas, H.R. 2012. Matric suction measurement of unsaturated soils with null-type axis-translation technique. *Geotechnical Testing Journal* 35(1).

- Tripathy, S., Elgabu, H. and Thomas, H.R. 2014. Soil-water characteristic curves from various laboratory techniques. *Unsaturated Soils: Research & Applications*, pp. 1701–1707.
- Tripathy, S., Al-Khyat, S., Cleall, P.J. and Baille, W. 2016. Soil Suction Measurement of Unsaturated Soils with a Sensor Using Fixed-Matrix Porous Ceramic Discs. *Indian Geotechnical Journal*.
- Tripathy, S. and Schanz, T. 2007. Compressibility behaviour of clays at large pressures. *Canadian Geotechnical Journal* 44(3), pp. 355–362.
- United States Salinity Laboratory 1954. Diagnosis and improvement of saline and alkali soils. *Agricultural Handbook No. 60. United States Department of Agriculture, Washington* (60).
- Upma, J. and Kumar, S. 2015. Effect of Cement Kiln Dust and Chemical Additive on Expansive Soil at Subgrade Level. , pp. 3759–3767.
- USEPA 1998. Technical Background Document on Ground Water Controls at CKD Landfills. *Office of Solid Waste U.S. Environmental Protection Agency*.
- Vanapalli, S.K., Fredlund, D.G., Pufahl, D.E. and Clifton, A.W. 1996. Model for the prediction of shear strength with respect to soil suction. *Canadian geotechnical journal* 33, pp. 379–392.
- Vanapalli, S.K., Fredlund, D.G. and Pufahl, D.E. 1996. The relationship between the soil-water characteristic curve and the unsaturated shear strength of a compacted glacial till. *Geotechnical Testing Journal* 19(3), pp. 259–268.
- Vanapalli, S.K., Fredlund, D.G. and Pufahl, D.E. 1997. Comparison of saturated-unsaturated shear strength and hydraulic conductivity behavior of a compacted sandy-clay till. *Proceedings of the 50 th Canadian Geotechnical Conference*, pp. 625–632.
- Vanapalli, S.K., Sillers, W.S. and Fredlund, M.D. 1998. The meaning and relevance of residual state to unsaturated soils. *Proceedings of the 51st Canadian Geotechnical Conference*, pp. 1–8.

- Vanapalli, S.K., Fredlund, D.G. and Pufahl, D.E. 1999. The influence of soil structure and stress history on the soil-water characteristics of a compacted till. *Geotechnique* 49(2), pp. 143–159.
- Vanapalli, S.K., Wright, A. and Fredlund, D.G. 2000. Shear strength behavior of a silty soil over the suction range from 0 to 1,000,000 kPa. *Proceedings of the 53th Canadian Geotechnical Conference*.
- Vanapalli, S.K. and Fredlund, D.G. 2000. Comparison of different procedures to predict unsaturated soil shear strength. In: *Advances in Unsaturated Geotechnics*. pp. 195–209.
- Varathungarajan, D.A., Garfield, S.M. and Wright, S.G. 2009. *Characterization of undrained shear strength profiles for soft clays at six sites in Texas*.
- Wan, A.W.L. 1996. The use of thermocouple psychrometers to measure in situ suctions and water contents in compacted clays. PhD thesis, University of Manitoba, Winnipeg, Manitoba, Canada.
- Wasemiller, M.A. and Hoddinott, K.B. 1997. *Testing soil mixed with waste or recycled materials*.
- Wheeler, S. 1986. The Stress-Strain Behaviour of soils containing Gas Bubbles. PhD thesis, University of Oxford.
- Wheeler, S.J. and Sivakumar, V. 1995. An elasto-plastic critical state framework for unsaturated soil. *Géotechnique* 45(1), pp. 35–53.
- Wijaya, M. and Leong, E.C. 2016. Swelling and Collapse of Unsaturated Soils Due to Inundation Under One-Dimensional Loading. *Indian Geotechnical Journal* 46(3), pp. 239–251.
- Williams, R.J. 2005. Effects of Cement Kiln Dust (CKD) Chemistry and Content on Properties of Controlled Low-Strength Materials (CLSM). University of South Carolina.

- Xu, Y., Wu, S., Williams, D.J. and Serati, M. 2018. Determination of peak and ultimate shear strength parameters of compacted clay. *Engineering Geology* 243, pp. 160–167.
- Yang, H., Rahardjo, H., Leong, E.C. and Fredlund, D.G. 2004. Factors affecting drying and wetting soil-water characteristic curves of sandy soils. *Canadian Geotechnical Journal* 41, pp. 908–920.
- Ye, Y. xue, Zou, W. lie, Han, Z. and Liu, X. wen 2019. Predicting the entire soil-water characteristic curve using measurements within low suction range. *Journal of Mountain Science* 16(5), pp. 1198–1214.
- Yilmaz, M.K. 2014. Improvement of expansive soils by using cement kiln dust. Thesis, Middle East Technical University.
- Zaman, M. 1992. Soil stabilization using cement kiln dust. In: *International conference on expansive soils*. pp. 347–351.
- Zapata, C.E. 1999. Uncertainty in soil-water-characteristic curve and impacts on unsaturated shear strength prediction. PhD Dissertation, Arizona State University, Tempe, United States.
- Zhai, Q. and Rahardjo, H. 2012. Determination of soil-water characteristic curve variables. *Computers and Geotechnics* 42, pp. 37–43.
- Zhang, J., Sun, D., Zhou, A. and Jiang, T. 2015. Hydromechanical behaviour of expansive soils with different suctions and suction histories. *Canadian Geotechnical Journal* 53(1), pp. 1–13.
- Zhou, A.N., Sheng, D. and Carter, J.P. 2012. Modelling the effect of initial density on soil-water characteristic curves. *Geotechnique* 62(8), pp. 669–680.
- Zhou, J. and Yu, J.L. 2005. Influences affecting the soil-water characteristic curve. *Journal of Zhejiang University: Science* 6 A(8), pp. 797–804.